Dynamics and Control of Multistage Membrane Plants

Department of Chemical and Process Engineering
University of Canterbury
Christchurch

A thesis presented in fulfilment of the requirement
for the degree of
Doctor of Philosophy
in Chemical and Process Engineering
to the University of Canterbury

Tristan J Hunter

2000

Acknowledgements

I wish to thank my supervisor Dr Ken Morison for his guidance and support during the course of this research. I always enjoyed our meetings, and your enthusiasm towards this project. I would also like to express my gratitude to Dr Pat Jordan for his input, particularly during the closing stages of this project. Tony Allen also deserves mention, for keeping my computer running smoothly. My thanks also go to Associate Professor Maurice Allen, who first introduced me to the challenges of process control. I must also mention my office mates, who supported and amused me during this project.

My greatest thanks goes to my wife Angela, whose support, faith and understanding helped me through stressful times.

The financial support provided by the New Zealand Dairy Board and University of Canterbury Doctoral Scholarship was greatly appreciated.

Summary

The controllability of multistage membrane separation processes is examined, and methods of improving closed-loop performance are assessed in this thesis. Membrane systems exhibit non-linear time-variant behaviour which poses special challenges. Extensive analysis of dynamic process characteristics was undertaken to develop an understanding of inherent system behaviour. In this work two case studies are examined, based on membrane separations performed in the New Zealand dairy industry, one manufacturing a retentate and the other a permeate product. Both produce a foodstuff, and are subject to operating constraints specified in the interests of product safety.

The initial part of this thesis reviews membrane separations, and develops a general framework for modelling the dynamic behaviour of multistage membrane processes. Specific models are developed for each case study, which exhibit characteristics representative of industrial membrane separations. These models are analysed extensively in this dissertation, and also used as the basis for open- and closed-loop process simulation.

In order to improve closed-loop process performance it was first necessary to develop an understanding of dynamic process behaviour. Qualitative analysis of structural system models showed the inherent characteristics of the two case studies to be similar, with inverse response and oscillatory characteristics feasible within both separations. It was found that multistage membrane processes have widespread disturbance propagation, due to concentration-dependent permeate fluxes and constant volume plant design. Numerical controllability assessment confirmed the presence of inverse response and oscillatory behaviour within both case studies. Oscillatory eigenvalues were not present in flowsheets with few stages, showing that flowsheet design has a significant impact on dynamic process behaviour. Analysis also showed that the use of diafiltration injection hastens the onset of oscillatory behaviour in systems with few stages. This illustrates the significant effect diafiltration injection has on dynamic process characteristics. The conclusions drawn in this thesis are valid for both retentate and permeate product separations.

Interaction between different control variable pairings was quantified using the relative gain array. This analysis tool indicated that high levels of interaction were present

within both case study systems for certain input-output variable pairings. The preferred variable pairings for the retentate product case study are consistent with industrial practice in New Zealand. No preferred variable pairings were identified for the permeate product case study, and instead it was concluded that directly controlling the permeate stream properties is generally undesirable. For a multistage membrane plant producing a permeate product, it is best to control the concentration and purity of the retentate stream, selecting setpoints corresponding to the desired permeate stream properties. This analysis contributes to a fundamental understanding of multistage process behaviour, and is applicable to any liquid-phase pressure-driven membrane separation.

Closed-loop simulation was used to examine achievable process performance. In both case studies, the retentate stream was controlled to achieve a composition corresponding to the desired retentate purity or permeate yield, using the preferred input-output variable pairings identified by the relative gain analysis. It was concluded that the performance of the multi-loop PID strategy is limited by the inherent characteristics of a membrane process. The regular addition of new separation stages also degrades the quality of control that can be achieved, and causes the dynamic process characteristics to change significantly over time. Analysis showed retentate composition control to be difficult in membrane plants, due to highly variable process dynamics and occasional inverse response behaviour. It was concluded that conventional diafiltration injection strategies limit the achievable closed-loop performance of multistage plants with variable membrane area. The closed-loop simulations successfully identified limitations on closed-loop performance, and highlighted the few options for the mitigation of these constraints.

The final part of this thesis presents an innovative multivariable controller which attempts to avoid the identified limitations on process performance associated with conventional diafiltration injection strategies. This strategy attempts to maintain the total solids concentration and purity of each fractionation stage somewhere on a specified reference trajectory, by simultaneously manipulating all variables in the input set. Diafiltration flow rate inputs are directly manipulated, rather than maintained as proportions of the permeate flows. A real-time model is used to supply estimates of current process conditions, and predictions of the process response to chosen input combina-

tions. The multivariable controller exhibits superior ability to reject measured system disturbances, such as those caused by the introduction of new separation stages. Most significantly, closed-loop simulation demonstrates the ability to maintain the desired retentate purity or permeate yield for the duration of production despite changes in process behaviour during this time. This controller strategy could easily be applied to any other multistage membrane plant using diafiltration injection to achieve enhanced separation.

Table of Contents

1 Introduction

Process optimisation was heralded as providing a competitive edge to companies through increased efficiency and reduced energy use (Lenhoff & Morari, 1982). However, price alone is no longer the definitive basis on which customers make purchasing decisions. "*Product quality...measured by product variability...is quickly becoming a discriminator among chemical suppliers*" (Downs *et al.*, 1994). At first glance, this demand may fall to the control engineer, but low product variability also relies on plant designs which are well behaved and limit disturbance propagation. Much work has been published in the field of plant controllability, particularly in the area of integrating process design and controllability assessment (for example Narraway *et al.*, 1991; Lear *et al.*, 1995; Lababidi & Alatiqi, 1996), directed mainly at the development and implementation of assessment methods for petrochemical operations.

Semi-permeable membrane separation operations have received comparatively little attention in process control literature, yet they can pose challenging control difficulties. This type of process is commonly associated with biochemical and food industries (Cheryan, 1998), offering energy efficient separation of heat labile products. Membrane separation is widely utilised in the New Zealand dairy industry, with existing plants each having processing capacity of up to 120 $m^3 hr^{-1}$ (Bennett, 1997). Winchester (1996) presented an analysis of a large-scale multistage membrane process, based on those used in the dairy industry. In this work he identified the presence of undesirable dynamic characteristics, contributing to poor closed-loop plant behaviour. The scale of membrane operations in New Zealand has grown hugely in the last two decades, meaning that controllability improvements now offer significant potential gains or, conversely, that the cost of poor process behaviour is becoming considerable. This thesis examines the dynamic characteristics of multistage membrane plants, in an effort to develop an understanding of process behaviour. Using this knowledge, opportunities for improving process controllability are considered, through modifications in process design, operating conditions and control strategies.

The widespread implementation of numerical design optimisation is based on the justification of minimising operating and capital costs. This is a valid argument since identification of the 'best' process design provides a competitive advantage to a com-

pany. However, to be successful the approach must be applied with caution. In addition to the typical design constraints such as processing capacity and product composition, a design brief usually also includes qualitative requirements covering aspects such as worker safety, environmental impact and consistency of product (Barton *et al.*, 1986; Lear, 1991). These requirements are often difficult to express within the framework of a numerical design optimisation. Furthermore, significant problems can arise if one of these qualitative factors becomes an active constraint. For a poorly behaved plant, process controllability and operability can be limiting factors. Although it is difficult to quantify process controllability (Skogestad, 1994), it is clear that poor plant behaviour can affect process efficiency (i.e. operating cost), worker safety, environmental risk and product consistency. Since the 1980's new plant design methodologies have increasingly focused on more efficient use of raw material and energy resources (Lenhoff & Morari, 1982). This has been achieved through highly integrated process designs which utilise recycle streams and heat recovery techniques (Price & Georgakis, 1993). Economic incentives have also lead to reduced plant inventories and less buffering, with smaller surge tanks between various parts of the plant (Luyben & Floudas, 1994). Each of these design trends, brought about by process optimisation, contribute to reduced controllability and product quality.

In some circumstances it quickly becomes clear during the design process that a plant is likely to be poorly behaved or have complex dynamics. The obvious solution is to implement some quantitative controllability assessment method, and define limits on the acceptable design region. Figure 1-1 shows such a situation, where feasible values of the design or operating variables DoF1 and DoF2 are constrained within a region which produces a plant design with acceptable controllability characteristics. Although a single global assessment tool may not exist, control literature contains many examples of useful tools which may be used at various times during the development of a process design (Perkins & Wong, 1985; Fararooy *et al.*, 1993). However, several issues make such an approach infeasible for any process:

1) *Definitions of 'acceptable' behaviour, or specification of controllability limits are arbitrary and imprecise.*
2) *Only limited tools are available for controllability assessment.* Some of these are very limited in scope, whilst others may give conflicting results.

3) *Difficulties in accurately modelling the dynamic behaviour of a process may cause the analysis to be inaccurate.* Hence, defining exact boundaries on the acceptable operating region may not be possible.

4) *Many assessment tools do not give a singular measure of process behaviour.*

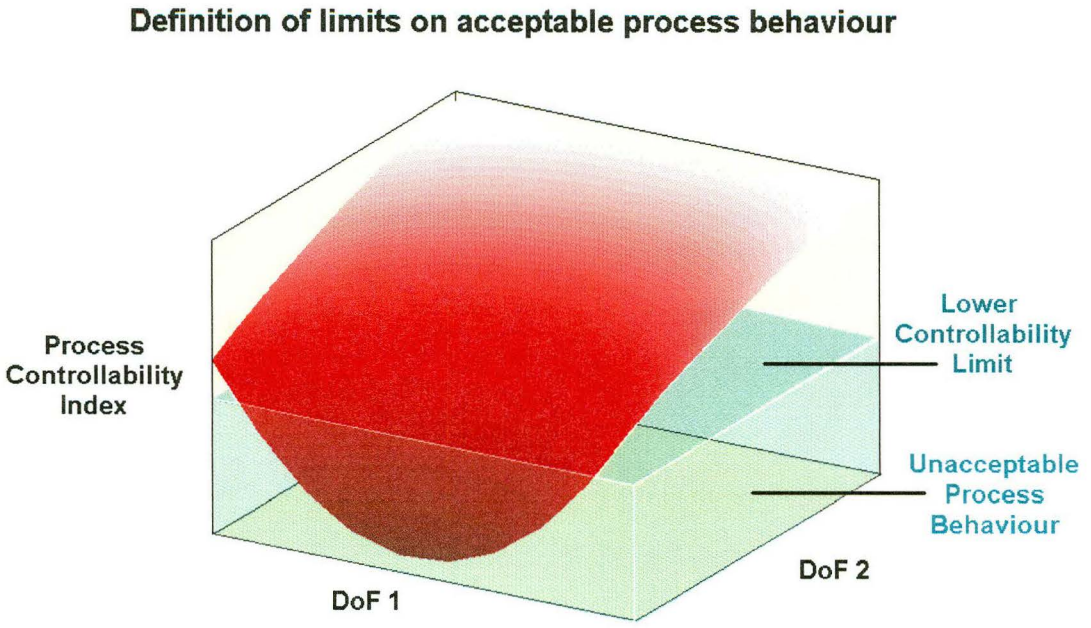

Figure 1-1 Quantitative controllability assessment
DoF 1 and DoF 2 represent two independent design or operating parameters

Given these difficulties, integrating formal controllability assessment within a global design optimisation is not easy, although work is continuing in this area (Bansal *et al.*, 2000; Russel *et al.*, 2000). Therefore, alternative approaches must be considered for poorly behaved processes. Heuristic methods, based on 'rules of thumb', have been widely used in the past to generate process flowsheets (Prince & Connolly, 1996). Such methods have also been used to predict process operability but they are not always reliable for complex systems (Price & Georgakis, 1993; Morud & Skogestad, 1996). In fact, the trend towards highly integrated plants with many recycle and heat recovery streams means that many of the past heuristics fail to be applicable (Morari, 1983). Moreover, changes in processing scale or, feed and product specifications can change the original design envelope and move the controllability boundaries of the system. Limited understanding of a well behaved process may not cause difficulties, but ignorance of some complex systems may result in a plant design with poor operability (such as the Tennessee Eastman process, Downs & Vogel, 1993) or one which needs extensive modification or retrofitting (Anderson, 1966; Oglesby *et al.*, 1992).

1.1 Scope of thesis

The aim of this work is to obtain a thorough understanding of multistage membrane plant behaviour. Several controllability assessment and analysis methods are used to investigate dynamic process characteristics and closed-loop controller performance. The effect of flowsheet design and operating conditions on process behaviour is also investigated. Two case studies are examined throughout this work; the first is the production of whey protein concentrate (WPC) and the second is the manufacture of a generic permeate product. The WPC case study requires the removal of unwanted permeable impurities, and dewatering of the remaining retentate product stream. The permeate product case study involves the separation of a permeable species from an unwanted impurity. The first process is widely used commercially in the dairy industry whilst the second is more typical of pharmaceutical applications. This thesis is divided into three parts; the first (Chapter 2 & 3) presents an overview of membrane separation, the second section (Chapter 4 & 5) explores open-loop process behaviour, and the third part (Chapter 6 & 7) focuses on closed-loop process controllability. This final section builds on the preceding chapters and explores options for improving controller performance.

In Chapter 2, important concepts of membrane separation are reviewed, and a range of multistage flowsheets examined for single phase membrane separations. The effect of qualitative and quantitative constraints on flowsheet selection is examined for the case studies. A suitable design, based on industrial plants operating in New Zealand is presented for subsequent analysis. Chapter 3 examines methods of representing the dynamic behaviour of multistage membrane flowsheets. A dynamic model is developed for each case study, using a general model of the process flowsheet, combined with specific models for the permeate characteristics (e.g. flux and composition).

Non-numerical analysis of the dynamic state space models is presented in Chapter 4, focusing specifically on identifying undesirable structural characteristics and disturbance propagation paths within the system. Such analysis offers an insight into system behaviour, and likely interaction between different input-output variable pairings. Chapter 5 examines process controllability and behaviour at steady state, using numerical assessment tools. The effect of operating conditions and process flowsheet design are examined in detail for each case study.

Single-input single-output (SISO) controller strategies are examined in Chapter 6, using preferred input-output variable pairings identified in Chapter 5. Of interest in this analysis are the effect of constraints and operating conditions on the closed-loop behaviour of each case study. Opportunities for improvements to existing designs and control strategies are reviewed in Chapter 7, for general membrane separations. An alternative control strategy is then presented, based on the process understanding developed in previous chapters. This strategy avoids or minimises closed-loop performance constraints that had been identified. Closed-loop performance under this strategy is then compared with the SISO simulations. Final conclusions and recommendations are presented.

1.2 References

Anderson J S (1966), A practical problem in dynamic heat transfer, *The Chemical Engineer,* **May**, CE97-CE103.

Bansal V, Perkins J B, Pistikopoulos F N & Van Schijndel J M G (2000), Simultaneous design and control optimisation under uncertainty, *Computers chem. Engng,* **24**, (2-7), 261-266.

Barton G W, Chan W K, Perkins J D & Prince R G H (1986), Controllability analysis of alternate process designs. *CHEMECA 86,* pp. 200-205, Adelaide.

Bennett R J (1997), Membrane applications in the New Zealand dairy industry, *Dairy Technology,* **11**, (1), 8-10.

Cheryan M (1998), *Ultrafiltration and Microfiltration Handbook,* 2nd Ed., Technomic Publishing Co., Lancaster, USA.

Downs J J, Hiester A C, Miller S M & Yount K B (1994), Industrial viewpoint on design/control tradeoffs. In *IFAC Workshop on Integration of Process Design and Control* (Ed. Zafiriou E), pp. 105-115, Pergamon Press, USA.

Downs J J & Vogel E F (1993), A plant-wide industrial process control problem, *Computers chem. Engng,* **17**, 245-255.

Fararooy S, Perkins J D, Malik T I, Oglesby M J & Williams S (1993), Process controllability toolbox (PCTB), *Computers chem. Engng.,* **17**, (5/6). 617-625.

Lababidi H M S & Alatiqi I M (1996), Application of controllability analysis tools during the conceptual design stage, *Computers chem. Engng.,* **20**, S207-S212.

Lear J B (1991), Optimising control as an economic design tool. *4th International Symposium on Process Systems Engineering,* pp. I.13.1-I.13.15, Montebello, Quebec.

Lear J B, Barton G W & Perkins J D (1995), Interaction between process design and process control: the impact of disturbances and uncertainty on estimates of achievable economic performance, *J. Proc. Cont.*, **5**, (1), 49-62.

Lenhoff A M & Morari M (1982), Design of resilient processing plants - I; process design under consideration of dynamic aspects, *Chem. Eng. Sci.*, **37**, (2), 245-258.

Luyben M L & Floudas C A (1994), Analyzing the interaction of design and control - 2. reactor-separator-recycle system, *Computers chem. Engng*, **18**, (10), 971-994.

Morari M (1983), Design of resilient processing systems III; a general framework for the assessment of dynamic resilience, *Chem. Eng. Sci.*, **38**, (11), 1881-1891.

Morud J & Skogestad S (1996), Dynamic behaviour of integrated plants, *J. Proc. Cont.*, **6**, (2/3), 145-146.

Narraway L T, Perkins J D & Barton G W (1991), Interaction between process design and process control: economic analysis of process dynamics, *J. Proc. Cont.*, **1**, 243-250.

Oglesby M J, Malik T I, Fararooy S & Geake V (1992), Early stage process controllability assessment. In *IFAC Workshop on Interactions between Process Design and Process Control* (Ed. Perkins J D), pp. 145-150, Pergamon Press, Oxford, UK.

Perkins J D & Wong M P F (1985), Assessing controllability of chemical plants, *Chem. Eng. Res. Des.*, **63**, (November), 358-362.

Price R M & Georgakis C (1993), Plantwide regulatory control design procedure using a tiered framework, *Ind. Eng. Chem. Res.*, **32**, 2693-2705.

Prince R G H & Connolly A F (1996), Heuristic decisions in an evolutionary design system, *Computers chem. Engng*, **32**, Suppl., S273-S278.

Russel B M, Henricksen J P, Jorgensen S B & Gani R (2000), Integration of design and control through model analysis, *Computers chem. Engng*, **24**, (2-7), 967-973.

Skogestad S (1994), A procedure for SISO controllability analysis - with application to design of pH processes. In *IFAC Workshop on Integration of Process Design and Control* (Ed. Zafiriou E), pp. 25-30, Pergamon Press, USA.

Winchester J (1996), *Computer Simulation and Controllability Studies of Multi-module Ultrafiltration Plants.* M.E. Thesis, Department of Chemical and Process Engineering, University of Canterbury, New Zealand.

2 Development Of A Membrane Process Flowsheet

A membrane plant must be correctly designed at both a micro- and macro-scale to successfully achieve all separation and operating objectives. At a molecular level, the correct membrane type must be selected to achieve the desired separation. On the macro-scale, the plant flowsheet should achieve the best possible separation efficiency subject to design and operating constraints. This chapter briefly reviews the main membrane types, then examines the macro-scale issues of maximising plant capacity and operating efficiency. The effect of operating constraints is also examined, particularly those specific to processing biological and food products. Two case studies are presented later in this chapter, representing the manufacture of foodstuffs, one a retentate and the other a permeate product. A single process flowsheet is presented as a design solution for both case studies. The operating conditions presented for this flowsheet are used when examining process behaviour in later chapters.

2.1 Overview of pressure driven membrane separation processes

Membrane separation technology has been employed by a diverse range of industries since initial commercial development during the 1960s (Le & Howell, 1985), including desalination, effluent treatment and enzyme concentration (Rautenbach & Albrecht, 1989). Most membrane operations are single-phase, offering energy savings over conventional multiphase separation operations such as distillation. More importantly, single phase separation preserves the functional properties of heat labile materials such as enzymic, biochemical and food products.

A number of different membrane types are available for the separation of liquid feed stocks. These may be broadly divided into four categories of pressure driven, single phase, membrane technologies (Figure 2-1):

- Microfiltration (MF)
- Ultrafiltration (UF)
- Nanofiltration (NF) or Loose Reverse Osmosis (LRO)
- Reverse Osmosis (RO)

All of the listed membrane types are semi-permeable and a pressure differential is used to force solvent through pores in the membrane. The permeate stream consists of

solvent and small, permeable species with the retentate consisting of the remaining solvent and material which did not pass through the membrane. Either retentate or permeate may be the desired product stream, depending on the nature of the separation. For a retentate product, membrane separation represents both fractionation (diffusion of the undesirable components through the membrane to the permeate stream) and concentration (loss of solvent through the membrane). Permeate product separations represent fractionation (by retention of less permeable impurities) but not usually concentration, since the permeate stream from each stage almost always contains species at a lower concentration than the retentate side of the membrane.

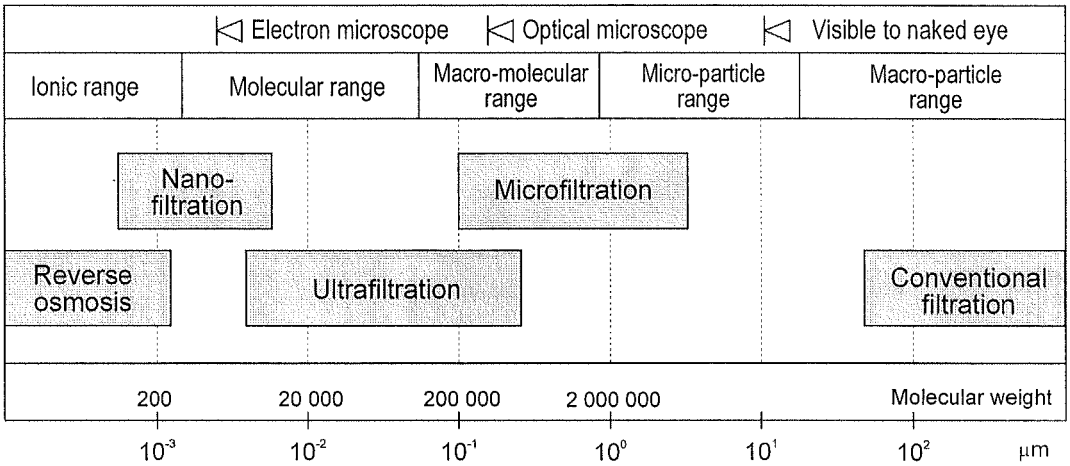

Figure 2-1 Molecular ranges of different membrane types used for liquid phase operations
Based on Bennett, 1997

Each membrane has a controlled pore size distribution which determines its molecular weight cut-off (MWCO) and selectivity. The manufacture, properties and applications of synthetic membranes are well understood and discussed in texts such as Cheryan (1998), Rautenbach & Albrecht (1989) and Mulder (1997). Each membrane type is produced by a number of manufacturers offering a range of designs and materials of construction. A review of these details is outside the scope of this work, but information of this type is presented by Scott (1995).

2.1.1 Microfiltration

Microfiltration (MF) separates very fine colloidal solid particles from liquids or gases, by means of mechanical sieving (Scott, 1995). Commercial applications of this technology include clarification of fruit juices (permeate product, Humphrey & Keller, 1997) and concentrating cell suspensions (retentate product, Grandison & Lewis, 1996). Separation can also be enhanced with the use of diafiltration, the addition

of clean solvent to 'wash' permeable species from the retentate. An example of this is the washing of colloidal suspensions such as pigment, metal hydroxide and grinding effluents. Generally the rate of permeation through the membrane is determined by the pressure differential (driving force) across the membrane. This pressure differential is usually less than 2 bar (Wagner, 1996). The MF systems can be operated in 'dead-end' mode (see Section 2.2) with feed flow perpendicular to the membranes, but this is only suitable for feeds containing very low solids concentration (Bowen, 1993).

2.1.2 Ultrafiltration

Ultrafiltration (UF) is widely used industrially to separate low molecular weight species or extremely fine particles from macromolecule compounds. Industrial applications include electropaint recovery and concentration of cheese whey (retentate product), as well as industrial effluent treatment (permeate product, Cheryan, 1998). Separation is primarily based on molecule size although molecular shape and interactions can also play a role. Permeation through the membrane is limited primarily by the accumulation of a layer of impermeable components at the membrane surface. For this reason, UF membranes are usually operated with feed flow parallel to the membrane surface, to sweep away retained components. Diafiltration is often employed to enhance separation for increased retentate purity or yield of permeable species. These membranes usually operate at intermediate differential pressure ranges of 1-10 bar (Wagner, 1996).

2.1.3 Nanofiltration

Nanofiltration (NF) is an emerging technology, developed from ultrafiltration. Smaller pores sizes result in partial retention of most ionic species but still allow higher permeate fluxes than reverse osmosis membranes. The technology is of particular interest for water treatment where it has been used for the removal of colour, hardness and radium (Field, 1996). Permeation rate through the membrane is limited by osmotic pressure (opposing permeation) and the accumulation of impermeable components at the membrane face. Again, these membranes operate with feed-flow parallel to the surface. Diafiltration can also be used with this technology to improve retentate product purity in separations such as the desalting of salty cheese whey (Field, 1996). Smaller pore size means that NF membranes operate at a higher differential pressure range of 5-35 bar (Wagner, 1996).

2.1.4 Reverse osmosis

Very small pore size and charge repulsion allows reverse osmosis (RO) membranes to completely retain most ionic species, with only pure solvent permeating through the membrane. Generally this technology is used to produce a permeate product (desalination and water treatment), but in some situations such as the dewatering of whey (Howell, 1990) a retentate product is produced. This technology is implemented on a larger scale than any other membrane type, particularly in the Middle East, with some installations producing over 50 000 tonnes of potable water per day (Howell, 1990). Unlike other membrane separations, diafiltration is not employed with RO. Again permeation rate through the membrane is affected by the accumulation of retained components on the membrane surface, so the feed flow moves parallel to the membrane. To achieve sufficient permeate flux and overcome (significant) opposing osmotic pressures, trans-membrane pressures of up to 150 bar may be necessary (Wagner, 1996).

2.2 Maximising long-term permeate flux

On a macro-scale, the throughput of a membrane plant design is most easily improved by increasing the long-term permeate flux, with corresponding increases in plant capacity. Traditional filtration operations use a filtercloth to collect solid material from a suspension or slurry, and generally operate with flow perpendicular to the filter (McCabe *et al.*, 1993). The process is referred to as dead-end filtration because the solids concentrate to a 'dead-end'. The cake of retained solids that forms on the filter (cloth) surface (Figure 2-2A) progressively thickens and causes a significant decline in permeate flux over time.

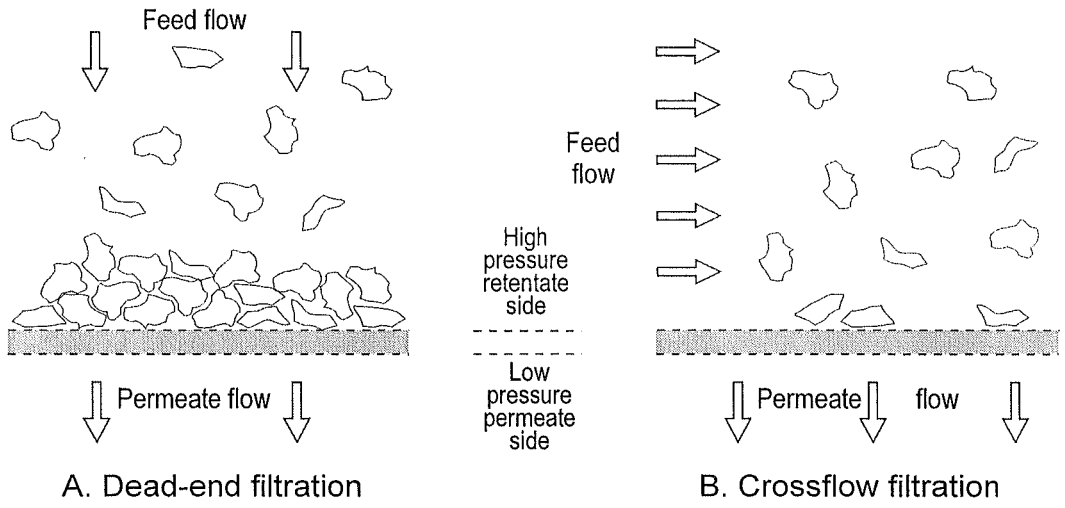

Figure 2-2 Schematic representation of fouling for different solvent flow regimes.

The high capital cost of membrane plant provides a strong incentive to increase the length of each filtration run, and maximise plant throughput. This is best achieved through the use of 'crossflow' (or 'tangential flow') designs, which force the solvent across the membrane surface at high velocities (Figure 2-2B). This tactic minimises fouling of the membrane surface since much of the impermeable material is swept from the membrane surface (Humphrey & Keller, 1997). Crossflow designs are successfully used for all membrane types.

A variety of fouling mechanisms occur with membrane separations. Microfiltration, like filtercloth filtration, sometimes suffers from the accumulation of fine colloidal solid material at the membrane surface. In contrast, molecular and ionic separation membranes (UF, NF and RO) suffer from 'concentration polarisation'. This is the accumulation of impermeable components as a concentrated layer at the membrane surface (Figure 2-3), which impedes the passage of solvent and small species through the membrane. The concentration polarisation boundary layer forms during the first few minutes of operation (Winchester, 1996) and is evident as a dramatic decline in permeate flux (Stage 1, Figure 2-4). During normal operation the accumulation is balanced by diffusion of the material back into the bulk solution. Permeate flux is therefore limited by the rate of diffusion away from the membrane surface. The thickness of the concentration boundary layer and hence concentration polarisation is significantly reduced by a high velocity crossflow regime, with a corresponding increase in overall permeate flux.

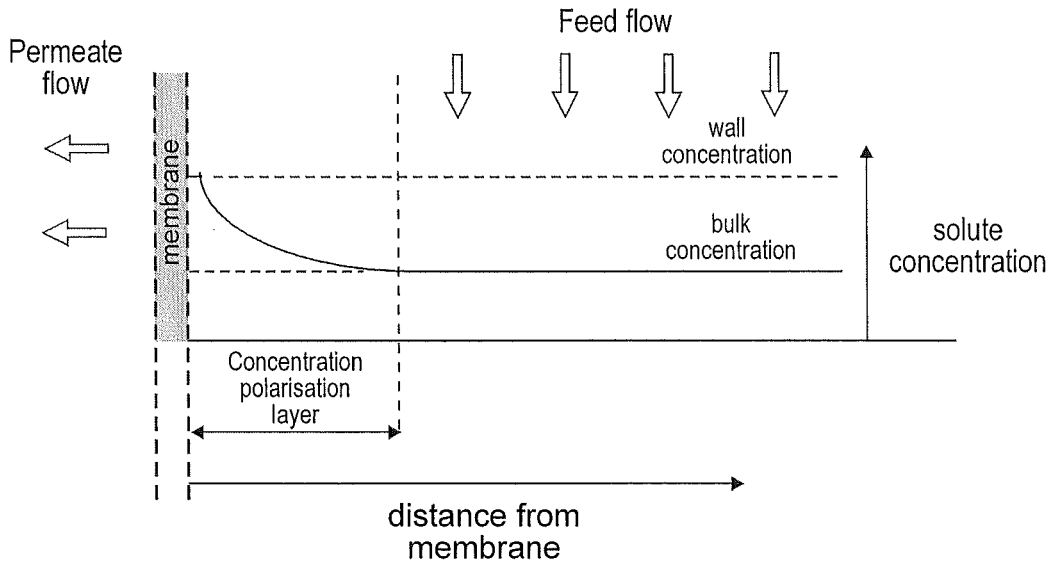

Figure 2-3 Schematic of concentration polarisation boundary layer at the membrane surface

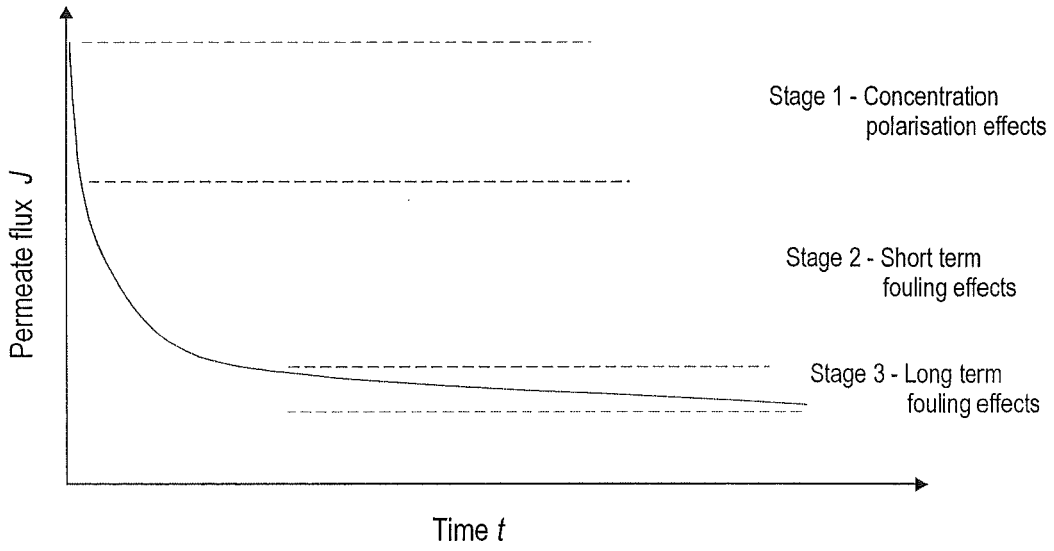

Figure 2-4 Effects of membrane fouling on permeate flux

Following the initial development of the concentration polarisation layer, a second stage of flux decline occurs, as components are adsorbed or deposited onto the membrane surface blocking access to pores. Finally the flux reaches a pseudo-steady state (Stage 3) with only a slow, near-linear decline with time. Many papers and books have been published on membrane fouling (for example Fane & Fell, 1987; Marshall *et al.*, 1993; Rao *et al.*, 1994), and the search for methods to reduce fouling effects continues.

2.3 Crossflow membrane flowsheet configurations

A number of configurations are possible for membrane separations. Selection of a flowsheet depends on the desired product specification and the nature of the separation. Optimal flowsheet design requires an understanding of the characteristics of each, so that the most appropriate choice is made. Overall, crossflow membrane flowsheets can be divided into two broad categories - batch and batchwise-continuous plants, with variations within each group.

2.3.1 Batch process flowsheets

Two common batch process designs exist for membrane plants (Figure 2-5), both based on a recirculating flow loop. Although not shown in the system schematics, a heat exchanger is often used to control the retentate temperature. Open-loop batch designs circulate the entire liquid volume around the flow loop and through the feed tank. This

results in the bulk concentration of the retentate continually increasing until processing is complete (Scott, 1995). In contrast, partial recycle designs return only a small volume back to the feed tank. Such designs offer reduced foaming in the feed tank, a small reduction in pumping costs and less mechanical damage to the product (Tutanjian, 1985). Batch filtration, like all batch operations, does not operate at a steady state point. As the separation progresses, and permeate is removed, the concentration of the retained components increases. Operation continues until a pre-determined product specification is reached. For a retentate product, there may be a large residence time and prolonged exposure to shear; two characteristics which can be problematic for biological or food products.

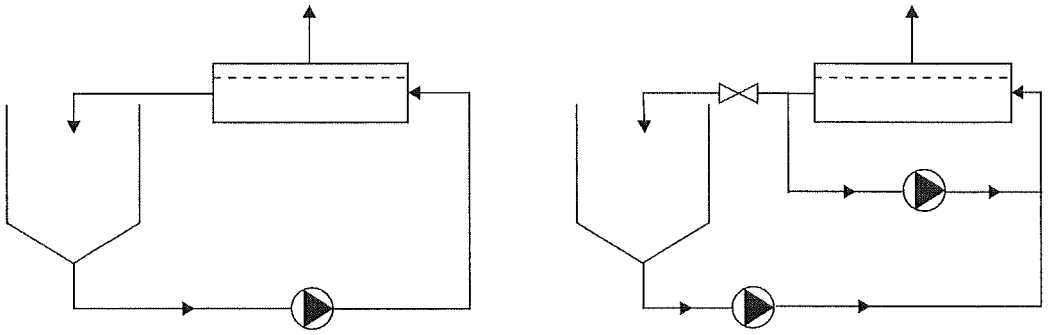

Figure 2-5 Batch process configurations

The behaviour of a batch membrane plant is most easily illustrated with a simple numerical example. Consider the separation of a two component feed using a semi-permeable membrane. Component A is a valuable species, initially present in lower concentrations (1 wt %), and almost completely impermeable. Component B is a highly permeable, unwanted impurity initially present in higher concentrations (5 wt %). Figure 2-6 shows the purification of a 200 L feed batch using a 0.5 m^2 membrane. Processing continues until the total solids (TS) concentration of the retentate reaches 12 wt %. Variation of the permeate flow rate with time (Figure 2-6B) is a significant characteristic of batch processing. This variation is entirely due to the concentration dependence of the permeate flux (membrane fouling was not included in the model). Overall, the average flux is comparatively high since the retentate concentration remains low for much of the processing cycle. The minimum permeate flow rate is marked by Point A in Figure 2-6B. Dynamic process behaviour is further investigated, using more sophisticated flux models, in Chapter 3.

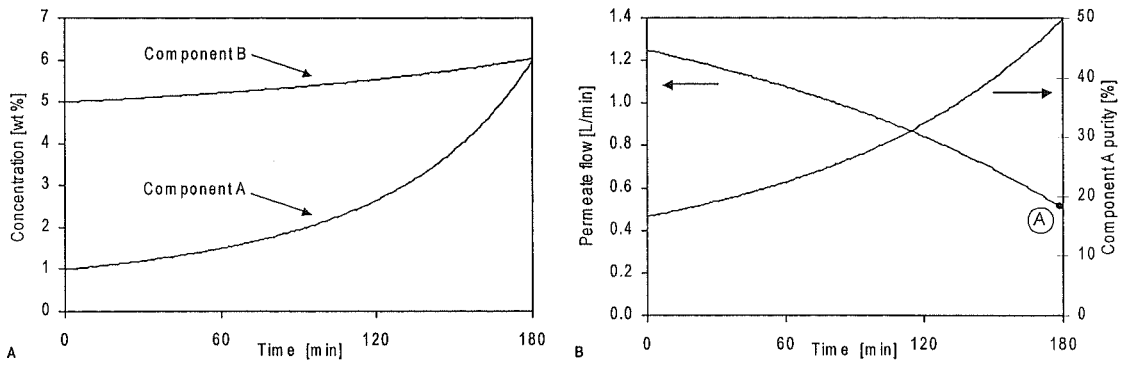

Figure 2-6 Time dependent behaviour of open-loop batch membrane plant
A simple system model was used; no membrane fouling, permeate flux dependent on the concentration of component A: Flux $J = 50(1\text{-}C_A/20)$, [L $m^{-2}hr^{-1}$]. Retention coefficients: Component A = 0.95, Component B = 0.1 Point A represents the permeate flow rate of an equivalent continuous single stage system. Retentate product specification = 12 wt %.total solids concentration.

From a process design perspective, a single batch plant has very few degrees of freedom since the feed composition, product specifications and membrane characteristics are usually fixed. This leaves only the membrane area and batch volume as significant design variables. Because the required processing time is uniquely determined by the feed, product and membrane parameters, opportunities for design optimisation are limited. However batch operations offer a high degree of flexibility since a single operation may be able to process a range of different feed stocks at various times (Douglas, 1988). In food and biological industries, individual batch operations can be difficult to integrate with other continuous processes, particularly when intermediate storage and residence times are restricted in the interests of product safety.

2.3.2 Simple continuous process flowsheets

Defined strictly, membrane plants cannot be operated as a continuous separation, unlike distillation for example, since progressive membrane fouling eliminates the possibility of steady state operation. However these plants can be operated in a batchwise-continuous manner, with production halted periodically and membranes cleaned to remove the accumulated foulants. These designs are commonly called 'continuous' flowsheets in literature, so this term will be used from now on. Continuous plants are more practical in many situations, particularly for large scale operations. Most importantly, they offer improved integration with upstream and downstream processes.

The production of a high concentration retentate product, particularly one with severe fouling or concentration polarisation, requires the use of a multipass plant design (Mulder, 1997). This configuration represents a single separation stage with the

retentate recycled past the membrane (Figure 2-7) to attain increased fractionation or retentate concentration. The flow rate around the recirculation loop may be up to ten times the flow rate of retentate leaving the loop (Cheryan, 1998).

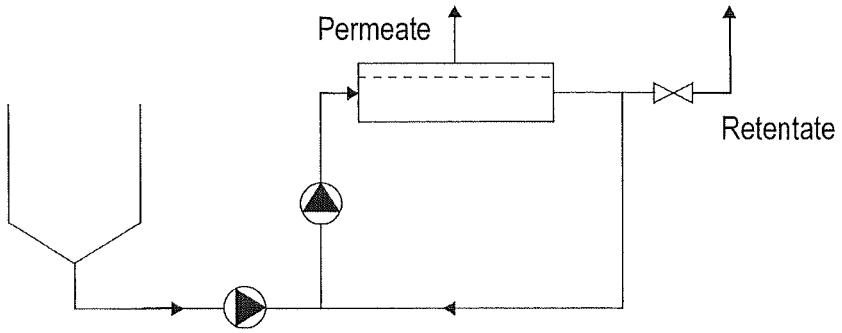

Figure 2-7 Continuous single stage plant design

However, a continuous plant such as that shown in Figure 2-7 must always operate at the required product concentration, with a correspondingly low permeate flux compared to a batch plant (represented by Point A, Figure 2-6B). The single stage process was also simulated using the same separation model and conditions as the batch process (see note under Figure 2-6). Table 2-1 shows the batch flowsheet to have twice the capacity (after 3 hours of operation) of the single stage design for an equivalent membrane area.

Table 2-1 Comparison of different separation flowsheets

Process design	Retentate TS conc. [wt %]	Component A purity [%]	Feed volume [L]	Product volume [L]
Open-loop batch	12	49.8	200.0	30.4
1 Stage continuous	12	54.4	94.4	10.2

Note: Analysis based on operating time of 3 hours, with total plant membrane area of 0.5 m^2.

Levenspiel (1972) showed that the operating efficiency of a cascaded train of small chemical reactors was superior to a single large reactor. The same is true for membrane systems, where a given area of membrane area is most efficiently utilised if split across a large number of small separation stages connected in series. This applies for both retentate and permeate product separations. Multistage designs consist of several recirculation loops connected in series (Figure 2-8) via a common baseline, into which feed is injected and where plant retentate is drawn. Feed to each stage is drawn from the baseline, pumped through the membrane housings and the retentate is returned to the baseline. Although the stages are connected via a manifold, and hence not truly in series, high recirculation flow rates mean that the flowsheet generally behaves as a

sequential arrangement of separate stages. Only the final stages operate at high concentrations so the overall permeate and component mass fluxes are greater, approaching those of a batch system.

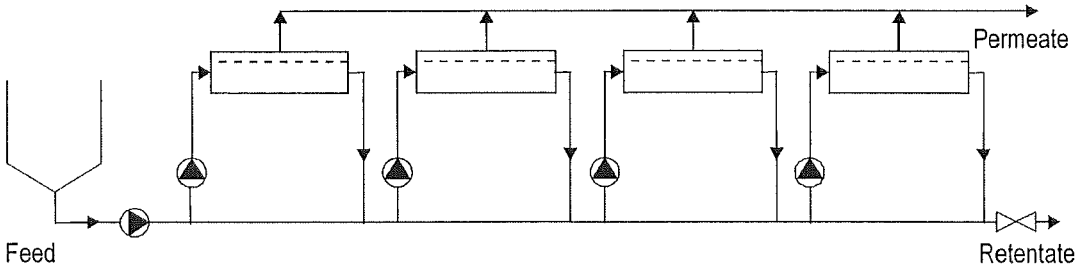

Figure 2-8 Example of a four stage plant design

Using the same separation model to simulate two and five stage process designs (Table 2-2) it is clear that operating capacity (for a given membrane area) increases with the number of stages in the flowsheet. However, even the separation with five stages cannot match the throughput of the batch plant (Table 2-1). In situations where continuous operation is required, plant designs with a large number of stages can provide significant economic advantages over equivalent single stage designs (Rautenbach & Albrecht, 1989).

Table 2-2 Performance of two multistage separation flowsheets

Process design	Retentate TS conc. [wt %]	Component A purity [%]	Feed volume [L]	Product volume [L]
2 Stage continuous	12	52.7	145.9	19.4
5 Stage continuous	12	51.1	178.2	25.7

Note: Analysis based on operating time of 3 hours, with total plant membrane area of 0.5 m^2.

A range of variables are available for optimisation during continuous flowsheet design, including the number of stages in the plant, total membrane area and its distribution through the plant. Design optimisation is often considered in terms of minimising the membrane area requirement, due to the relatively high capital cost of separation membranes. Alternate design objectives include maximising separation efficiency or mass flux, however these still result in minimum membrane area designs. Morison (1997) showed that the minimum membrane area requirement occurs as the required number of stages tends to infinity. Obviously capital and pumping costs will limit the number of stages actually used in a flowsheet, so a continuous commercial process design will never achieve the true minimum area optimum.

2.3.3 *Continuous membrane process flowsheets for 'difficult' separations*

Separation of a feedstock using membranes with low selectivity (i.e. separating components with similar permeabilities) can be achieved using a flowsheet based on a distillation analogy (Seader & Henley, 1998). A multistage column utilises reflux at top and bottom to achieve good separation. For a retentate product, membrane stages may be arranged using recycle streams in a manner much like reflux in the stripping section of a distillation column (Figure 2-9). Reflux flowsheets give enhanced purification but only achieve limited concentration of the retentate, since almost all permeate is reinjected.

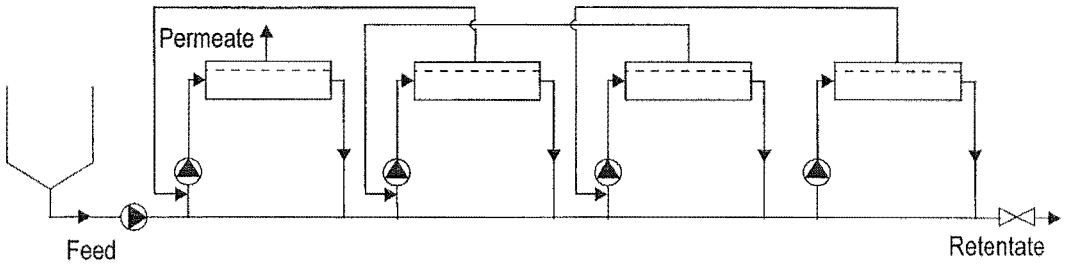

Figure 2-9 Multistage reflux plant design - retentate product

For a permeate product the flowsheet may be based on the enrichment section of a staged separation column (Figure 2-10). This flowsheet shows the feed stream to be positioned just before to the final membrane stage. Alternatively, a plant design may combine both stripping and enrichment sections for the overall design. Wankat (1990) calls this a 'fractionation' flowsheet. Design variables for these flowsheets are the same as the previous section, with the number of stages and distribution of membrane area over these of particular importance.

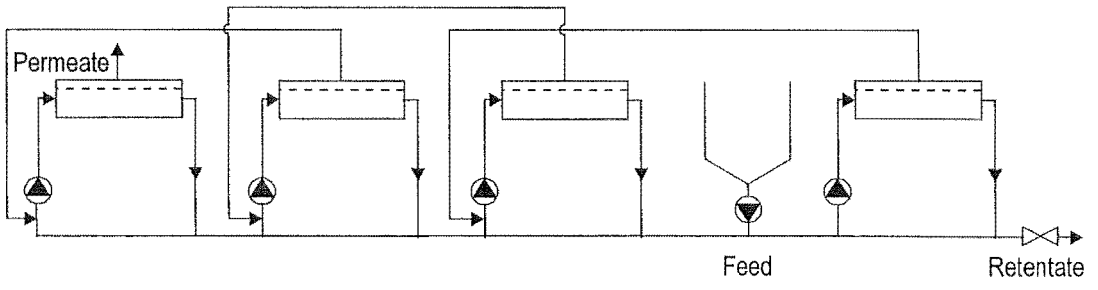

Figure 2-10 Multistage reflux plant design - permeate product

For less difficult separations, the level of reflux (reinjection of permeate) employed in the flowsheet is often excessive and the required membrane area can become prohibitive. A variation on this approach is the use of partial reflux, with a 'reflux ratio' used to represent the proportion of each permeate stream reinjected. This provides an

additional degree of freedom for flowsheet optimisation. The most widely discussed industrial application of reflux flowsheets is the enrichment of Uranium ^{235}U (Rautenbach & Albrecht, 1989). This separation is actually performed in the gas phase, but a reflux-style flowsheet design is used. It is sometimes desirable to separate food components with similar permeabilities, such as the fractionation of proteins (Grandison & Lewis, 1996). In such a situation, the large residence time of the plant (due to extensive use of recycle between stages) becomes a problem. The use of reflux flowsheets for processing food products is therefore rather restricted.

2.3.4 Membrane process flowsheets for high purity products

Attaining a particularly high retentate purity or yield of a permeable species may sometimes prove difficult. The injection of additional solvent (usually water) can improve product purity by 'flushing' or 'washing' small species through the membrane to the permeate stream. This technique, called diafiltration (DF) injection, improves permeate fluxes by lowering the retentate concentration and increasing the mass flux of permeable components across the membrane. Increased purification is achieved at the cost of reduced retentate concentration. This approach can be applied to both retentate and permeate product situations, however for a retentate product it is best suited to systems with an (almost) impermeable product, otherwise there may be significant losses of the valuable product species (Zeman & Zydney, 1996).

Diafiltration injection can be applied to both batch and continuous membrane operations. For a batch process (Figure 2-11), diafiltration injection can be by one of two modes; continuous or discontinuous addition (Cheryan, 1998). Continuous diafiltration injection is the addition of pure solvent to the feed tank during plant operation. This need not occur at all times during the batch. For example, diafiltration injection may

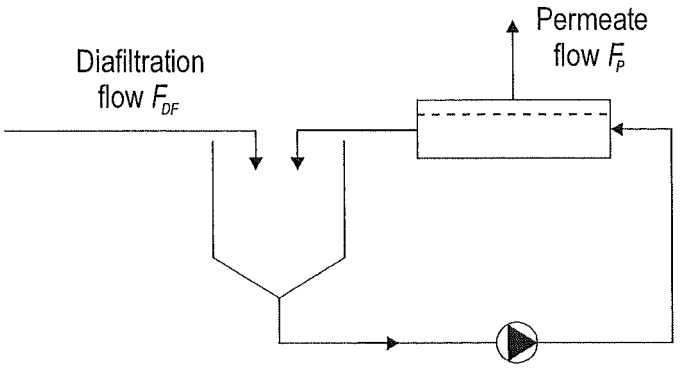

Figure 2-11 Batch flowsheet with diafiltration injection

start only after a certain amount of permeate has been removed. Discontinuous diafiltration is a two-stage process; beginning with initial feed volume V_1 the separation proceeds until the batch volume reduces to some amount V_2. At this point a volume of diafiltration solvent is quickly added to the feed tank and processing will then continue until the retentate volume has returned to the desired value (V_2). This sequence may be repeated a number of times until the desired retentate purity or permeate yield has been achieved. Discontinuous diafiltration is more efficient than the continuous method, taking less time and producing smaller volumes of permeate (Tutanjian, 1985; Asbi & Cheryan, 1992). By providing more degrees of freedom, diafiltration injection provides greater opportunity for flowsheet and scheduling optimisation.

For a continuous process, the flow rate of diafiltration water F_{DF} injected into a stage can be specified as a fraction of the permeate flow rate F_P. This is expressed as the diafiltration ratio ϕ, which must be positive, and usually lies within the range of zero (no diafiltration) to one ('constant volume' diafiltration). Diafiltration injection can be applied to both single and multistage plant designs (Figure 2-12), with different diafiltration ratios possible for each stage. The diafiltration ratio of the i^{th} separation stage is calculated as:

$$\phi_i = \frac{F_{DF,i}}{F_{P,i}} \qquad \textbf{(2-1)}$$

Merry (1996) calls this technique 'cross-current diafiltration'. Generally diafiltration is only applied to the final few stages in a plant where retentate concentrations are higher and washing efficiency is greater. Beaton & Klinkowski (1983) and Grandison & Lewis (1996) present an extensive analysis of the effect of diafiltration on plant performance, but they only consider 'constant volume' diafiltration, where the rate of solvent addition matches the permeate flow (i.e. $\phi_i = 1.0$).

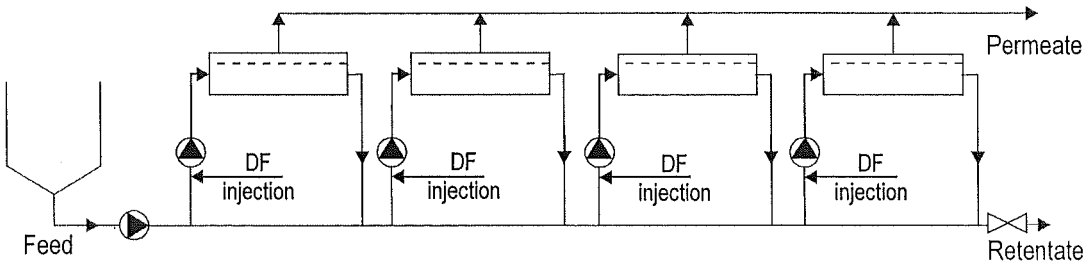

Figure 2-12 Multistage process flowsheet with diafiltration injection

Design optimisation of continuous membrane designs using diafiltration injection involves selecting the number of stages in a plant, as well as specifying the membrane area distribution and diafiltration ratios for all stages. Given that a large commercial membrane separation plant may have 15 stages or more (Morison, 1997), this poses a large and complex design optimisation.

2.3.5 Specialised solvent recovery flowsheets

A specific flowsheet exists for the recovery of solvent from a feed stream. This design is still a crossflow configuration, but does not recirculate the retentate (Figure 2-13). High permeate fluxes and short residence times are achieved by this 'single-pass' design (Merry, 1996), with high crossflow velocities maintained by tapering the plant. The flowsheet suits desalination operations (Gutman, 1987) where disposal of the retentate is not a problem. Such a design is not suited to standard permeate product separations, since the yield of permeate species is very low.

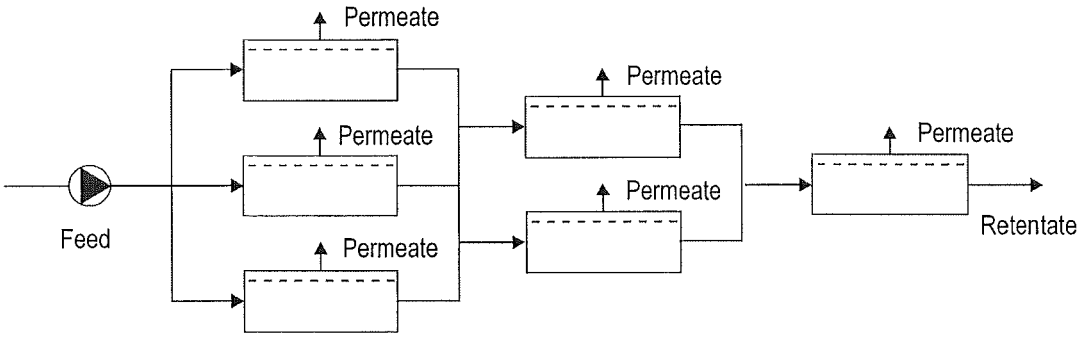

Figure 2-13 Continuous single pass (tapered) plant design

2.4 Constraints on process operation for the separation of biological feedstocks

Single-phase membrane separations are well suited to heat-labile components such as enzymic, biochemical and food products, but processing these materials is often subject to significant operating constraints. Of particular concern is the growth of undesirable and potentially dangerous microbial contaminants. Since the risk of microbial growth and product contamination increases with time, it is strongly desirable to minimise residence time both within the plant and intermediate storage between unit operations. In large food industries, continuous processing is strongly preferred over batch operations since it offers superior integration with upstream and downstream processes, and shorter residence times. Intermediate storage can be further reduced by operating all

units in a process at constant throughput. This is possible with membrane separations, but has some impact on flowsheet design.

Production capacity of membrane plants is primarily controlled by the permeate flux. Volumes of literature have been written on methods to maximise permeate flux, but in an integrated plant it is necessary to regulate rather than maximise flux. Permeate flux is dependent on the trans-membrane pressure (Figure 2-14) and increasing this will, up to a point, increase the permeate flux (Zeman & Zydney, 1996). At higher pressures, mass transfer effects (concentration polarisation) become dominant. For separation with little fouling, manipulation of the trans-membrane pressure can reduce variation in the permeate fluxes and plant feed flow rate. For heavily fouling separations a constant plant throughput is best maintained by varying the number of stages operating at any time. In this strategy only a small number of stages in the plant are used initially, with additional membrane area added as necessary, and trans-membrane pressure usually manipulated at the same time to maintain a constant feed flow rate.

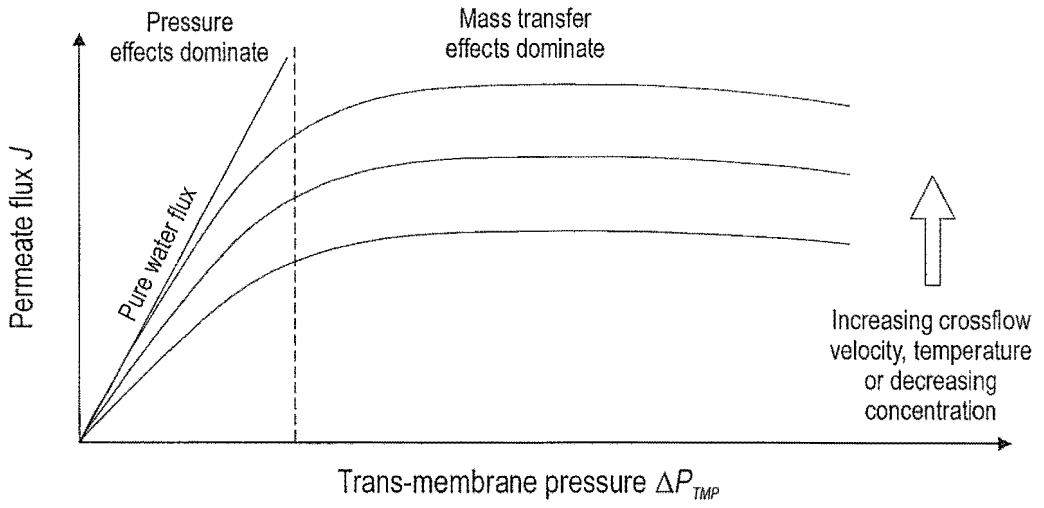

Figure 2-14 Schematic of permeate flux - pressure relationship

For a biological separation the maximum operating time of a plant may actually be limited by food safety requirements rather than membrane fouling effects. For food-grade products it is likely that processing times will be restricted to a matter of hours, rather than days as is possible for electropaint ultrafiltration separations (Cheryan, 1998). At the end of production, the plant will be chemically cleaned and sanitised to reduce levels of biological activity within the plant and product.

2.5 Case study scenarios

The dynamic characteristics and closed-loop performance of two case studies are examined in later chapters. Of particular interest in this thesis are the dynamic characteristics of large scale membrane separation plants achieving high levels of fractionation. Design scenarios for each case study are discussed in Sections 2.5.1 and 2.5.2, with a proposed plant design presented in Section 2.6. One separation produces a retentate and the other a permeate product, and so they are subject to different product specifications. Both are biological separations and subject to operating constraints, imposed in the interests of product safety.

2.5.1 Case study 1: Whey protein concentrate production

Industrial scale purification of whey protein via ultrafiltration is well understood, and discussed in many publications including Cheryan (1998) and Hobman (1992). WPC plants process dilute whey streams, a by-product of casein or cheese production. Ultrafiltration membranes are used to produce a concentrated and partially purified retentate product. An optimal process flowsheet is therefore a compromise between fractionation and concentration design objectives. Typically the feed stream contains low concentrations of lactose, lactic acid, whey protein, non-protein nitrogen (NPN), fat and minerals (Hickey *et al.*, 1980; Bylund, 1995). The composition of whey produced by a casein plant and used in this case study is presented in Table 2-3. Fat and whey protein are (essentially) completely impermeable whilst lactose, lactic acid, NPN and minerals are only partially retained by an ultrafiltration membrane.

Table 2-3 Whey composition - case study 1

Feed stream composition	Protein = 0.56 wt %
	NPN = 0.19 wt %
	Lactose = 4.89 wt %
	Lactic acid = 0.05 wt %
	Minerals = 0.78 wt %
	Fat = 0.04 wt %

Membrane separation is only one part of the WPC process, and must be integrated with the casein plant upstream, and an evaporator and spray drier downstream (Figure 2-15). Typically, the value of the powder product is related to its purity, so a high degree of fractionation is usually desired. In a large scale operation the permeate contains significant quantities of lactose which may be concentrated, purified and dried in a

separate downstream process. This case study represents only part of the complete design scenario for the WPC plant.

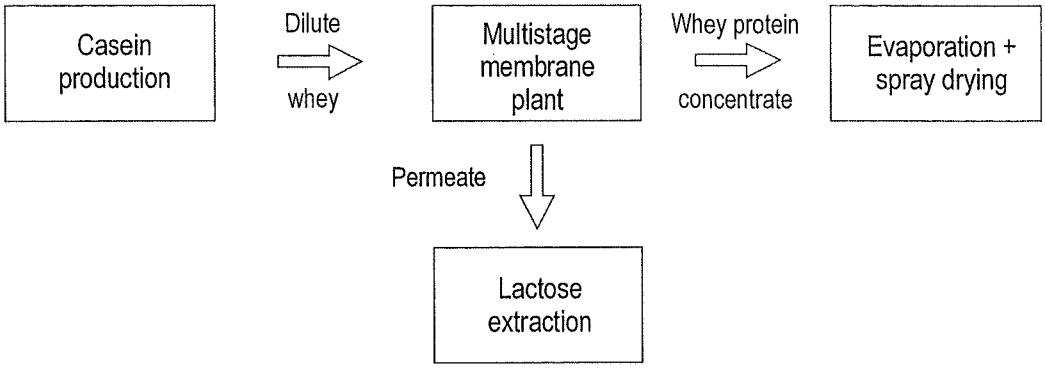

Figure 2-15 Schematic of WPC production flowsheet

Primary design specifications for this membrane separation are presented in Table 2-4. A desired dry basis protein purity of 85 wt % means that 85 % of the mass of total solids in the retentate stream must be protein. The required retentate concentration would usually be influenced by the preliminary evaporator design. It is desirable for the plant to be capable of producing a range of product purities from the same feedstock. Since downstream operations only involve dewatering, product final composition is determined by the membrane plant.

Table 2-4 Design specifications - case study 1

Processing capacity	1 250 000 L day^{-1}
Retentate protein purity	60 - 85 wt % dry basis
Retentate concentration	27 wt % total solids

Food safety requirements place additional constraints on how the plant can be operated. It is desirable to operate the plant continuously and at constant capacity so that it can easily be integrated with upstream and downstream operations (Figure 2-15). The maximum continuous processing time is restricted by hygiene requirements, after which production ceases and the plant is chemically cleaned. In this case study it is assumed that the maximum continuous operating time is nine hours, followed by three hours cleaning. Two production runs are possible daily.

2.5.2 Case study 2: Permeate product separation

Two food-grade components are separated in this case study; a valuable species (Component B) which is partially permeable, is recovered from an unwanted impermeable

species (Component A). Both components are present in the feed stream in equal concentrations (Table 2-5). Commercial examples of permeate product situations include protein fractionation using ultrafiltration (Grandison & Lewis, 1996) and recovery of pharmaceuticals from fermentation broths (Scott, 1995).

Table 2-5 Feed stream composition - case study 2

Component A	1.2 wt %
Component B	1.2 wt %

Like the first case study, this separation will also use ultrafiltration membranes. It is desirable to recover as much of the valuable component from the retentate stream as practical, hence a design optimisation would usually focus on maximising retentate fractionation in order to achieve the desired permeate yield. Diafiltration injection will be necessary to enhance recovery of the permeable component, but will decrease the overall concentration of the permeate stream, placing increased load on dewatering processes downstream (Figure 2-16).

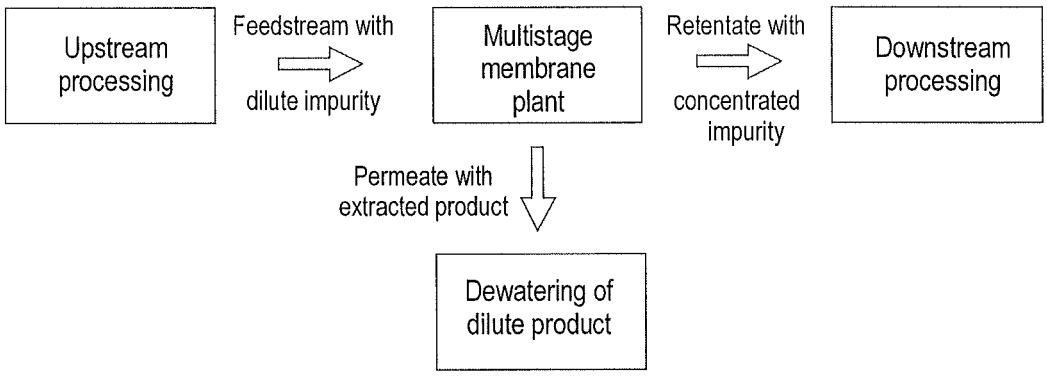

Figure 2-16 Schematic of permeate product flowsheet

Unlike the WPC case study, only two main design specifications exist (Table 2-6); desired yield of valuable Component B, and required operating capacity. No requirements are set for the overall concentration of the permeate stream. Degree of freedom analysis (Seider *et al.*, 1999) shows that such a constraint would result in an over-specified design problem for which no solutions exist. Product safety constraints require that the plant be operated continuously and with constant throughput. Maximum continuous processing time is limited to nine hours before chemical cleaning is necessary (three hours), allowing two production runs per day.

Table 2-6 Design specifications - case study 2

Processing capacity	970 000 L day^{-1}
Desired recovery of Component B	75 wt %

2.6 Design solution for case study analysis

The intention of this thesis is to analyse the dynamic behaviour of multistage membrane processes and investigate methods of improving plant control. Rigorous process design falls outside the scope of this work, but decisions made during the selection of flow-sheets and operating conditions can have considerable impact on process controllability. It is also important to realise that both case studies are part of a larger design problem, and cannot be considered independently of downstream processes. Indeed, membrane plant design is usually only one part of a larger design optimisation. Identifying the factors that cause poor plant controllability is particularly important, otherwise a global design optimisation may produce a membrane plant design which operates in a region of very poor dynamic behaviour.

The development of a complete membrane plant design requires extensive information such as membrane fouling characteristics, retentate viscosities and retention coefficients. Such information was not given in Sections 2.5.1 and 2.5.2 since it was intended that these sections provide only a general overview of each case study without becoming distracted by the large amount of information required for a rigorous plant design. For a detailed review of design methods, the work of She (1998) is recommended. A single membrane plant design will be used for both case studies for simplicity, based loosely on commercial WPC plants operating in New Zealand. Details of this design are presented in Table 2-7. The use of a single plant also allows comparisons to be made in later chapters between the behaviour of the two case studies. Permeate flux and retentate coefficient models are presented for each case study in Chapter 3, and closed-loop plant behaviour is simulated in Chapter 6. In certain situations the required total processing capacity may not be achieved, i.e. the desired feed flow rate may be possible but cannot be maintained for the required duration. This is not considered to be a significant problem in the context of this work, since it is the general dynamic behaviour of the process which is of interest.

Table 2-7 Final design specifications of case study plant

Stage	Membrane area [m^2]	Stage volume [m^3]
1	285	0.18
2	285	0.18
3	285	0.17
4	285	0.17
5	285	0.18
6	285	0.18
7	285	0.17
8	285	0.17
9	230	0.16
10	215	0.16
11	215	0.16
12	168	0.16
13	178	0.16
14	178	0.15
15	134	0.14
16	59	0.12

In the permeate flux models presented in the next chapter, membrane fouling effects are significant. For this reason the plant feed flow rate is controlled by manipulating the feed pressure in conjunction with the addition of membrane area. Because trans-membrane pressure is dependent on the plant feed pressure (Equation 3-30), varying the feed pressure of a plant is equivalent to manipulating the trans-membrane pressure and hence permeate flux (provided the plant is not operating in the mass-transfer controlled region of the flux-pressure curve, Figure 2-14). Plant feed pressure is manipulated either using a variable-speed controller on the pump motor or a valve on the pump outlet. The position of this pump on the baseline, between the balance tank and first stage, is shown in Figure 2-8. Manipulation of the plant feed pressure is a technique which is commonly employed in large, modern plants in New Zealand.

2.7 Conclusion

A brief outline of the different membrane types was presented in this chapter, along with an overview of several separation flowsheets, each offering advantages in certain situations. Details of the case studies were presented, along with the operating constraints imposed by the products being a foodstuff. Rigorous plant design methods are outside the scope of this work so a single process flowsheet was chosen for use with

both case studies, based on WPC plant designs used commercially in New Zealand. In later chapters the impact of flowsheet design and operating methods on plant behaviour will be considered, and the flowsheets presented in this chapter will be revisited.

2.8 References

Asbi B A & Cheryan M (1992), Optimizing process time for ultrafiltration and diafiltration, *Desalination,* **86**, 49-62.

Beaton N C & Klinkowshi p R (1983), Industrial ultrafiltration design and application of diafiltration process, *Journal of Separation Process Technology,* **4**, (2), 1-10.

Bennett R J (1997), Membrane applications in the New Zealand dairy industry, *Dairy Technology,* **11**, (1), 8-10.

Bowen R (1993), Understanding flux patterns in membrane processing of protein solutions and suspensions, *Trends in Biotechnology,* **11**, 451-460.

Bylund G (1995), *Dairy Processing Handbook,* Tetra Pak Processing Systems, Lund, Sweden.

Cheryan M (1998), *Ultrafiltration and Microfiltration Handbook,* 2nd Ed., Technomic Publishing Co., Lancaster, USA.

Douglas J M (1999), *Conceptual Design of Chemical Processes,* McGraw-Hill International, Singapore.

Fane A G & Fell C J D (1987), A review of fouling and fouling control in ultrafiltration, *Desalination,* **62**, 117-136.

Field R (1996), Fundamentals of transport in dense membranes. *Proceedings of Application of Membrane Technologies,* pp. 2.1-2.8, The University of Auckland, New Zealand.

Grandison A S & Lewis M J (1996), *Separation Processes in the Food and Biotechnological Industries: Principles and Applications,* Woodhead Publishing Ltd, Cambridge, England.

Gutman R G (1987), *Membrane Filtration: The Technology of Pressure-driven Cross-flow Processes,* Adam Higler, Bristol.

Hickey M W, Hill R D & Smith B R (1980), Investigations into the ultrafiltration and reverse osmosis of wheys 1. The effects of certain pretreatments, *New Zealand Journal of Dairy Science and Technology,* **15**, 109-121.

Hobman P G (1992), Ultrafiltration and manufacture of WPC. In *Whey and Lactose Processing* (Ed. Zadow J G), pp. 489, Elsevier Applied Science, Great Britain.

Howell J A (1990), Overview of membranes. In *The Membrane Alternative; Energy Implications for Industry* (Ed. Howell J A), Watt Committee on Energy, Report 21 pp. 1-8, Elsevier Applied Science, Oxford, England.

Humphrey J L & Keller G E (1997), *Separation Process Technology,* McGraw Hill, USA.

Le M S & Howell J A (1985), Ultrafiltration. In *Comprehensive Biotechnology: the Principles, Applications and Regulations of Biotechnology in Industry, Agriculture and Medicine* (Ed. Cooney C L & Humphrey A E), Vol 2, pp. 383-408, Pergamon Press, England.

Levenspiel N (1972), *Chemical Reaction Engineering,* 2nd Ed., John Wiley & Sons, Singapore.

Marshall A D, Munro P A & Tragardh G (1993), The effect of protein fouling in microfiltration and ultrafiltration on permeate flux, protein retention and selectivity: a literature review, *Desalination,* **91**, 65-108.

McCabe W L, Smith J C & Harriott P (1993), *Unit Operations of Chemical Engineering,* 5th Ed., McGraw-Hill Inc., USA.

Merry A J (1996), Membrane equipment and plant design. In *Industrial Membrane Separation Technology* (Ed. Scott K & Hughes R), pp. 32-66, Blackie Academic & Professional, Glasgow.

Morison K R (1997), Developing a design methodology for ultrafiltration plants. *CHEMECA 97,* pp. PD4e:1-PD4e:11, Rotorua, New Zealand.

Mulder M (1997), *Basic Principles of Membrane Technology,* 2nd Ed., Kluwer Academic Publishers, The Netherlands.

Rao H G R, Grandison A S & Lewis M J (1994), Flux pattern and fouling of membranes during ultrafiltration of some dairy products, *J. Sci. Food Agric.,* **66**, 563-571.

Rautenbach R & Albrecht R (1989), *Membrane Processes,* John Wiley & Sons, New York.

Scott K (1995), *Handbook of Industrial Membranes,* 1st Ed., Elsevier Science Publishers, Oxford, UK.

Seader J D & Henley E J (1998), *Separation Process Principles,* John Wiley & Sons.

Seider W D, Seader J D & Lewin D R (1999), *Process Design Principles: Synthesis, Analysis and Evaluation,* John Wiley and Sons, Inc, USA.

She X (1998), *Design and Optimisation of Multistage Ultrafiltration Plants.* M.E. Thesis, Department of Chemical and Process Engineering, University of Canterbury, New Zealand.

Tutanjian R S (1985), Ultrafiltration processes in biotechnology. In *Comprehensive Biotechnology: The Principles, Applications and Regulations of Biotechnology in Industry, Agriculture and Medicine* (Ed. Moo-Young M), pp. 411-438, Pergamon Press, Great Britian.

Wagner J (1996), *Membrane Filtration Handbook,* Wagner Publishing, Denmark.

Wankat P C (1990), *Rate-controlled Separations,* Elsevier Science Publishers, Essex, England.

Winchester J (1996), *Computer Simulation and Controllability Studies of Multi-module Ultrafiltration Plants.* M.E. Thesis, Department of Chemical and Process Engineering, University of Canterbury, New Zealand.

Zeman L J & Zydney A L (1996), *Microfiltration and Ultrafiltration: Principles and Applications,* Marcel Dekker, New York.

3 Modelling The Behaviour Of Membrane Processes

The design specifications of a multistage membrane plant were presented in the previous chapter. From these a dynamic process model can be developed for each case study, representing all of the main process characteristics. This chapter reviews published membrane plant models, and details the development of a general process model which can describe any multistage membrane flowsheet configuration. Specific models are then developed for each case study, for use in later chapters. Implementation details are discussed, and simulated open-loop process behaviour is presented for both case studies.

3.1 Methods of describing a process

To successfully design a process flowsheet and carry out all equipment sizing, some representation or model of the operation is needed. Himmelblau & Bischoff (1968) define three types of process models:

1) *Empirical* - a mathematical equation fitted to physical data
2) *Population balance* - residence time distribution models and other population age distributions
3) *Transport phenomena* - continuum equations describing the conservation of mass, momentum and energy

Empirical models have been widely used in engineering, particularly before the availability of computers. Early design methods for distillation separations often used a series of empirical relationships for equipment design and sizing (Rose, 1985). However each empirical model only applies to a specified range of conditions and so can be quite limiting, particularly for new or novel operations. Population balance models are best suited to predicting characteristics such as residence time distributions. Because of this, they are limited to specialised applications such as reactor design.

Transport phenomena models are most widely used for flowsheet development and equipment sizing, particularly since the widespread availability of computers which have simplified the solution of numerical models. These transport phenomena models are further divided into five sub-groups by Himmelblau & Bischoff (1968):

1) *Molecular and atomic* - used in quantum mechanics and kinetic theory to predict distribution functions and collision integrals
2) *Microscopic* - used in laminar and turbulent transport theories to predict phenomenological coefficients such as viscosity and thermal conduction
3) *Multiple gradient* - used in transport theory for porous media, to predict 'effective' transport coefficients
4) *Maximum gradient* - used in reaction theory to predict kinetic constants
5) *Macroscopic* - widely used in process engineering and design to predict friction factors, 'overall' kinetic constants and transport coefficients

Molecular, microscopic, multiple and maximum gradient models are all distributed parameter systems, which use partial differential equations to describe spatial gradients within a subsystem or process. Macroscopic models are lumped parameter methods which use ordinary differential equations to represent concentrations or temperatures as single values averaged over the volume of the subsystem or unit operation. Lee *et al.* (1998) uses the term 'model fidelity' to represent the desired accuracy of a process model. A model with high fidelity will have greater complexity, but will more closely represent the actual behaviour or characteristics of a system. The challenge when developing a process model, is to select a level of model fidelity which is consistent with both the intended use of the model and the available data.

3.2 Review of published membrane plant models

At this point it would be usual to present a thorough review and critique of all dynamic process models that have been published for membrane operations. Unfortunately, very little literature presents a complete theoretical process model suitable for simulation and dynamic analysis of large-scale multistage flowsheets. The general concepts and characteristics of membrane separations have been discussed in many publications (see references quoted in Section 2.1), along with a wide range of permeate flux and fouling models which describe observed phenomena. However these generally strive to explain only what occurs at the membrane surface on a microscopic level. In this work, it is the macroscopic behaviour of the separation that is of interest, in particular the open- and closed-loop dynamic characteristics of the process. The desired plant model must therefore combine a macroscopic equation set describing system response dynamics,

with microscopic models predicting phenomena at the membrane surface (permeate fluxes and retentate fractionation).

van Boxtel (1994) published a simple multistage dynamic model of an reverse osmosis plant, using a permeate flux which accounted for membrane fouling. However the method of modelling the concentration dynamics of each stage was not explained. No results were given showing (modelled) real-time plant behaviour. A dynamic membrane plant model was published by Niemi & Palosaari (1994) which calculated the concentration profile and associated permeate flux at internals along each membrane in a stage, and at different points around the recirculation loop. Concentrations were calculated by the iterative solution of the equation set for each stage in sequence, repeated at each time step of the simulation. Unfortunately, this model did not fully represent microscopic phenomena occurring at the membrane, since it requires the assumption of equal permeate flow rate from each stage. For this work, it is desirable to avoid such gross assumptions. This could be achieved by adopting the same macroscopic model framework, then implementing a complete set of suitable microscopic models to describe events occurring at the membrane surface. However the distributed parameter structure of such a model does not accommodate the application of dynamic analysis tools in the frequency or state space domains. Given the importance of these tools for analysing process behaviour, it is therefore desirable to instead develop a lumped parameter model, which is compatible with frequency and state space domain theory.

3.3 Generating an equation set for a membrane separation stage

The development of a plant model is often simplified by decomposing the process into a number of parts and examining each separately (Morari *et al.*, 1980). It is logical to cleave any multi-stage operation into single stages, model these individually, and then combine the stages to represent the complete process flowsheet. To develop a lumped parameter model, it is necessary to assume that a separation stage with constant volume and high crossflow velocity (i.e. recirculation rate) is sufficiently well mixed that it has the same concentration at all points within the recirculation loop. Cheryan (1998) states that the recirculation velocity within a separation stage may be up to ten times that of the retentate stream.

A single recirculation loop is shown schematically in Figure 3-1A, with the dashed line representing the process boundary. In a lumped parameter model this may be represented as shown in Figure 3-1B. Although there are usually several components in a feed stream, only one is represented here for simplicity. For convenience, flows are expressed on a volume basis, and concentrations are weight percent.

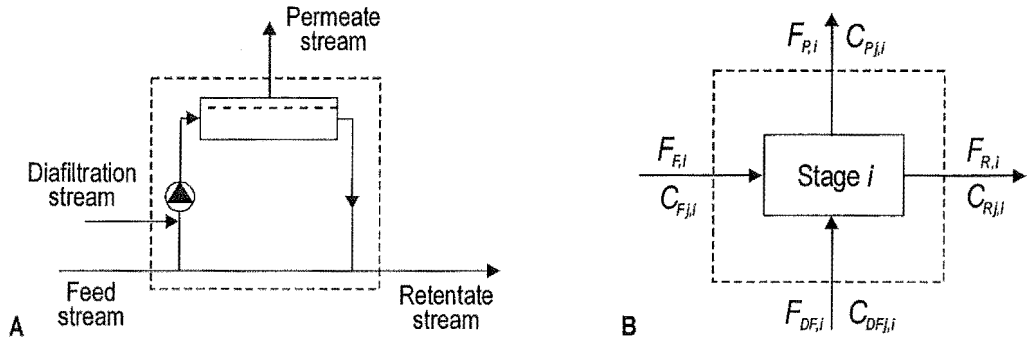

Figure 3-1 Schematic representations of a separation stage

When operating at steady state, the balance for component j over stage i can be stated algebraically:

$$\rho_{F,i}F_{F,i}\frac{C_{Fj,i}}{100} + \rho_{DF,i}F_{DF,i}\frac{C_{DFj,i}}{100} = \rho_{P,i}F_{P,i}\frac{C_{Pj,i}}{100} + \rho_{R,i}F_{R,i}\frac{C_{Rj,i}}{100} \qquad (3\text{-}1)$$

where the feed, diafiltration, permeate and retentate flow rates for stage i are given by $F_{F,i}$, $F_{DF,i}$, $F_{P,i}$ and $F_{R,i}$ respectively. Stream densities are denoted ρ [kg m^{-3}] and subscripted in the same manner. Component j mass fractions in the feed, diafiltration, permeate and retentate streams are given by $C_{Fj,i}/100$, $C_{DFj,i}/100$, $C_{Pj,i}/100$ and $C_{Rj,i}/100$ respectively. For convenience, the mass fractions have been multiplied by 100 in later equations.

However it is known that membrane systems do not operate at steady state (Wankat, 1990), hence a differential component balance is required to describe changes in the concentration of component j within a stage. An ordinary differential equation is used since the concentration is assumed to be uniform throughout the stage:

$$\frac{d\left(\rho_{R,i}V_iC_{Rj,i}\right)}{dt} = \rho_{F,i}F_{F,i}C_{Fj,i} + \rho_{DF,i}F_{DF,i}C_{DFj,i} - \rho_{P,i}F_{P,i}C_{Pj,i} - \rho_{R,i}F_{R,i}C_{Rj,i} \qquad (3\text{-}2)$$

where V_i is the stage volume [m^3]. At this point, a general non-linear equation describing changes in component concentration has been developed. For a process stream with j components in solution, a set of j differential equations is required to completely

model the separation stage. The solvent concentration can be calculated by difference from the remaining component concentrations, hence a differential model is not necessary (Morison, 1997). A complete process flowsheet can be constructed by combining the equation sets representing each separation stage.

To develop a complete system model, all parameters must either be specified as manipulated inputs or explicitly calculated. Ramirez (1997) states "*the major difference between a simulation study and a design study is the type of variables that are specified*". The purpose here is to develop a dynamic simulation of a membrane process, hence all input variables and equipment parameters must be specified. For each stage, the specified input variables are the component concentrations in the diafiltration and feed streams, along with the diafiltration and feed (or retentate) flow rates. The remaining variables must be specified algebraically.

For the i^{th} separation stage with constant volume V_i, processing a liquid at a constant temperature, the system flow rates can be calculated by simple volume balance:

$$F_{F,i} + F_{DF,i} = F_{P,i} + F_{R,i} \tag{3-3}$$

Depending on the flowsheet, either the feed or retentate flow rate of the plant will be a manipulated variable.

It is common for both the permeate flux relationship and retention coefficients to be determined experimentally, since the main design constraints of product composition and processing capacity are heavily dependent on these terms. For the purposes of constructing a dynamic process model, either empirical or phenomenological representations of flux and retention coefficients can be used. The choice is clearly a compromise between accuracy and complexity with the best selection dependant on the purpose of the model. If it is desired to extend the model beyond experimental data, a phenomenological model is needed. However, if the model needs only to exhibit behaviour characteristic of a plant operating within the limits of the current data then a simple empirical model may suffice.

3.3.1 Prediction of permeate stream compositions

The ability of a species to permeate through a membrane is dependent on the molecular size and shape of the component, characteristics of the membrane (usually expressed in

terms of MWCO) and sometimes the valency of the component. For a specific component and membrane, the ability of component j to diffuse through the membrane is defined by the observed retention coefficient (de Rham & Chanton, 1986; Pradanos *et al.*, 1994):

$$R_j = 1 - \frac{C_{Pj}}{C_{Rj}} \tag{3-4}$$

The true retention coefficient has been used for microscopic models (Cheryan, 1998) but is not useful for the dynamic plant model being developed here. The retention coefficient R_j need not be constant; it may be dependent on the concentration of a retained component. Fouling causes the effective pore size of the membrane to change, hence so too does the retention of the membrane. Therefore the observed retention coefficient is actually a time-variant function:

$$R_{j,i} = f\left(C_{R\,foul,i}, t\right) \tag{3-5}$$

where $C_{R\,foul,i}$ is the sum of concentrations of retained components that affect diffusion across the membrane in stage i. This situation is best described by a microscopic model which accounts for binding of molecules to the membrane and pore constriction, but a simple time-invariant empirical model often suffices:

$$R_{j,i} = a_j + b_j C_{R\,foul,i} \tag{3-6}$$

where a_j and b_j are fitting coefficients, and concentrations are on weight percent basis. The retention coefficient model presented in Equation 3-6 is used in this thesis to predict permeate stream compositions in the two case studies.

3.3.2 Prediction of permeate flux

For stage i, the permeate flow rate $F_{P,i}$ can be calculated from the membrane area A_i and permeate flux J_i:

$$F_{P,i} = A_i J_i \tag{3-7}$$

Accurate prediction of permeate flux is difficult since it is a complex time-variant function dependent on both operating and membrane characteristics. For any given membrane design, the factors affecting permeate flux and fouling are numerous:

$$J_i = f\left(\mu_{R,i}, \mu_{P,i}, \Delta P_{TMP}, u_i, \Delta\pi_i, C_{R\,foul,i}, t\right) \tag{3-8}$$

where:

$\mu_{R,i}$ = retentate dynamic viscosity [Pa.s]

$\mu_{P,i}$ = permeate dynamic viscosity [Pa.s]

ΔP_{TMP} = trans-membrane pressure driving force [Pa]

u_i = retentate crossflow velocity [m s^{-1}]

$\Delta\pi_i$ = osmotic pressure difference across membrane [Pa]

t = operating time [sec]

Several phenomenological models have been proposed to predict permeate flux (Rautenbach & Albrecht, 1989), likewise empirical relations also exist for specific sets of operating conditions (Kuo & Cheryan, 1983; Rao *et al.*, 1994; She, 1998a). A definitive review of flux modelling is beyond the scope of this work. The aim of this thesis is to examine the dynamic characteristics of multistage membrane plants. Numerical controllability assessment and closed-loop simulation of the case studies requires a permeate flux model which exhibits behaviour representative of a physical separation process. Winchester (1996a) developed a permeate flux model for ultrafiltration separations. Subsequent industrial trials (unpublished) validated the characteristics of the permeate flux model. For this reason, the same model is utilised in this work, to produce a complete process model suitable for dynamic analysis. The intention of this work is not to develop a rigorous process model, but rather to produce a representation that exhibits appropriate dynamic characteristics (e.g. fouling, dependence on concentration and trans-membrane pressure). Provided this is achieved, the exact form of the model is of little importance. The development of this model is outlined in the remainder of this section.

The relationship between trans-membrane pressure and permeate flux was shown in Figure 2-14 to be complex, showing two regions of dissimilar behaviour. When operating at a high trans-membrane pressure, mass transfer effects are dominant, and a simple mass transfer model may suitably predict the permeate flux (Le & Howell, 1985):

$$J_i = J_{mt} = K_m \ln\left(\frac{C_{W\,foul,i} - C_{P\,foul,i}}{C_{R\,foul,i} - C_{P\,foul,i}}\right) \qquad \textbf{(3-9)}$$

where:

J_{mt} = mass transfer permeate flux [m s^{-1}]

K_m = mass transfer coefficient [m s^{-1}]

$C_{W\,foul,i}$ = concentration of limiting species at membrane wall [kg kg^{-1}]

$C_{P\,foul,i}$ = concentration of limiting species in permeate stream [kg kg^{-1}]

However to implement this model the mass transfer coefficient and wall concentration of the limiting components must be estimated. The wall concentration $C_{W\,foul,i}$ represents the component concentration in the concentration-polarisation boundary layer at the membrane surface. Unfortunately, estimation of this concentration is extremely difficult, so the term is usually replaced with C_{gel}, a limiting bulk concentration above which there is no permeation:

$$J_i = K_{m,i} \ln\left(\frac{C_{gel} - C_{P\,foul,i}}{C_{R\,foul,i} - C_{P\,foul,i}}\right) \quad \textbf{(3-10)}$$

Equation 3-10 is called the gel-concentration flux model and is empirical, since $C_{gel,i}$ is essentially an arbitrary fitting coefficient that is manipulated in accordance with experimental data (Winchester, 1996a). When retained components limit the permeate flux and permeate concentrations are low Equation 3-10 can be simplified:

$$J_i = K_{m,i} \ln\left(\frac{C_{gel}}{C_{R\,foul,i}}\right) \quad \textbf{(3-11)}$$

The mass transfer coefficient K_m is generally not constant since fouling of the membrane reduces the permeate flux making it some complex function of time and component concentrations:

$$K_{m,i} = f\left(C_{R\,foul,i}, t\right) \quad \textbf{(3-12)}$$

A number of extensions to this model exist, but are not examined here.

It may instead be possible to model the complete relationship between trans-membrane pressure and permeate flux (Figure 2-14) by using a phenomenological model. One widely presented model is expressed in terms of a resistance analogy (Yeh & Cheng, 1993). If a semi-permeable membrane is considered as a porous media then permeation through this body can be described by Darcy's Law (Cussler, 1984):

$$J_i = \frac{\Delta P_{TMP}\, L_{P,i}}{\mu_{P,i}} \quad \textbf{(3-13)}$$

where

$L_{P,i}$ = membrane permeability [m]

If the overall resistance R across a membrane is considered to be inverse of its permeability, then the flux resistance model can be expressed as:

$$J_i = \frac{\Delta P_{TMP}}{\mu_{P,i} R_i} \tag{3-14}$$

where

R_i = overall resistance across membrane [m^{-1}]

It is known from diffusion theory that an osmotic pressure is exerted in the direction from high to low concentration. Osmotic pressure gradients favour diffusion in the opposite direction to permeate flux, hence the driving pressure for the separation is the difference between the trans-membrane pressure ΔP_{TMP} and the opposing osmotic pressure $\Delta \pi_i$:

$$J_i = \frac{\Delta P_{TMP} - \Delta \pi_i}{\mu_{P,i} R_i} \tag{3-15}$$

Osmotic pressures are higher for smaller components such as ionic species, and are particularly significant for NF and RO separations.

The overall resistance R_i is commonly expressed as the sum of three separate terms; the inherent flux resistance of the membrane R_m, concentration polarisation (mass transfer) resistance at the membrane surface $R_{p,i}$, and fouling resistance $R_{f,i}$.

$$J_i = \frac{\Delta P_{TMP} - \Delta \pi_i}{\mu_{P,i}\left(R_m + R_{p,i} + R_{f,i}\right)} \tag{3-16}$$

This form of the resistance model is widely presented, although Gekas *et al.* (1993) argue that it is incorrect to include osmotic pressure in Equation 3-16 when is it already included in the polarisation resistance $R_{p,i}$. In this work osmotic pressure effects were assumed negligible since only large components were retained and concentration gradients of ionic species across the membrane were low.

Neither Equation 3-16 nor Equation 3-11 provide a complete model for the effects of trans-membrane pressure, concentration or fouling. An overall permeate flux relation is best developed by combining individual models for each resistance term. A number of models exist for each resistance, again a detailed description of these is beyond the scope of this work. Generally though, the membrane resistance R_m is considered constant, since the membrane characteristics do not significantly change during

operation. The concentration polarisation resistance can be determined experimentally if it is assumed that $R_{p,i}$ represents the difference between the overall and the membrane resistances, prior to the occurrence of significant long-term fouling:

$$R_{p,i} = R_i - R_m \tag{3-17}$$

If the flux model of Equation 3-15 is equated with the mass transfer relation (Equation 3-11) and substituted into Equation 3-17, this gives a relationship for the concentration polarisation resistance of stage *i*:

$$R_{p,i} = \frac{\Delta P_{TMP} - \Delta\pi_i}{\mu_{P,i} K_{m,i} \ln\left(\frac{C_{gel,i}}{C_{R\,foul,i}}\right)} - R_m \tag{3-18}$$

The mass transfer coefficient $K_{m,i}$ is assumed constant, since membrane fouling is accounted for in the fouling resistance $R_{f,i}$. At low concentrations the mass transfer resistance may be less than the membrane resistance hence $R_{p,i}$ is taken as:

$$R_{p,i} = \max\left\{\begin{array}{c}\dfrac{\Delta P_{TMP} - \Delta\pi_i}{\mu_{P,i} K_{m,i} \ln\left(\dfrac{C_{gel,i}}{C_{R\,foul,i}}\right)} - R_m \\ 0\end{array}\right\} \tag{3-19}$$

The polarisation resistance relation in Equation 3-19 was developed specifically for ultrafiltration separations (She, 1998b). Alternative models may be required for RO and MF separations. Most importantly, the resistance exhibits concentration dependence, which is representative of behaviour reported in literature. The resistance is also dependant on trans-membrane pressure ΔP_{TMP}, provided the separation is not operating in the mass-transfer dominated region of Figure 2-14.

Membrane fouling is particularly difficult to characterise since it is dependent on both time and the species in the feed stream (see Marshall *et al.*, 1993 for an overview). Some models are phenomenological, seeking to explain the events in terms of physical occurrence (e.g., adsorption isotherms Le & Howell, 1984), whilst others use population-balance (Koltuniewicz & Noworyta, 1994) or empirical models (Rao *et al.*, 1994). For the purposes of controllability assessment, particularly closed-loop simulation, it is important to include fouling effects in the flux model.

The fouling model presented by Winchester (1996a) is based on a general description of the fouling event, with the fouling resistance $R_{f,i}$ actually consisting of a short- and a long-term fouling resistance:

$$R_{f,i}=R_{sf,i}+R_{lf,i} \tag{3-20}$$

represented by $R_{sf,i}$ [m^{-1}] and $R_{lf,i}$ [m^{-1}] respectively. Such a model form allows concentration effects to be expressed within the short-term fouling resistance $R_{sf,i}$, and cumulative fouling effects to be accounted for in the long-term resistance $R_{lf,i}$. In both cases, a differential model is necessary to describe changes in the fouling resistances.

$$\frac{dR_{sf,i}}{dt} = \frac{k_1 J_i C_{R\,foul,i} \mu_{R,i}}{\rho_{R,i}} - k_2 R_{sf,i} \tag{3-21}$$

$$\frac{dR_{lf,i}}{dt} = k_3 R_{sf,i} \tag{3-22}$$

Since the membranes are free of fouling initially, the initial conditions for the fouling models are given by:

$$R_{sf,i}(0)=R_{lf,i}(0)=0$$

The rate of fouling is primarily determined by the coefficients k_1, k_2 and k_3. Manipulation of these parameters allows the decline in predicted permeate flux to match behaviour observed in a physical system.

3.3.3 Prediction of physical stream properties

To predict the permeate flux, and solve the mass and component balances over each stage, it is necessary to calculate the physical properties of streams within the plant. For biological separations operating at constant temperature, variation in physical properties will be primarily due to changes in component concentrations within each stream (Kuo & Cheryan, 1983). The effect of concentration on stream density and viscosity can be determined using analytical relationships, however these relationships can make the differential equation sets numerically difficult to solve, since they become more tightly coupled. Assuming a constant stream viscosity or density simplifies the model, but can significantly change the characteristics of the model.

Preliminary analysis of the case studies showed the retentate viscosity to vary significantly along the plant, and have a strong effect on the polarisation resistance $R_{p,i}$ calculated for each stage. For this reason it was chosen to model viscosity as a function

of concentration. The dynamic viscosity of a stream containing k components was predicted using (Winchester, 1996a):

$$\mu_{R,i} = \mu_w \, e^{\sum_{j=1}^{k} B_{v,j} C_{Rj,i}} \tag{3-23}$$

where

μ_w = dynamic viscosity of water at operating temperature [Pa.s]

$B_{v,j}$ = fitting parameter for component j [kg kg^{-1}]

It is also possible to predict permeate viscosity, however this remains essentially constant since the permeate streams contain little protein or fat (macromolecules), and concentrations of the other components remain low. Permeate stream viscosities are therefore assumed constant and equal to the viscosity of water at 50 °C (processing temperature of the plant).

Retentate and permeate densities were also required for the differential component balances (Equation 3-2). Rao *et al.* (1994) state that density generally changes little with concentration in macromolecule solutions. Preliminary calculations for case studies one and two concurred, exhibiting density variations of less than 6 % and 4 % respectively. On this basis, and in the interests of numerical simplicity, stream densities were assumed to be constant and equal to water at 50 °C.

3.3.4 Overall differential material balance for a component

Returning to the differential balance for component j (Equation 3-2), the algebraic relations developed for the mass balance over stage i (Equation 3-3) and retention coefficient (Equation 3-4) can be substituted. Depending on the flowsheet, either the feed or retentate flow rate of the plant will be specified. For a manipulated feed flow:

$$\begin{aligned} \frac{d\left(\rho_i V_i C_{Rj,i}\right)}{dt} = {} & \rho_{F,i} F_{F,i} C_{Fj,i} + \rho_{DF,i} F_{DF,i} C_{DFj,i} \\ & - \rho_{P,i} F_{P,i} \left(1 - R_{j,i}\right) C_{Rj,i} - \left(\rho_{F,i} F_{F,i} + \rho_{DF,i} F_{DF,i} - \rho_{P,i} F_{P,i}\right) C_{Rj,i} \end{aligned} \tag{3-24}$$

and for a manipulated retentate flow:

$$\begin{aligned} \frac{d\left(\rho_i V_i C_{Rj,i}\right)}{dt} = {} & \left(\rho_{R,i} F_{R,i} - \rho_{DF,i} F_{DF,i} + \rho_{P,i} F_{P,i}\right) C_{Fj,i} + \rho_{DF,i} F_{DF,i} C_{DFj,i} \\ & - \rho_{P,i} F_{P,i} \left(1 - R_{j,i}\right) C_{Rj,i} - \rho_{R,i} F_{R,i} C_{Rj,i} \end{aligned} \tag{3-25}$$

The diafiltration flow rate $F_{DF,i}$ and component concentration $C_{DFj,i}$ will be dependent on the flowsheet configuration, so are not explicitly defined in this general model. To completely describe the dynamic behaviour of a separation stage processing a feed stream with n components (excluding the solvent), a set of n+2 ordinary differential equations are required; n equations for the differential component balances (Equation 3-24 or 3-25) plus an additional 2 differential fouling resistance equations (Equation 3-21 and 3-22).

3.4 Overall equation set for a multistage flowsheet

A complete multistage process model can be constructed by combining the sets of differential equations in a manner that represents the actual flowsheet. Equivalent process variables are substituted as necessary to 'connect' the stages. For example in Figure 3-2 the retentate concentrations from stage one become the feed concentrations to stage two. In this situation the retentate flow rate from stage two is specified, hence the retentate flow rate for stage one is specified by the calculated feed flow rate of stage two. Both diafiltration flow rates $F_{DF,1}$ and $F_{DF,2}$ are manipulated. Pure solute is used for diafiltration hence $C_{DFj,1} = C_{DFj,2} = 0$. The overall equation set for component j is therefore:

$$\begin{aligned}\frac{d\left(\rho_{R,1}V_1C_{Rj,1}\right)}{dt} &= \left(\rho_{R,2}\tilde{F}_{R,2} - \rho_{DF,2}\tilde{F}_{DF,2} + \rho_{P,2}F_{P,2} - \rho_{DF,1}\tilde{F}_{DF,1} + \rho_{P,1}F_{P,1}\right)\tilde{C}_{Fj,1} \\ &\quad - \rho_{P,1}F_{P,1}\left(1 - R_{j,1}\right)C_{Rj,1} - \left(\rho_{R,2}\tilde{F}_{R,2} - \rho_{DF,2}\tilde{F}_{DF,2} + \rho_{P,2}F_{P,2}\right)C_{Rj,1}\end{aligned} \quad \textbf{(3-26)}$$

$$\begin{aligned}\frac{d\left(\rho_{R,2}V_2C_{Rj,2}\right)}{dt} &= \left(\rho_{R,2}\tilde{F}_{R,2} - \rho_{DF,2}\tilde{F}_{DF,2} + \rho_{P,2}F_{P,2}\right)C_{Rj,1} \\ &\quad - \rho_{P,2}F_{P,2}\left(1 - R_{j,2}\right)C_{Rj,2} - \rho_{R,2}\tilde{F}_{R,2}C_{Rj,2}\end{aligned} \quad \textbf{(3-27)}$$

where the manipulated variables are marked with a tilde. This sequence of substitution considerably reduces the number of manipulated variables in the model. The final, completed process model for a multistage flowsheet with i feed components and n stages will consist of a set of $(n+2) \times i$ non-linear ordinary differential equations. The actual number of manipulated variables will depend on the diafiltration regime and structure of the flowsheet.

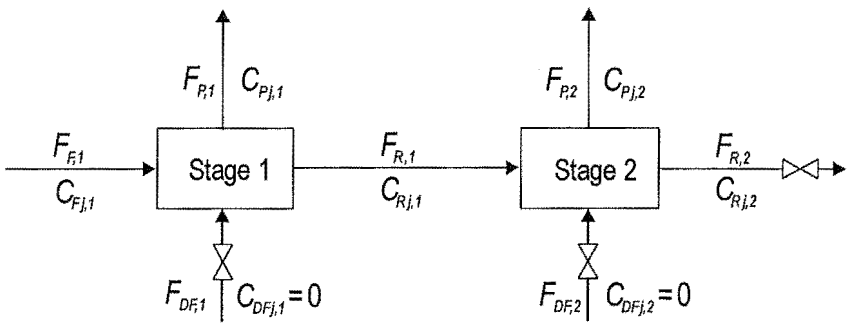

Figure 3-2 Two stage example flowsheet with diafiltration injection

The differential model that has been developed (Equation 3-24 and 3-25) is entirely generic, representing any type of crossflow membrane separation (e.g. UF, NF or RO). Substitution of the appropriate algebraic relations for retention coefficients, permeate flux and stream physical properties will allow a specific separation to be modelled. The differential model can be used either for batch or continuous process situations. A model for a batch plant can be created using the same basic equation set, with the addition of differential equations to model the feed tank contents.

3.5 Case study models

In the previous chapter, design scenarios were presented for two case studies; one manufacturing a retentate and the other a permeate product. Both of these case studies share a common plant design which has 16 stages connected in series. The structure of the generic equation set is therefore identical for each, but the required number of equations differs since there are a different number of components in each feed stream.

3.5.1 Case study 1: Whey protein concentrate production

A substantial amount of research has been carried out on the membrane separation of whey. For this reason retention coefficient and flux models are reasonably well known, although exact values of these parameters will depend on the characteristics of the membranes. Membrane fouling is primarily based on the retained components fat and whey (Winchester, 1996a), hence for this case study:

$$C_{R\,foul,i} = C_{R\,Protein,i} + C_{R\,Fat,i} \quad \textbf{(3-28)}$$

The concentration dependent retention coefficient model (Equation 3-6) is used for this case study.

The retention coefficients used are based on those known for acid whey (Rao *et al.*, 1994; Rao *et al.*, 1995; She, 1998a). It can be seen in Table 3-1 that the unwanted fat is completely retained whereas the valuable protein component is slightly permeable. The use of diafiltration injection will therefore increase protein losses from the retentate stream. For simplicity, all retention coefficients were assumed to be independent of membrane fouling.

Table 3-1 Coefficients for retention model (Equation 3-6) - case study 1

Component	Coefficient a_j	Coefficient b_j
Protein	0.993	0.0004
NPN	0.080	0.0390
Lactose	0.120	0
Lactic Acid	0.120	0
Minerals	0.034	0.0130
Fat	1.000	0

The resistance model (Equation 3-16) was selected to predict permeate flux from each stage, with resistance R_p, R_{sf} and R_{lf} calculated using Equations 3-19, 3-21 and 3-22 respectively. Osmotic pressure effects were assumed negligible. Coefficients for the flux model are given in Table 3-2. Values for the constants were based on unpublished WPC modelling work performed by Winchester (1996b).

Table 3-2 Flux coefficients - case study 1

Mass transfer constant	$K_m = 1.39\text{x}10^{-5}$ m s^{-1}
Gel concentration	$C_{gel} = 40$ wt %
Membrane resistance	$R_m = 1.3\text{x}10^{13}$ m^{-1}
Fouling constants	$k_1 = 1.25\text{x}10^{22}$ - $2.5\text{x}10^{23}$ s m^{-4} (see Appendix A for details)
	$k_2 = 8.33\text{x}10^{-4}$ s^{-1}
	$k_3 = 1.67\text{x}10^{-5}$ s^{-1}

Retentate viscosity is predicted using the algebraic model presented in Equation 3-23, based on the component concentrations within each stage, and the dimensionless coefficients presented in Table 3-3. For WPC, the retained macromolecules protein and fat have greatest effect on retentate viscosity. Permeate viscosities and stream densities were less variable (see Section 0) and assumed to remain constant and equal to those of water at 50 °C. A summary of the model equation set and parameters is presented in Appendix A.

Table 3-3 Physical properties and operating conditions - case study 1

Maximum trans-membrane pressure	$\Delta P_{TMP,max} = 3.0 \times 10^5$ Pa
Minimum trans-membrane pressure	$\Delta P_{TMP,min} = 1.75 \times 10^5$ Pa
Retentate viscosity model fitting coefficients	$B_{v,Protein} = 17$
	$B_{v,NPN} = 5$
	$B_{v,Lactose} = 5$
	$B_{v,Lactic\ Acid} = 5$
	$B_{v,Minerals} = 5$
	$B_{v,Fat} = 20$
Permeate viscosity	$\mu = 5.44 \times 10^{-4}$ Pa.s
Stream density	$\rho = 998.14$ kg m^{-3}

3.5.2 Case study 2: Permeate product separation

Unlike the first case study, the second is not based on any industrial separation, so specification of appropriate values for the retention coefficient and flux models is arbitrary. For this separation, the fouling component concentration was specified by:

$$C_{R\,foul,i} = C_{R\,A,i} \tag{3-29}$$

Retention coefficients for the two components in the feed stream were assumed constant and independent of concentration (Table 3-4).

Table 3-4 Coefficients for retention model (Equation 3-6) - case study 2

Component	Coefficient a_j	Coefficient b_j
A	1.0	0
B	0.7	0

Permeate fluxes were predicted using the same model as the first case study, but with parameters given in Table 3-5.

Table 3-5 Flux coefficients - case study 2

Mass transfer constant	$K_m = 1.6\text{x}10^{-5}$ m s^{-1}
Gel concentration	$C_{gel} = 20$ wt %
Membrane resistance	$R_m = 1.3\text{x}10^{13}$ m^{-1}
Fouling constants	$k_1 = 1\text{x}10^{22}$ - $4\text{x}10^{23}$ s m^{-4} (see Appendix A for details)
	$k_2 = 6.67\text{x}10^{-4}$ s^{-1}
	$k_3 = 1.33\text{x}10^{-5}$ s^{-1}

Dynamic viscosities were assumed to be concentration dependent for retentate streams (predicted using Equation 3-23 and the dimensionless coefficients given in Table 3-6), but permeate viscosity and all stream densities were assumed constant, with properties

equal to water at 50 °C. A summary of the model equation set and parameters is presented in Appendix A.

Table 3-6 Physical properties and operating conditions - case study 2

Maximum trans-membrane pressure	$\Delta P_{TMP,max} = 3.0 \times 10^5$ Pa
Minimum trans-membrane pressure	$\Delta P_{TMP,min} = 1.75 \times 10^5$ Pa
Viscosity model fitting coefficients	$B_{v,A} = 10$
	$B_{v,B} = 4$
Permeate viscosity	$\mu = 5.44 \times 10^{-4}$ Pa.s
Stream density	$\rho = 998.14$ kg m^{-3}

3.6 Implementation of dynamic case study simulations

With the equation sets now complete for each case study and all necessary plant and model information specified, it is now possible to develop a dynamic process simulation. Simulink is a simulation environment that operates with the Matlab software package (MathWorks, 1999). Simulink provides a convenient environment in which to develop dynamic non-linear differential algebraic models, whilst Matlab provides a range of useful tools for solving these, including a suite of numerical integration methods.

The basic Simulink model has a fixed structure with 16 stages, with dynamic behaviour described using the differential equation set developed in Section 0. As discussed in Section 2.6, it is possible in a modern membrane plant to control the number of stages in operation by manipulating valves (Figure 3-3) which isolate a stage from the plant baseline. The trans-membrane pressure of a stage can be calculated from a specified feed pressure using She (1998a):

$$\Delta P_{TMP} = \Delta P_{Feed} + \frac{\Delta P_{crossflow}}{2} \qquad \textbf{(3-30)}$$

where:

ΔP_{Feed} = plant feed pressure [kPa gauge]

$\Delta P_{crossflow}$ = crossflow pressure drop over the length of the membrane within the retentate flow channel [kPa]

A crossflow pressure drop of 2 bar is used in the Simulink case study models.

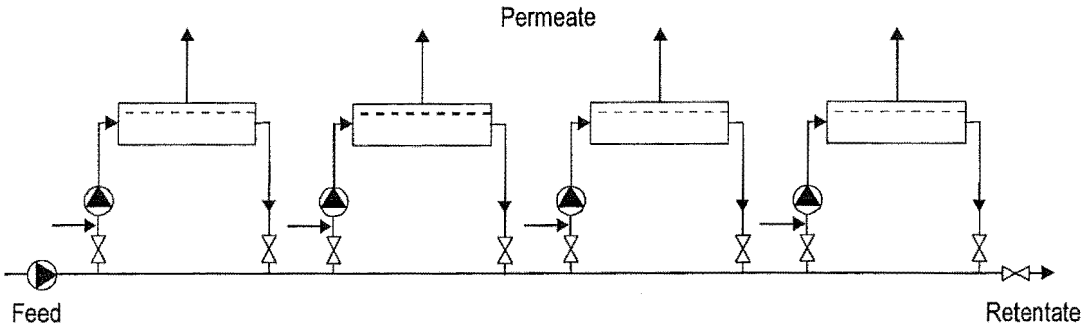

Figure 3-3 Schematic of separation stages with isolation from the plant baseline

When production begins from a commercial membrane plant, it initially contains pure water (because the membranes should not dry out), so all stage concentrations are initially zero. Identical initial conditions are set for the simulation. To completely remove an 'idle' stage from the simulation the membrane area is set to zero, and the retentate concentration is set equal to its feed concentration (rather than being calculated from the differential component balances).

In practice a new, water-filled, stage is brought into operation in a plant by opening the isolating values and starting the recirculation pump. In the simulation, this is achieved by setting the stage membrane area to the correct value, and using the differential equation set to model the stage concentrations. The 'new' membrane increment initially contains water, some of which will pass through the membrane to the permeate stream, with the remainder recirculated around the stage. It is possible to represent this behaviour within a lumped parameter model, provided the numerical integration method is capable of solving systems containing discontinuities. The Matlab integration method '*ode13s*' (Shampine & Reichelt, 1997) was used to simulate process behaviour using the piece-wise continuous models. This is a variable order numerical integration algorithm suited to stiff systems, and capable of solving systems of equations containing discontinuities.

The model described here is an open-loop representation of the plant (Figure 3-4) with the addition of new stages supervised by an external controller. This has been implemented in Simulink in a way that allows the plant to be operated in two distinct ways:

- *Uncontrolled processing capacity* - fixed number of stages and area
- *Controlled processing capacity* - addition of complete stages as necessary

Methods of managing the addition of new stages, and general closed-loop plant control are examined in later chapters.

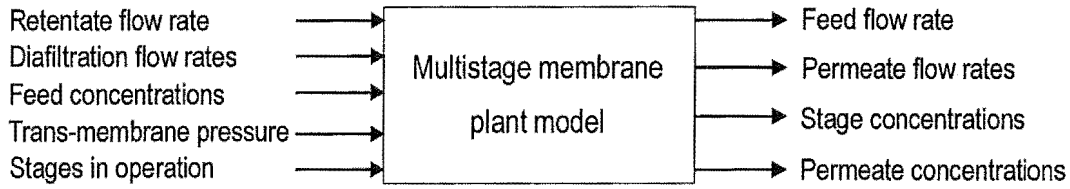

Figure 3-4 Input and output variable sets for dynamic process model

3.7 Open-loop behaviour of case study simulations

Closed-loop control of the case study simulations is not considered until Chapter 6, but the open-loop behaviour of each can be examined using the Simulink model represented in Figure 3-4. To do this, no diafiltration was added, trans-membrane pressure remained constant, and the retentate flow rate of the plant was maintained at a fixed value. In both case studies, the plant operated with all 16 stages.

3.7.1 Case study 1: Whey protein concentrate production

The open-loop characteristics of the WPC plant are shown in Figure 3-5, for a fixed retentate flow rate of 2×10^{-3} m^3 sec^{-1} and feed pressure of 2.0 bar (She, 1998a). As expected the plant showed no steady state, due to the continual decline in the permeate flux of each stage. A protein purity of 60 % was feasible with no diafiltration, but higher purities, particularly the 85 % protein specification will require significant use of diafiltration injection. The delay in the total solids concentration response (Figure 3-5B) suggests that it took some time for the water initially in the plant to be displaced by the whey feed stream. This graph shows that plant start-up should be carefully controlled, otherwise unnecessarily dilute retentate will be sent to the evaporator downstream. Significant variation in feed flow rate to the plant shows the importance of implementing some form of feed flow control when the plant is integrated with an upstream process.

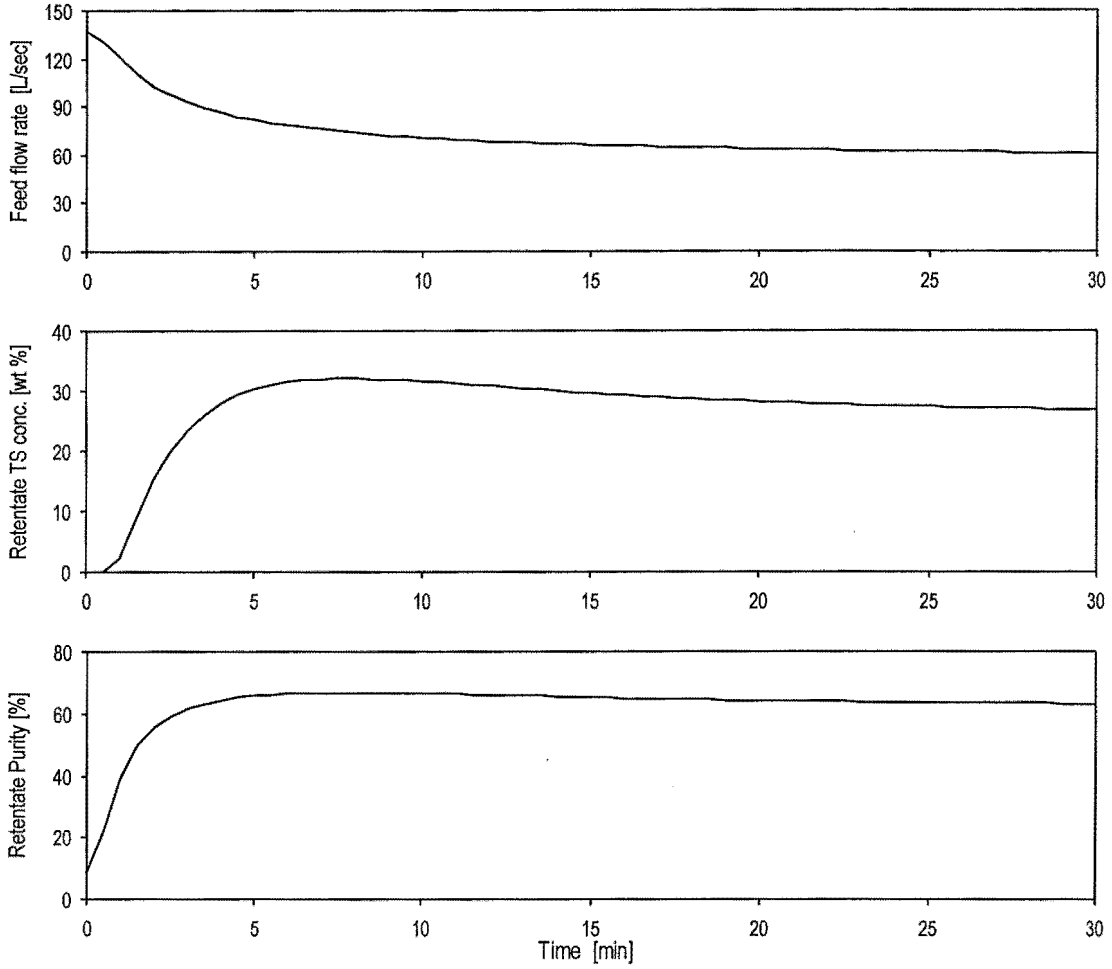

Figure 3-5 Graphs of open-loop plant behaviour - case study 1

3.7.2 Case study 2: Permeate product separation

Open-loop simulation of the permeate product plant is shown in Figure 3-6, for a fixed retentate flow rate of 6 L sec^{-1} and feed pressure of 2.0 bar. The total solids concentration of the combined permeate stream did not show any delay following plant start-up, unlike the retentate stream in case study 1. Overall the permeate stream compositions showed a much faster response than the retentate stream compositions of the other case study. Reasons for this are explored in the next chapter. It is clear that achieving the desired 75 % recovery of Component B will require substantial diafiltration injection. With different parameters in the resistance model (compared to case study 1) the permeate flux showed faster decline, and lower plant feed flow rate after 30 minutes. Again the plant showed no steady state operating point although it is likely that with manipulation of the feed pressure and area distribution of the plant, it will be possible to maintain a constant feed flow rate.

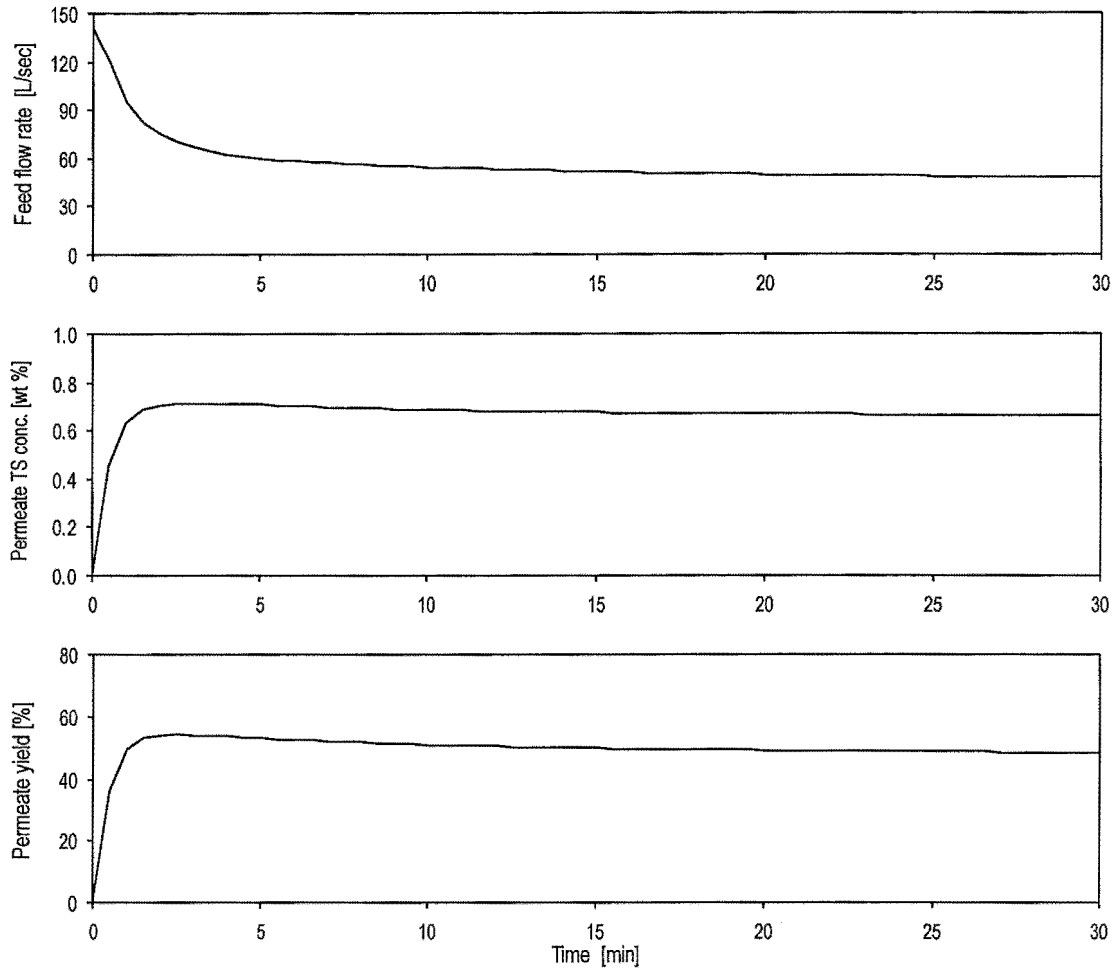

Figure 3-6 Graphs of open-loop plant behaviour - case study 2

3.8 Conclusion

In this chapter the basic equations for a general dynamic process model have been developed. A representation of the overall process flowsheet is generated by combining the equation sets for each stage. Both batch and continuous flowsheets can be represented using this approach. Substituting appropriate retention coefficient, permeate flux and physical property equations produces a model specific to a given separation.

Continuous dynamic process models were developed for each case study, and implemented in Simulink. Open-loop simulation showed these models to exhibit the expected, non-steady state behaviour. Using the continuous process models, the characteristics of each case study will be examined in later chapters in an effort to gain an understanding of general process behaviour. Armed with this knowledge the closed-loop performance of continuous industrial processes will be examined and improvements in control strategy proposed.

3.9 References

Cheryan M (1998), *Ultrafiltration and Microfiltration Handbook,* 2nd Ed., Technomic Publishing Co., Lancaster, USA.

Cussler E L (1984), *Diffusion: Mass Transfer in Fluid Systems,* Cambridge University Press, UK.

de Rham O & Chanton S (1986), An empirical mathematical model of retentate composition in ultrafiltration of dairy products, *Journal of Dairy Research,* **53**, 271-283.

Gekas V, Tragardh G & Hallstrom B (1993), *Ultrafiltration Membrane Performance Fundamentals,* Swedish foundation for membrane technology, Lund.

Himmelblau D M & Bischoff K B (1968), *Process Analysis and Simulation: Deterministic Systems,* John Wiley and Sons, USA.

Koltuniewicz A & Noworyta A (1994), Dynamic properties of ultrafiltration systems in light of the surface renewal theory, *Ind. Eng. Chem. Res.,* **33**, 1771-1779.

Kuo K P & Cheryan M (1983), Ultrafiltration of acid whey in a spiral-wound unit: effect of operating parameters on membrane fouling, *Journal of Food Science,* **48**, 1113-1118.

Le M S & Howell J A (1984), Alternative model for ultrafiltration, *Chem. Eng. Des.,* **62**, (Nov), 373-318.

Le M S & Howell J A (1985), Ultrafiltration. In *Comprehensive Biotechnology: the Principles, Applications and Regulations of Biotechnology in Industry, Agriculture and Medicine* (Ed. Cooney C L & Humphrey A E), Vol 2, pp. 383-408, Pergamon Press, England.

Lee P L, Newell R B & Cameron I T (1998), *Process Control and Management,* Blackie Academic and Professional, Australia.

Marshall A D, Munro P A & Tragardh G (1993), The effect of protein fouling in microfiltration and ultrafiltration on permeate flux, protein retention and selectivity: a literature review, *Desalination,* **91**, 65-108.

MathWorks (1999), *Matlab User's Guide v 5.3,* The MathWorks Inc., USA.

Morari M, Arkun Y & Stephanopoulos G (1980), Studies in the synthesis of control structures for chemical processes, *AIChE Journal,* **26**, (2), 220-232.

Morison K R (1997), Cheese Manufacture as a Separation and Reaction Process, *Journal of Food Engineering,* **32**, 179-198.

Niemi H & Palosaari S (1994), Flowsheet simulation of ultrafiltration and reverse osmosis processes, *Journal of Membrane Science,* **91**, 111-124.

Pradanos P, Arribas J I & Hernandez A (1994), Retention of proteins in cross-flow UF through asymmetric inorganic membranes, *AIChE Journal,* **40**, (11), 1901-1910.

Ramirez W F (1997), *Computational Methods for Process Simulation,* 2nd Ed., Butterworth-Heinemann, Oxford UK.

Rao H G R, Grandison A S & Lewis M J (1994), Flux pattern and fouling of membranes during ultrafiltration of some dairy products, *J. Sci. Food Agric.,* **66**, 563-571.

Rao H G R, Lewis M J & Grandison A S (1995), Effect of pH on flux decline during ultrafiltration of sweet whey and buttermilk, *Journal of Dairy Research,* **62**, 441-449.

Rautenbach R & Albrecht R (1989), *Membrane Processes,* John Wiley & Sons, New York.

Rose L M (1985), *Distillation Design,* Elsevier, New York.

Shampine L F & Reichelt M W (1997), The Matlab ODE suite, *SIAM Journal on Scientific Computing,* **18**, (Jan), 1-22.

She X (1998a), *Design and Optimisation of Multistage Ultrafiltration Plants.* M.E. Thesis, Department of Chemical and Process Engineering, University of Canterbury, New Zealand.

She X (1998b), New Zealand Dairy Group, Personal communication

van Boxtel A J B (1994), Optimal operation policies in Food Processing. In *Automatic Control of Food and Biological Processes* (Ed. Bimbenet J J, Dumoulin E & Trystram G), pp. 449-456, Elsevier Scence, Netherlands.

Wankat P C (1990), *Rate-controlled Separations,* Elsevier Science Publishers Ltd, Essex, England.

Winchester J (1996a), *Computer Simulation and Controllability Studies of Multi-module Ultrafiltration Plants.* M.E. Thesis, Department of Chemical and Process Engineering, University of Canterbury, New Zealand.

Winchester J (1996b), Personal communication

Yeh H M & Cheng T W (1993), Resistance-in-series for membrane ultrafiltration in hollow fibres of tube-and-shell arrangement, *Separation Science and Technology,* **28**, (6), 1341-1355.

4 Non-Numerical Analysis Of Multistage Membrane Plants

A set of equations was developed in the previous chapter describing the dynamic behaviour of a membrane separation stage. By combining several of these sets, the behaviour of a complete process flowsheet can be modelled. Examining the characteristics of individual equations, and the overall structure of the equation set can provide useful information about inherent system behaviour, including disturbance propagation pathways and interaction between important variables. The intention of this chapter is to develop and analyse non-numerical membrane separation models for each case study, as a preliminary analysis into the general dynamic characteristics of multistage membrane processes.

4.1 Qualitative analysis of membrane separation characteristics

The general characteristics of a membrane separation stage can be identified by examining the differential component balance, permeate flux and retention coefficient models that were developed in Chapter 3. Qualitative relationships between flow rate and the concentration of protein and lactose for case study 1 were determined by inspection. These are presented in Figure 4-1, with retentate flow rate F_R, diafiltration flow rate F_{DF} and feed pressure ΔP_{Feed} all specified as manipulated variables. Component concentrations in the feed and diafiltration streams were assumed to be fixed. The fouling concentration $C_{R\,foul}$ was defined in Section 3.5.1 as:

$$C_{R\,foul} = C_{R\,Protein} + C_{R\,Fat} \tag{3-28}$$

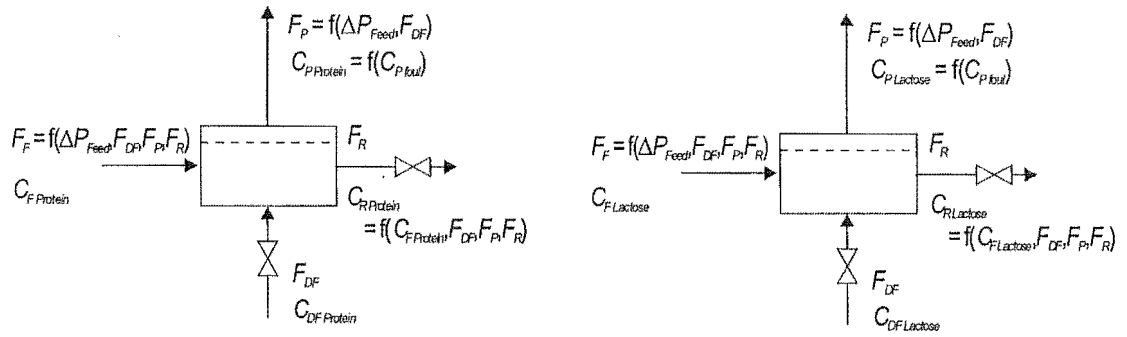

Figure 4-1 Relationships between concentration and flow rate variables within a separation stage

This representation shows a high degree of interdependence between the variables, suggesting that a separation stage is highly interactive. The manipulation or disturbance

of any input will have widespread, complex effects within the stage. Consider the situation when the retentate flow rate is manipulated. The differential component balance for each component predicts that such an action will affect retentate concentrations $C_{R\,Lactose}$ and $C_{R\,Protein}$, meaning that $C_{R\,foul}$ will change also. Changes in these variables will disturb the permeate stream concentrations $C_{P\,Lactose}$ and $C_{P\,Protein}$, and flow rate F_P. Because a separation stage has constant volume, the feed flow rate will be directly affected by the changes in the flow rates F_P and F_R. In a multistage flowsheet, changes in the feed flow rate of a stage will propagate to upstream stages, since $F_{R,i-1} = F_{F,i}$. Thus, any flow rate variation, or disturbance in $C_{R\,foul}$ which affects the permeate flux within a stage, will propagate to all upstream stages.

A lactose feed concentration disturbance entering the stage will affect the permeate and retentate concentrations ($C_{P\,Lactose}$ and $C_{R\,Lactose}$ respectively), but will not propagate to any other variables. In comparison, a protein feed concentration disturbance will affect both the permeate and retentate concentrations, $C_{P\,Protein}$ and $C_{R\,Protein}$ as well as $C_{R\,foul}$. Variation in $C_{R\,foul}$ will then disturb the permeate flux (Equation 3-18), and feed flow rate as a result. Thus concentration disturbances which affect $C_{R\,foul}$ cause additional flow rate disturbances which propagate upstream through the plant.

The characteristics of case study 2, which produces a permeate product, can also be analysed in a similar manner. In this situation, the fouling component is Component A:

$$C_{R\,foul} = C_{R\,A} \tag{3-29}$$

Equivalent conclusions can be drawn for this case study, since it was also found that disturbances affecting system flow rates (e.g. F_P and F_{DF}) will propagate through all upstream stages of a multistage plant. Concentration disturbances which affect $C_{R\,foul}$ will spawn additional flow rate disturbances within the stage, and ultimately within the plant. Even though case study 2 has fixed retention coefficients, the general dynamic behaviour of the process remains the same as case study 1.

The behaviour identified in this analysis is caused by two specific characteristics of membrane separation; constant volume plant design, and concentration dependent permeate fluxes. This combination makes a multistage membrane plant a challenging prospect to control. The action of the controller, in manipulating variables, will actually cause disturbances to propagate into other variables and control loops in the system.

4.2 Structural system analysis as a flowsheet assessment tool

The non-numerical analysis presented in the previous section provided a useful insight into the dynamic characteristics of a membrane separation stage, and disturbance propagation between multiple stages connected in series. Structural system models provide a framework within which to examine the dynamic characteristics of a complete process flowsheet. This approach also allows non-numerical controllability assessment to be performed, to identify types of dynamic behaviour which may exist within a process. Numerical analysis methods can then be used as necessary to determine whether these traits are actually present, or under what conditions they may be encountered. Structural systems analysis can also be used to prove that certain characteristics are not present and cannot occur within a given structural system.

4.2.1 Developing a structural system representation

Structural system representations can provide a non-numerical alternative to a state space model when there is an absence of complete or accurate numerical data. The use of structural systems for process analysis was first proposed by Lin (1974). He suggested that the numerical evaluation of entries in the state space model was not really necessary, claiming that most coefficients in a model are only known within limits of experimental or modelling error. In reality, the only entries known with 100 % certainty are terms equal to zero, where no relation exists between states, inputs or outputs. In a structural system model, non-zero terms are denoted 'X' and known zero terms are usually omitted.

A structural system representation has an identical structure to a numerical state space model:

$$\dot{x} = \mathbf{A}x + \mathbf{B}u \qquad \textbf{(4-1)}$$

where **A** and **B** are coefficient matrices associated with the vector of states x and inputs u. The model output vector y is calculated from:

$$y = \mathbf{C}x + \mathbf{D}u \qquad \textbf{(4-2)}$$

where **C** and **D** are coefficient matrices. Applying this approach, it is possible to construct a structural representation for any system, once the input, output and state variables have been defined. This follows the same sequence as the development of a numerical state space model, but linearisation of the equation set and evaluation of the matrix coefficients is not necessary.

4.2.2 Structural controllability assessment

The concept of structural controllability for systems with feedback control was introduced by Lin (1974), based on the complete state controllability definition of Kalman (Nagrath & Gogal, 1982). Once extended to multiple input systems by Glover & Silverman (1976) and Shields & Pearson (1976), structural controllability theory offered the first true preliminary assessment tool for use during initial flowsheet development. A thorough review of this theory is presented by Morari & Stephanopoulos (1980). Formal structural controllability methods are particularly useful as a preliminary flowsheet assessment tool, where limited numerical data is available. These tools are able to identify flowsheets which have a 'defective' or 'dilated' structure (Lin, 1974; Johnston & Barton, 1985), where it is not possible to independently control the system states and outputs using the specified input variables.

However, the complete state controllability criterion of Kalman requires that all system states must be observable and independently manipulated by the specified input set (Nagrath & Gogal, 1982). Examples have been presented by several authors (Morari & Stephanopoulos, 1980; Russell & Perkins, 1987; Lin *et al.*, 1991) where feasible control schemes exist for systems which are not state structurally controllable. Output structural controllability was presented by Lin *et al.* (1991), as an alternative controllability assessment method which did not require complete state controllability. Instead, it only required that the specified output variables be independently manipulated by the specified input variable set. This avoided unnecessary states being included in the accessibility requirements. Hopkins *et al.* (1993) presented examples where output structural controllability was used to assess industrial process flowsheets.

Formal structural controllability assessment offers useful information during preliminary design, but for existing process designs these methods generally have limited use; industrial experience has already proven the operability of multistage membrane flowsheets. Structural system models do however, offer a useful insight into the dynamic characteristics of a process since they can be used to identify disturbance propagation pathways and interaction between different input-output variable pairings. Dynamic 'resilience' is a concept first introduced by Lenhoff & Morari (1982) to explain the desired characteristics of operability, controllability and flexibility. For a feedback controller, performance is limited by the dynamic characteristics of the plant.

Analysis of a structural system model can therefore be considered as non-numeric assessment of process resilience, where dynamic characteristics which may limit controller performance are identified.

4.2.3 Analysis of structural system models

To develop a complete state space model of a process, it is necessary to linearise the differential equation set, and determine numeric values of all model coefficients. For a membrane process, numerical analysis is further complicated by progressive fouling, which prevents the process from attaining steady state. Structural system models offer a clear, simple insight into the dynamic characteristics of each case study, without the difficulties associated with developing numerical state space models.

Analysis of structural system models is easiest when the model states correspond to physical system variables, i.e. the structural model is not presented in canonical or phase variable form (Nagrath & Gogal, 1982). In this situation, the **A** matrix of the model provides information on disturbance propagation and interaction between states within a process. Of particular interest are the number and placement of off-diagonal terms within this matrix. The **B** and **C** matrices of the model show relationships between the process inputs and outputs, including the existence of interaction between input and output variables. The presence of non-zero terms in the **D** matrix represents direct connections between process inputs and outputs. Such characteristics are undesirable from a process control perspective.

4.2.4 Structural analysis of a simple three tank example system

Structural modelling and analysis techniques are not widely discussed in process control literature or texts. For this reason it is useful to briefly examine a simple example system; in this case a three tank, variable volume flowsheet. The tanks may either be arranged in series or in a cascade, as shown in Figure 4-2. In both situations the system states are given by the liquid levels h_1, h_2 and h_3 in the three tanks. The control objective is to maintain the flow rate F_3 from the third tank at a desired value by manipulating the inlet flow rate F_{in}. The objective of this analysis is to determine if one of the systems will be easier to control than the other.

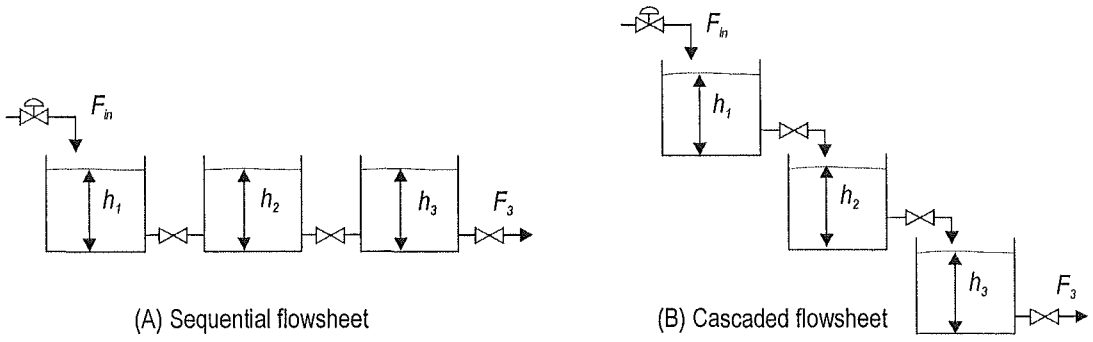

Figure 4-2 Flowsheet of sequential and cascaded tank systems

In the sequential flowsheet (Figure 4-2A) the flow rate between any two tanks is related to the differential head between the two:

$$A_1 \frac{dh_1}{dt} = F_{in} - k_1\sqrt{h_1 - h_2} \quad \textbf{(4-3)}$$

$$A_2 \frac{dh_2}{dt} = k_1\sqrt{h_1 - h_2} - k_2\sqrt{h_2 - h_3} \quad \textbf{(4-4)}$$

$$A_3 \frac{dh_3}{dt} = k_2\sqrt{h_2 - h_3} - k_3\sqrt{h_3} \quad \textbf{(4-5)}$$

The structural system model for the sequential flowsheet can then be developed from the differential equation set:

$$\begin{bmatrix} \dot{h}_1 \\ \dot{h}_2 \\ \dot{h}_3 \end{bmatrix} = \begin{bmatrix} X & X & \\ X & X & X \\ & X & X \end{bmatrix} \begin{bmatrix} h_1 \\ h_2 \\ h_3 \end{bmatrix} + \begin{bmatrix} X \\ \\ \end{bmatrix} \begin{bmatrix} F_{in} \end{bmatrix} \quad \textbf{(4-6)}$$

$$\begin{bmatrix} F_3 \end{bmatrix} = \begin{bmatrix} & & X \end{bmatrix} \begin{bmatrix} h_1 \\ h_2 \\ h_3 \end{bmatrix} + \begin{bmatrix} \ \end{bmatrix} \begin{bmatrix} F_{in} \end{bmatrix} \quad \textbf{(4-7)}$$

For the cascaded arrangement (Figure 4-2B) the flow rate from a tank is solely dependent on the head of the discharging tank:

$$A_1 \frac{dh_1}{dt} = F_{in} - k_1\sqrt{h_1} \quad \textbf{(4-8)}$$

$$A_2 \frac{dh_2}{dt} = k_1\sqrt{h_1} - k_2\sqrt{h_2} \quad \textbf{(4-9)}$$

$$A_3 \frac{dh_3}{dt} = k_2\sqrt{h_2} - k_3\sqrt{h_3} \quad \textbf{(4-10)}$$

This gives a structural system model of the form:

$$\begin{bmatrix} \dot{h}_1 \\ \dot{h}_2 \\ \dot{h}_3 \end{bmatrix} = \begin{bmatrix} X & & \\ X & X & \\ & X & X \end{bmatrix} \begin{bmatrix} h_1 \\ h_2 \\ h_3 \end{bmatrix} + \begin{bmatrix} X \\ \\ \end{bmatrix} \begin{bmatrix} F_{in} \end{bmatrix} \tag{4-11}$$

$$\begin{bmatrix} F_3 \end{bmatrix} = \begin{bmatrix} & & X \end{bmatrix} \begin{bmatrix} h_1 \\ h_2 \\ h_3 \end{bmatrix} + \begin{bmatrix} \ \end{bmatrix} \begin{bmatrix} F_{in} \end{bmatrix} \tag{4-12}$$

Formal controllability assessment methods for structural models were discussed in Section 4.2.2, where it was suggested that these tools are often of limited use. In this example neither flowsheet shown in Figure 4-2 satisfies the criterion of Lin (1974) for state structural controllability, since the three states cannot be independently manipulated with a single input. Conversely, both flowsheets fulfil the requirements of Lin *et al.* (1991) for output structural controllability since the output can be manipulated using the input. Thus, formal structural controllability assessment has not aided flowsheet selection. However, examination of the structural models (Equations 4-6 and 4-7, 4-11 and 4-12) can be surprisingly useful for identifying the flowsheet with superior dynamic resilience.

Reviewing the structural system models (Equations 4-6 and 4-7, 4-11 and 4-12), it can be seen that the difference between the flowsheets is represented in the arrangement and number of non-zero terms in the **A** matrix. The diagonal structure of the **A** matrix in Equation 4-11 means that the cascaded flowsheet will never exhibit oscillatory behaviour, since it is not structurally possible for the model to have complex eigenvalues (assuming the model is a fair representation of the actual process). In comparison, the structure of the **A** matrix in Equation 4-6 has sufficient off-diagonal terms that complex eigenvalues are structurally possible. Whether or not the process flowsheet actually exhibits such behaviour can only be determined by analysis of a numerical state space model.

The structural models also provide information of the dynamic relationships between input and output variables. In both situations, there is only a single manipulated input (F_{in}) and controlled output (F_3), and the relationship between these is much the same for

the two process configurations. For both the sequential and cascaded systems, F_3 has an overdamped third order response to a change in F_{in}:

$$F_3 = \frac{K_p}{(\tau_1 s + 1)(\tau_2 s + 1)(\tau_3 s + 1)} F_{in} \quad \textbf{(4-13)}$$

Overall the structural analysis suggests that the cascaded flowsheet has superior controllability characteristics.

4.3 Structural analysis of the multistage membrane processes

The three tank example in the previous section highlighted the difference between formal structural controllability assessment, and general analysis of the structural models. The aim of this thesis is to investigate the characteristics of multistage membrane plants, and develop an understanding of dynamic process behaviour. Construction and analysis of structural system models for each case study is consistent with this aim.

Before a structural system model can be developed it is first necessary to identify the process inputs, outputs and states. Generally, state variables are those whose behaviour is best described by a differential equation. The equation set developed in Section 3.3 described the behaviour of each component concentration in a stage using a differential component balance. Thus component concentrations within all stages are system states. Other states may also exist, depending on the choice of relations describing permeate concentration and flux. For both case studies, permeate concentrations were calculated algebraically from the retentate concentration (Equation 3-4) so are not states. However the permeate flux relation adds two states to the model for each separation stage, corresponding to the differential models for short- and long-term fouling resistances (Equations 3-21, 3-22).

An analysis of multi-stage membrane plant characteristics was carried out by Winchester (1996a) based on a rigorous plant model, using a resistance flux model of identical form to that presented in Section 3.3.2. However analysis of this was complex and the results difficult to interpret, due mainly to the large number of state variables in the model. It is desirable to simplify the structural model to aid analysis in this chapter. This is most easily achieved by replacing the differential short- and long-term fouling

models with constant values evaluated at an operating point of interest. This produces a simplified permeate flux model of the form:

$$J = \frac{\Delta\tilde{P}_{TMP}}{\mu_p\left(\frac{\Delta\tilde{P}_{TMP}}{\mu_p K_m ln\left(C_g / \tilde{C}_{R\,foul,i}\right)} + R_{sf} + R_{lf}\right)} \tag{4-14}$$

where variables are denoted with tilde and the remaining terms are constant. It was specified in Section 2-6 that new stages would be brought into operation as necessary in each case study to maintain the desired feed flow rate. As the number of stages in the process increases, so too does the number of states in the system model. To maintain the analysis at a manageable scale, structural models were developed for each case study when operating with only four stages.

Controlled process outputs differ for each case study, since one is producing a retentate and the other a permeate product. For case study 1, the structural system outputs are specified as the plant feed flow rate F_F, as well as retentate total solids concentration $C_{R\,TS,n}$ and protein purity $P_{R\,Protein,n}$ (Section 2.5.1). Controlled system outputs for case study 2 were specified in Section 2.5.2 as Component B permeate yield Y_B and plant feed flow rate F_F. Permeate stream total solids concentration $C_{P\,TS}$ is also included in this analysis, as a point of interest.

Identical manipulated inputs were specified in Section 3.7 for both case studies; plant feed pressure ΔP_{Feed}, retentate flow rate $F_{R,n}$ and the amount of diafiltration applied to each stage. Although diafiltration control strategies are not formally defined or analysed until later chapters, a brief consideration of diafiltration injection control is necessary at this point. As explained earlier, progressive membrane fouling means that the permeate flux of each separation stage continually declines. It is therefore necessary to regularly update the diafiltration flow rates to ensure they track changes in permeate flows. Failure to do so can result in undesirable concentration peaks within the plant. The strategy commonly employed industrially is to maintain the diafiltration flow rate as a specified proportion or ratio of the permeate flow. Alternative strategies are examined in Chapters 6 and 7. However for the purposes of this structural analysis, manipulated diafiltration inputs are specified as the diafiltration ratio ϕ_i to each stage. It is also useful

to include likely disturbances in the input set, so the effect of these inputs can be examined. For this reason, the feed concentrations of selected components have been included as inputs in the structural model for each case study.

4.3.1 Case study 1: Whey protein concentrate production

The structural system model of the whey protein case study, operating with four stages, is presented in Equations 4-15 and 4-16. Although a total of six components were specified in the case study description (Section 2.5) only two, protein and lactose, are shown here. Limiting the number of stages and components in the structural system model makes it easier to concisely present the structural system model. Trends identified in this model can easily be extended to the omitted components and stages.

$$\begin{bmatrix} \dot{C}_{R\,Protein,1} \\ \dot{C}_{R\,Protein,2} \\ \dot{C}_{R\,Protein,3} \\ \dot{C}_{R\,Protein,4} \\ \dot{C}_{R\,Lactose,1} \\ \dot{C}_{R\,Lactose,2} \\ \dot{C}_{R\,Lactose,3} \\ \dot{C}_{R\,Lactose,4} \end{bmatrix} = \begin{bmatrix} X & X & X & X & & & & \\ X & X & X & X & & & & \\ & X & X & X & & & & \\ & & X & X & & & & \\ X & X & X & X & X & & & \\ X & X & X & X & X & X & & \\ & X & X & X & & X & X & \\ & & X & X & & & X & X \end{bmatrix} \begin{bmatrix} C_{R\,Protein,1} \\ C_{R\,Protein,2} \\ C_{R\,Protein,3} \\ C_{R\,Protein,4} \\ C_{R\,Lactose,1} \\ C_{R\,Lactose,2} \\ C_{R\,Lactose,3} \\ C_{R\,Lactose,4} \end{bmatrix} + \begin{bmatrix} X & & X & X & X & X & X & X \\ & & & X & X & X & X & X \\ & & & & & X & X & X & X \\ & & & & & & X & X & X \\ & X & X & X & X & X & X & X \\ & & & X & X & X & X & X \\ & & & & & X & X & X & X \\ & & & & & & X & X & X \end{bmatrix} \begin{bmatrix} C_{F\,Protein} \\ C_{F\,Lactose} \\ \phi_1 \\ \phi_2 \\ \phi_3 \\ \phi_4 \\ F_R \\ \Delta P_{Feed} \end{bmatrix} \quad \textbf{(4-15)}$$

$$\begin{bmatrix} C_{R\,TS,4} \\ P_{R\,Protein,4} \\ F_F \end{bmatrix} = \begin{bmatrix} & & & X & & & & X \\ & & & X & & & & X \\ X & X & X & X & & & & \end{bmatrix} \begin{bmatrix} C_{R\,Protein,1} \\ C_{R\,Protein,2} \\ C_{R\,Protein,3} \\ C_{R\,Protein,4} \\ C_{R\,Lactose,1} \\ C_{R\,Lactose,2} \\ C_{R\,Lactose,3} \\ C_{R\,Lactose,4} \end{bmatrix} + \begin{bmatrix} & & & & & & & \\ & & & & & & & \\ & & & & X & X & X & X \end{bmatrix} \begin{bmatrix} C_{F\,Protein} \\ C_{F\,Lactose} \\ \phi_1 \\ \phi_2 \\ \phi_3 \\ \phi_4 \\ F_R \\ \Delta P_{Feed} \end{bmatrix} \quad \textbf{(4-16)}$$

In this analysis fat and protein are considered 'key' components, since they influence the permeate fluxes and retention coefficients of the separation:

$$C_{R\,foul,j} = C_{R\,Protein,j} + C_{R\,Fat,j} \quad \textbf{(3-28)}$$

Lactose, NPN, lactic acid and minerals are all 'non-key' components since the concentrations of these species to not affect the permeate fluxes or retention coefficients.

The diagonal arrangement of non-zero terms, in the portion of the **A** matrix corresponding to the lactose states (Equation 4-15), suggests that system dynamics for this component mirror those of the cascaded tank example (Section 4.2.4). A concentration disturbance in this component will pass down the plant, being attenuated by each successive stage. Because lactose is a non-key component it does not affect the

retention coefficient of any component, or permeate flux of any stage, thus concentration disturbances in this component do not propagate to any other. For a process with n stages, a feed concentration disturbance in a non-key component will slowly pass through each stage, emerging as an n^{th} order concentration disturbance in the retentate stream:

$$C_{R\ Lactose,n} = \frac{K_p}{(\tau_1 s+1)(\tau_2 s+1)\ldots(\tau_n s+1)} C_{F\ Lactose} \qquad \textbf{(4-17)}$$

As a general conclusion, plants with more stages will provide increased attenuation of concentration disturbances, although the concentration disturbance reaching the retentate stream will be of a higher order.

The presence of key components introduces additional non-zero terms to the **A** matrix of the structural system model (Equation 4-15). Sufficient off-diagonal terms are present in this section of the **A** matrix that the occurrence of complex eigenvalues becomes structurally possible, meaning that the plant may exhibit underdamped oscillatory behaviour. By tracing the main paths of a protein feed concentration disturbance (Equation 4-18) it can be seen that the presence of non-zero terms to the third (lower-left) quadrant of the **A** matrix allows this concentration to propagate to other component concentrations within the process. Thus key components, by affecting permeate fluxes, create widespread propagation paths within a multistage plant. Additional propagation pathways also exist for the key components via concentration dependent retention coefficients, but these are generally not as significant.

$$\begin{bmatrix} \dot{C}_{R\ Protein,1} \\ \dot{C}_{R\ Protein,2} \\ \dot{C}_{R\ Protein,3} \\ \dot{C}_{R\ Protein,4} \\ \dot{C}_{R\ Lactose,1} \\ \dot{C}_{R\ Lactose,2} \\ \dot{C}_{R\ Lactose,3} \\ \dot{C}_{R\ Lactose,4} \end{bmatrix} = \begin{bmatrix} X & X & X & X & & & & \\ X & X & X & X & & & & \\ & X & X & X & & & & \\ & & X & X & & & & \\ X & X & X & X & X & & & \\ X & X & X & X & X & X & & \\ & X & X & X & & X & X & \\ & & X & X & & & X & X \end{bmatrix} \begin{bmatrix} C_{R\ Protein,1} \\ C_{R\ Protein,2} \\ C_{R\ Protein,3} \\ C_{R\ Protein,4} \\ C_{R\ Lactose,1} \\ C_{R\ Lactose,2} \\ C_{R\ Lactose,3} \\ C_{R\ Lactose,4} \end{bmatrix} + \begin{bmatrix} X & X & X & X & X & X & \\ & X & X & X & X & X & \\ & & X & X & X & X & \\ & & & X & X & X & \\ X & X & X & X & X & X & X \\ & X & X & X & X & X & \\ & & X & X & X & X & \\ & & & X & X & X & \end{bmatrix} \begin{bmatrix} C_{F\ Protein} \\ C_{F\ Lactose} \\ \phi_1 \\ \phi_2 \\ \phi_3 \\ \phi_4 \\ F_R \\ \Delta P_{Feed} \end{bmatrix} \qquad \textbf{(4-18)}$$

The lack of non-zero terms in the second (upper-right) quadrant of the **A** matrix means that disturbances can propagate from key to non-key components but not in the reverse direction, i.e. a one-way interaction exists between the key and non-key components.

The widespread disturbance propagation characteristics of key components means that the total solids response of a process with n stages to a protein feed concentration disturbance will be n^{th} order, with complex lead-lag dynamics. Inverse response behaviour is structurally possible in the response of both components to a $C_{F\ Protein}$ disturbance, although such behaviour will only be exhibited if there is an odd number of positive roots (zeros) in the numerator of the transfer function (Nagrath & Gogal, 1982). As the number of stages in a plant increases, so too will the order of the process response. Because a feed concentration disturbance in a key component will propagate to all other components in the process, the complexity of the process response will increase with the number of components in the feed stream.

Qualitative system analysis performed in Section 4.1 suggested that there was strong interconnection between flow rate and concentration variables within a separation stage. The structural system analysis model developed in this section proves this to be primarily due to the behaviour of the key components protein and fat. A process without concentration-dependent permeate flux or retention coefficients would not have such complex disturbance propagation characteristics or possible oscillatory behaviour.

From the **B** matrix (Equation 4-15) it can be seen that retentate flow rate and feed pressure both directly affect all concentrations within the plant. As with feed concentration disturbances, the order of the plant response to these inputs will be proportional to the number of stages operating in the plant. Equation 4-19 shows that the manipulation of a diafiltration ratio associated with a stage will directly affect the component concentrations within that stage, as well as creating disturbances which propagate up and downstream from this point. As stages are progressively added to the plant to maintain the desired feed flow rate, the relationship between manipulated diafiltration ratios and retentate composition will change. This suggests that the performance of fixed parameter feedback controllers will also change over time.

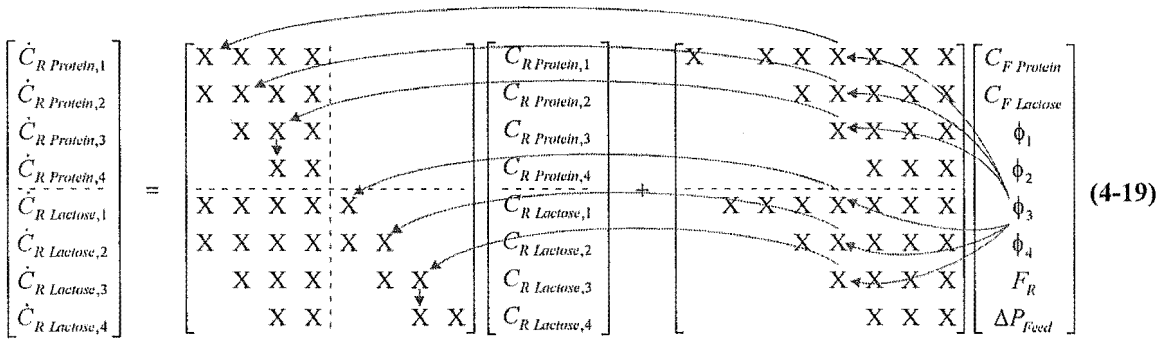

(4-19)

The **C** matrix (Equation 4-16) provides information on the relationship between system states and the controlled process outputs. Total solids concentration $C_{R\,TS,4}$ is the sum of component concentrations in the retentate stream, so is susceptible to concentration disturbances in multiple components passing down the plant in parallel. Retentate protein purity $P_{R\,Protein,4}$ is dependent on the total solids concentration, so exhibits equivalent behaviour. The response dynamics for these variables will therefore be high order lead-lag relations. Inverse response behaviour is structurally possible for these outputs, raising the possibility of controllability difficulties.

All four manipulated variables are also shown in the **D** matrix (Equation 4-16) to directly affect the feed flow rate. This is due to the fixed volume plant design, and a manipulated retentate flow rate $F_{R,4}$. Overall, this means there will be a significant amount of interaction between the input and output variables. Such behaviour suggests that it is likely the plant will be difficult to control using individually tuned, single variable control loops.

Prior to plant startup each separation stage contains pure water. Plant startup can therefore be considered as a step change in feed stream concentration (from zero) occurring simultaneously for all components. Returning to the 16 stage open-loop simulation for this case study (Figure 3-5), it is now apparent that the delay in retentate total solids concentration response is in fact a 16^{th} order response to the step change in feed concentration. The faster response of the protein purity was due to it being calculated from the ratio of concentrations in the retentate stream.

4.3.2 Case study 2: Permeate product separation

The structural model of the second case study (Equations 4-20 and 4-21) has much in common with case study 1, since the process flowsheet and flux relations are the same.

$$\begin{bmatrix} \dot{C}_{RA,1} \\ \dot{C}_{RA,2} \\ \dot{C}_{RA,3} \\ \dot{C}_{RA,4} \\ \hline \dot{C}_{RB,1} \\ \dot{C}_{RB,2} \\ \dot{C}_{RB,3} \\ \dot{C}_{RB,4} \end{bmatrix} = \left[\begin{array}{cccc:cccc} X & X & X & X & & & & \\ X & X & X & X & & & & \\ & X & X & X & & & & \\ & & X & X & & & & \\ \hdashline X & X & X & X & X & & & \\ X & X & X & X & X & X & & \\ & X & X & X & & X & X & \\ & & X & X & & & X & X \end{array}\right] \begin{bmatrix} C_{RA,1} \\ C_{RA,2} \\ C_{RA,3} \\ C_{RA,4} \\ \hline C_{RB,1} \\ C_{RB,2} \\ C_{RB,3} \\ C_{RB,4} \end{bmatrix} + \left[\begin{array}{ccccccc:c} X & & X & X & X & X & X & X \\ & & & X & X & X & X & X \\ & & & & X & X & X & X \\ & & & & & X & X & X \\ \hdashline & X & X & X & X & X & X & X \\ & & & X & X & X & X & X \\ & & & & X & X & X & X \\ & & & & & X & X & X \end{array}\right] \begin{bmatrix} C_{FA} \\ C_{FB} \\ \phi_1 \\ \phi_2 \\ \phi_3 \\ \phi_4 \\ F_R \\ \Delta P_{Feed} \end{bmatrix} \quad \textbf{(4-20)}$$

$$\begin{bmatrix} Y_B \\ C_{PTS} \\ F_F \end{bmatrix} = \left[\begin{array}{cccc:cccc} X & X & X & X & X & X & X & X \\ X & X & X & X & X & X & X & X \\ & & X & X & & & & \end{array}\right] \begin{bmatrix} C_{RA,1} \\ C_{RA,2} \\ C_{RA,3} \\ C_{RA,4} \\ \hline C_{RB,1} \\ C_{RB,2} \\ C_{RB,3} \\ C_{RB,4} \end{bmatrix} + \left[\begin{array}{ccccccc:c} & X & X & X & X & X & X & X \\ & & & & & & & X \\ & & X & X & X & X & X & X \end{array}\right] \begin{bmatrix} C_{FA} \\ C_{FB} \\ \phi_3 \\ \phi_3 \\ \phi_3 \\ \phi_3 \\ F_R \\ \Delta P_{Feed} \end{bmatrix} \quad \textbf{(4-21)}$$

The structural system dynamics of the **A** matrix for this separation are identical to those examined in the previous case study. In this separation Component A, the unwanted impurity, is the key component, influencing the permeate fluxes of each stage (Equation 3-29):

$$C_{R\,foul,i} = C_{RA,i} \quad \textbf{(3-29)}$$

One-way interaction is again present in this system, due to the presence of non-zero terms in the third (lower-left) quadrant of the **A** matrix but not the second (upper-right). As a result, a concentration disturbance in Component A (the key component) will propagate to the non-key component, however the reverse cannot occur. Manipulated variables remain the same for this case study, as are the system response dynamics for each.

In this particular case study, the key component is completely retained by the membrane. Regardless of this, disturbances in a key component concentration still affect the permeate product, since concentration disturbances in this component will cause flow rate disturbances within the plant. These will cause secondary concentration disturbances in the permeable component (Component B) which will affect the permeate stream. The responses of permeate stream total solids concentration and yield will therefore be lead-lag relations, the order of which will be proportional to the number of

stages operating in the plant. The total solids response dynamics will also be dependent on the number of permeable components in the feed stream.

The **C** matrix (Equation 4-21) provides information on the system outputs. Given that this case study produces a permeate product, compared with the retentate product of the first case study, it is not surprising that the **C** matrix for this separation has a different structure. Most significantly, the permeate total solids concentration $C_{P\,TS}$ and yield Y_B show direct dependence on all stage concentrations. This is somewhat different to the first case study where only the final stage concentrations directly affected product concentration and composition. Therefore, a feed concentration disturbance entering the first separation stage will first pass directly to the permeate stream, then repeatedly propagate to the permeate stream as it passes through each stage down the plant. Such behaviour will occur for both key and non-key components, provided they are able to permeate through the membrane.

Manipulation of a stage diafiltration ratio will cause a concentration disturbance within that stage, which will directly propagate to the permeate stream. However, like the first case study, disturbances will propagate upstream and downstream from this point, each propagating through to the permeate stream from each stage. Thus the permeate response to the input will have first order dynamics initially, followed by secondary high order disturbance dynamics propagating from other stages. The main disturbance paths from this input are illustrated in Equation 4-22. Other paths also exist but are not shown.

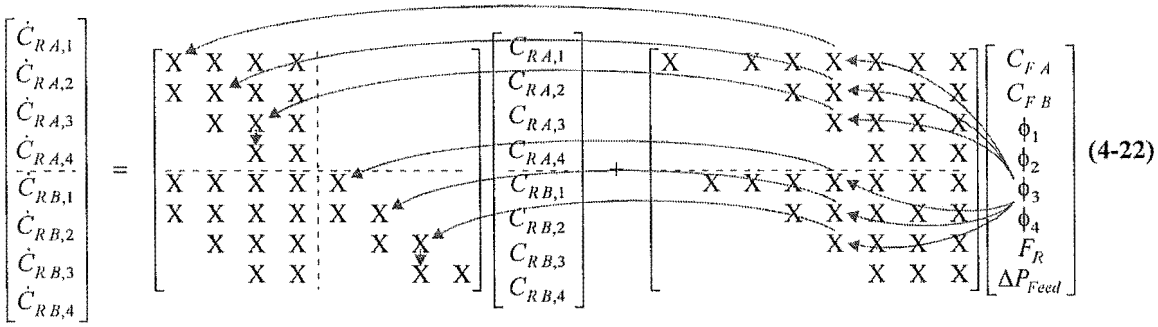

(4-22)

From the **D** matrix (Equation 4-21) it can be seen that direct connections exist between the manipulated inputs and outputs of the process. This is undesirable, and suggests that there will be interaction difficulties when controlling the plant, since the actions of one controller will affect variables controlled by another.

Open-loop plant behaviour at startup (Figure 3-6) showed the total solids concentration of the permeate stream to increase almost immediately. This was due to the feed stream immediately entering the product stream via the first stage. Overall, both the permeate yield Y_B and total solids concentration $C_{P\,TS}$ had much faster dynamics than the retentate stream of case study 1. Generally this suggests that permeate product systems may have superior dynamic resilience, and better potential for good feedback controller performance.

4.4 Conclusion

Non-numerical models were constructed in this chapter for the two case study systems. Analysis of these showed the presence of interaction between system concentrations and flow rates, due to concentration dependent permeate fluxes within each stage. This characteristic played a significant role in determining process behaviour. Inverse response was also structurally possible for disturbances in key component concentrations.

Constant volume plant design caused flow rate disturbances to propagate widely throughout the plant. Such flow disturbances caused component concentrations to vary, affecting both the retentate and permeate streams. The natural dynamics of each system were found to be a function of both the number of stages in the plant design, and the number of components in the feed stream. The sequential flowsheet of the plant was found to cause high order response dynamics in the retentate product case study. Permeate stream dynamics exhibited a mixture of low and high order disturbance response dynamics. Interaction between the inputs and outputs of the system suggests poor performance when operating the plant with individually tuned single-variable control loops.

When drawing conclusions from this theoretical analysis, it must be remembered that the dynamic models used here have not been rigorously validated against physical multistage membrane plants. However, unpublished work by Winchester (1996b) has shown that the dynamic model characteristics are representative of observed industrial plant behaviour.

4.5 References

Glover K & Silverman L M (1976), Characterization of structural controllability, *IEEE Trans. Autom. Control.*, **21**, 534-537.

Hopkins L, Lant P & Newell B (1993), Output structural controllability; a tool for integrated process design and control, *J. Proc. Cont.*, **8**, (1), 57-68.

Johnston R D & Barton G W (1985), Structural equivalence and model reduction, *Int. J. Control,* **41**, (6), 1477-1491.

Lenhoff A M & Morari M (1982), Design of resilient processing plants - I; process design under consideration of dynamic aspects, *Chem. Eng. Sci.*, **37**, (2), 245-258.

Lin C (1974), Structural controllability, *IEEE Trans. Autom. Control.*, **AC-19**, (3), 201-208.

Lin C (1974), Structural controllability, *IEEE Trans. Autom. Control.*, **AC-19**, (3), 201-208.

Lin X, Tade M O & Newell R B (1991), Output structural controllability condition for the synthesis of control systems for chemical processes, *Int. J. Systems Sci.*, **22**, (1), 107-132.

Lin X, Tade M O & Newell R B (1991), Output structural controllability condition for the synthesis of control systems for chemical processes, *Int. J. Systems Sci.*, **22**, (1), 107-132.

Morari M & Stephanopoulos G (1980), Part II; Structural aspects and the synthesis of alternative feasible control schemes, *AIChE Journal,* **26**, (2), 232-246.

Morari M & Stephanopoulos G (1980), Part II; Structural aspects and the synthesis of alternative feasible control schemes, *AIChE Journal,* **26**, (2), 232-246.

Nagrath I J & Gopal M (1982), *Control Systems Engineering,* 2nd Ed., New Age International Ltd, India.

Russell L W & Perkins J D (1987), Towards a method for diagnosis of controllability and operability problems in chemical plants, *Chem. Eng. Res. Des.*, **65**, 453-461.

Shields R W & Pearson J B (1976), Structural controllability of multi-input linear systems, *IEEE Trans. Autom. Control.*, **AC-21**, (2), 203-212.

Winchester J (1996a), *Computer Simulation and Controllability Studies of Multi-module Ultrafiltration Plants.* M.E. Thesis, Department of Chemical and Process Engineering, University of Canterbury, New Zealand.

Winchester J (1996b), Personal communication.

5 Numerical Analysis Of Multistage Membrane Plants

Non-numerical structural models were developed in the previous chapter to provide an insight onto the general dynamic characteristics of multistage membrane plants. Examination of these revealed several potentially undesirable characteristics which, if present, would limit the achievable quality of control for each case study. Numerical state space models are developed for both case studies in this chapter, and further analysis performed to determine whether these undesirable characteristics are actually present. This chapter explores some of the fundamental characteristics of membrane process behaviour along with the effects of diafiltration injection. The understanding developed here is used as a basis for closed-loop controller development and trials in the following chapters. Because simplified models are used for the purposes of explanation, emphasis is placed on trends in the results rather than the absolute values of the numbers generated.

5.1 Development of numerical membrane plant models

Numerical analysis of a membrane plant can be a difficult task, since the process does not attain steady state. Controllability is not easy to quantify, particularly for rate-controlled non-linear systems which are continually changing. Analysis in this chapter is performed using the permeate flux model presented previously (Section 3.3.2). The behaviour of a non-linear system is dependent on the operating point, which for this process is continually changing. For this analysis, system behaviour is examined at the beginning of plant operation when membrane fouling is not significant, hence R_{sf} and R_{lf} are zero. Unlike a complete resistance model, the resulting flux relations allow a membrane separation plant to achieve steady state. Most importantly, the simplified flux model still exhibits concentration dependence, which was identified in the previous chapter as being a fundamental characteristic of membrane processes. Using this flux model, it is possible to examine the general characteristics of both retentate and permeate product plants. Equivalent steady state permeate flux models have been used in literature during the analysis of process designs and operating conditions (Le & Howell, 1985; Rautenbach & Albrecht, 1989; Field, 1996).

This chapter focuses extensively on the effect of diafiltration injection on membrane plant behaviour. A number of strategies exist for controlling the injection of diafiltra-

tion into a multistage membrane plant, and dynamic analysis of diafiltration is performed in the next chapter. For the steady state investigation presented in this chapter the flow rate of diafiltration to a stage is specified as a fraction or ratio of the permeate flow from that stage:

$$\phi_i = \frac{F_{DF,i}}{F_{P,i}} \tag{2-1}$$

In this chapter, whenever diafiltration injection is applied to part of a plant, the same diafiltration ratio is used for all stages.

5.2 Concepts of membrane plant behaviour

Membrane separations simultaneously achieve both fractionation and concentration of the feed stream. Fractionation can be enhanced through the use of diafiltration injection, but system concentrations will be reduced as a result. Diafiltration injection can be applied to a multistage plant in a number of ways, with different effects on separation efficiency. Membrane plant design would seem like a simple optimisation, and in most ways it is, but it will be shown in this chapter that design trade-offs also have a significant effect on process behaviour and achievable closed-loop performance. Analysis of the case studies provides an insight into the effect of diafiltration on process characteristics.

5.2.1 Case study 1: Whey protein concentrate production

Provided excessive diafiltration is not applied, the retentate stream from each successive stage down the membrane plant is more highly concentrated and purified than the previous. The concentration and purity profiles along a plant depend on the physical properties of the separation (e.g. permeate flux and retention coefficients), design parameters (e.g. membrane area distribution) and operating conditions (e.g. diafiltration and retentate flow rates). The effect of different diafiltration injection regimes on process characteristics is best illustrated with a numerical example. Figure 5-1 shows concentration and protein purity profiles through the 16 stage WPC case study plant for four different diafiltration regimes, for a fixed plant feed stream (stage 0). Each regime represents a different method of applying diafiltration to the plant to achieve the desired retentate concentration and purity (stage 16). In the example shown in Figure 5-1, the desired retentate stream specifications were 27 wt % total solids concentration and 85 % protein purity. The dynamic model equation set is summarised in Appendix A.

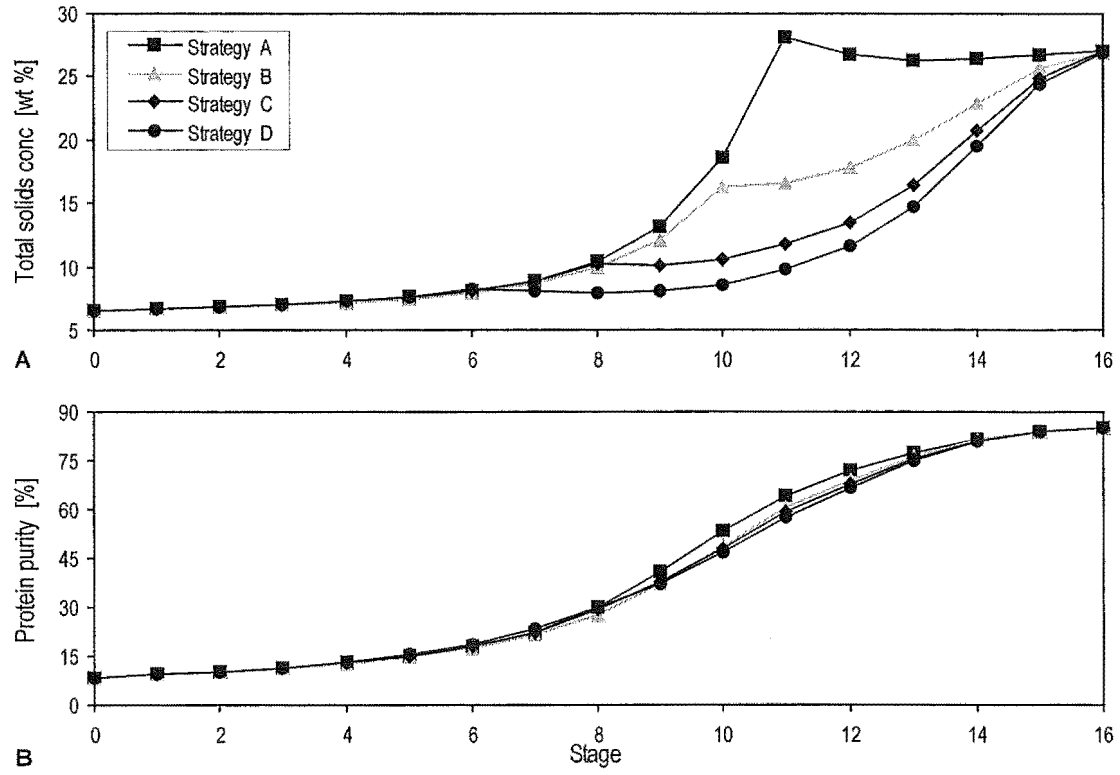

Figure 5-1 Concentration and purity profiles for different diafiltration regimes - case study 1
See Table 5-1 for full details of the diafiltration strategies shown in this figure. The separation trajectory plotted in grey is used as the basis for further analysis in Figure 5-6 Simulation conditions are presented in Appendix B.

Specific details of these regimes are presented in Table 5-1. Strategy A is the most 'aggressive' diafiltration regime, applying greater amounts of diafiltration into fewer stages. This regime produces a noticeable peak in concentration (often called 'backup') just prior to the first diafiltration stage (Figure 5-1A). Such an effect is undesirable within a plant, since high concentrations generally cause excessive membrane fouling. Very high protein concentrations within a WPC plant also cause a significant increase in viscosity (called 'gelling'), and pumping difficulties as a result. The other strategies apply diafiltration at a lower rates (smaller ϕ_i) to a greater number of stages, achieving the desired retentate concentration and purity without causing backup within the plant.

Table 5-1 Details of steady state diafiltration strategies - case study 1

Diafiltration regime	Number of stages receiving diafiltration	Stage diafiltration ratio ϕ_i	Overall diafiltration ratio ϕ_o
Strategy A	5	0.910	0.061
Strategy B	6	0.660	0.089
Strategy C	8	0.495	0.158
Strategy D	10	0.418	0.240

The amount of diafiltration injected into a plant can be expressed as a fraction of the feed flow rate F_F, called the overall diafiltration ratio ϕ_o:

$$\phi_o = \frac{\sum_{i=1}^{n} F_{Pi}\phi_i}{F_F} \qquad \textbf{(5-1)}$$

For the WPC case study, the application of large amounts of diafiltration into the final stages of a plant gives a low overall diafiltration ratio (Figure 5-2), corresponding to greater separation efficiency and minimal diafiltration water requirements. Diafiltration Strategy A (Figure 5-2, Table 5-1) offers the lowest overall diafiltration ratio and most efficient use of diafiltration water. This strategy also gives a higher permeate concentration, which is desirable if lactose is recovered from the permeate stream. However, as discussed above, this strategy also causes undesirable concentration peaks within the plant. Thus there is evidence of a conflict between optimal process design (maximising separation efficiency) and process controllability (avoiding undesirable behaviour such as extreme backup).

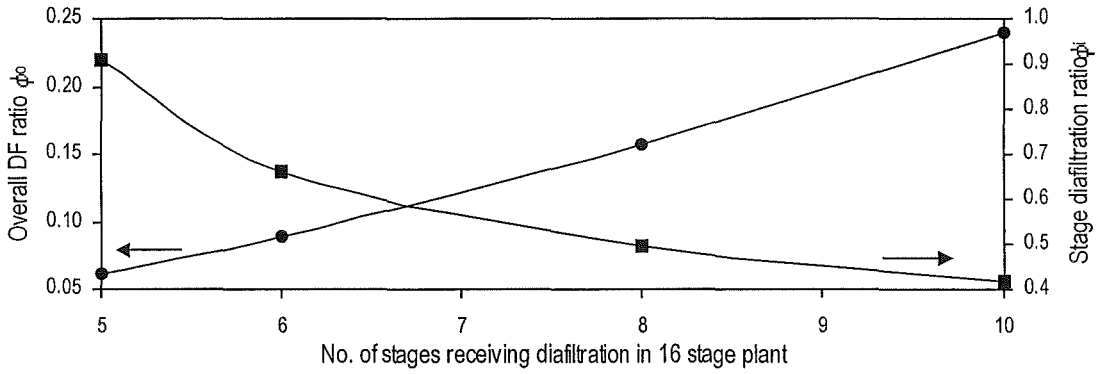

Figure 5-2 Effect of different diafiltration regimes on overall diafiltration ratio - case study 1
See Table 5-1 for full details of the diafiltration strategies shown in this figure.

She (1998) showed that the fundamental characteristics of a separation could be examined by plotting purity against total solids concentration (Figure 5-3A) with Point 1 representing the feed stream and Point 2 the desired retentate stream properties. For a process with no diafiltration, a theoretical plant with many small stages has a trajectory from Point 1 that is uniquely specified by the characteristics of the separation (i.e. retention coefficients) This path is independent of plant design or permeate fluxes. Likewise, the path to a desired retentate stream (Point 2) can also be calculated. It was demonstrated by She (1998) that these properties also hold for a physical plant with fewer stages, with the concentration and purity of each stage falling very close to this trajectory (Figure 5-3B). For a plant operating with a variable number of stages, the

positions of the operating stages will change over time, but the trajectory will remain nearly the same.

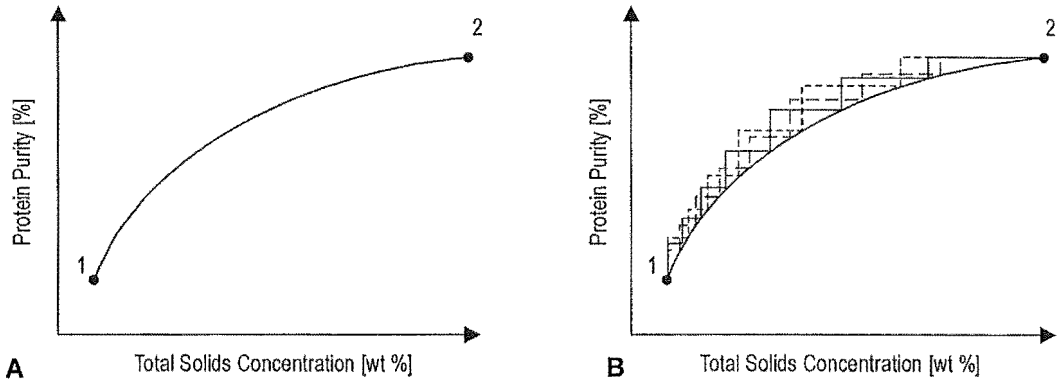

Figure 5-3 Separation trajectory schematics - case study 1

For the WPC case study diafiltration is necessary to move from the low purity trajectory beginning at Point 1 to the high purity path finishing at Point 2 (Figure 5-4). Therefore, the separation can be considered as a two-point boundary value system, with a number of possible paths (diafiltration regimes) between these points.

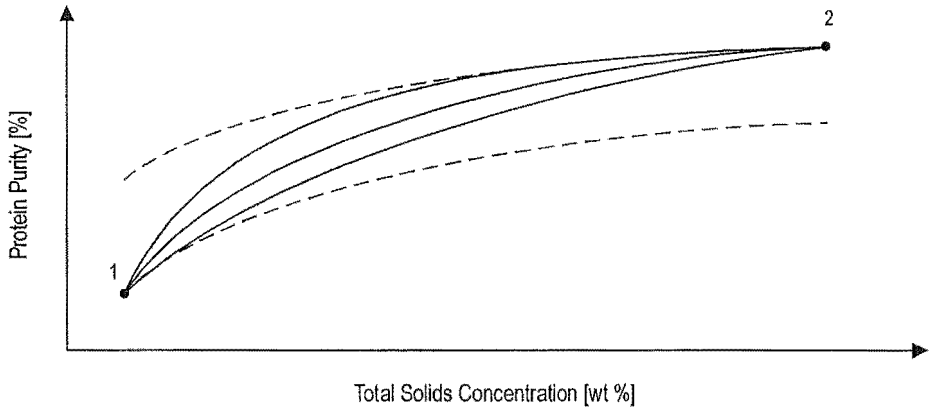

Figure 5-4 Separation trajectory schematics for multistage separation with diafiltration - case study 1

Dashed lines represent the trajectory with no diafiltration injection

Replotting the plant profiles presented in Figure 5-1 it can be seen that the diafiltration regimes produce significantly different separation trajectories (Figure 5-5). In this representation the effect of diafiltration injection is clear, with significant purification (fractionation) achieved at the cost of reduced concentration. The concentration peak for the 'optimal' diafiltration regime (Strategy A) can still be seen.

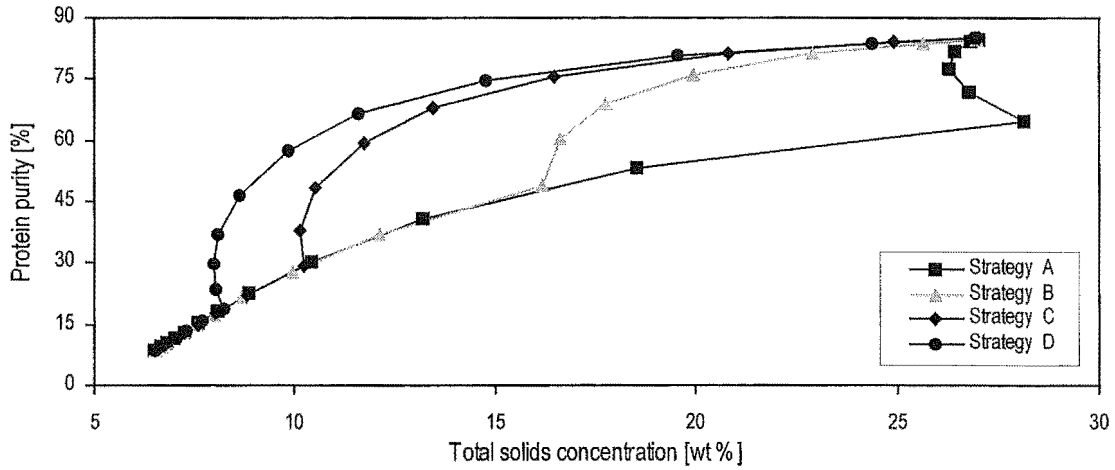

Figure 5-5 Separation trajectories for different diafiltration regimes - case study 1
See Table 5-1 for full details of the diafiltration strategies shown in this figure. The separation trajectory plotted in grey is used as the basis for further analysis in Figure 5-6. Simulation conditions are presented in Appendix B.

For a plant receiving diafiltration injection, the effect of new stage addition on the separation trajectory is not clear. Steady state simulation for Strategy B (Figure 5-6) shows that the separation trajectory remains a stable, even when new stages are added. For a given value of ϕ_{max}, there exists a single value of ϕ_0 which produces the desired retentate stream concentration and purity. Figure 5-7 shows that the value of ϕ_0 remains (almost) constant as new stages were added. This is in contrast with Figure 5-2.

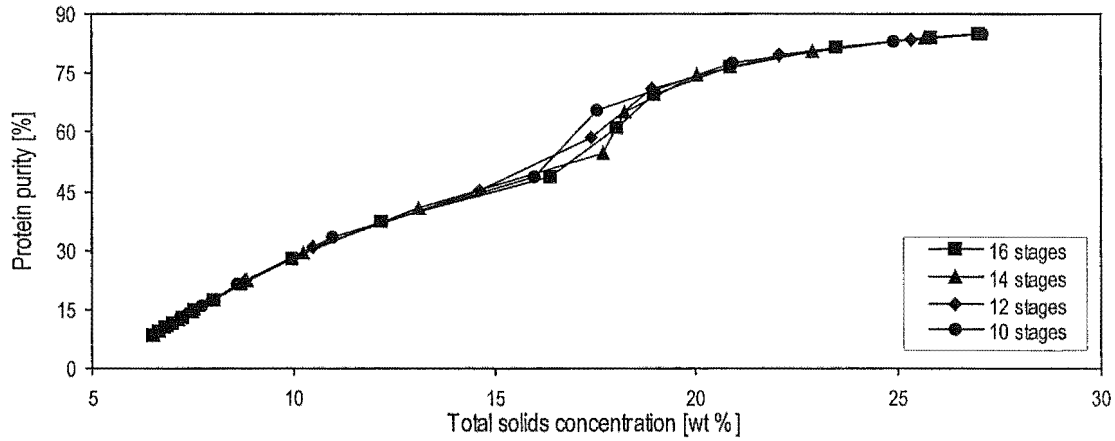

Figure 5-6 Separation trajectories for process operating with different number of stages but achieving the same product specification - case study 1
The maximum diafiltration ratio to any stage ϕ_{max} = 0.66, based on Strategy B in Figure 5-5. Overall diafiltration ratios associated with each separation trajectory are shown in Figure 5-7. Simulation conditions are presented in Appendix B.

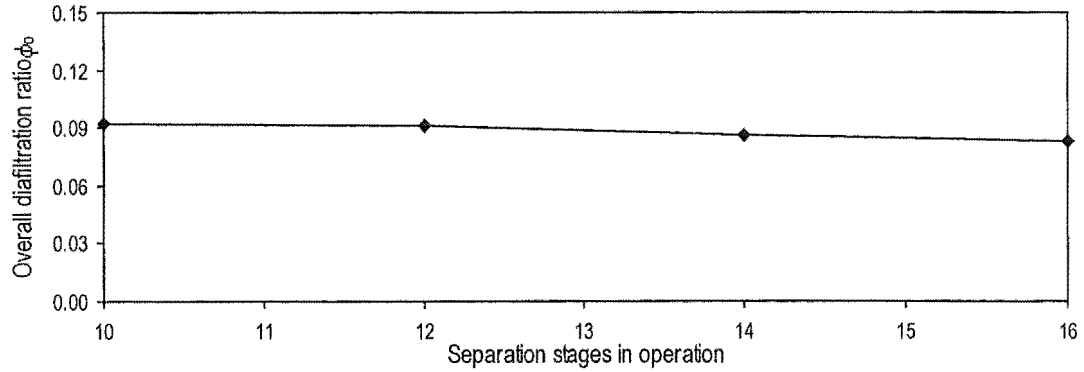

Figure 5-7 Diafiltration requirements for process operating with different number of stages but achieving the same product specification - case study 1

Maintaining a constant overall diafiltration ratio can only be achieved by manipulating some or all stage ratios in the plant. This is best achieved by varying the ratio of the first diafiltration stage, and fixing the remaining stage ratios at a chosen value ϕ_{max}. For a given overall diafiltration ratio, the value of the manipulated or variable diafiltration ratio ϕ_v can be calculated using the algebraic relation:

$$\phi_v = \phi_o F_F - \sum_{j=2}^{k} \phi_{\max} F_{P,j} \tag{5-2}$$

where the current number of stages k receiving diafiltration was manipulated as necessary to maintain ϕ_v within the limits

$$0 \leq \phi_v \leq \phi_{\max} \tag{5-3}$$

Two main conclusions regarding the control of multistage membrane processes can be drawn from this analysis; a conflict may occur between process design optimisation and process controllability, and the overall diafiltration ratio is an important parameter for the control of plants operating with a variable number of stages.

5.2.2 Case study 2: Permeate product separation

Permeate product separations have many similarities to retentate product systems (the mechanisms are of course the same), but the variables of interest are different. It is desired in this case study that a valuable permeable component be recovered from a feed stream containing an impermeable impurity. A yield of 75 % is desired for this separation, so diafiltration injection will be necessary. The total solids concentration profile for the 16 stage plant is shown in Figure 5-8A, for four different diafiltration strategies. Specific details of these regimes are presented in Table 5-2. Strategy A is the most aggressive, but unlike case study 1, this strategy does not cause backup to

occur within the process. The propensity of a process to exhibit backup is determined by the feed stream concentrations, and retention coefficients of the components. In this case study, Components A and B have reasonably similar retention coefficients (1.0 and 0.7 respectively), making the occurrence of backup within the plant less likely.

Table 5-2 Details of steady state diafiltration strategies - case study 2

Diafiltration regime	Number of stages receiving diafiltration	Stage diafiltration ratio ϕ_i	Overall diafiltration ratio ϕ_o
Strategy A	8	0.648	0.123
Strategy B	10	0.466	0.175
Strategy C	12	0.379	0.241
Strategy D	14	0.330	0.315

In this case study, the retentate total solids concentration is maintained as high as possible (17 wt %), in order to increase the residence time within the plant, and maximise recovery of the valuable component (Component B) in the permeate stream. Operation at a higher concentration is undesirable, due to concentration polarisation limits (C_{gel} = 20 wt %). The cumulative yield profile shown in Figure 5-8B is essentially independent of diafiltration strategy, much like the purity profile in the first case study.

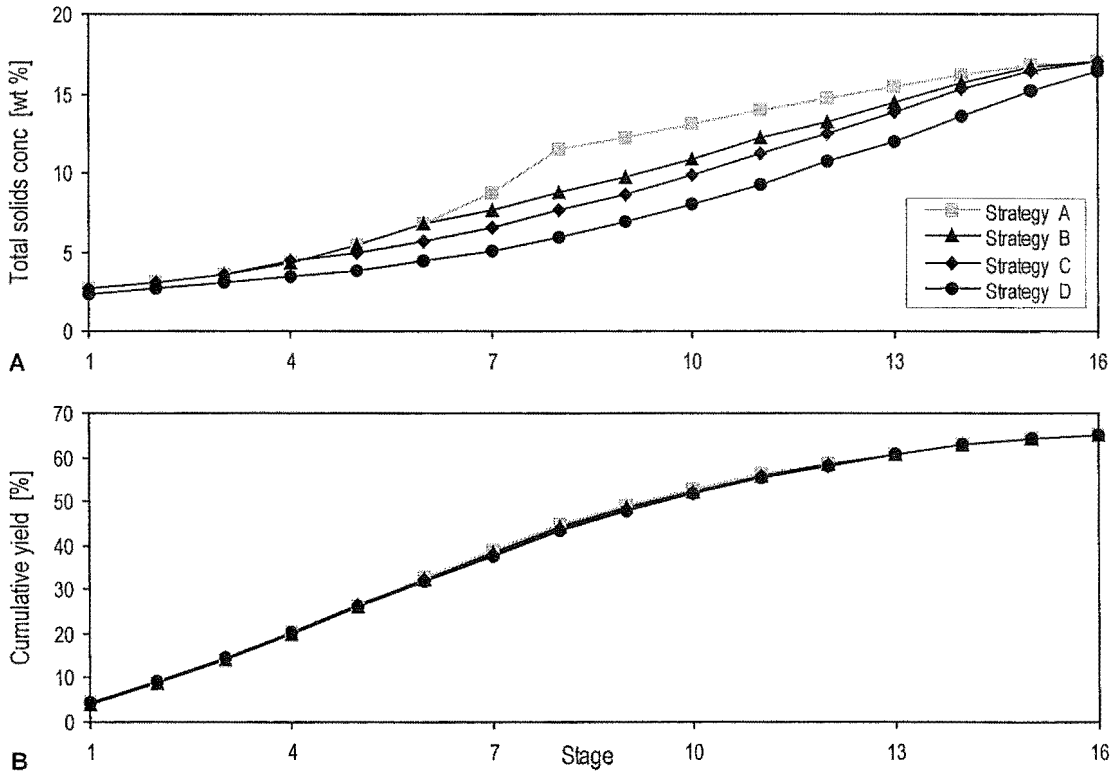

Figure 5-8 Concentration and purity profiles for different diafiltration regimes - case study 2
See Table 5-2 for full details of the diafiltration strategies shown in this figure. The separation trajectory plotted in grey is used as the basis for further analysis in Figure 5-12. Simulation conditions are presented in Appendix B.

More aggressive diafiltration strategies have little effect on the yield profile, although Figure 5-9A shows that such strategies do reduce the total diafiltration water requirements of a plant. With a smaller volume of water injected into the plant, permeate total solids concentration (Figure 5-9B) is higher, reducing the load on the permeate dewatering process downstream.

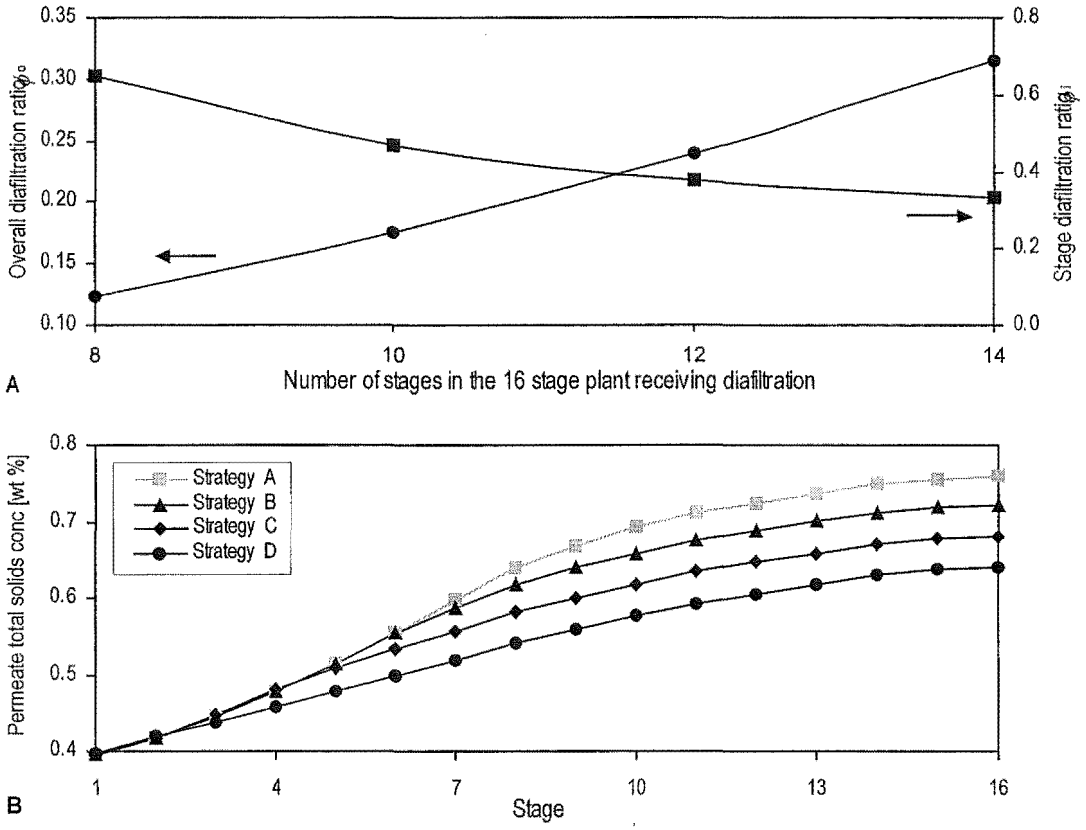

Figure 5-9 Effect of different diafiltration regimes - case study 2
See Table 5-2 for full details of the diafiltration strategies shown in this figure. The separation trajectory plotted in grey is used as the basis for further analysis in Figure 5-12. Simulation conditions are presented in Appendix B.

The separation trajectory concept presented by She (1998) was originally applied to retentate product systems, but it still applicable to permeate product separations. As for case study 1, a representation is sought that gives a single trajectory which is independent of membrane fouling and permeate flux. For case study 2, the separation trajectory can be created by plotting Component A purity against total solids concentration for each stage (Figure 5-10). Defining the separation in terms of the purity of the retained component may seem unusual, but it can be shown that permeate yield is proportional to the composition of the retentate stream (for a given feed stream composition). Provided the retentate stream maintains the desired composition, then the desired permeate yield will also be achieved.

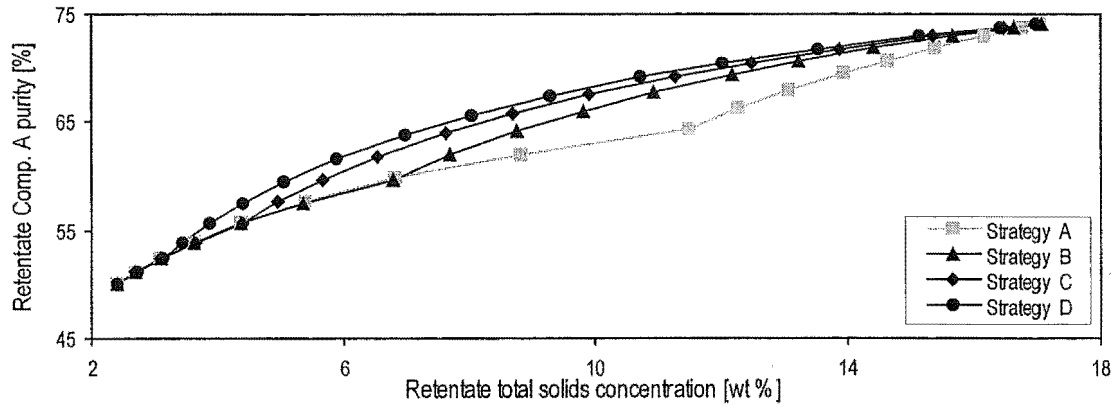

Figure 5-10 Retentate-based separation trajectories for different diafiltration regimes - case study 2
The separation trajectory plotted in grey is used as the basis for further analysis in Figure 5-12. Simulation conditions are presented in Appendix B.

It is possible also to construct a separation trajectory in terms of permeate yield (Figure 5-11), but this representation is more dependent on operating conditions (e.g. retentate flow rate) than Figure 5-10, so does not possess the attractive characteristics of the concentration-purity trajectory. It is undesirable to use the yield as a direct control variable, since accumulation within the plant and the addition of new stages will cause large fluctuations in this calculated variable.

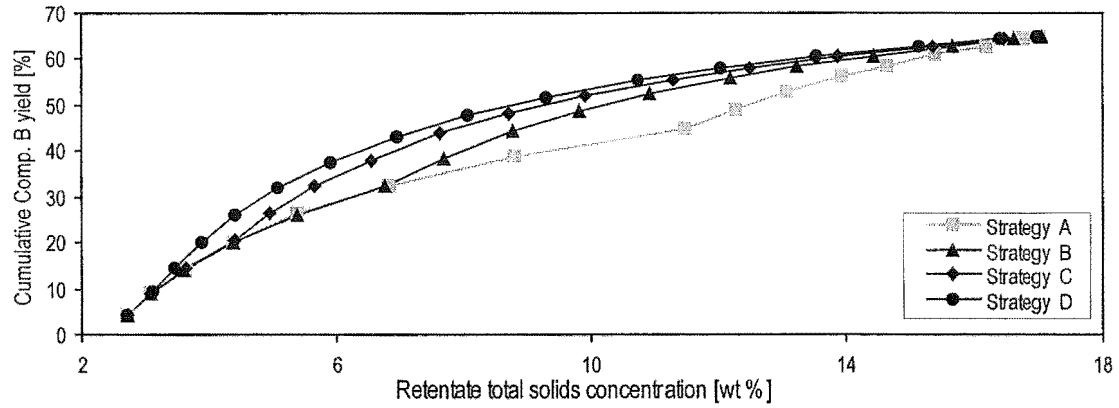

Figure 5-11 Yield-based separation trajectories for different diafiltration regimes - case study 2
The separation trajectory plotted in grey is used as the basis for further analysis in Figure 5-12. Simulation conditions are presented in Appendix B.

Using a simple example, it can be shown that the separation trajectory of this case study also remains constant even when the number of stages in the plant varies. The maximum diafiltration ratio of any stage ϕ_{max} was restricted to 0.65 which corresponded to Strategy A (shown in grey in Figure 5-10 and Figure 5-11). Diafiltration was applied to the final stages of the plant. Steady state separation trajectories are shown in Figure 5-12 for the case study plant operating with 10, 12, 14 and 16 stages. Since all four simulations follow the same path, regardless of membrane area distribution, it is clear

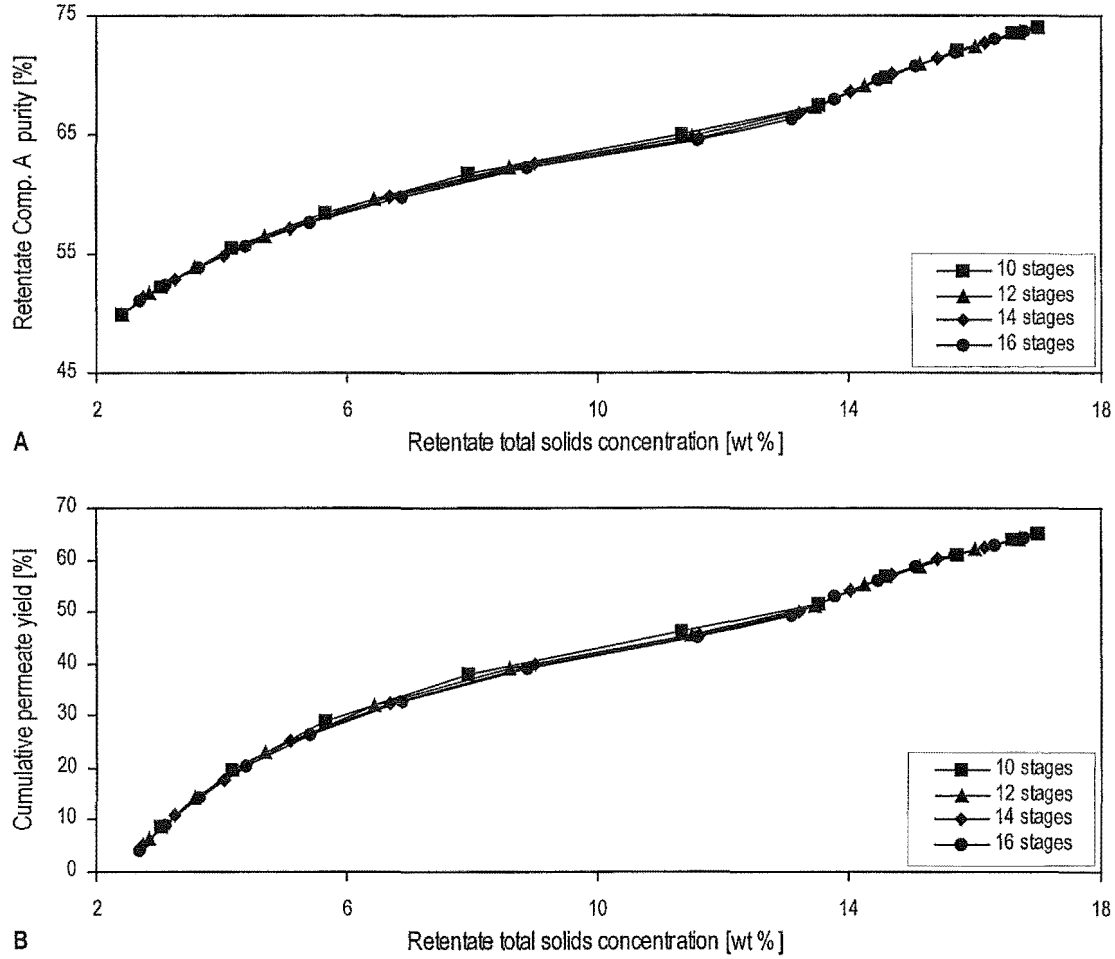

Figure 5-12 Separation trajectories for several flowsheets achieving the same product specification - case study 2

Simulation conditions are presented in Appendix B.

that the yield objective can be consistently achieved by maintaining an appropriate separation trajectory. The overall diafiltration ratio (Figure 5-13) can be seen to be little affected by the number of stages operating in the process.

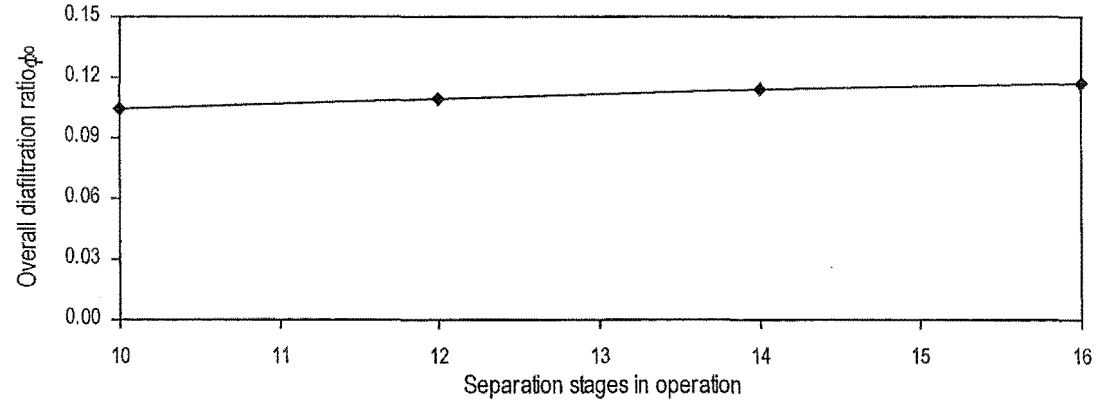

Figure 5-13 Diafiltration requirements for several flowsheets achieving the same product specification - case study 2

Simulation conditions are presented in Appendix B.

It is evident that the overall diafiltration ratio is an important parameter for process control. This is the same conclusion as that presented for the case study 1 in Section 5.2.1, despite this separation producing a permeate product. The analysis presented in this section highlights the usefulness of the separation trajectory concept, as a tool for investigating membrane separations. Although backup did not occur in this case study, it is possible that it may still occur in other permeate product separations.

5.3 Controllability assessment using linearised process models

A number of tools exist for dynamic controllability assessment, but the vast majority require a linear time invariant system (Morari & Perkins, 1995). Unfortunately, the general equation set developed in Section 3.3 for a multistage membrane plant is non-linear, and so must be linearised. A state space model of the form:

$$\begin{aligned} \dot{x} &= \mathbf{A}x + \mathbf{B}u \\ y &= \mathbf{C}x + \mathbf{D}u \end{aligned}$$

is a complete representation of dynamic system behaviour about a chosen operating (linearisation) point for a specified set of inputs u and outputs y.

Analysis of the structural system models in Chapter 4 focused on the properties of the **A** matrix. The positions of entries in this matrix provided information on the inherent behaviour of the system. In both case studies, oscillatory system states and inverse response behaviour were identified as being structurally feasible. Analysis of numerical state space models allows the presence of such behaviour to be confirmed or rejected.

A steady state Simulink model was developed for each case study, using the same system inputs and outputs as the structural models of Chapter 4, with the exception of the manipulated diafiltration ratios. For the analysis performed in this chapter, the manipulated diafiltration ratio input ϕ_r was chosen as either the first or last stage in the process receiving diafiltration injection. This allowed the system response to be compared for these two inputs, and a preferred position identified for the manipulated ratio ϕ_r (Equation 5-2).

Linearised state space models were constructed at the desired steady state operating point using the linear time invariant methods available in the Control Toolbox (MathWorks, 1999) in Matlab.

5.4 Pole-zero analysis of numerical system models

In Section 4-3 it was determined that 'key' components, i.e. those affecting permeate fluxes, had a significant effect on dynamic plant behaviour. In particular, it was found that the response dynamics for disturbances in key components were complex lead-lag functions, with both oscillatory and inverse response behaviour structurally possible. Numerical system models can be used to determine if these undesirable characteristics actually occur in each case study. The dynamic response of a specific process output y to a given input or disturbance u can be expressed as a transfer function $g_{uy}(s)$, constructed from the state space model of the system. Pole-zero maps are a means of graphically presenting information about this transfer function (Stephanopoulos, 1984). Poles (denoted '×') are roots of the denominator, and zeros (denoted 'o') roots of the numerator of $g_{uy}(s)$.

The presence and number of poles and zeros for each input-output sequence in the case studies were examined in Chapter 4 using the structural system model. However, the actual placement of the poles and zeros could not be determined from a structural model, since this was dependant on the characteristics of the plant, parameters used in the permeate flux and retention coefficient models, and operating conditions. The availability of a numerical state space model for each case study allows the positions of these poles and zeros to be mapped, and the actual characteristics of each process (under the specified operating conditions) to be determined.

5.4.1 Pole-zero map properties

A pole-zero map is a graphical representation of the transfer function relating a given input to a specified output. It provides information on the general dynamic characteristics of the process, but does not predict the plant response to a specific input (e.g. a ramp input), nor does it supply information on the process gains between an input-output pairing. Pole-zero maps also do not determine the level of interaction between this and any other input-output pairings. Interaction information can only be determined using other controllability assessment analysis tools such as the relative gain array (RGA). An overview of this tool, and its application to the separation case studies is presented in Sections 5.6 and 5.7.

Significant information can be gleaned from the position of poles and zeros on a map (Nagrath & Gogal, 1982):

1) A system pole with a positive real component, i.e. one lying in the right half plane, shows the process is unstable.
2) The presence of an imaginary component in a pole indicates underdamped or oscillatory behaviour within the system.
3) A polemap with an odd number of zeros with a positive real component indicates the presence of inverse response behaviour within the system (Morari & Zafiriou, 1989).
4) A pole positioned on the origin of a pole-zero map is a pure integrator, which makes it difficult for plant to achieve steady state.
5) The existence of a zero on, or close to a pole represents a cancellation in the transfer function $g_{wp}(s)$, and the associated dynamics are not exhibited in the system output.
6) A process time constant can be calculated from the real component of a pole or eigenvalue λ by:

$$\tau_i = \frac{-1}{\lambda_i} \tag{5-4}$$

A pole positioned near the origin has a large time constant τ, and slow system dynamics.

The presence of characteristics 1) to 4) are undesirable, since they limit the closed-loop performance of a feedback controller (Morari, 1983). Likewise, the presence of very slow system dynamics limits achievable closed-loop performance since slow process startup and setpoint changes are unavoidable.

5.4.2 Pole-zero analysis of a simple three tank example system

Before examining pole-zero maps for each case study, it is useful to briefly return to the three tank system presented in Section 4.2.4. In this example, the dynamic characteristics of sequential and cascaded flowsheet arrangements were examined. Analysis of the non-numerical models showed that underdamped response characteristics were structurally possible in the sequential flowsheet. The cascaded flowsheet had a less complex dynamics, with no possibility of oscillatory behaviour occurring in this system.

If the coefficients for the sequential (Equation 4-3 to 4-5) and cascaded (Equation 4-8 to 4-10) equation sets are specified it becomes possible to construct complete (linearised)

state space models representing the two flowsheets. In the interests of simplicity it was assumed that all three tanks had equal cross-sectional area (A_{Tank} = 2 m^2) and discharge coefficients (k_d = 0.04 m$^{2.5}$ s^{-1}). Placement of the poles and zeros on the map is also determined by the operating conditions of the system. In this case, it was assumed that both flowsheets operated with a constant feed flow rate, F_{in} = 0.05 m^3 s^{-1}.

Equation 4-13 predicted the presence of third-order dynamics within both flowsheets. The corresponding pole-zero map shown in Figure 5-14 had three poles, all of which lay in the left half plane, meaning that the open-loop system was stable. The absence of imaginary components in the system poles shows that the process does not contain oscillatory process characteristics (at that operating point), even though they were structurally possible. The transfer functions for the two flowsheets were identical, yet the pole-zero map for the cascaded process (Figure 5-14B) appears to show only a single pole (eigenvalue). This process actually has three identical poles, due to the parameters for the three tanks being the same. As predicted, the poles were not complex and did not contain imaginary components.

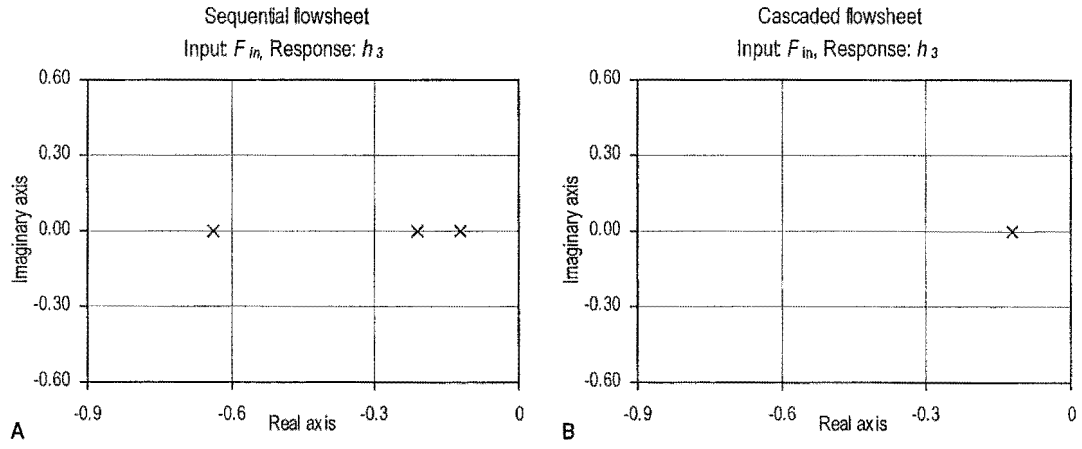

Figure 5-14 Pole-zero maps for three tank example system

Placement of the real components of the poles also provides information on the speed of the system dynamics (Equation 5-4). In the sequential system, the system time constants differed significantly between the tanks (24, 72 and 125 seconds). The cascaded flowsheet had three identical time constants of τ = 125 seconds, making this system the slower of the two. Contrary to the structural system analysis, the numerical analysis suggests that the sequential flowsheet may actually have superior controllability. This situation highlights the difficulties encountered when assessing the controllability of a process, where conflicting results may be provided by different assessment methods.

5.4.3 *Case study 1: Whey protein concentrate production*

A 16 stage WPC plant was simulated in Simulink with 2 bar feed pressure, and retentate total solids concentration of 27 wt %. Diafiltration was applied according to the strategy presented in Equations 5-2 and 5-3, with and $\phi_{10} = 0.1$ and ϕ_{11} to $\phi_{16} = 0.7$. A linearised state space model was constructed for analysis at this steady state operating point. Pole-zero maps were generated from this model using the linear time invariant system tools in the Matlab Control Toolbox (MathWorks, 1999) for selected input and output variable pairings.

Figure 5-15 shows pole-zero maps representing the dynamic relationship between retentate total solids concentration and protein (key component) and lactose (non-key component) feed concentration inputs. For the lactose feed concentration (Figure 5-15A), there were 16 poles corresponding to the number of stages in the plant. These poles contained no imaginary components meaning that process dynamics corresponding to the lactose concentrations (states) were non-oscillatory; a result that was demonstrated in Section 4-3 to be true for all non-key components in a multistage membrane separation. The absence of zeros was also predicted by the lactose response transfer function (Equation 4-17). Using the pole-zero map it can now be determined that the system is open-loop stable for any lactose feed concentration input, since all poles lie in the left half plane.

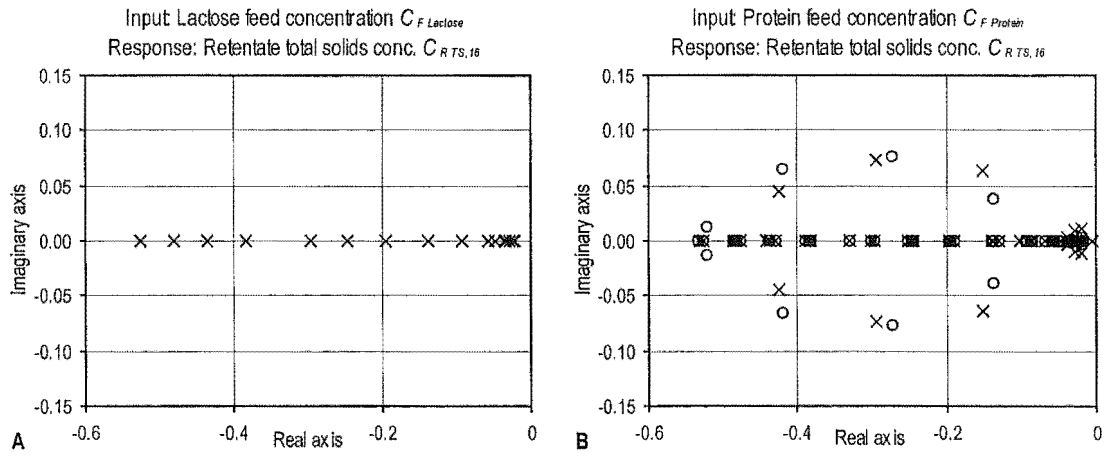

Figure 5-15 Pole-zero maps for transfer functions relating retentate total solids concentration to lactose and protein feed concentration

The lactose time constant $\tau_{Lactose,i}$ for a separation stage can be derived by rearranging and linearising the differential component balance (Equation 3-25):

$$\tau_{Lactose,i} = \frac{\rho_i V_i}{F_{p,i}(1-R_{Lactose}) + F_{R,i}} \quad (5\text{-}5)$$

Since the retentate flow rate from each stage $F_{R,i}$ decreases more than stage volume V_i, the largest time constants in the process generally correspond to the downstream separation stages. Therefore the eigenvalue closest to the origin in the pole-zero map (Figure 5-15A) is that of the final stage, from which the product stream is drawn. Thus λ_{16} = -0.022 corresponds to a final stage time constant $\tau_{Lactose,16}$ of 45 seconds.

The dynamic characteristics of the relationship between the retentate total solids concentration and feed concentration input is much more complicated for key components such as protein (Figure 5-15B). It was determined from analysis of the structural model that the response had high order lead-lag dynamics, and this was shown in the pole-zero map. Because the retentate total solids concentration is the sum of all concentrations in this stream, the number of poles in the plot depends on both the number of stages n in operation and the number of components j in the feed stream. The pole-zero map for this case study contained a total of 96 poles (all system states), since the plant had 16 stages and was processing a feed stream containing six components. Such behaviour is caused by the widespread disturbance propagation characteristics of key components in membrane separations, where a concentration disturbance in one stage propagates to all components in all other stages of the plant.

It was shown in Section 4.3 that it was structurally feasible for the states of key components to exhibit oscillatory characteristics. The presence of conjugate pairs of poles in Figure 5-15B proves such behaviour to be present in the process. However the existence of zeroes close to all oscillatory poles suggests reasonable cancellation, meaning that whilst the states have oscillatory characteristics, underdamped behaviour is unlikely to be apparent in the behaviour of the retentate total solids concentration. With no zeros lying in the right half plane, the process did not exhibit inverse response characteristics. Analysis in Section 4.3 showed that oscillatory system behaviour was only structurally possible when concentration dependent permeate fluxes were present, causing concentration-flow rate interaction within the plant.

The 'slowest' eigenvalue in the pole-zero map (Figure 5-15B) corresponded to a time constant of 236 seconds. Because the section of the **A** matrix corresponding to the key component states was not diagonal, it is not possible to relate individual time constants to specific components or stages. However, as a general trend the time constants for each component are dependent on the retention coefficient (Equation 5-5). Components with large retention coefficients (e.g. protein and fat) will therefore have larger time constants than the more permeable components such as lactose and minerals. This is clearly illustrated in Figure 5-16, where the concentrations of protein and lactose in the retentate stream have significantly different response speeds during start-up. Retentate total solids concentration is the sum of all component concentrations in the stream, but is usually dominated by the slower dynamics of fat and protein, particularly at high product purities.

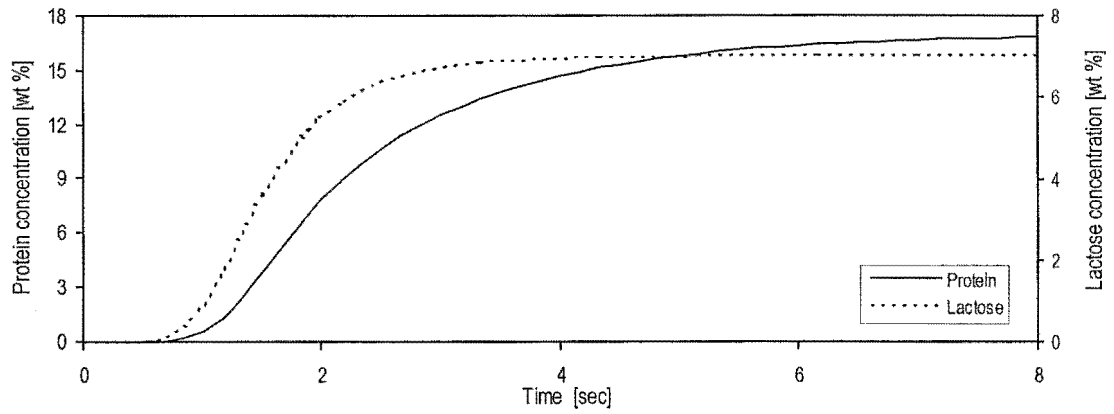

Figure 5-16 Behaviour of protein and lactose in retentate stream during start-up - case study 1
Based on the open-loop simulation for case study 1, presented in Figure 3.7.1.

Feed flow rate to the plant is usually controlled through the addition of membrane area and manipulation of the plant feed pressure. A pole-zero map for feed flow rate response to a feed pressure input is shown in Figure 5-17A. It can be seen that there was almost perfect pole-zero cancellation, suggesting no significant response dynamics existed and there was an almost direct relationship between the input and output variables. Cancellation of the imaginary system poles means that oscillatory behaviour will not be evident in the feed flow rate response to changes to feed pressure.

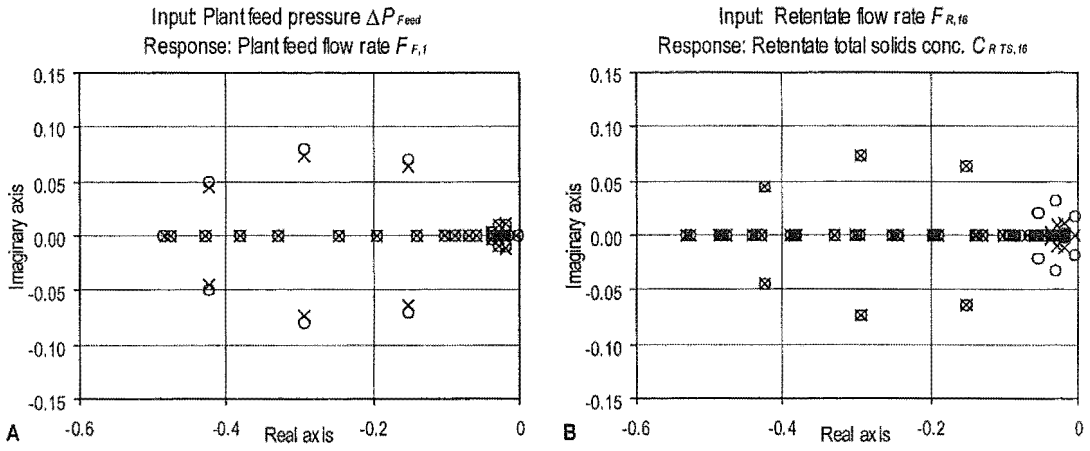

Figure 5-17 Pole-zero maps for transfer functions relating feed pressure to feed flow rate, and retentate flow rate to retentate total solids concentration

Simulation conditions are presented in Appendix B.

Retentate flow rate is commonly used to control the total solids concentration of the stream, and a pole-zero map of this pairing shown in Figure 5-17B. The system response had very high order lead-lag dynamics as predicted from structural model analysis, but almost complete cancellation of the faster process dynamics. Therefore the behaviour exhibited by the plant, and seen by a total solids controller, will be of much lower order and dominated by the poorly cancelled slower poles and zeros.

The effect of flowsheet design on system behaviour was examined by constructing a series of linearised plant models, each with different number of stages but the same operating point (27 wt % retentate total solids concentration). Analysis of the eigenvalues for each system showed oscillatory behaviour to be present in all flowsheet designs with 11 stages or more, regardless of retentate protein fraction. Plants with more stages had a greater number of oscillatory poles. This analysis was repeated for different permeate flux parameters and operating conditions, and it was consistently found that oscillatory poles appeared, and became more prevalent, as the number of stages in the flowsheet increased. Whilst there was some variation in the exact point at which the oscillatory behaviour first appeared, it can be concluded that the presence of such behaviour is influenced by flowsheet design. Separation efficiency increases with the number of stages in a flowsheet, and so design optimisations tend to favour such plants. However the analysis performed here suggests that process controllability is reduced in the region of the design optimum.

5.4.4 Case study 2: Permeate product separation

The steady state behaviour of this permeate product case study was modelled in Simulink, for a plant operating with 16 stages. Diafiltration was applied according to the strategy presented in Equations 5-2 and 5-3. Significant amounts of diafiltration were required to achieve the desired recovery of Component B in the permeate stream, with $\phi_6 = 0.4$, and ϕ_7 to $\phi_{16} = 0.7$. Linearisation of the Simulink model was performed when the process was operating with a feed pressure of 2 bar and retentate total solids concentration of 17 wt % .

Analysis of this case study focuses on permeate stream response characteristics for several different inputs. The key component (A) was not permeable, so did not directly affect the permeate stream composition or yield. However, the concentration dependence of the permeate flux meant that disturbances in the key component still affected the permeate stream (Figure 5-18A). Unfortunately, with pole-zero maps, it is not possible to determine the magnitude of these disturbances. The zero in the right half plane represents the presence of inverse response behaviour, which has very undesirable effects on controller performance. Analysis shows permeate yield to have almost identical response dynamics (pole-zero map) for the same input.

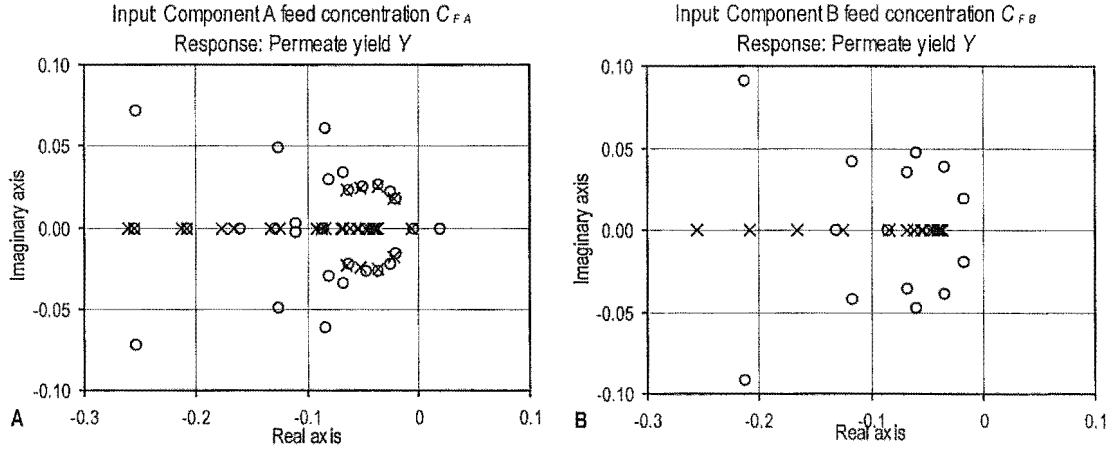

Figure 5-18 Pole-zero maps for transfer functions relating permeate yield to Component A and B feed concentration

Simulation conditions are presented in Appendix B.

Retentate stream response to a disturbance in the non-key component (B) was found to be 16th order and non-oscillatory, as was the situation for lactose in case study 1. The response dynamics of the permeate stream total solids concentration were almost identical to yield (Figure 5-18B) for a feed concentration disturbance in Component B.

However, unlike case study 1 the pole-zero map contained a number of zeros, due to the calculated permeate yield being simultaneously dependent on the Component B mass flux from every stage in the plant. Thus a disturbance in a key component will propagate to component concentrations in other stages causing simultaneous disturbances to pass into the plant permeate stream in parallel.

The effect of flowsheet design on the behaviour of this second case study was examined by constructing and analysing several flowsheets each with different number of stages, but identical retentate total solids concentration. It was found that a plant design with 7 stages or more had oscillatory eigenvalues. Equivalent behaviour was found for a range of different permeate flux parameters and operating conditions, although the onset of oscillatory behaviour was dependent on the conditions. The general conclusion was that oscillatory poles appeared, and were present in greater numbers, as the number of stages in the flowsheet increased. This result was expected since the problem of interaction, and the disturbance propagation mechanisms within multistage membrane plants (i.e. inherent plant characteristics represented in the **A** matrix of the process model) were identical for both retentate and permeate product situations. Only the outputs (**C** matrices) of the case study systems differ. Therefore, both situations have the same characteristics, but their apparent behaviour is not the same, because different streams are being observed.

Feed flow rate for this case study is controlled by manipulation of the plant feed pressure. The pole-zero map for this input-output pairing (Figure 5-19A) showed a high degree of cancellation. The poles in this plot corresponded to the key component, since permeate flow rate (and hence feed flow rate) were dependent on this component alone. The level of cancellation means that most response dynamics for this input-output pairing will not be observed. The relationship between retentate flow rate and permeate total solids was more complex (Figure 5-19B), since it depended on all system states. There was again a high level of cancellation suggesting that the permeate total solids concentration may not be visibly oscillatory, even though oscillatory characteristics may be present within the **A** matrix.

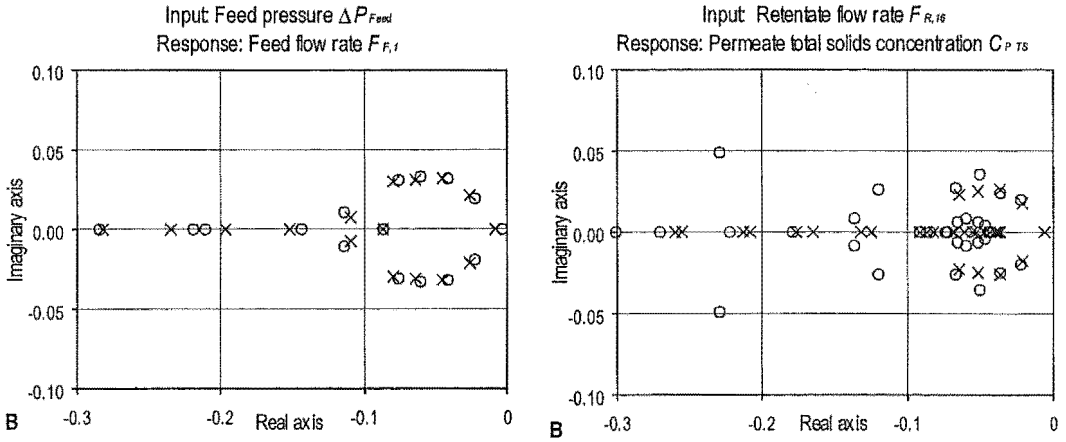

Figure 5-19 Pole-zero maps for transfer functions relating feed flow rate to feed pressure and permeate total solids concentration to retentate flow rate

Simulation conditions are presented in Appendix B.

5.5 Effect of diafiltration on plant behaviour

It was stated in Section 5.4 that each case study became oscillatory with increasing number of separation stages. Winchester (1996) suggested that the presence of such behaviour was influenced by diafiltration injection. The effect of diafiltration on the onset of oscillatory behaviour was examined for each case study using linearised steady state Simulink models. In both separations ratio-controlled diafiltration injection was applied to the downstream half of the plant. Equal ratios ϕ were used for all stages, with comparisons made at constant retentate total solids concentration.

5.5.1 Case study 1: Whey protein concentrate production

The effect of diafiltration injection on natural system dynamics is shown in Figure 5-21, for several different plant flowsheets, each producing a retentate stream with total solids concentration of 27 wt %, and operating at a feed pressure of 2 bar. The critical diafiltration ratio plotted in this graph represents the lowest diafiltration ratio at which the linearised plant model exhibited oscillatory eigenvalues. The corresponding retentate protein purity is also plotted on the same graph. An 85 % protein purity specification for the 16 stage WPC plant (Section 2.5.1) places this plant well inside the region of oscillatory behaviour, above the critical diafiltration curve. The results calculated for this example cannot be directly applied to an industrial WPC plant due to simplifications made developing the model, but the results suggest that oscillatory behaviour is highly possible for a large industrial plant producing a high purity retentate product.

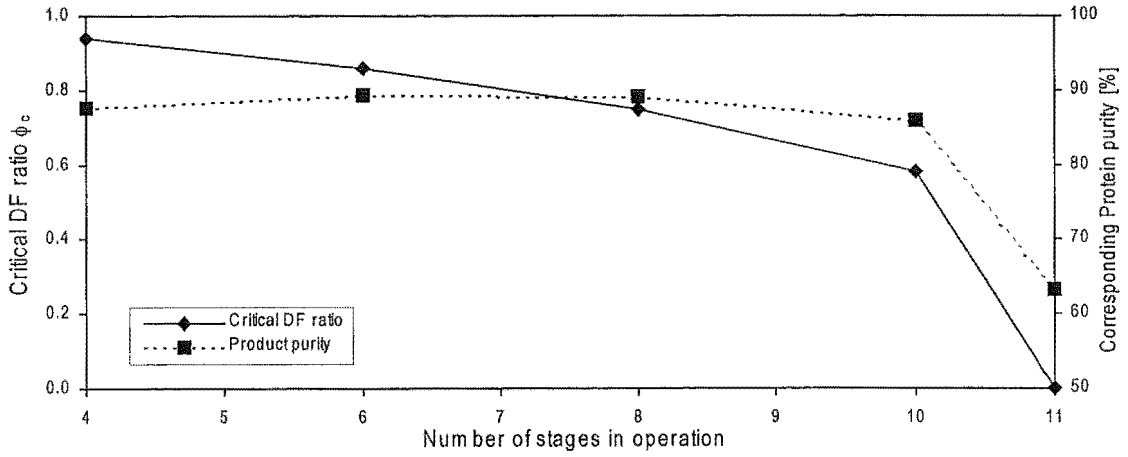

Figure 5-21 Effect of diafiltration on the onset of oscillatory behaviour - case study 1

Process response of the 16 stage plant to diafiltration injection disturbances or inputs was discussed in Section 4.3.1, and it was concluded that the order of the retentate purity response was dependent on the point of injection. The pole-zero maps presented in Figure 5-20 are in agreement. The transfer function relating retentate protein purity response to manipulation of the diafiltration ratio to stage 10 (the first stage receiving diafiltration injection in the steady state example system) was particularly complex. Of concern was the presence of zeros in the right half plane representing inverse response behaviour. Simulation has shown such behaviour can occur during closed-loop operation of a plant with diafiltration injection (Hunter & Morison, 1997). Retentate protein purity response to manipulation of the stage 16 diafiltration ratio (the final stage of the plant) was much less complex, although the magnitude of the resulting protein purity disturbance cannot be determined from the pole-zero map. The diafiltration ratio of the final separation stage is not usually manipulated industrially, since disturbances

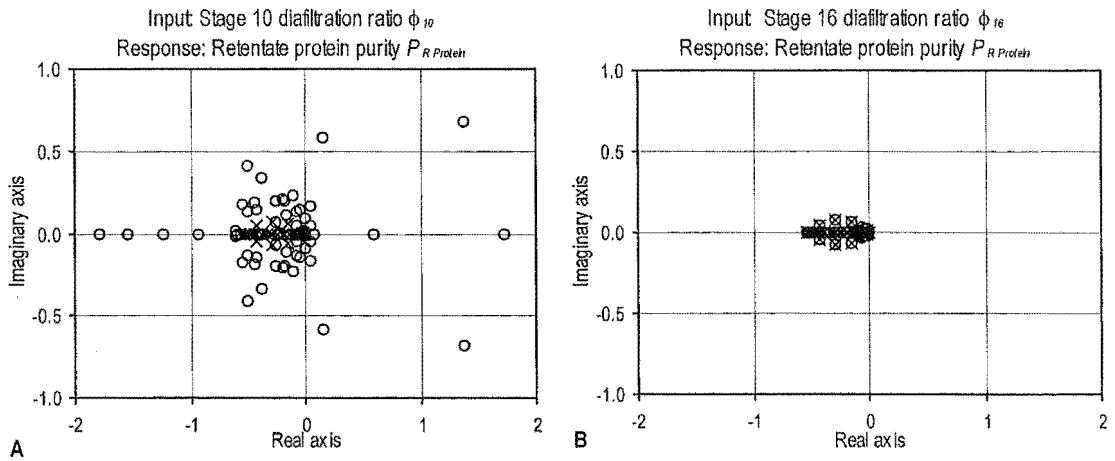

Figure 5-20 Pole-zero maps for transfer functions relating stage 10 and stage 16 diafiltration ratios to retentate protein purity
Stage 10 was the first stage receiving diafiltration in this 16 stage simulation. Simulation conditions are presented in Appendix B.

caused by this input pass directly into the retentate product stream with little attenuation. This analysis, although specific to a certain set of operating conditions, suggests that as stages are added to the plant and the points of diafiltration alter, dramatic changes in system response dynamics may occur. Such a situation means that selection of the manipulated diafiltration ratios for closed-loop control of retentate purity should be made with care.

5.5.2 Case study 2: Permeate product separation

The onset of oscillatory behaviour was also examined for the second case study, for a variety of plant flowsheets operating at a feed pressure of 2 bar, and producing a retentate stream with total solids concentration of 17 wt %. Corresponding permeate yield Y_B is also plotted. The onset of oscillatory behaviour was again hastened by the use of ratio-controlled diafiltration (Figure 5-22). For this case study it was desired that 75 % of the valuable component (B) be recovered in the permeate stream. From Figure 5-22 it is clear that this will only be possible with extensive diafiltration injection, suggesting that for much of the time the plant will be operating in the oscillatory region. As explained earlier, the presence of oscillatory characteristics in the plant is independent of whether the product stream is the permeate or retentate.

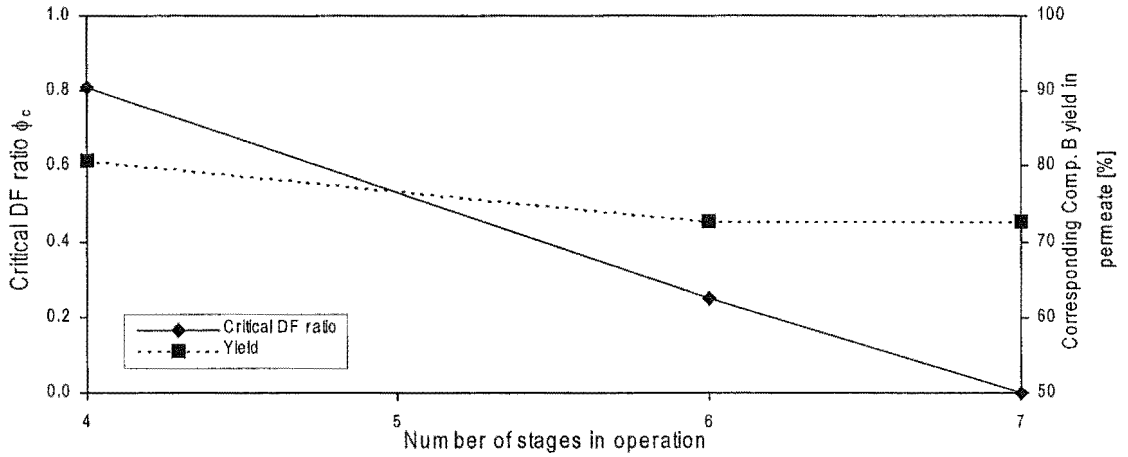

Figure 5-22 Effect of diafiltration on the onset of oscillatory behaviour - case study 2

The case study 1, the protein purity response dynamics to diafiltration inputs were complex and extremely dependent on the point of injection. In the second case study, the pole-zero maps (Figure 5-23A & B) for the permeate yield response were almost identical for both manipulated diafiltration ratios (Stage 6 and 16). In this case study the input passed directly into the permeate stream, to give a first order initial response, with (partially cancelled) secondary response dynamics occurring in upstream and down-

stream stages. This result, as for the feed concentration disturbance, was due to the parallel path from input to output via all stages, rather than the sequential propagation path exhibited by the retentate product separation. However the speed of the system response will still depend on the point of injection, since each stage has a different time constant. The positioning of zeros close to all imaginary poles suggests that the majority of the undesirable oscillatory system dynamics were cancelled, and will not be evident in the time domain behaviour of the plant. Unlike the first case study, there were no zeros present in the right half plane of either pole-zero map. However, pole-zero maps for a stage 6 input and retentate purity output showed the presence of zeros in the right half plane. This suggests that closed-loop retentate composition control of the plant proposed in Section 5.2.2 may encounter control difficulties similar to the retentate product case study.

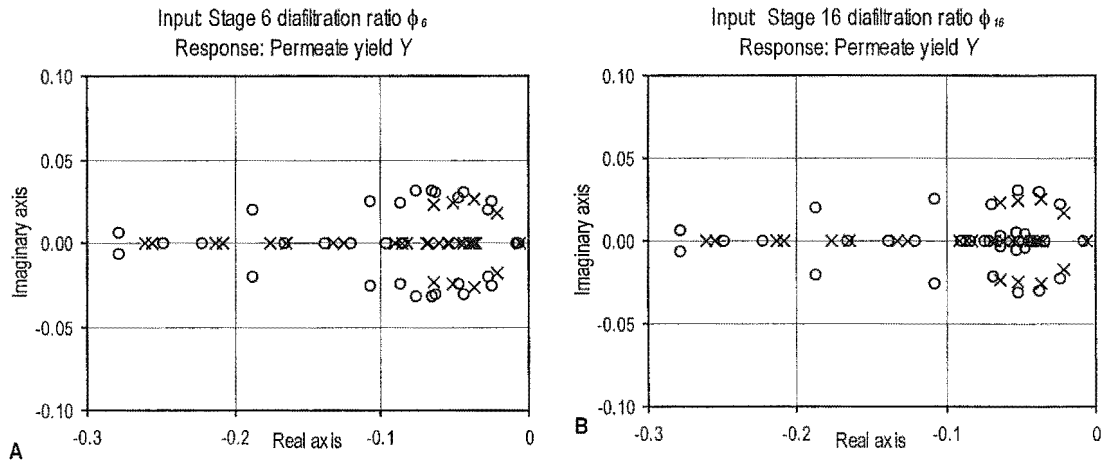

Figure 5-23 Pole-zero maps for transfer functions relating stage 6 and stage 16 diafiltration ratios to permeate yield

Stage 6 was the first stage receiving diafiltration in this 16 stage simulation. Simulation conditions are presented in Appendix B.

5.6 Interaction analysis using the relative gain array (RGA)

Analysis in previous sections has shown that complex disturbance propagation and response dynamics in membrane plants are caused by concentration dependent permeate fluxes. The concentration-flow rate interaction that results is of concern since it represents potential control difficulties which may lead to performance degradation. The relative gain array (RGA) quantifies steady state interaction within a process, between specific combinations of input and output variables. First proposed by Bristol (1966), this tool has been extremely widely used for controllability analysis of multivariable systems (Jafarey *et al.*, 1979; Grosdidier *et al.*, 1985; Stanley *et al.*, 1985). Dynamic relationships between preferred input-output pairings were

examined for the case studies using pole-zero maps in Section 5.4. RGA analysis offers the opportunity to determine the level of steady state interaction between these pairings, and can easily be applied and interpreted over a range of operating conditions.

5.6.1 Theory

The theoretical basis of the RGA was originally published by Bristol (1966), with a thorough review of this theory presented by Grosdidier *et al.* (1985). The behaviour of a multivariable system *G(s)* around a chosen operating point can be approximated by a steady state gain matrix **K**. A linear, time invariant *2 × 2* multivariable process can be modelled as:

$$\begin{bmatrix} y_1 \\ y_2 \end{bmatrix} = \begin{bmatrix} k_{11} & k_{12} \\ k_{21} & k_{22} \end{bmatrix} \begin{bmatrix} u_1 \\ u_2 \end{bmatrix} \tag{5-6}$$

which is assumed to be open-loop stable. The response of the output y_1 to an asymptotically constant disturbance entering through the variable u_1 (dashed line in Figure 5-24) is given by:

$$y_1 = k_{11} u_1 \tag{5-7}$$

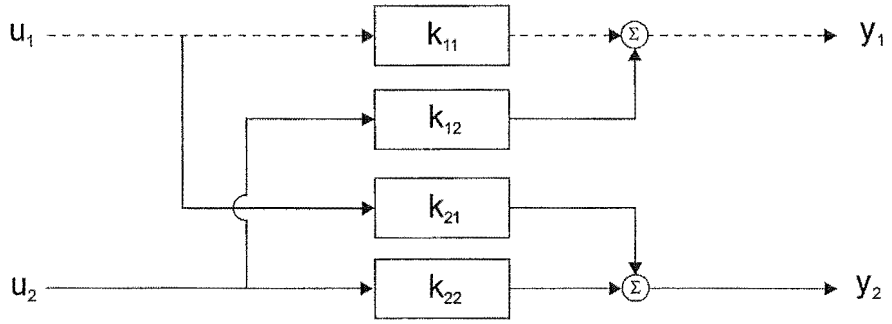

Figure 5-24 Disturbance propagation for open-loop 2 x 2 multivariable system

The open-loop disturbance propagation through this path can be defined as:

$$\left(\partial y_1 / \partial u_1\right)_{OL} = k_{11} \tag{5-8}$$

Suppose that a stable controller with gain k_{c2} is added to the system to maintain y_2 constant by manipulating input u_2, as shown in Figure 5-25. To achieve perfect steady state control the controller k_{c2} must be integral-based to ensure zero offset. When the the u_2 - y_2 loop is closed, there are two disturbance propagation paths from u_1 to y_1; one is direct and the other passes through loop 2, as shown by the dashed lines in Figure 5-25.

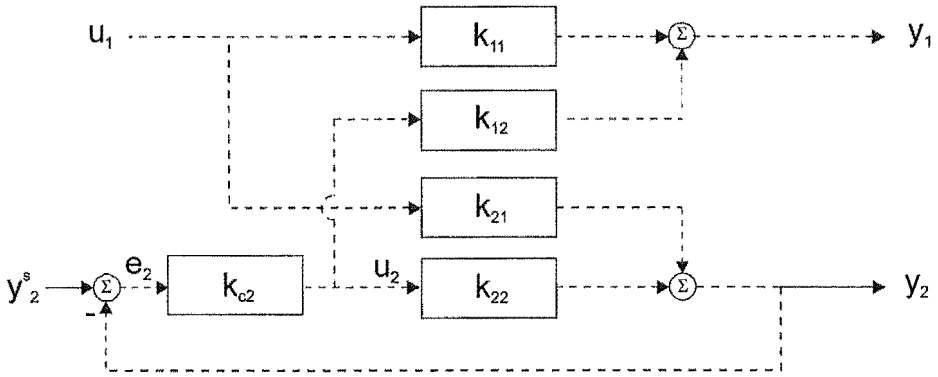

Figure 5-25 Disturbance propagation for 2 x 2 multivariable system with loop 2 closed

The relative gain λ_{ij} from u_j to y_i represents the ratio of system gains:

$$\lambda_{11} = \frac{open-loop\ gain\ between\ u_1\ and\ y_1\ with\ all\ other\ control\ loops\ open}{open-loop\ gain\ between\ u_1\ and\ y_1\ with\ all\ other\ control\ loops\ closed}$$

Relative gain terms close to one are desirable, since this signifies that there is little interaction between this input-output pairing and others in the system. Values approaching 0.5-0.6 represent significant levels of interaction. A negative value is extremely undesirable (Bristol, 1966) since the sign of the process gain k_{ij} is changed by the action of the other control loops. In such a situation a control loop tuned individually with all others in manual will have very poor performance or even become unstable when the plant is operated with all control loops closed. Whilst a 'small' relative gain (e.g. $\lambda < 2$) does not guarantee good system performance, a large relative gain (e.g. $\lambda > 20$) will always be associated with poor closed-loop performance (Skogestad & Morari, 1987).

The relative gain array Λ is a grouping of the relative gains for all combinations of system input and output variables:

$$\Lambda = \begin{bmatrix} \lambda_{11} & \lambda_{12} \\ \lambda_{21} & \lambda_{22} \end{bmatrix} \quad \textbf{(5-9)}$$

It is easily calculated directly from the steady state gain matrix **K** using the relation:

$$\Lambda = \mathbf{K} \times \left(\mathbf{K}^T\right)^{-1} \quad \textbf{(5-10)}$$

where ' × ' represents element-by-element multiplication.

5.6.2 *RGA properties*

The RGA has a number of interesting and useful properties (Bristol, 1966):

1) *Any row or column of Λ sums to one.* For the 2×2 system case, all terms in Λ can be calculated from the single term λ_{11}. In certain situations not all process gains are available, and so the resulting RGA is incomplete. The summation property means that it may be possible to calculate values for the missing terms.
2) *Λ is scaling independent.* This is a significant property which allows different system models to be compared with little effort. Some other analysis tools such as condition number are scaling dependent (Wolff *et al.*, 1992) and hence require more numerical manipulation prior to comparing different systems.
3) *Reordering of the gain matrix* **K** *only alters the row and column order in Λ.* Therefore, the RGA need only be rearranged, rather than recalculated to examine alternate controller pairings.
4) Λ=*I for all non-interacting processes,* i.e. processes with diagonal gain matrix.
5) *Λ=I for systems with one-way interaction,* i.e. processes with a triangular gain matrix.

5.7 Application of RGA analysis to multistage membrane plants

Steady state plant models for each 16 stage case study were linearised about the chosen operating point, and full state space models produced for a set of 3 inputs and outputs. Diafiltration was applied to the downstream half of the plant. In both case studies, inputs were retentate flow rate $F_{R,16}$, feed pressure ΔP_{Feed} and manipulated diafiltration ratio ϕ_1 (the first stage receiving diafiltration). Equal ratios ϕ were used for all stages receiving diafiltration. The retentate product case study had outputs of feed flow rate F_F, retentate total solids concentration $C_{R\ TS,16}$ and protein purity $P_{R\ Protein,16}$, whilst the system variables for the permeate product case study were feed flow rate F_F, permeate total solids concentration $C_{P\ TS}$ and yield Y_B. From the linearised state space model, the transfer function matrix **G**(s) was constructed, and evaluated at steady state (i.e. **G**(0)), to produce the gain matrix **K** from which the RGA was calculated using Equation 5-10. Interpretation of RGA analysis for complex systems is not necessarily simple, but relative gain terms close to one are generally desirable, signifying an input-output pairing that interacts little with the other variables. Relative gains greater than one are acceptable, but input-output variable pairings with negative gains should be avoided.

5.7.1 *Case study 1: Whey protein concentrate production*

System interaction was examined for a range of different diafiltration injection strategies, each achieving the desired retentate total solids concentration $C_{R\ TS,16}$ and protein purity $P_{R\ Protein,16}$ (Figure 5-26). The RGA analysis provides information on levels of interaction within the WPC plant for a range of different diafiltration strategies. Diafiltration ratios for the different regimes differed between $\phi = 0.75$ (six stages receiving diafiltration injection) and $\phi = 0.33$ (16 stages). Only one set of variable pairings (Strategy A, shown in grey, Figure 5-26) do not have any negative relative gain terms. This set is identical to that commonly used industrially for WPC plants. Surprisingly, the most aggressive diafiltration strategy also had the lowest levels of interaction (i.e. relative gains closest to one).

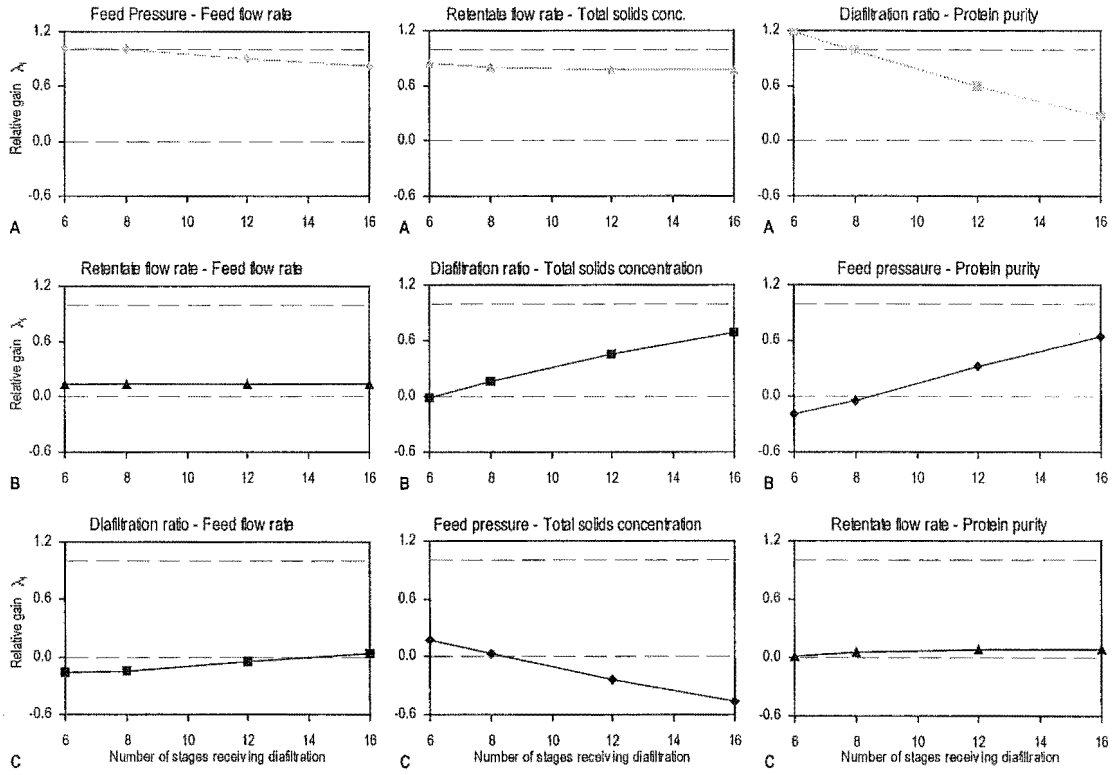

Figure 5-26 Interaction analysis using the RGA - case study 1
Simulation conditions are presented in Appendix B.

When interpreting the RGA results it should be remembered that this analysis was based on the steady state system gain matrix **K**. The system model used to produce the pole-zero maps was modified to allow it attain steady state, but the analysis utilised the full dynamic description of the process. This highlights the fundamental difference between the two analysis tools - one examines steady state and the other dynamic system behaviour. The most significant, and widely discussed weaknesses of RGA analysis is

that it applies only to steady state system behaviour. Examples are presented in literature (e.g. Stanley *et al.*, 1985; Jensen *et al.*, 1986; Huang *et al.*, 1994) where the properties of the RGA are inconsistent with the dynamic system behaviour. It is possible that multistage membrane separation are another example. Frequency dependent forms of the RGA tool have been developed (Bristol, 1977; Tung & Edgar, 1981; Hovd & Skogestad, 1992) and it is likely that they would provide additional information on interaction within the process, but it becomes very difficult to determine trends in the results with such a large amount of information. Comparisons of different behaviour at different frequencies becomes daunting, when each data point in Figure 5-26 becomes a complete frequency spectra.

5.7.2 Case study 2: Permeate product separation

This case study represents a membrane separation that is not as widely used industrially on a multistage scale, and so preferred pairings of measured and manipulated variables are generally not discussed in the literature. Steady state relative gains were calculated for a range of diafiltration strategies, each achieving the required 75 % permeate stream yield Y_B, operating at 17 wt % retentate total solids concentration $C_{P\,TS}$ (Figure 5-27). Diafiltration ratios for the different regimes differed between $\phi = 0.91$ (nine stages receiving diafiltration injection) and $\phi = 0.43$ (16 stages). Trends in the relative gains λ_i

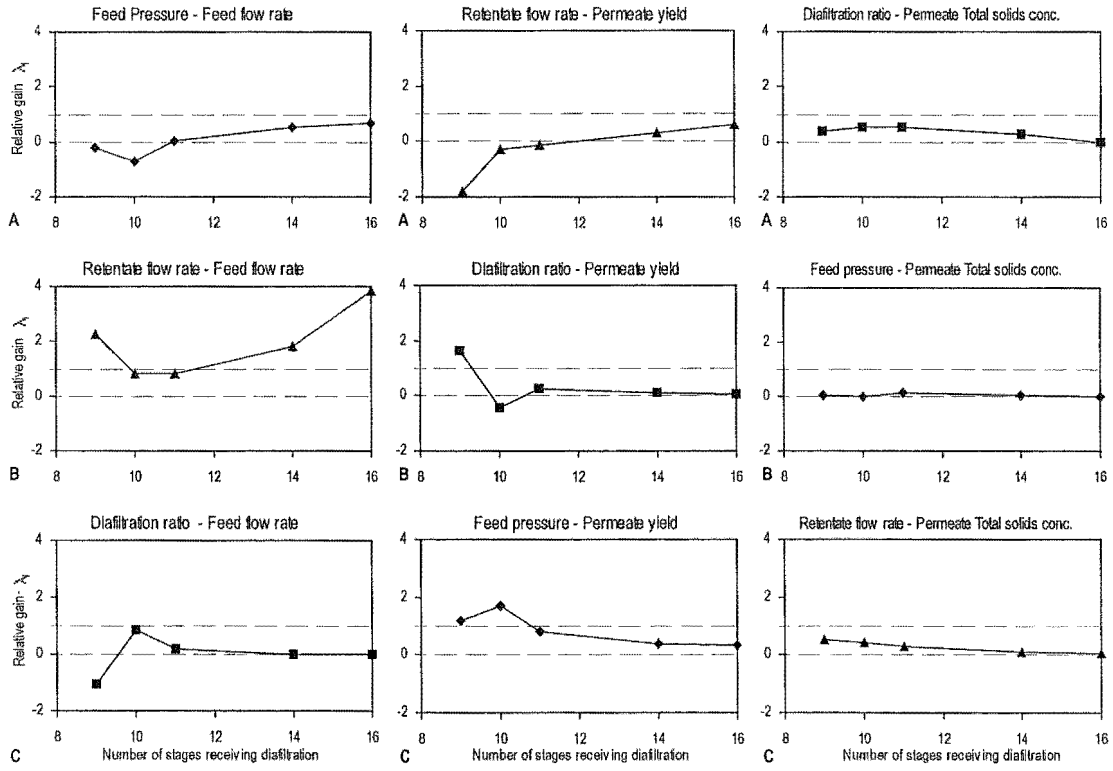

Figure 5-27 Interaction analysis using the RGA - case study 2
Simulation conditions are presented in Appendix B.

were less clear for this case study and overall exhibited greater variation and deviation from the preferred value of 1.0, particularly for the more aggressive diafiltration strategies. Overall it can be concluded from the RGA analysis that the selection of permeate stream yield and total solids concentration as controlled variables is undesirable. None of the input-output pairings produce consistent relative gain terms over a range of diafiltration regimes, few gains are close to one, and several are negative. For this case study there are no preferred input-output pairings, and it is concluded that the retentate, rather than the permeate stream, should be controlled.

5.8 Conclusion

Numerical analysis of multistage membrane plant characteristics for selected input-output pairings was carried out using a steady state and a dynamic assessment tool. Dynamic system characteristics were examined using pole-zero analysis. For both case studies, flowsheets with many states exhibited undesirable oscillatory characteristics for disturbances in the key components. Such behaviour was independent of any chosen control system. Fortuitously, pole-zero cancellation means that this oscillatory behaviour is not likely to be evident in the process outputs. Inverse response was also observed in the WPC case study for some manipulated diafiltration ratios. The use of diafiltration was shown to hasten the onset of oscillatory behaviour. Although this analysis was performed using a simplified permeate flux model, the conclusions drawn apply to all multistage membrane separations with concentration dependent permeate fluxes. Neglecting membrane fouling effects made it possible to investigate the steady state process characteristics, but precluded experimental validation of the results.

Steady state interaction between pairings of input and output variables was examined under a range of different diafiltration regimes, using the relative gain array (RGA). The results suggested that there was little interaction within the retentate product case study for the preferred variable pairings, but more significant interaction was present for the permeate product situation, particularly under more aggressive diafiltration strategies. On this basis, it was concluded that direct control of the permeate stream properties is undesirable, and closed-loop control strategies should focus on the plant retentate stream, in the same manner as case study 1.

5.9 References

Bristol E H (1966), On a new measure of interaction for multivariable process control, *IEEE Trans. Autom. Ctrl,* **AC-11**, 133-134.

Bristol E H (1966), On a new measure of interaction for multivariable process control, *IEEE Trans. Autom. Ctrl,* **AC-11**, 133-134.

Bristol E H (1977), Dynamic effects of interaction. *16th IEEE Conference on Decision and Control,* pp. 1096-1100, New York.

Field R (1996), Workshop session on membrane process design. *Proceedings of Application of Membrane Technologies,* pp. 5.1-5.2, Auckland, New Zealand.

Grosdidier P, Morari M & Holt B R (1985), Closed-loop properties from steady-state gain information, *Ind. Eng. Chem. Fundamen.,* **24**, (2), 221-235.

Grosdidier P, Morari M & Holt B R (1985), Closed-loop properties from steady-state gain information, *Ind. Eng. Chem. Fundamen.,* **24**, (2), 221-235.

Hovd M & Skogestad S (1992), Simple frequency-dependent tools for control system analysis, structure selection and design, *Automatica,* **28**, (5), 989-996.

Huang H, Ohshima M & Hashimoto I (1994), Dynamic interaction and multiloop control system design, *J. Proc. Cont.,* **4**, (1), 15-27.

Hunter T J & Morison K R (1997), Characterisation of the effects of diafiltration water injection on multi-stage ultrafiltration plants. *CHEMECA 97,* pp. PC2b:1-PC2b:13, Rotorua, New Zealand.

Jafarey A, McAvoy T J & Douglas J M (1979), Analytical relationships for the relative gain for distillation control, *Ind. Eng. Chem. Fundamen.,* **18**, (2), 181-187.

Jensen N, Fisher D G & Shah S L (1986), Interaction analysis in multivariable control systems, *AIChE Journal,* **32**, (6), 959-970.

Le M S & Howell J A (1985), Ultrafiltration. In *Comprehensive Biotechnology: the Principles, Applications and Regulations of Biotechnology in Industry, Agriculture and Medicine* (Ed. Cooney C L & Humphrey A E), Vol 2, pp. 383-408, Pergamon Press, England.

MathWorks (1999), *Control System Toolbox User's Guide v4.2,* The MathWorks Inc., USA.

Morari M (1983), Design of resilient processing systems III; a general framework for the assessment of dynamic resilience, *Chem. Eng. Sci.,* **38**, (11), 1881-1891.

Morari M & Perkins J (1995), Design for operations. In *Fourth International Conference on: Foundations of Computer-Aided Process Design* (Ed. Biegler L T & Doherty M F), Vol. 91, No. 304, pp. 105-114, AIChE Symposium Series.

Morari M & Zafiriou E (1989), *Robust Process Control,* Prentice-Hall International, New Jersey.

Nagrath I J & Gopal M (1982), *Control Systems Engineering,* 2nd Ed., New Age International Ltd, India.

Rautenbach R & Albrecht R (1989), *Membrane Processes,* John Wiley & Sons, New York.

She X (1998), *Design and Optimisation of Multistage Ultrafiltration Plants.* M.E. Thesis, Department of Chemical and Process Engineering, University of Canterbury, New Zealand.

Skogestad S & Morari M (1987), Implications of large RGA elements on control performance, *Ind. Eng. Chem. Res.,* **26**, (11), 2323-2330.

Stanley G, Marino-Galarraga M & McAvoy T J (1985), Shortcut operability analysis 1.The relative disturbance gain, *Ind. Eng. Chem. Process Des. Dev.,* **24**, (4), 1181-1191.

Stephanopoulos G (1984), *Chemical Process Control: An Introduction to Theory and Practice,* Prentice-Hall International, New Jersey.

Tung L S & Edgar T F (1981), Analysis of control-output interactions in dynamic systems, *AIChE Journal,* **27**, (4), 690-693.

Winchester J (1996), *Computer Simulation and Controllability Studies of Multi-module Ultrafiltration Plants.* M.E. Thesis, Department of Chemical and Process Engineering, University of Canterbury, New Zealand.

Wolff E A, Skogestad S, Hovd M & Mathisen K W (1992), A procedure for controllability analysis. In *IFAC Workshop on Interactions Between Process Design and Process Control* (Ed. Perkins J D), pp. 127-132, Pergamon Press, UK.

6 Closed-Loop Behaviour Of Multistage Membrane Plants

The dynamic behaviour of multistage membrane separation plants was examined in the previous chapter, and the presence of undesirable characteristics established. This chapter investigates how these characteristics affect closed-loop system behaviour and the achievable level of controller performance. Controller strategies are developed for each case study and closed-loop system behaviour simulated. Disturbance rejection capabilities of these processes are examined, as well as plant behaviour at startup.

6.1 Preferred control variable pairings

Membrane separation plants have commonly been controlled using multiple independent single-input single-output (SISO) control loops (Winchester, 1996) allowing the use of simple PID-style controllers. This strategy is relatively simple to develop, but can be implemented in a number of configurations, each subject to different performance constraints.

Significant experience in controlling and operating multistage membrane plants has been accumulated in New Zealand, primarily in the production of whey protein concentrate. Control strategies have been developed and refined in the industrial arena, but these are generally the result of trial and error experiences rather than theoretical analysis or formal controllability assessment. It is possible, for case study 1, to examine the industrially applied input-output variable pairings and compare the closed-loop process performance of these with the findings of the controllability assessment performed in the previous chapters.

The lack of theoretical basis in industrial practice makes it difficult to extend current retentate product strategies to permeate product separations. Very little literature is available regarding control strategies for permeate product separations, so preferred variable pairings for the second case study must be developed from the understanding of process behaviour developed in the previous chapters. Proposed control strategies for this case studies can then be examined using closed-loop simulation.

6.1.1 Case study 1: Whey protein concentrate production

The input-output pairings presented in the Table 6-1 represent preferred variable pairings often used industrially in New Zealand (Morison, 1998).

Table 6-1 Commonly employed control variable pairings - case study 1

Manipulated input	Measured output
Feed pressure	Feed flow rate
Retentate flow rate	Retentate total solids concentration
Diafiltration injection	Retentate composition

Analysis in previous chapters has examined the relationship between feed pressure ΔP_{Feed} and feed flow rate to the plant. Pole-zero analysis in Section 5.4.3 showed there to be complete cancellation of system dynamics, meaning that the process output responds directly to the input giving very fast control. Steady state interaction analysis using the relative gain array (RGA) also showed these input-output pairings to have least interaction with each other (Section 5.7.1). The strategy presented in Table 6-1 can be applied to either fixed area plants or used in conjunction with the addition of membrane area as required.

In this strategy, retentate total solids concentration is controlled by manipulating the setpoint to a cascade loop controlling the retentate flow rate. Varying this flow rate changes the residence time within the plant and the retentate total solids concentration. RGA analysis in Section 5.7.1 indicated that this practice interacts least with other control loops. Pole-zero analysis suggested that there was extensive cancellation of dynamics within the system, with the resulting input-output dynamics being of relatively low order. The process behaviour is therefore unlikely to be visibly oscillatory. Both industrial experience and analysis agree that this pairing is superior to the available alternatives, so will be employed for all WPC simulations performed in this chapter.

Industrial practice suggests that retentate composition is best controlled by manipulating the injection of diafiltration water to the plant. RGA analysis concurred, showed little interaction between this control loop and others in the process. However, the pole-zero maps showed suggested that the dynamic response of the system was heavily dependent on the choice of manipulated input. Overall, selection of suitable diafiltration ratio(s) to manipulate is not clear. For this reason closed-loop composition control is further investigated in Sections 6.3 and 6.4.

6.1.2 Case study 2: Permeate product separation

The lack of large scale permeate product separations in the New Zealand dairy industry means that industrially preferred control variable pairings are not widely known. This situation is not aided by a lack of control literature for such processes. Operating requirements stipulated in Section 3.5.2 specified only a required feed flow rate and desired recovery of permeable component. This separation therefore has three manipulated variables available (feed pressure, diafiltration injection and retentate flow rate) but only two outputs to be controlled (yield and feed flow rate). From this perspective permeate plant control is substantially different from case study 1.

RGA analysis performed on this system (Section 5.7.2) suggested that significant interaction occurred between certain variable pairings. Interaction levels also varied markedly under different diafiltration strategies. Overall, no set of variable pairings proved suitable. It was instead suggested that a retentate-style control strategy be implemented instead, where the retentate purity is maintained at a value corresponding to the desired permeate yield. Provided the concentration of valuable component (Component B) in the retentate stream is only 25 % of that in the feed stream, then the desired 75 % yield is achieved. On this basis, retentate total solids concentration would be best controlled by manipulating retentate flow rate, with retentate composition controlled by diafiltration injection. Maintaining a high total solids concentration in the retentate stream increases the residence time of the process, and provides greater opportunity to recover the permeable component. As with the first case study, several stages receive diafiltration injection, and it is difficult to specify which one(s) should be selected as the manipulated variable(s). This makes the development and implementation of composition control strategies a complex issue, worthy of further consideration in the next two sections.

6.2 Development and analysis of diafiltration injection strategies for composition control

Although the RGA analysis provided information on the presence and degree of interaction within each case study, findings from this tool must be used with great care. This controllability assessment technique, like most published in the literature, is intended for use on linear time-invariant systems. Forcing a membrane separation to conform to such requirements by neglecting fouling, non-linearity and the addition of

new stages creates the risk that significant characteristics of the process may have been omitted. The absence of key behaviour from the analysis could conceivably produce a result which is relevant for the simplified model, but inappropriate for the actual process. It is therefore important that any conclusions drawn from steady state analysis in Chapter 5 be confirmed by closed-loop simulation, using the complete non-linear process model.

Analysis of the two case study systems in the previous chapter consistently highlighted diafiltration injection as having a significant effect on dynamic process behaviour. Several strategies exist for applying and controlling diafiltration injection to multistage plants. For this reason it is useful to fully investigate the effect of diafiltration injection on closed-loop process behaviour, and consider different strategies for retentate composition control. Diafiltration injection strategies for fixed area plants are examined in Section 6.3; the two strategies considered are those of maintaining fixed diafiltration flow rates (Section 6.3.1), and maintaining the diafiltration flow rates as specified fractions of the permeate flows (Section 6.3.2). The feasibility of closed-loop composition control for fixed area plants is considered in Section 6.3.3. Section 6.4 investigates strategies for composition control of multistage membrane plants operating with the periodic addition of new stages (variable area operation). Of interest is the implementation of a diafiltration strategy that is able to modify how diafiltration is injected into a plant, to maintain a constant retentate purity in the face of a changing process flowsheet and operating conditions.

6.3 Composition control strategies for fixed area membrane plants

Diafiltration control is a complex issue for multistage membrane separations. Progressive membrane fouling causes operating conditions within the plant to continually change, whilst high levels of interaction within and between stages result in widespread disturbance propagation. System behaviour must therefore be considered for both short-term disturbances and long-term changes during production. A diafiltration control strategy must be able to successfully reject disturbances entering the process (regulatory control) as well as track changing operating conditions (servo control) caused by membrane fouling.

The issues associated with composition control are best illustrated using an example system. The WPC case study was chosen for this purpose. For ease of presentation, the plant is restricted to operating with only eight separation stages during the fixed area analysis. All simulations use the complete flux model developed in Section 3.3.2, which includes both short- and long-term fouling effects. Feed flow rate and retentate total solids concentration are controlled using the feed pressure and retentate flow rate respectively, as discussed in Section 6.1.1. Fixed-term PID controllers are used to maintain the desired setpoints; $F_{F,1}$ = 21.7 L/s and $C_{R\ TS,8}$ = 27 wt %. The total solids controller remains in manual until the retentate concentration reaches 25 wt %, when automatic control begins. Diafiltration is applied to the final three stages of the process to produce the desired protein purity (85 wt %, dry basis). The maximum diafiltration ratio of any stage was restricted (ϕ_{max} = 0.7). The analysis in this section focuses on composition control in fixed area membrane plants. A summary of the simulation conditions is presented in Appendix B.

Closed-loop performance is affected by the characteristics and tuning of the controllers manipulating the process. When examining the closed-loop behaviour of a process it is therefore preferable to use a 'standard' tuning method. To do this the process of interest must be identified (e.g. using a process reaction curve) and the controller parameters calculated (using a set of tuning rules). Identification methods for this purpose require the plant to be self-regulatory and exhibit approximately first order dynamics (Marlin, 1995), whilst tuning rules for fixed parameter controllers generally assume the process is reasonably linear, with little interaction (Ogunnaike & Ray, 1994). Unfortunately, multi-stage membrane separation plants generally possess none of these properties. Given these limitations, the feed flow rate and retentate concentration controllers used in these closed-loop simulations were manually tuned, with emphasis placed on minimising setpoint overshoot. Two-term (PI) controllers were used for all loops. Sensor and actuator dynamics were assumed to be negligible. A summary of the controller parameters is presented in Appendix B.

Dynamic resilience is a concept originally introduced by Lenhoff & Morari (1982), which states that the achievable performance of a feedback controller is actually limited by the characteristics of the process. For example, a plant with large deadtime will always have poor performance when rejecting input disturbances. In the case of multi-

stage membrane plants, feedback controller performance will be limited by large process time constants and high order dynamics, regardless of the controller tuning technique employed. For this reason, the rise-time at startup will be limited by the process rather than controller tuning (see Figure 3-5). On this basis, the use of manually tuned controllers when investigating closed-loop process behaviour is assumed to be acceptable, since in most cases it is the process characteristics which limit performance rather than loop tuning. It is unlikely that the use of formal tuning methods will provide performance improvements over controllers which have been carefully tuned by hand.

6.3.1 Composition control using fixed diafiltration flow rates

The closed-loop behaviour of the eight stage WPC process is presented in Figure 6-1, when operating with fixed diafiltration flow rate to each stage. During startup the diafiltration flow rates to stages 6, 7 & 8 were maintained as fixed ratios of the permeate

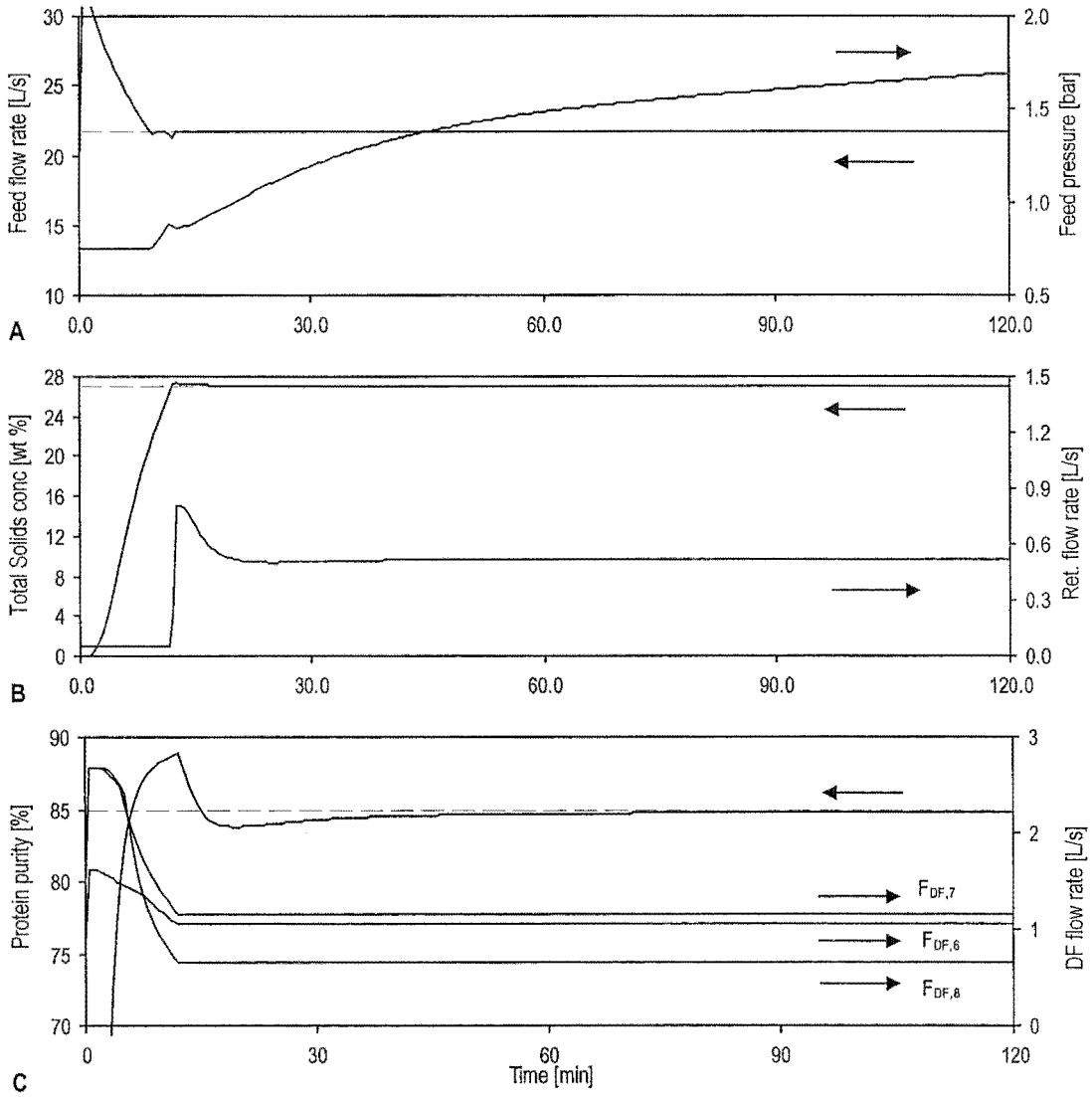

Figure 6-1 Closed-loop operation of WPC system - fixed diafiltration flow rates
Simulation conditions and controller parameters are presented in Appendix B.

flow rates from these stages (ϕ_6 = 0.35, ϕ_7,ϕ_8 = 0.7). The diafiltration flow rate to each stage remained constant (Figure 6-1C) once the total solids reached setpoint.

At startup the plant was full of water and so very high permeate fluxes occurred. Permeate fluxes and the plant feed flow rate dropped rapidly as water was flushed from each stage and concentration polarisation boundary-layers become established. With the diafiltration flow rates fixed, the amount of diafiltration added to each stage became a greater proportion of the permeate flow, as the membranes fouled. This caused the slow rise in retentate purity evident in Figure 6-1C. The initial plant feed flow rate exceeded the setpoint, even though the feed pressure remained low. Control of the plant feed flow rate only became possible once the initial pure-water permeate fluxes had declined after about 10 minutes.

6.3.2 Composition control using fixed diafiltration ratios

The inability of fixed flow rate diafiltration to maintain the desired retentate composition (Figure 6-1C) highlights the need for servo-style characteristics (Stephanopoulos, 1984; Lee *et al.*, 1998) in the diafiltration control strategy. Such behaviour is best achieved by maintaining the diafiltration flow rate as a set proportion of the permeate flow rate for each stage, i.e. $F_{DF,i} = \phi_i F_{P,i}$. The permeate flow rate therefore acts as the setpoint for the flow rate of diafiltration to that stage.

Ratio-controlled diafiltration (as it is called in this thesis) has been extensively discussed in previous chapters and forms the basis of all diafiltration strategies used in New Zealand. Figure 6-2 shows the closed-loop behaviour of the WPC case study system operating with eight stages and fixed diafiltration ratios of ϕ_6 = 0.35 and ϕ_7,ϕ_8 = 0.7. Diafiltration control dynamics were assumed negligible compared to the (slow) speed of the plant, and so were ignored. Like the first simulation, diafiltration injection began at startup. Ratio-controlled diafiltration successfully allowed the diafiltration flow rates to track long-term changes in process operating conditions caused by membrane fouling, and produced a more constant product composition (Figure 6-2C). Because the diafiltration flow rates track changes in permeate flows, this strategy ensures that backup does not develop within any plant as the membranes foul.

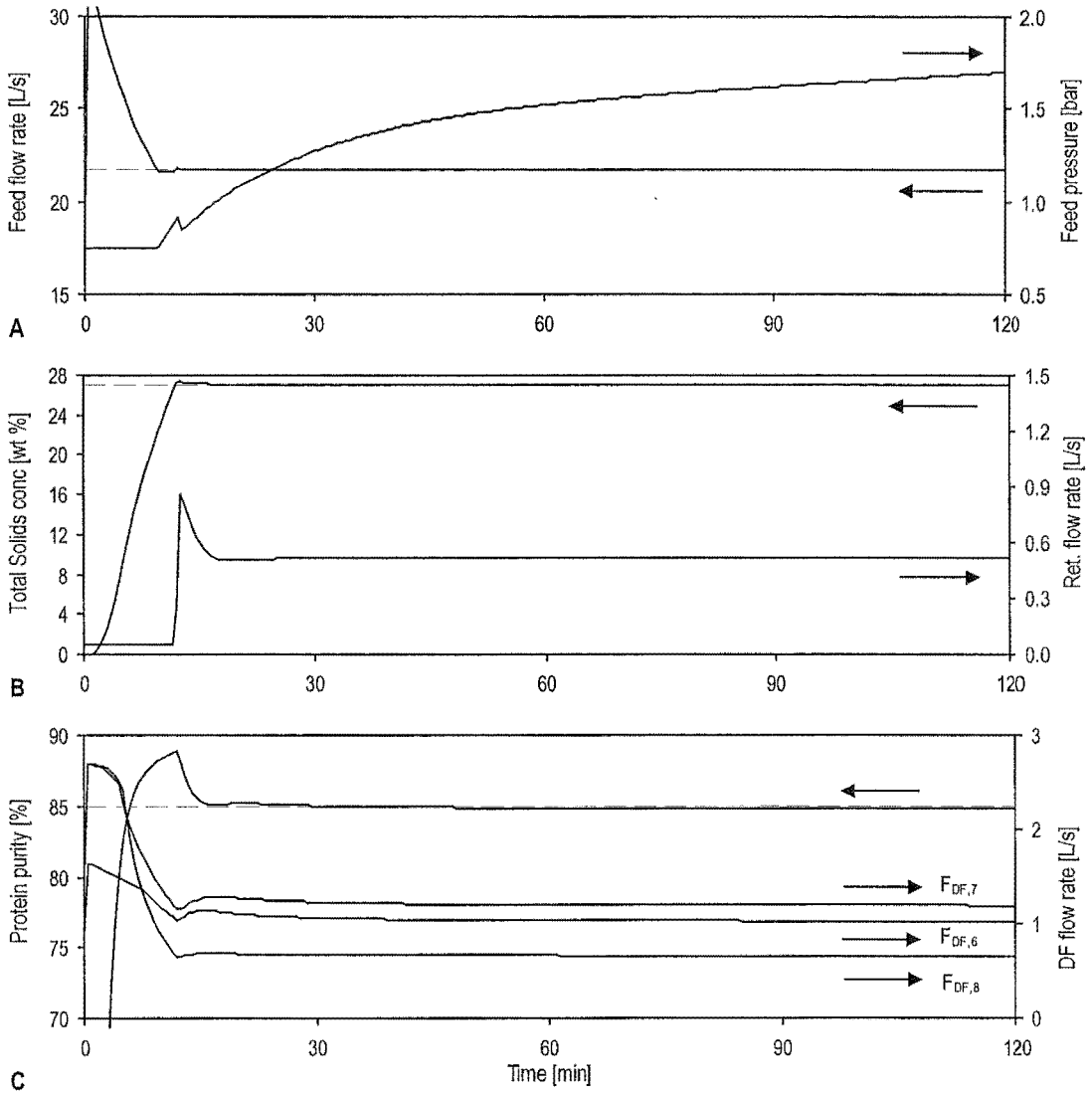

Figure 6-2 Closed-loop operation of WPC system - fixed stage diafiltration ratios
Simulation conditions and controller parameters are presented in Appendix B.

6.3.3 Closed-loop retentate composition control

The analysis performed so far shows that ratio-controlled diafiltration can successfully maintain the retentate composition of separation processes with fixed membrane area. This is an impressive achievement for an open-loop strategy. So far no feedback control has been implemented using the measured retentate composition; selection of the diafiltration ratio values has been based on previous experience, with no guarantee of achieving the desired retentate purity. Assuming that the measured composition is available on-line, implementing closed-loop feedback control would ensure that the product specification is achieved and maintained over the duration of production. The overshoot in protein purity evident at startup could also be avoided.

An obvious feedback configuration is to manipulate the diafiltration ratio of one or more stages in order to maintain the desired retentate stream composition. However pole-zero analysis for the WPC case study in Section 5.5.1 showed that there may be an odd number of right half plane zeros in transfer function relating the protein purity response to changes in certain diafiltration ratios (Figure 5-19A). Intriguingly, manipulation of a different diafiltration ratio within the same plant (Figure 5-19B) did not cause equivalent behaviour. An odd number of right half plane zeros corresponds to inverse response behaviour (see pole-zero map properties in Section 5.4.1), where the initial direction of the response is opposite to the direction of the final steady state. Such behaviour is extremely undesirable, and very detrimental to closed-loop controller performance (Ogunnaike & Ray, 1994).

Feedback composition control for multistage diafiltration plants therefore presents two significant obstacles; difficulties associated with online composition measurement (often expensive or impractical), and the potential presence of undesirable response dynamics. In certain circumstances, inverse response behaviour may not be present but this will depend on the process flowsheet, operating conditions and manipulated diafiltration ratio. The presence of this behaviour is difficult to predict without a rigorous model. It is also highly likely, particularly for biological separations, that online composition measurement will not be available.

Returning to Figure 6-2C it can be seen that following startup the retentate composition of the plant remains relatively consistent. The simplest, and probably most feasible solution for constant area plants is to employ fixed ratio diafiltration injection, with off-line composition measurement (where available) used to periodically update the diafiltration ratio used for some or all stages.

6.4 Composition control strategies for variable area membrane plants

The eight stage WPC case study examined so far has been a useful tool, but differs from both case studies in one significant aspect; the membrane area of the plant is fixed. In both case studies examined in this thesis, membrane area is added to maintain a constant feed flow rate when the upper feed pressure limit is reached because of fouling. Under such an operating strategy a plant may begin production with five stages, and finish with perhaps 16 stages. What was initially the first separation stage (receiving the feed

stream) will become the second, with the new stage now receiving the feed. This reflects the operating practice employed in many industrial plants in New Zealand.

With variable area operation the distribution of diafiltration across the plant cannot remain static. If the initial diafiltration ratios are not changed as further stages are added, then the total volume of diafiltration injected into the plant will reduce over time, as the diafiltration stages foul and permeate fluxes decline. The amount of diafiltration applied to the plant will soon become insufficient to maintain the desired retentate composition. It is therefore necessary to employ some form of supervisory controller or 'adaptive' diafiltration strategy to add further diafiltration capacity to the plant as necessary. Measurement difficulties and controllability issues preclude the implementation of any closed-loop composition control, so open-loop or inferential strategies must be considered for composition control.

The concept of an overall diafiltration ratio ϕ_o was introduced in Section 5.2.1, where the total flow of diafiltration water injected into a plant was maintained as a constant fraction of the feed flow rate:

$$\phi_o = \frac{\sum_{i=1}^{n} F_{Pi}\phi_i}{F_F} \qquad \textbf{(5-1)}$$

It was shown in each case study that this strategy was able to maintain the separation trajectory and retentate purity (almost) constant, regardless of the number of stages in operation. It was shown in Section 5.2.2 that an equivalent relationship between overall diafiltration ratio and permeate yield also existed, so this strategy can also be applied to permeate product systems. The overall diafiltration ratio approach remains an open-loop composition control strategy, since a value for ϕ_o must be chosen arbitrarily. This approach is commonly employed industrially in New Zealand for WPC production (Morison, 1998), although it is likely that this strategy was developed as a result of operational experience rather than in the context of separation trajectories as presented here.

Maintaining a constant overall diafiltration ratio can only be achieved by manipulating some or all stage ratios in the plant. Several options are available when deciding which ratio(s) should be manipulated. Returning to the separation trajectories plotted in

Section 5.2, it was shown that ϕ_o remained constant only if the separation trajectory was stable, i.e. followed the same general path. This can be achieved by varying the ratio of the first diafiltration stage, and fixing the remaining k stage ratios at a chosen value ϕ_{max}:

$$\phi_v = \phi_o F_F - \sum_{j=2}^{k} \phi_{\max} F_{P,j} \tag{5-2}$$

In a closed-loop simulation, a supervisory controller would set the value of the manipulated or variable diafiltration ratio ϕ_v using Equation 5-2, where the current number of diafiltration stages k was manipulated as necessary to maintain ϕ_v within the limits

$$0 \leq \phi_v \leq \phi_{\max} \tag{5-3}$$

When the manipulated diafiltration ratio ϕ_v reaches the upper limit, diafiltration injection must begin in a new (upstream) stage, hence the position of the manipulated diafiltration ratio changes as stages are added to the process. This approach is very similar to that used industrially, although the basis for this implementation was originally to keep the disturbance source (ϕ_v) as far as possible from the product stream (Morison, 1998).

With the general diafiltration strategy defined, a startup policy can now be considered for the multistage process. When the plant begins operation it contains water which must be displaced from each stage by the process stream. At startup this occurs sequentially down the plant until, after a delay, the total solids concentration of the final stage begins to increase (see Figure 3-5). The injection of diafiltration is best delayed until most of the water initially in the plant has been displaced, hence diafiltration is not usually applied (i.e. $\phi_o = 0$) until the total solids concentration in the retentate stream of the plant has risen to a specified value.

It is useful to explore the closed-loop behaviour of a variable area membrane plant, operating under the constant overall diafiltration ratio strategy. The WPC case study is again simulated, this time with five stages in operation initially and new stages added when necessary to maintain the desired feed flow rate. In this simulation diafiltration injection commenced (via a step increase in ϕ_o from 0 to 0.118) when the total solids concentration of the retentate stream reached 25 wt %, with the maximum diafiltration ratio to any stage limited ($\phi_{max} = 0.7$). Diafiltration was injected into the final stages of the plant as before. Complete details of the control strategy for case study 1 are presented in Table 6-2. This strategy is similar to industrial practice in New Zealand. A summary of the controller parameters is presented in Appendix B.

Table 6-2 Implementation details of process control strategy - Case study 1

Manipulated variable	Measured variable	Implementation details
Retentate flow rate	Retentate total solids concentration	Fixed term PI controller, manually tuned. Retentate flow rate fixed initially at F_R = 0.05 L/s, with controller switching to automatic when total solids concentration reaches 25 wt %. Controller setpoint = 27 wt %. Maximum retentate flow rate limited to 2.5 L/s. Sensor and actuator dynamics neglected in simulation.
Plant feed pressure	Plant feed flow rate	Fixed term PI controller manually tuned. New membrane area added in whole stage increments when the feed pressure reaches upper limit. Plant operating range $0.75 \leq P_F \leq 2$ bar. Controller setpoint = 21.7 L/s. Each new stage is added upstream of existing stages, and receives the plant feed. Five stages in operation at startup. Sensor and actuator dynamics neglected in simulation.
Diafiltration flow rate to each stage	Permeate flow rate from each stage	Flow rate setpoint for each diafiltration stage calculated from $F_{DF,i} = \phi_i F_{P,i}$. Diafiltration ratio for one stage is manipulated to maintain the total flow rate of diafiltration water to the plant as a fixed ratio ϕ_o of the plant feed flow rate. Manipulated ratio ϕ_i corresponds to the first (upstream) diafiltration stage. ϕ_o = 0 initially with step change to 0.118 when retentate total solids concentration reaches 25 wt %. Stage ratios limited, within range $0 \leq \phi_i \leq 0.7$. Perfect flow control assumed in simulation, with all dynamics ignored.

Simulation results for the WPC example system (Figure 6-3) show that the plant feed flow rate reached setpoint more quickly than the fixed area strategy, though the addition of new stages disturbed the total solids controller, forcing it to manipulate the retentate flow rate. Close scrutiny showed the retentate protein purity to increase with the addition of new stages (see Figure 7-9). This behaviour was consistent with the characteristics of the overall diafiltration ratio for a given retentate concentration and purity, which showed minor dependence on the number of separation stages operating in a plant (Figure 5-5). For a plant operating with variable area and fixed ϕ_o this means that the retentate purity will increase each time a new stage is added. This is not particularly desirable since the product stream will either be over-purified near the end of production, or below specification initially. It is feasible to update the values of ϕ_o to maintain the desired retentate composition, if off-line composition measurements are available.

Analysis of process characteristics in previous chapters has shown significant interaction to be present within a multistage plant. During closed-loop operation, this means that the actions of one controller impact on the others. In terms of both frequency and

magnitude, it is the actions of the feed flow rate controller that disturb the process most significantly. To maintain the desired feed flow rate the controller must periodically add a new stage to the process and reduce the plant feed pressure. These actions can be seen to affect both the total solids control loop (visible in the manipulated variable response) and retentate composition (evident in the protein purity) after approximately 40 minutes of operation. Interaction analysis performed in Section 5.7.1 suggested less interaction was present when the WPC process was operating at high protein purity. However, the relative gains calculated in Section 5.7.1 related to a plant operating with closed-loop composition control using a measured retentate composition. This is not representative of industrial practice.

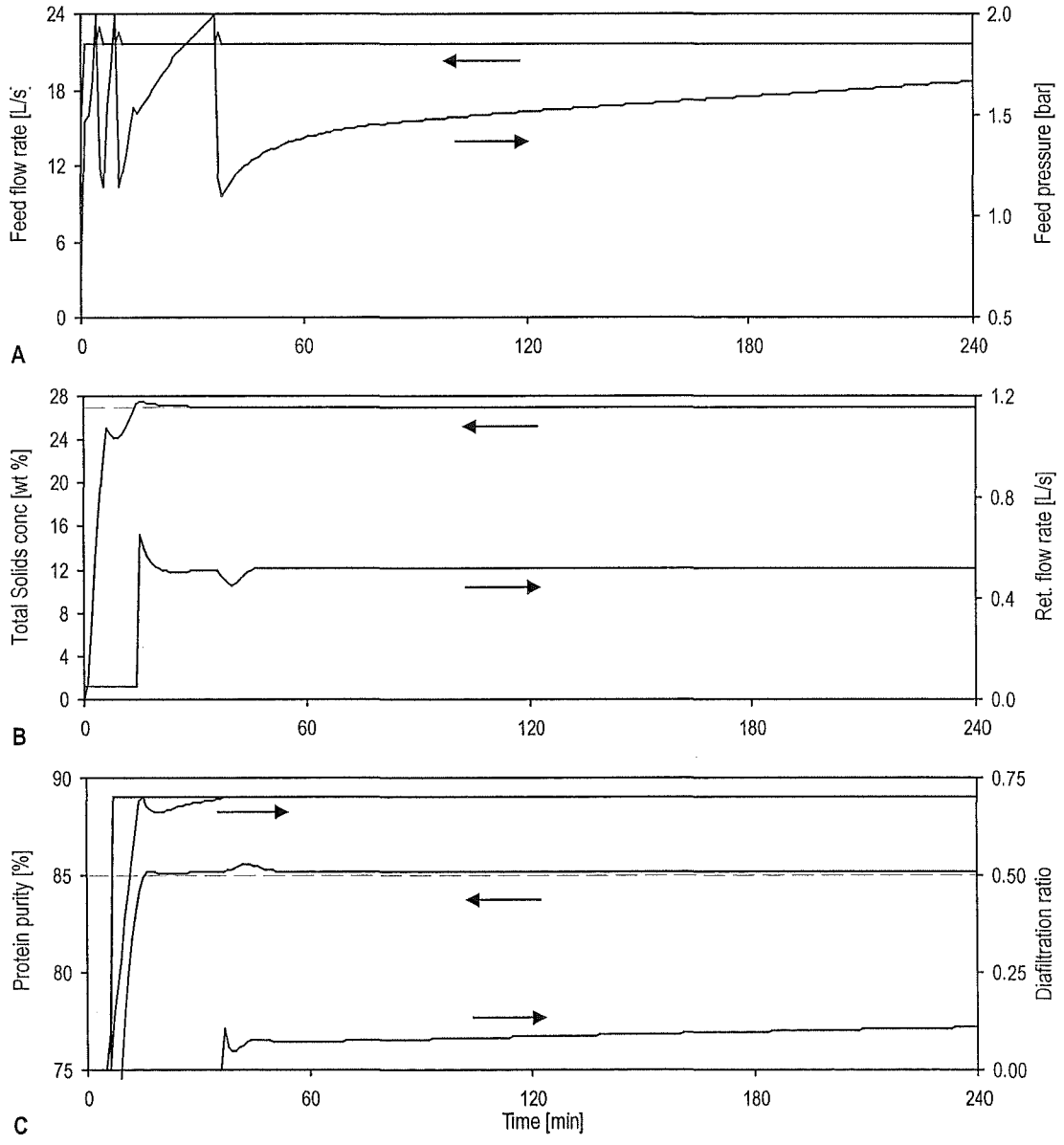

Figure 6-3 Closed-loop operation - case study 1 with variable membrane area
Simulation conditions and controller parameters are presented in Appendix B.

Closed-loop simulation (Figure 6-4) showed the addition of a new stage disturbed the feed flow rate, changing the manipulated diafiltration ratio ϕ_v (Figure 6-4C) and creating further feed flow rate disturbances. The amount of diafiltration water added to the plant must then be adjusted by the controller to maintain the desired overall diafiltration ratio ϕ_o. Therefore, the overall diafiltration ratio strategy creates a disturbance feedback loop that interacts with the feed flow rate controller. This is in addition to the feedback loops that exist within each diafiltration stage in the plant. Some of these disturbance feedback dynamics are avoidable if the total amount of diafiltration water added to the plant is calculated as a fraction of the feed flow rate setpoint rather than the measured value. For this reason, it is recommended that overall diafiltration ratio control be based on the feed flow rate setpoint of the plant. It is likely that any reduction in retentate variation will only be small, but it is desirable to break this disturbance feedback loop.

It is difficult to develop an understanding of multi-stage plant characteristics if the process behaviour is not considered in the context of the internal states (stage concentrations) of the plant. Separation trajectories (Figure 6-3) are a concise means of displaying this volume of data. Blue points represent stages with diafiltration injection, while red points correspond to stages receiving no diafiltration water. Most importantly, the separation trajectories shown in Figure 6-3 demonstrate the existence of a stable separation trajectory which (provided the process is well controlled) is maintained for the duration of production. From a control perspective this result suggests that in addition to pursuing specific setpoints for the retentate stream, there also exists a reference trajectory for the entire separation.

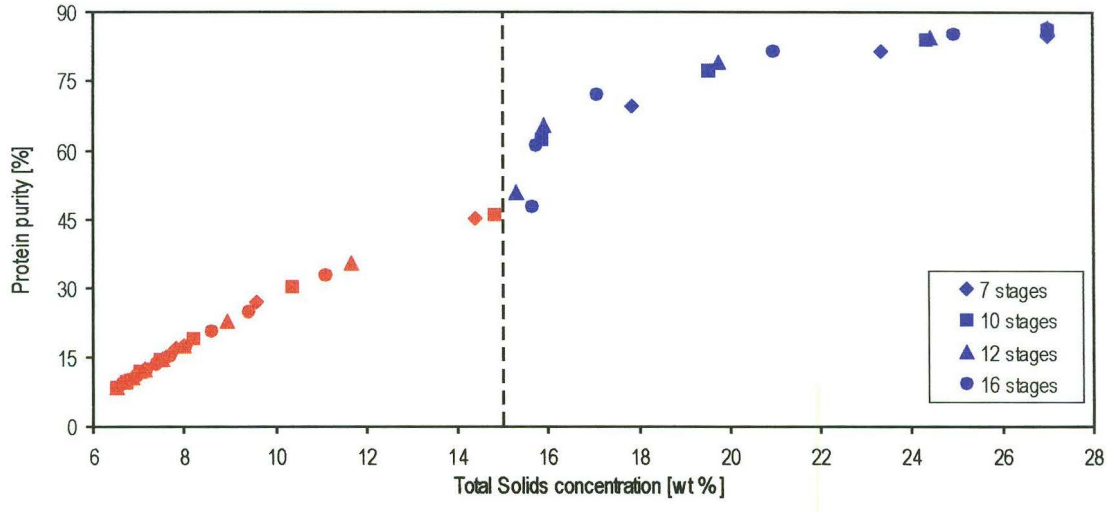

Figure 6-3 Separation trajectories - case study 1 with variable membrane area
Simulation conditions and controller parameters are presented in Appendix B.

The trajectories for this case study show that the plant can be considered as performing two separation operations in series; dewatering (concentration) and purification (fractionation). It is desirable that the feed stream to be concentrated up to approximately 15 wt % total solids prior to entering the first diafiltration stage. Winchester (1996) made an equivalent suggestion, proposing that the total solids concentration prior to the first diafiltration stage be used as the basis for a feed-forward control strategy. However the exact point of measurement in the plant (both simulated and real) moves as new stages are added. Alternative methods of adding membrane area are examined in the next chapter, including strategies allowing measurement of this total solids concentration at a fixed point within the plant.

6.5 Closed-loop behaviour of variable area multistage membrane plants

It has become evident in the previous sections of this chapter that what seems to be a simple separation requires a surprisingly complicated control strategy. The process is not difficult to model, nor is the control technology complex, yet the implementation of a control strategy for a variable area membrane plant is not straightforward. It is not surprising then, that analysis of closed-loop process behaviour poses difficulties also. With non-linear and discontinuous characteristics, a variable area plant makes formal controllability assessment a challenging task. In the previous chapter, controllability assessment methods were successfully applied by neglecting membrane fouling and linearising the resulting process model about a chosen operating point. However for closed-loop analysis, membrane fouling is a fundamental characteristic of the process and cannot be neglected. A plant that does not foul will not require the periodic addition of membrane area, and the requirement for an overall diafiltration ratio strategy is lost. Morari & Perkins (1995) point out that there are essentially no non-linear controllability assessment methods currently available. Linearising the complete (fouling) plant model achieves little unless this analysis is repeated over a number of operating conditions. This leaves only qualitative analysis tools, such as examining plant behaviour in the time domain. Separation trajectories are useful in this context since they provide a means to visualise the behaviour of internal system stages.

6.5.1 Case study 2: Permeate product separation

Whilst the objective of the second case study differs from the first, analysis in the previous chapter and Section 6.4 suggests that the same retentate-based control strategy can be applied to this process. Achieving good control of the retentate total solids concentration and composition will achieve stable permeate stream conditions. Implementing this control strategy therefore becomes a matter of selecting appropriate setpoints for the retentate controllers, so that the desired permeate yield Y_B and a suitable total solids concentration $C_{P\,TS}$ will be achieved for the permeate stream. Implementation details for this control strategy are provided in Table 6-3. A summary of the controller parameters is presented in Appendix B.

Table 6-3 Implementation details of process control strategy - case study 2

Manipulated variable	Measured variable	Implementation details
Retentate flow rate	Retentate total solids concentration	Fixed term PI controller, manually tuned. Retentate flow rate fixed initially at F_R = 0.1 L/s, with controller switching to automatic when total solids concentration reaches 15 wt %. Controller setpoint = 17 wt %. Maximum retentate flow rate limited to 2.5 L/s. Sensor and actuator dynamics neglected in simulation.
Plant feed pressure	Plant feed flow rate	Fixed term PI controller manually tuned. New membrane area added in whole stage increments when the feed pressure reaches upper limit. Plant operating range $0.75 \le P_F \le 2$ bar. Controller setpoint = 15 L/s. Each new stage is added upstream of existing stages, and receives the plant feed. Sensor and actuator dynamics neglected in simulation.
Diafiltration flow rate to each stage	Permeate flow rate from each stage	Flow rate setpoint for each diafiltration stage calculated from $F_{DF,i} = \phi_i F_{P,i}$. Diafiltration ratio for one stage is manipulated to maintain the total flow rate of diafiltration water to the plant as a fixed ratio ϕ_o of the plant feed flow rate. Manipulated ratio ϕ_o corresponds to the diafiltration stage furthest from the retentate stream. ϕ_o = 0 initially with step change to 0.26 when retentate total solids concentration reaches 15 wt %. Stage ratios limited, within range $0 \le \phi_i \le 0.7$. Perfect control assumed in simulation, with all control dynamics ignored.

Feed flow rate control (Figure 6-5A) is not as smooth for this simulation compared to case study 1. In this simulation the process begins operation with 5 stages, producing a higher feed flow rate initially. However this soon reduces as concentration polarisation boundary layers become established in each stage. The differences in feed flow rate behaviour between the two case studies are primarily due to differences in permeate flux model parameters, and operating conditions within the plant.

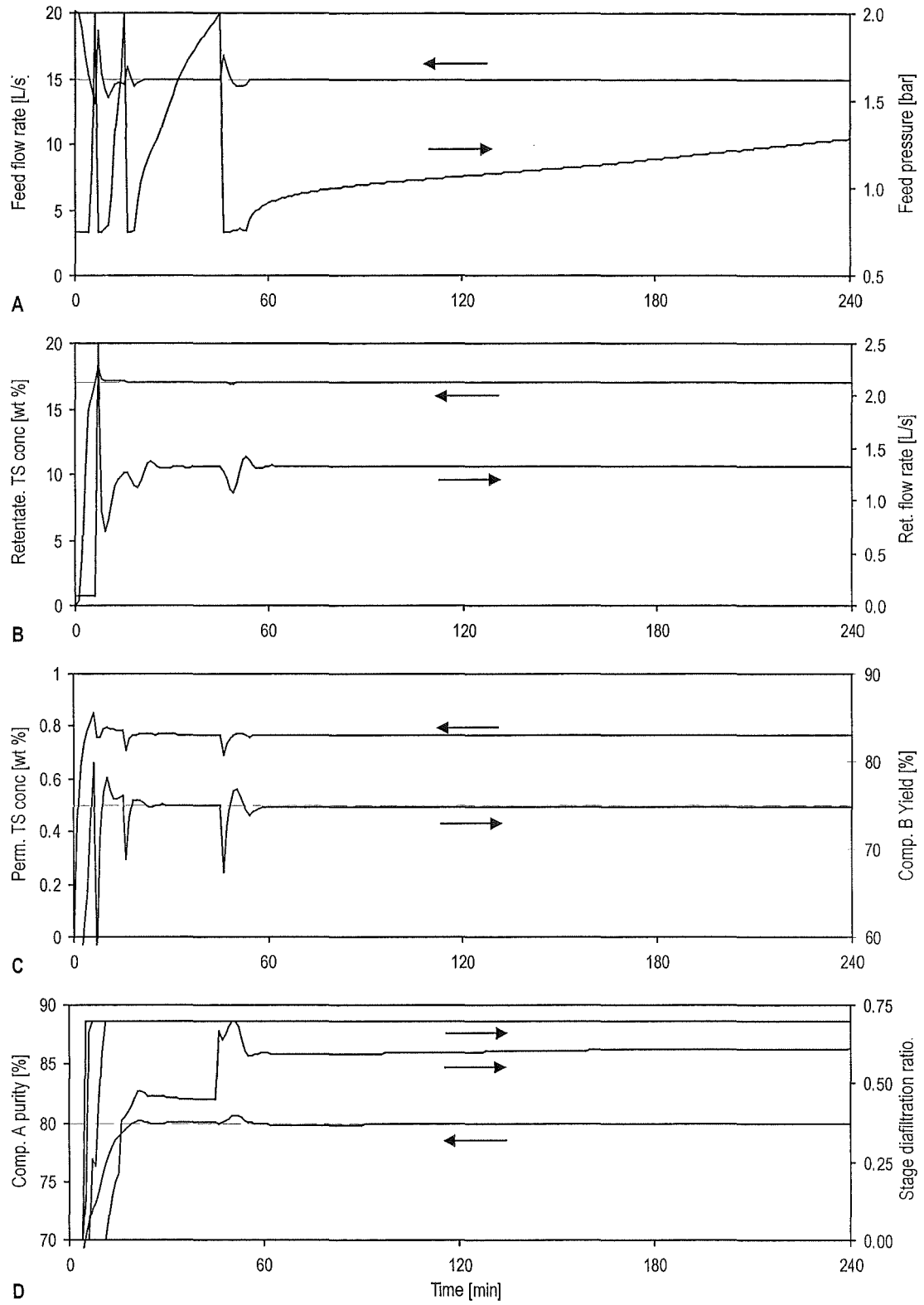

Figure 6-5 Closed-loop operation - case study 2 with variable membrane area
Simulation conditions and controller parameters are presented in Appendix B.

Figure 6-5 shows the both retentate total solids concentration and composition reached setpoint faster than the WPC case study. From the dynamic resilience concepts discussed in Section 6.3, it is known that this superior performance is due to the plant characteristics rather than controller tuning. Examination of the pole-zero maps

presented in Section 5.4.4 confirms this, showing the eigenvalues to be closer to the origin (slower) for case study 1. Of particular interest for this separation are the permeate stream conditions shown in Figure 6-5C. Permeate total solids concentration rose particularly quickly at startup, since this stream is simultaneously dependent on the concentrations of all stages operating in the plant. Therefore, the response of the first stage at startup immediately propagates through into the permeate stream without transport delay. Surprisingly, the yield did not increase with the addition of new separation stages, in fact it actually reduced slightly with the addition of each new stage. Some explanation for this behaviour is provided by Figure 5-11 where ϕ_o declined with increasing number of separation stages (unlike case study 1, shown in Figure 5-5).

For this case study there again exists a constant trajectory (Figure 6-6) for the separation. For this process it would seem desirable to maintain the feed stream to the diafiltration section of the plant at a total solids concentration of 9.25 wt %. The stability of the separation trajectory over time suggests that an alternative control strategy may be feasible, where the process inputs are manipulated to control the total solids concentration and purity of all stages, not just the retentate stream. To implement such an approach all stage compositions would have to be known (to construct the separation trajectory), and a multivariable controller would have to be developed. The feasibility and development of such a control strategy is examined in detail in the next chapter.

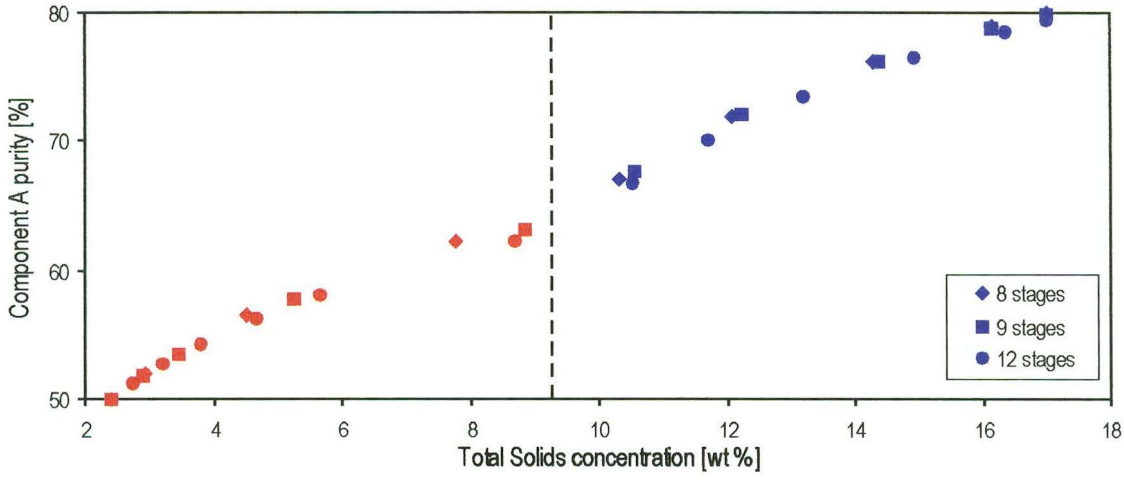

Figure 6-6 Separation trajectories - case study 2 with variable membrane area
Simulation conditions and controller parameters are presented in Appendix B.

6.6 Startup strategies for multistage plants

Membrane plants producing a food grade product usually contain water prior to the start of processing. The startup sequence therefore involves the displacement of water initially within each stage. At startup it is desirable to bring the process smoothly up to setpoint whilst minimising the volume of off-specification product created (Lee *et al.*, 1998). For a retentate product separation, the initial retentate is usually recycled and reprocessed. The volume of off-specification retentate can be reduced if the retentate flow rate remains low prior to the total solids controller switching to automatic. It is theoretically possible to draw no retentate from the plant during startup and produce no off-specification product, however the long residence time associated with this strategy subjects the process stream to excessive shear. Control difficulties also become more likely as the time constant of the final stage tends to infinity (Equation 5-5).

For a membrane process, a successful plant startup is one that quickly develops a stable separation trajectory. A suitable startup strategy for diafiltration injection will help to achieve this. To examine plant startup behaviour and determine the best strategies for each separation, it is necessary to return to the case studies and focus on the initial period of operation.

As a point of reference, it is useful to re-examine the closed-loop behaviour of case study 1, operating under a constant overall diafiltration ratio. Simulated process behaviour was presented in Figure 6-3, for a step increase in ϕ_0 from 0 to 0.118 when the retentate total solids concentration 25 wt %. The first 30 minutes of this simulation are replotted in Figure 6-7, allowing process startup to be more closely examined. It can be seen (Figure 6-7B) that the total solids concentration of the retentate stream deviated significantly when diafiltration injection commenced after 6 minutes. Most importantly, both retentate stream specifications (purity and concentration) reached setpoint simulta-

Table 6-4 Comparison of pre-production retentate volumes for different startup strategies - case study 1

Total Solids concentration setpoint for commencing diafiltration injection [wt %]	Off-specification retentate volume produced initially [L]
15 (step increase in ϕ_0)	49
25 (step increase in ϕ_0)	75
27 (step increase in ϕ_0)	251
15 (ϕ_0 ramped over 7 minutes)	44

neously with minimal overshoot. The off-specification retentate volume for this startup strategy, along with three others, is given in Table 6-4. At startup, the stage concentrations rise and the separation trajectory (Figure 6-4) begins to develop from the feed toward the desired retentate condition. If diafiltration injection does not commence at some point during startup the desired retentate composition (85 % protein purity) will not be attained. Two things occurred simultaneously when the retentate concentration reached 25 wt % after 6 minutes (Figure 6-7B); the total solids controller switched to automatic, and diafiltration injection into the plant began, due to a step increase in ϕ_0. The separation trajectory immediately begins to change in response to the new operating conditions, and the diafiltration profile started to develop. After 15 minutes the full trajectory was established, and the desired retentate conditions were achieved.

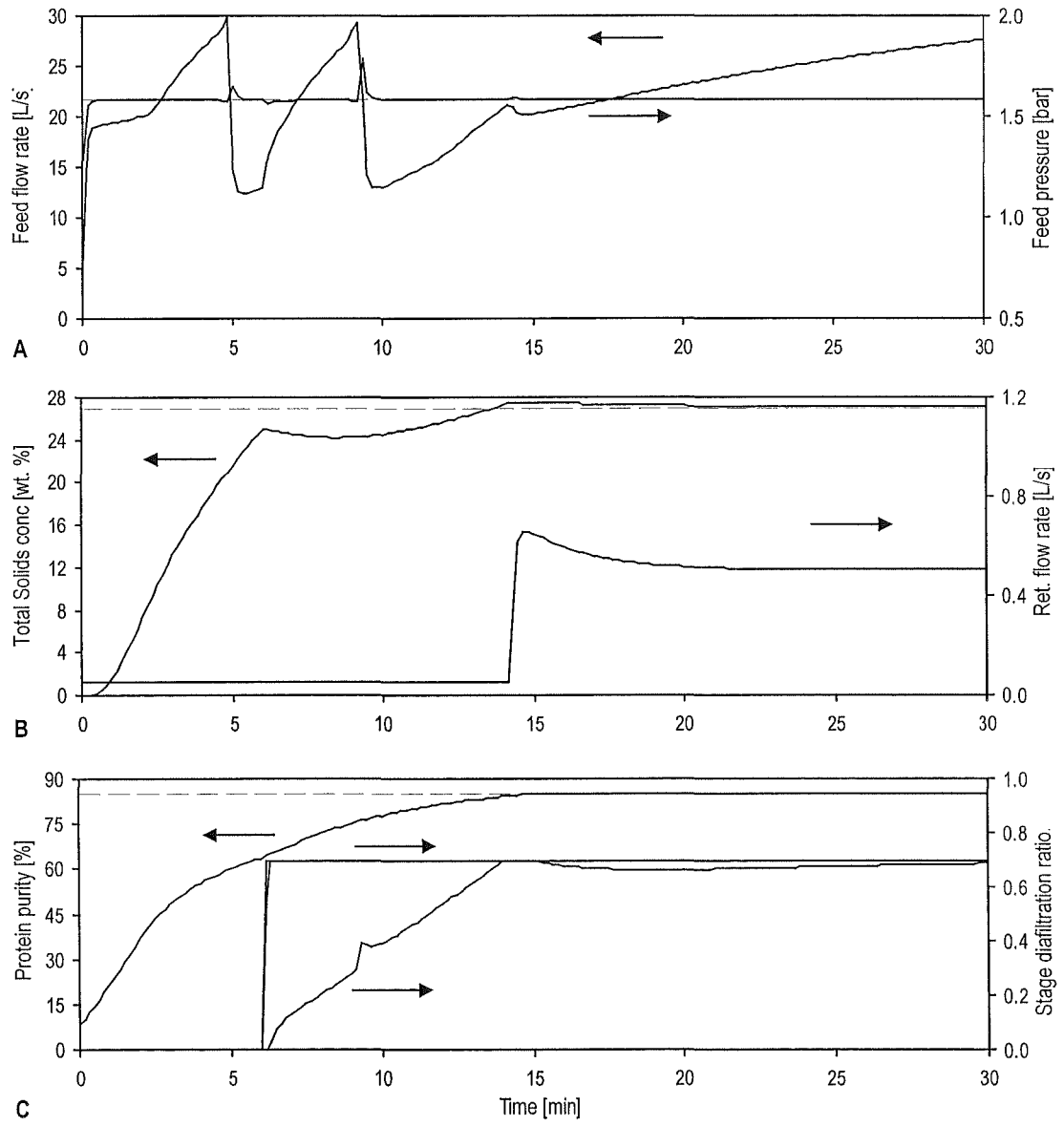

Figure 6-7 Startup operation - case study 1 with a step increase in diafiltration at 25 % total solids
Simulation conditions and controller parameters are presented in Appendix B.

An alternative approach is to delay diafiltration injection until the desired total solids concentration is reached. In this situation, the plant will develop the complete (non-diafiltration) separation trajectory from the feed to the retentate totals concentration, prior to diafiltration injection commencing. Startup profiles for this approach (Figure 6-8) show no overshoot occurred in protein purity, but there was a significant delay in the setpoint being achieved. This resulted in an excessive volume of off-specification retentate being produced (Table 6-4), since the retentate flow rate was much greater once the total solids controller has switched to automatic.

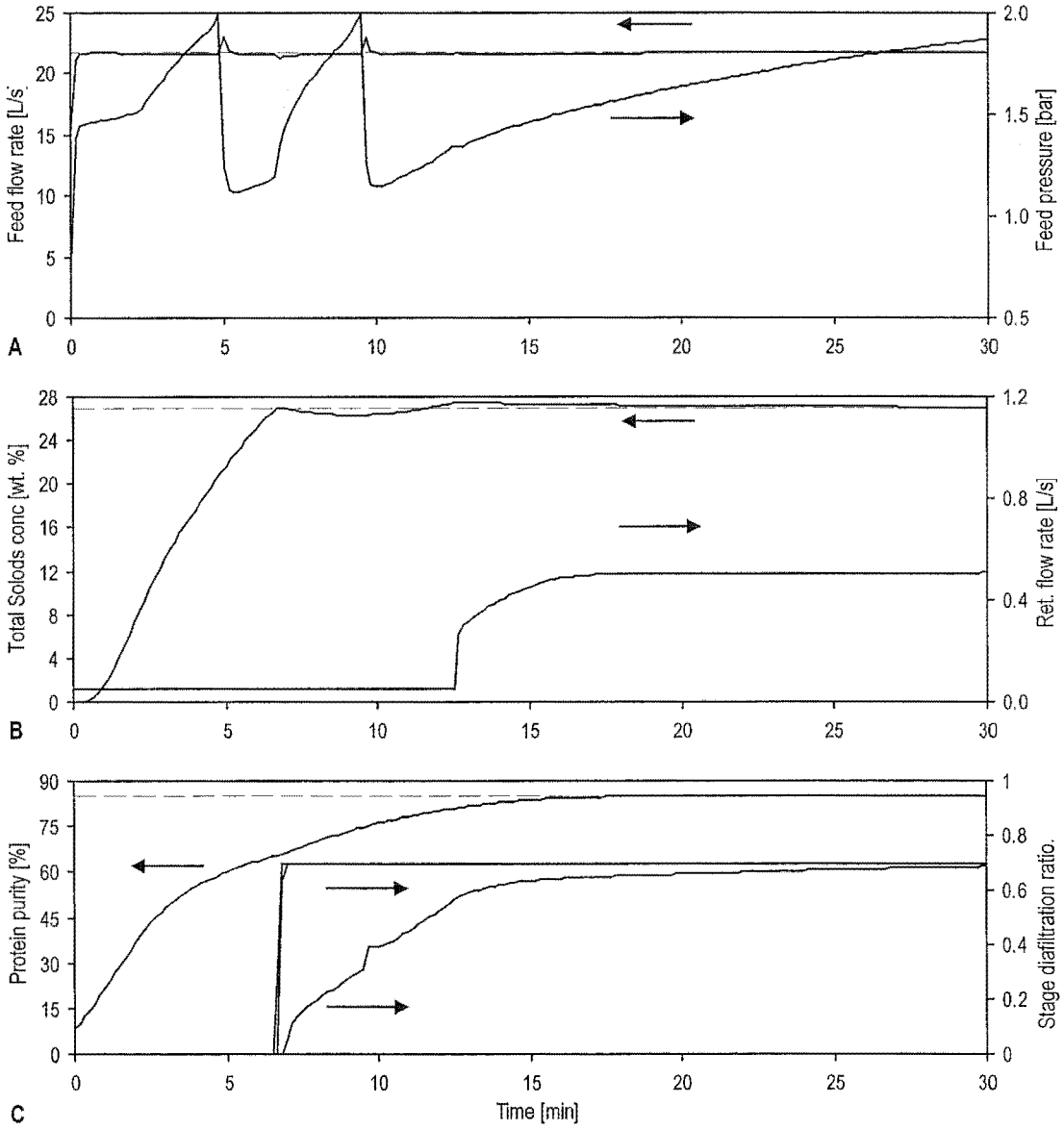

Figure 6-8 Startup operation - case study 1 with a step increase in diafiltration at 27 % total solids
Simulation conditions and controller parameters are presented in Appendix B.

An interesting alternative is to attempt to follow the stable separation trajectory at startup (Figure 6-4). To do this, diafiltration injection must commence when the

retentate total solids concentration reaches 15 wt %. Startup profiles for this strategy are shown in Figure 6-9 for a step increase in ϕ_o. Examining the simulation it can be seen that this strategy delayed the total solids concentration reaching setpoint, and caused overshoot in the protein purity. The deviation in retentate total solids concentration at the introduction of diafiltration suggests that the process did not completely follow the desired trajectory during startup.

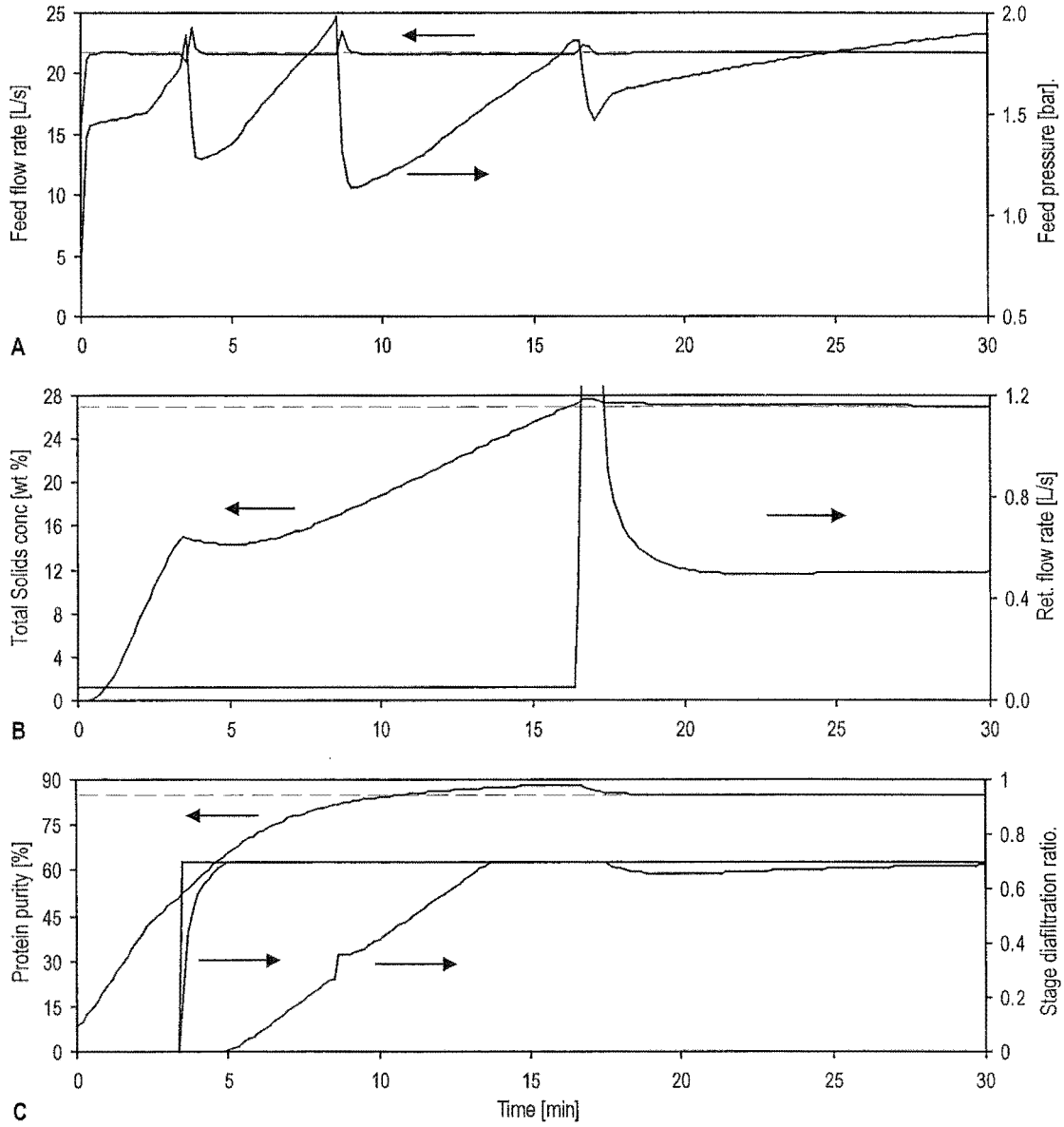

Figure 6-9 Startup operation - case study 1 with a step increase in diafiltration at 15 % total solids
Simulation conditions and controller parameters are presented in Appendix B.

It is clear that the abrupt introduction of diafiltration to the plant during startup, via a step increase in ϕ_o, causes a brief but undesirable reduction in the retentate total solids concentration. A less aggressive approach to introducing the diafiltration water may solve this problem. Figure 6-10 shows the startup profiles for the plant when diafiltra-

tion injection was initiated in a less abrupt manner, by smoothly increasing (ramping) ϕ_0 from zero to 0.118 over a period of 7 minutes. This allowed both the concentration and composition of the retentate stream to reach setpoint simultaneously, and reduced the volume of off-specification retentate produced (Table 6-4). Overall, this approach disturbed the plant less, produced a smoother startup and allowed the plant to settle to a stable separation trajectory more quickly. From this sequence of simulations it would seem that the slow introduction of diafiltration water at a suitable total solids concentration is a superior alternative to the abrupt startup methods currently employed industrially.

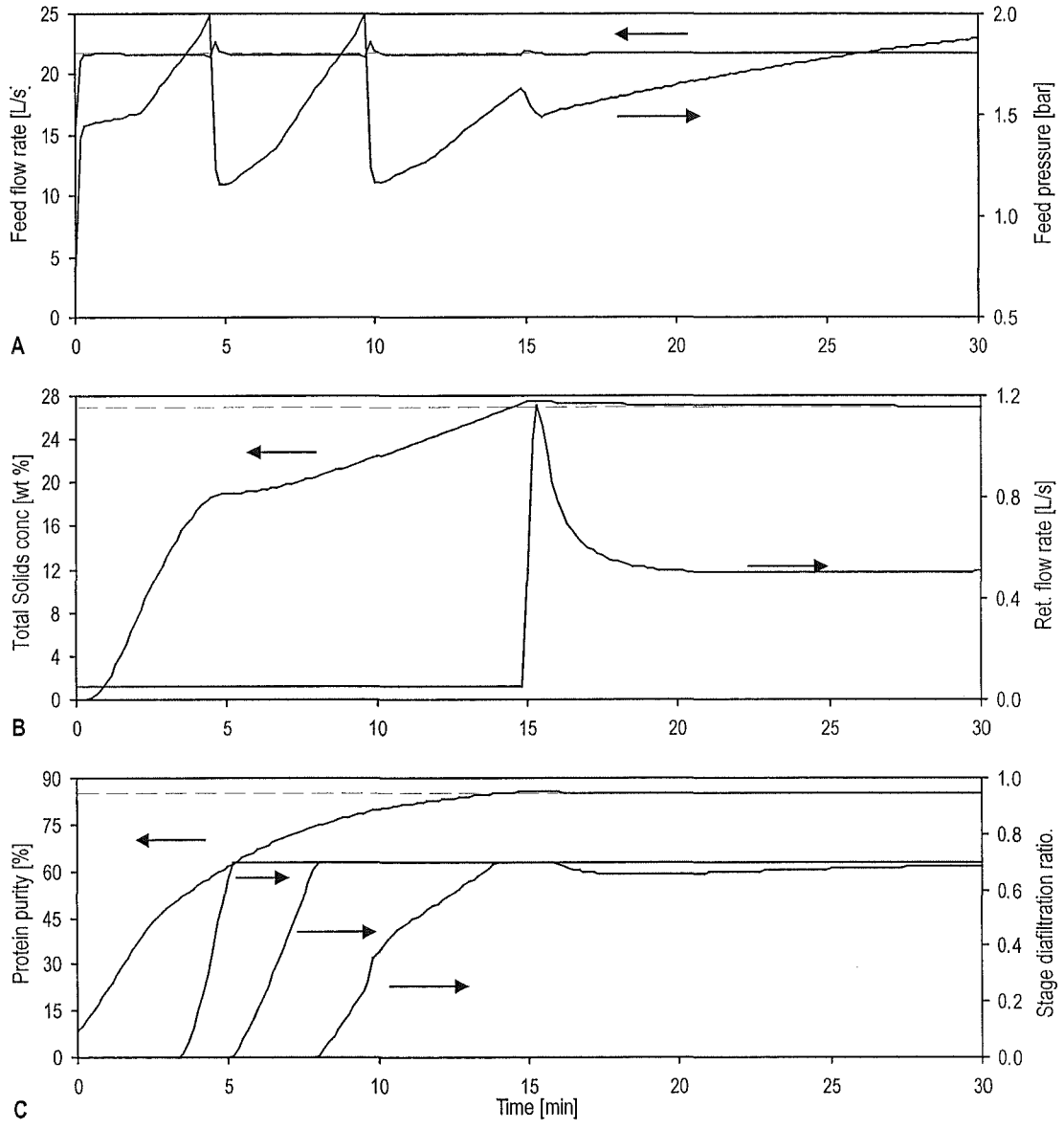

Figure 6-10 Startup operation - case study 1 with a ramped increase in diafiltration from 15 % total solids

Simulation conditions and controller parameters are presented in Appendix B.

Startup requirements for the second case study differ somewhat from the first, since a permeate rather than a retentate product is manufactured. Startup time is not as significant in this situation because recovery of the permeable component begins as soon as the feed stream enters the first stage. Figure 6-11 shows the first 30 minutes of

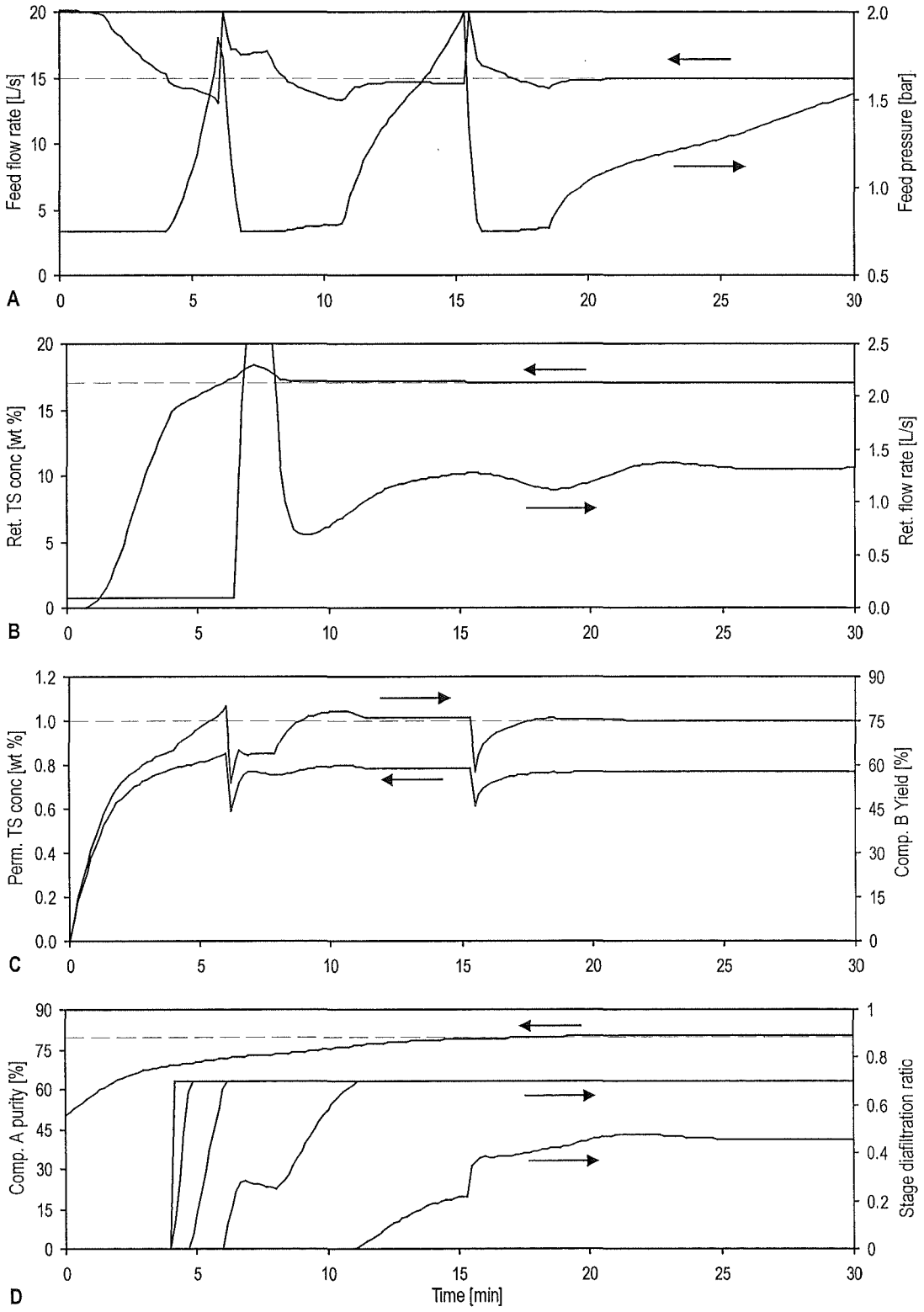

Figure 6-11 Startup operation - case study 2 with a step increase in diafiltration at 15 % total solids

Simulation conditions and controller parameters are presented in Appendix B.

plant operation under the constant overall diafiltration strategy first shown in Figure 6-5. Figure 6-11 clearly shows that the process achieves a high yield relatively quickly, even though the retentate stream concentration and composition are slow to change.

Plant startup behaviour (Figure 6-11C) clearly shows the permeate yield to have much lower order and faster response dynamics than the retentate concentration or purity (Figure 6-11A & D). Such behaviour was predicted in Sections 4.3.2 and 5.4.4. The concepts of dynamic resilience (Lenhoff & Morari, 1982) are particularly evident in this simulation, where superior permeate startup performance is achievable, but only because the plant dynamics are favourable. Slow retentate rise-times cannot be improved by alternative feed back control strategies, since it is the plant dynamics that limit achievable controller performance.

Following initial startup the permeate yield showed a significant increase following the introduction of diafiltration injection. Figure 6-11C suggests then, that the desired yield could be attained more quickly if diafiltration injection commenced sooner. Separation trajectories for this case study (Figure 6-6) agree with this assessment, suggesting that diafiltration injection should commence (via a step increase in ϕ_0) when the total solids concentration reached 9.25 wt %. Simulating this startup strategy (Figure 6-12) shows the yield to now rise more quickly to the desired value. Coincidentally, the retentate concentration and composition also reached their respective setpoints almost simultaneously. This startup strategy would seem to satisfy all requirements and provide the best possible startup performance for this case study.

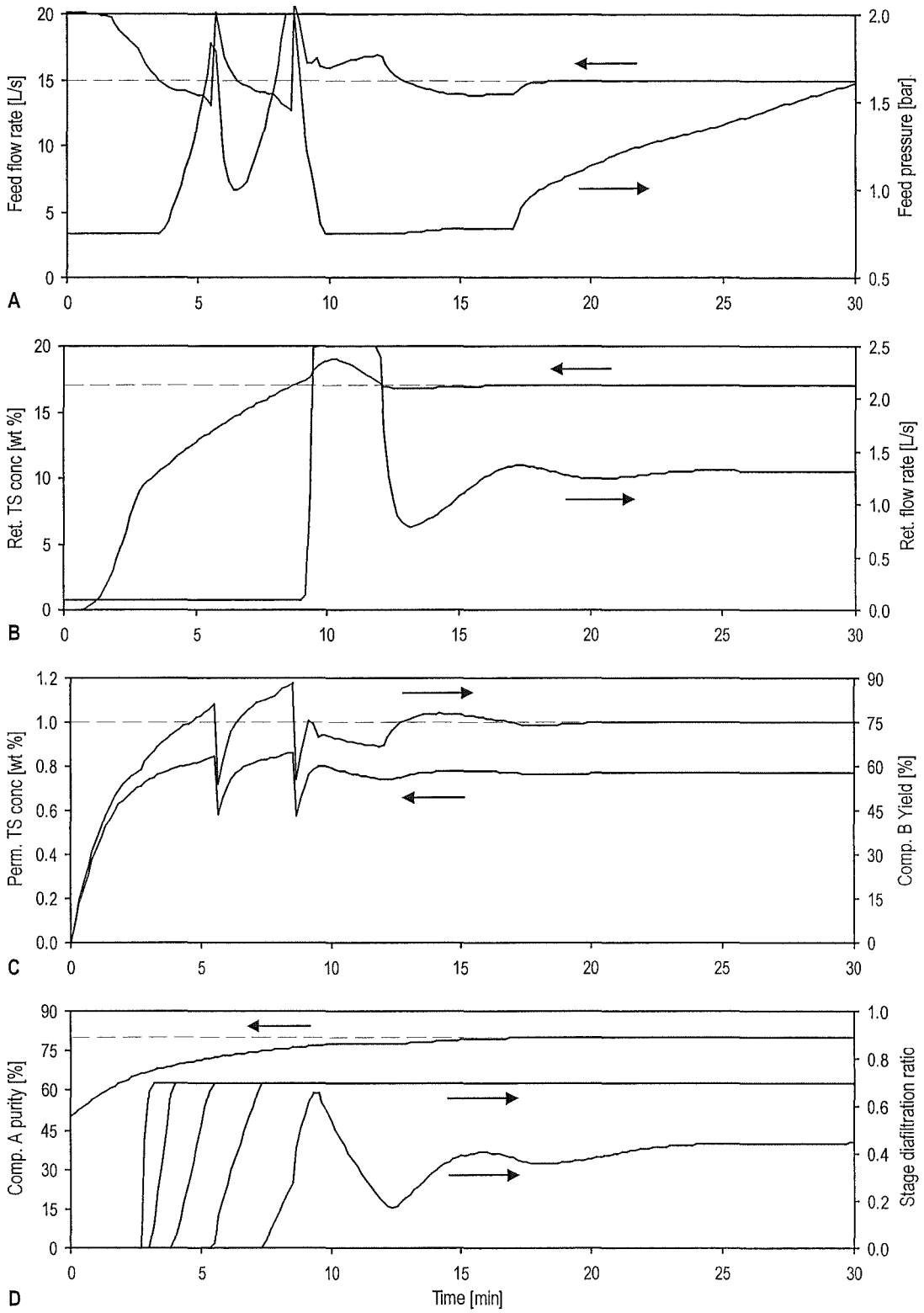

Figure 6-12 Startup operation - case study 2 with a step increase in diafiltration at 9.25 % total solids

Simulation conditions and controller parameters are presented in Appendix B.

6.7 Effect of membrane area addition on multistage plants

It was stated in Sections 6.4 and 6.5.1 that the addition of a new stage was a significant disturbance to a membrane plant. Ideally it would be possible to use some numerical

tool to provide a quantitative assessment of this disturbance. Methods for minimising this disturbance index could then be investigated However, for reasons previously discussed in Chapter 5 this is not particularly feasible and a qualitative assessment method must be used instead. The effect of area addition on internal states is best visualised by plotting a series of separation trajectories following the addition of a new stage. Figure 6-13 shows such a sequence for case study 1, for the addition of the 8th stage, at time $t = 37$ minutes in Figure 6-3. Immediately prior to this event the plant was operating at the desired setpoints and the separation trajectory was stable. This stable seven stage trajectory is shown in Figure 6-13A-D for comparison.

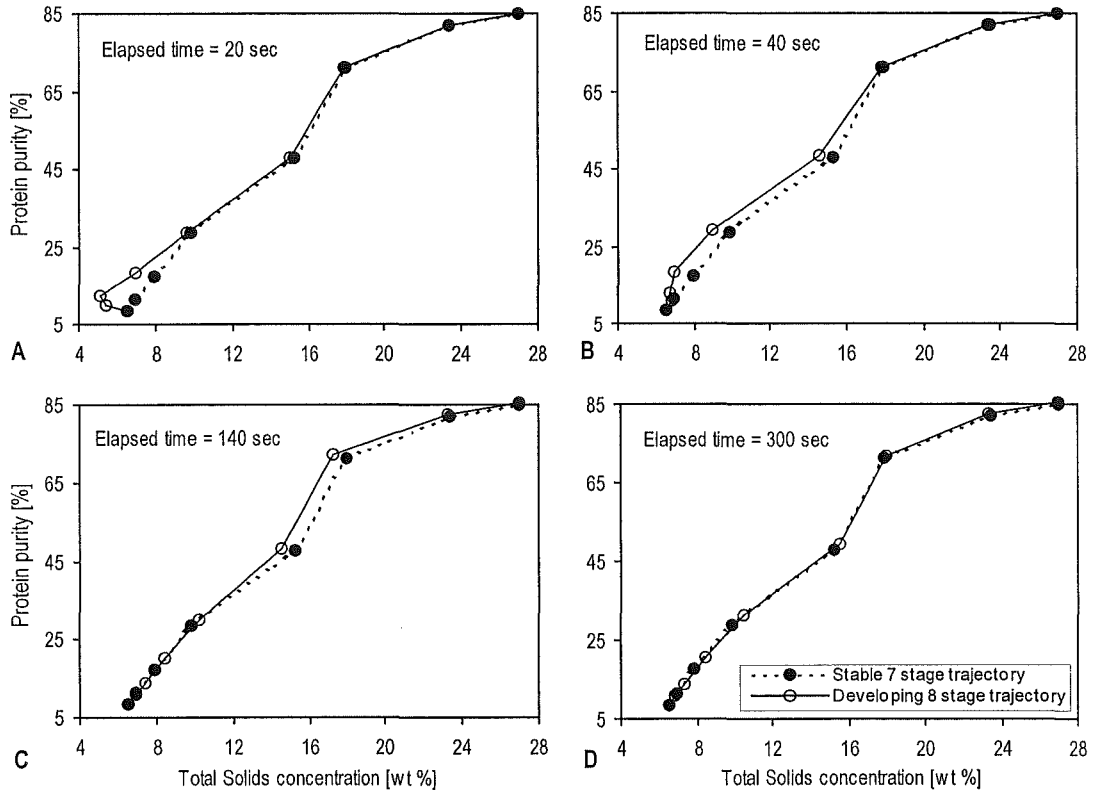

Figure 6-13 Separation trajectories - effect of stage addition on case study 1

Separation trajectories produced from simulation presented in Figure 6-3 following the addition of a new stage at $t = 37$ minutes.

In an industrial plant, the addition of a new stage is achieved by opening the isolation values and starting the recirculation pump (see Section 3.6 for details). Some of the water initially contained in the stage will pass through the membrane to the permeate stream with the remainder recirculating around the stage and being displaced by the feed stream over time. It is common practice to add new stages upstream of those currently in operation, with the feed stream always entering the most recently added stage. In the closed-loop process simulation, the addition of a new stage caused the separation trajectory to briefly distend to the left of the feed point, due to dilution from the water in

the new stage (Figure 6-13A). As water was displaced from the first stage it passed through each successive stage down the plant acting much like a volume of diafiltration water (Figure 6-13B). This concentration-composition disturbance continued down the process (Figure 6-13C) until it reached the retentate stream and passed from the plant, allowing the stable trajectory to become re-established (Figure 6-13D). For this WPC case study, it took approximately 5 minutes for the plant to return to a stable separation trajectory.

The process response following the addition of a new stage is much the same for case study 2. Figure 6-14 shows a sequence of separation trajectories following this event, corresponding to t = 25 minutes in Figure 6-5. Water initially in the new stage was again displaced and passed down the plant as a combined concentration-purity disturbance. However for this case study it took significantly longer for the process to return to a stable separation trajectory (Figure 6-14D).

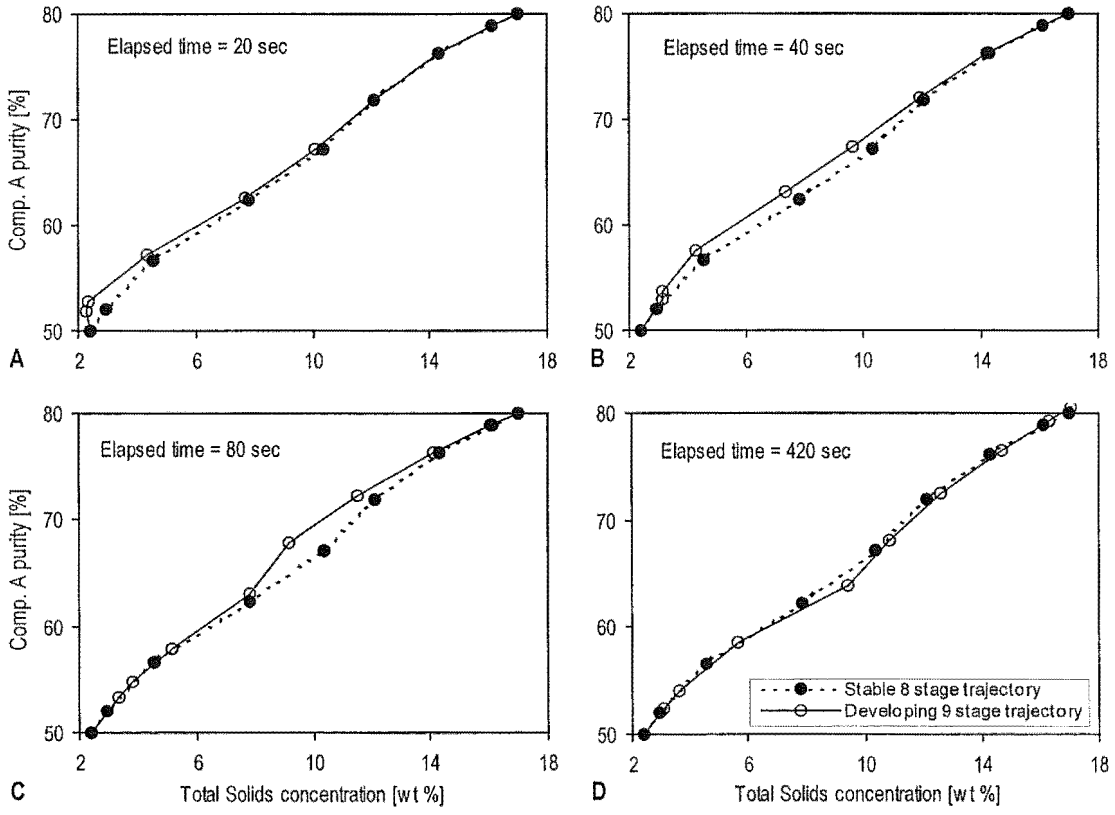

Figure 6-14 Separation trajectories - effect of stage addition on case study 2
Separation trajectories produced from simulation presented in Figure 6-5.

Overall it can be concluded for both case studies that the addition of a new stage significantly disturbs a multistage stage membrane plant. However, each new stage is deliberately added upstream of all existing ones, to allow maximum attenuation before

the resulting disturbances enter the retentate stream. This is a sound approach for a retentate product separation, but may seem less logical for a permeate product plant. However, given that the control strategy still focuses on the retentate stream properties it is still desirable to attenuate disturbances before they enter the retentate stream of the permeate product plant.

6.8 Effect of feed concentration disturbances in multistage plants

Structural analysis in Chapter 4 suggested that feed concentration disturbances in non-key components (those not affecting permeate fluxes) were well attenuated by the plant, and not particularly significant. The effect of feed concentration disturbances on a closed-loop process is most easily determined by simulation and analysis in the time domain. To do this it is necessary that the plant be operating at setpoint in a stable manner.

For case study 1, a 10 % step increase in lactose feed concentration was introduced at t = 65 minutes when the plant was operating at a constant total solids concentration and protein purity. The simulation was performed using the same operating conditions as Figure 6-3. The process response (Figure 6-15) showed the retentate total solids controller to have excellent disturbance rejection abilities. Unfortunately open-loop composition control, like most open-loop strategies, could not reject the unmeasured

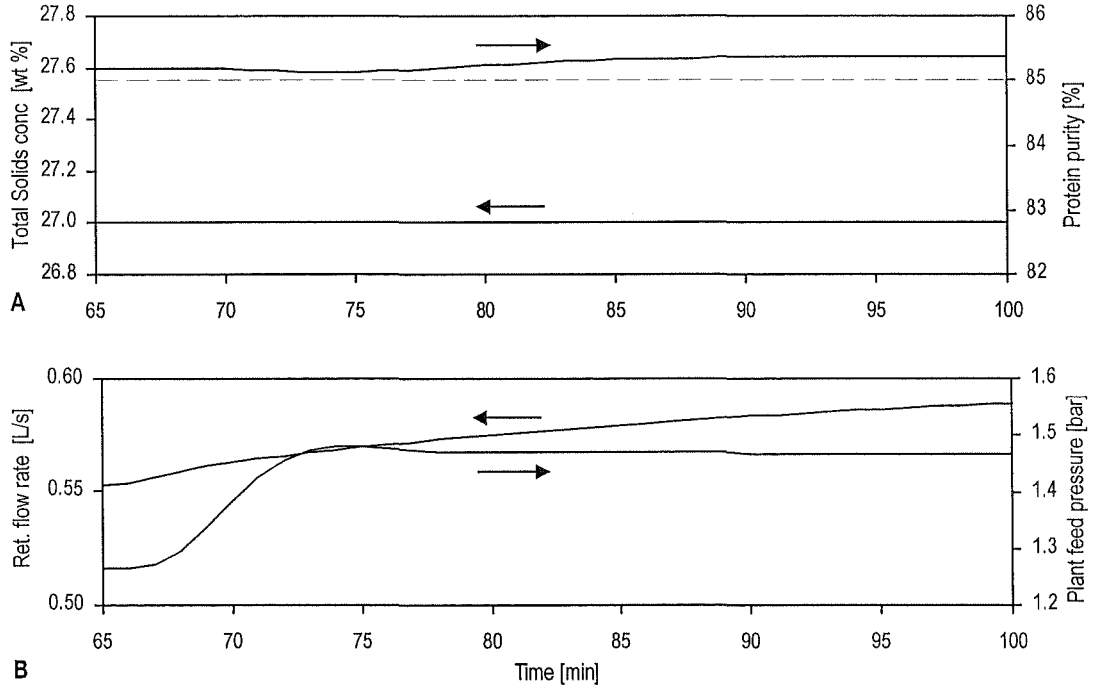

Figure 6-15 Disturbance response for 10 % step increase in lactose feed concentration - case study 1
Constant overall diafiltration ratio strategy. See Figure 6-3 for simulation conditions.

composition disturbance. For this reason the retentate composition varied noticeably, dropping below the purity specification several minutes after the concentration of lactose (impurity) in the feed stream increased.

Figure 6-16 shows the closed-loop system response to a 10 % step increase in protein feed concentration at t = 65 minutes (Figure 6-3). Protein is a key component, the concentration of which can affect permeate fluxes and system flow rates. Structural analysis in Chapter 4 suggested that a protein feed concentration disturbance would have complex, widespread effects on a multistage membrane plant. The system response is indeed complex, with the retentate purity showing inverse response characteristics several minutes after the disturbance entered the process. As predicted this disturbance had significant effect on process conditions, causing the controllers to manipulate both the retentate flow rate and plant feed pressure (Figure 6-16B). The overall diafiltration ratio control strategy was surprisingly successful at mitigating this disturbance, ironically due to the concentration disturbance propagating through to the system flow rates. In maintaining a constant overall diafiltration ratio, the action of the diafiltration strategy partially mitigated the change in feed concentration. A lactose (non-key component) disturbance did not affect system flow rates, so the feed concentration variation was not detected.

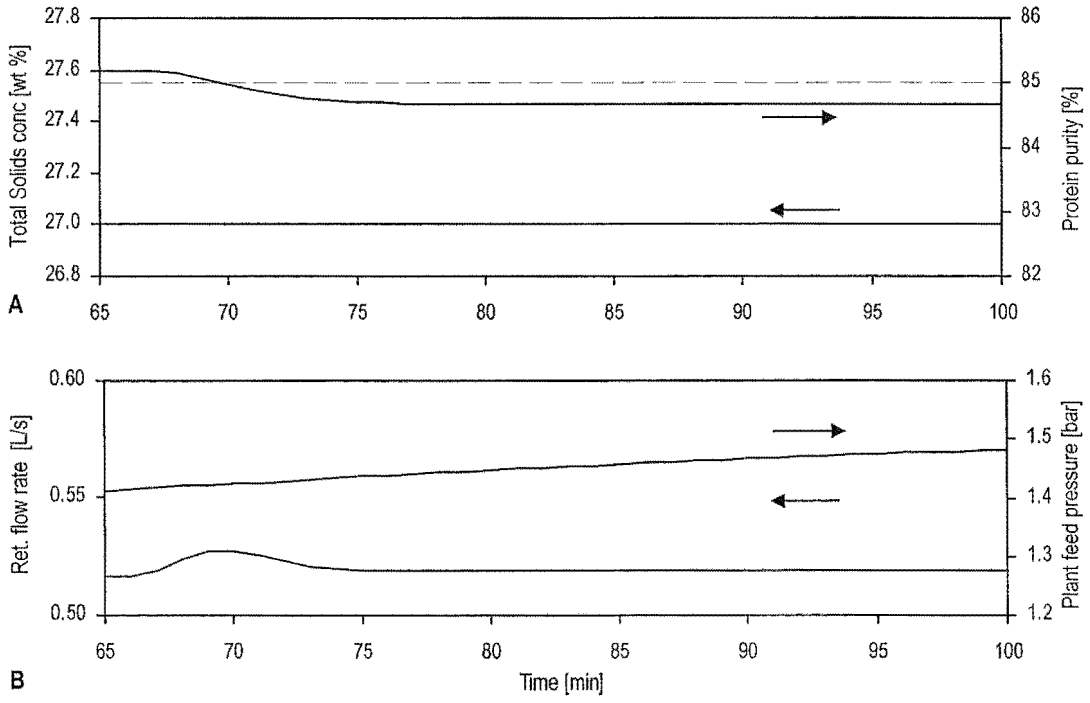

Figure 6-16 Disturbance response for a 10 % step increase in protein feed concentration - case study 1
Constant overall diafiltration ratio strategy. See Figure 6-3 for simulation conditions.

The behaviour of the variable (manipulated) diafiltration ratios ϕ_v are compared in Figure 6-17 for the 10 % protein and lactose feed concentration disturbances. Greater action was taken by the overall diafiltration controller following the protein (key component) feed concentration disturbance due to the resulting changes in permeate fluxes. The diafiltration controller response to the lactose feed concentration disturbance was smaller, since the lactose disturbance did not affect permeate fluxes. The diafiltration controller response was actually caused by the actions of the retentate total solids controller. This highlights the significance of interaction effects between individual control loops operating on a membrane process.

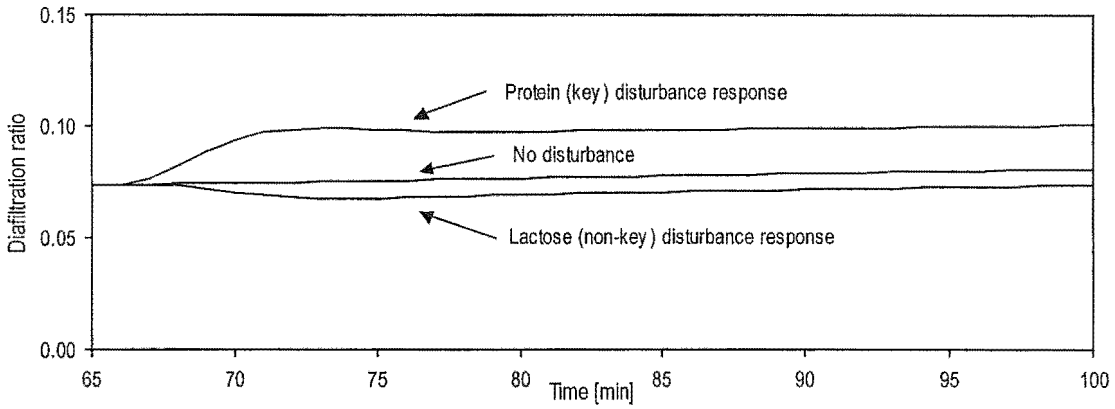

Figure 6-17 Action of manipulated diafiltration ratio ϕ_v following feed concentration disturbance - case study 1
Constant overall diafiltration ratio strategy. See Figure 6-3 for simulation conditions.

The disturbance rejection capabilities for case study 2 were examined by introducing a step increase in feed concentration at t = 65 minutes while the plant was operating at setpoint under conditions associated with Figure 6-5. The effect of a 10 % increase in (non-key) Component B was evident in the retentate stream several minutes later (Figure 6-18A), and was equivalent to the behaviour observed in case study 1, for a non-key component disturbance. However, both permeate yield and concentration showed an immediate response to the disturbance (Figure 6-18B), much like that seen during plant startup. The increased feed concentration passed into the first stage then diffused directly into the permeate stream, to produce a fast system response.

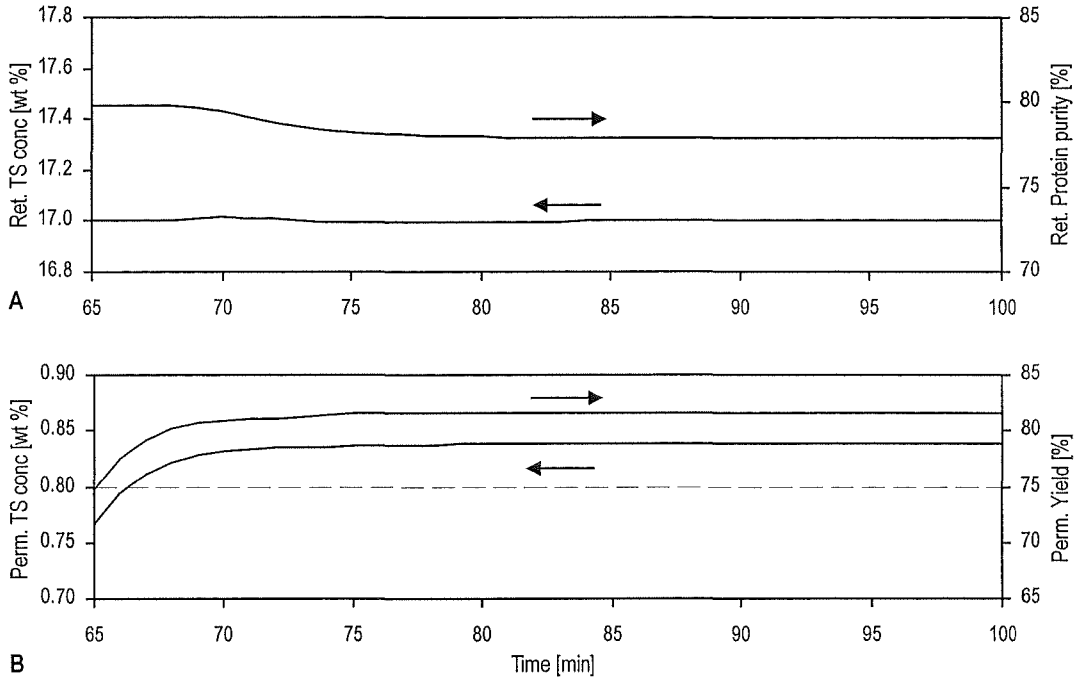

Figure 6-18 Disturbance response for a 10 % step increase in Component B feed concentration - case study 2
Constant overall diafiltration ratio strategy. See Figure 6-5 for simulation conditions.

A step increase in Component A (key) feed concentration (Figure 6-19) had a less significant effect on the permeate stream. Although component A was impermeable, the disturbance still propagated through to the permeate stream (Figure 6-19B), via the permeate flow rate disturbances that occurred. However, without direct propagation pathways the permeate stream response was much slower.

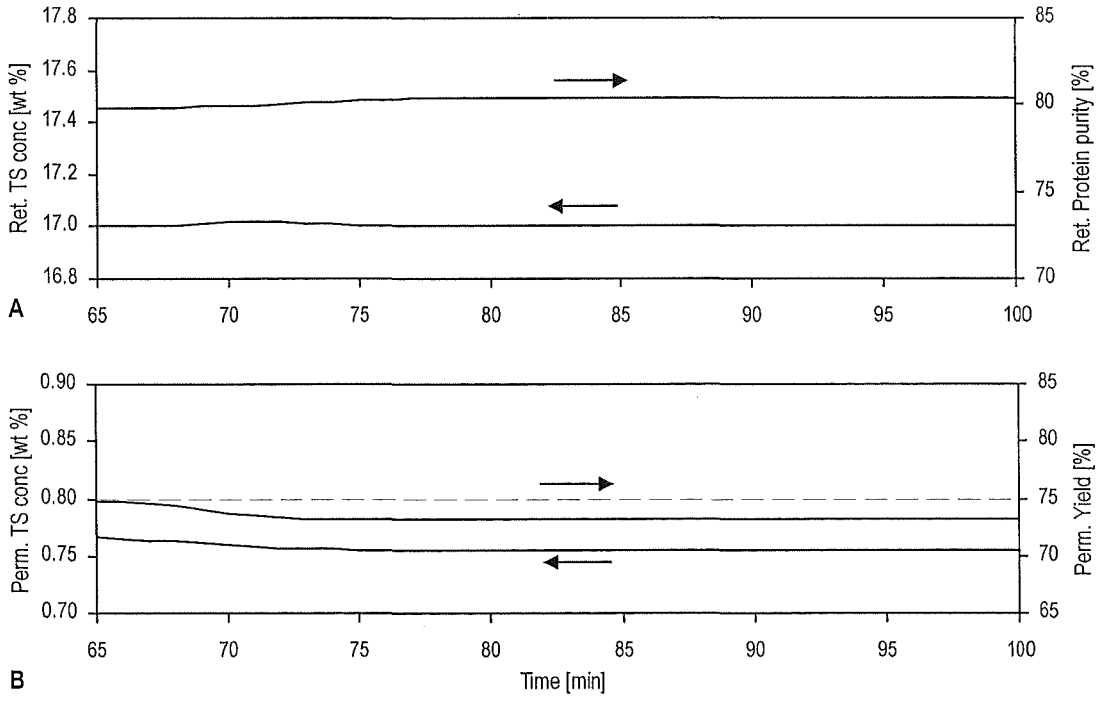

Figure 6-19 Disturbance response for a 10 % step increase in Component A feed concentration - case study 2
Constant overall diafiltration ratio strategy. See Figure 6-5 for simulation conditions.

Overall, disturbances in Component A generally had less effect on the process. This is primarily because disturbances in this key component caused subsequent disturbances in the system flow rates which were detected by the diafiltration strategy. In reacting to these flow rate changes, the controller partially mitigated the original concentration disturbance (Figure 6-20). Component B (non-key) disturbances did not propagate to system flow rates, and so the diafiltration strategy did not take action. The variation in ϕ_r shown in Figure 6-20 for the Component B disturbance was in response to the actions of the retentate total solids controller.

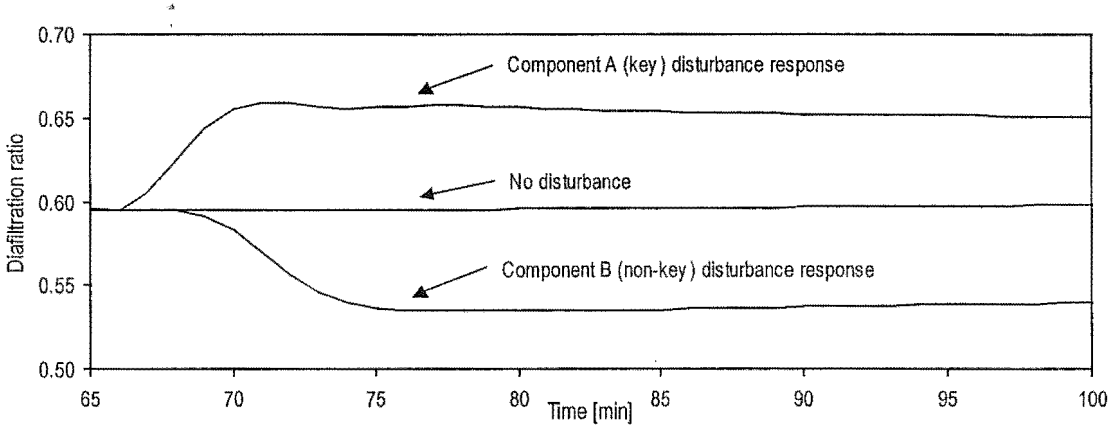

Figure 6-20 Action of manipulated diafiltration ratio ϕ_r following feed concentration disturbance - case study 2
Constant overall diafiltration ratio strategy. See Figure 6-5 for simulation conditions.

6.9 Conclusion

This chapter has examined the closed-loop behaviour of multi-stage membrane plants, focusing primarily on composition control strategies and difficulties. Significant interaction occurred between the individual SISO control loops operating on the plant, as predicted by the structural controllability assessment (Chapter 4) and open-loop steady state analysis (Chapter 5). The addition of new separation stages to maintain the desired feed flow rate was found to be the most significant source of disturbances entering the process. Analysis showed that in trying to reject such disturbances, ratio-controlled diafiltration stages created significant new disturbances for the other control loops.

Feed concentration disturbance analysis showed that key components (affecting permeate fluxes) were generally better mitigated, since disturbances in the permeate flow rates were detected by the diafiltration strategy. The overall diafiltration controller did not react directly to non-key component disturbances, meaning that these had a

greater effect on the retentate stream concentration and purity as a result. These results, based on closed-loop simulations, contradicted the open-loop structural analysis of Chapter 4, highlighting the complexity of closed-loop process behaviour. Experimental validation of the results presented in this chapter was not undertaken, but it is believed that contradictions between the open-and closed-loop results were due to limitations in the controllability assessment tools, rather than modelling issues.

The existence of a stable separation trajectory for each case study allowed improved plant startup strategies to be developed. They also helped to visualise the propagation of disturbances caused by the addition of a new stage to a plant. It was suggested that the desired separation trajectory of a process could perhaps be used as the basis for a plantwide control strategy, instead of using single setpoints for individual SISO control loops. Such an approach would require the implementation of a multivariable control strategy, and the development of a unique framework for specifying an appropriate control objective. These concepts are considered and developed in the next chapter.

6.10 References

Lee P L, Newell R B & Cameron I T (1998), *Process Control and Management,* Blackie Academic and Professional, UK.

Lenhoff A M & Morari M (1982), Design of resilient processing plants - I; process design under consideration of dynamic aspects, *Chem. Eng. Sci.,* **37**, (2), 245-258.

Marlin T E (1995), *Process Control: Designing Processes and Control Systems for Dynamic Performance,* McGraw-Hill International, Singapore.

Morari M & Perkins J (1995), Design for operations. In *Fourth International Conference on: Foundations of Computer-Aided Process Design* (Ed. Biegler L T & Doherty M F), Vol. 91, No. 304, pp. 105-114, AIChE Symposium Series.

Morison K R (1998), Department of Chemical and Process Engineering, University of Canterbury, Personal communication

Ogunnaike B A & Ray W H (1994), *Process Dynamics, Modeling, and Control,* Oxford University Press, New York.

Stephanopoulos G (1984), *Chemical Process Control: An Introduction to Theory and Practice,* Prentice-Hall International, New Jersey.

Winchester J (1996), *Computer Simulation and Controllability Studies of Multi-module Ultrafiltration Plants.* M.E. Thesis, Department of Chemical and Process Engineering, University of Canterbury, New Zealand.

7 Novel Strategies For Improving Membrane Plant Behaviour

An extensive analysis of multistage membrane plant behaviour has been presented in the previous chapters of this thesis. Initially, structural system models were employed to examine disturbance propagation and interaction characteristics, followed by the use of steady state simulations for the numerical assessment of open-loop process controllability. SISO controller strategies were then developed and used in the simulation and analysis of closed-loop system characteristics. Some minor improvements were identified during this analysis, but significant improvements in controller performance were not achieved. It is the intention of this chapter to review the process from a fresh perspective, using the understanding that has been gathered thus far to develop new approaches to improving closed-loop plant behaviour.

Process performance can be considered in the contexts of both operating efficiency and controller performance. Analysis in previous chapters has shown that the requirements of these two objectives are generally conflicting. The desire here is to enhance controller performance without making significant sacrifices in operating efficiency.

7.1 Opportunities for improving membrane plant behaviour

Membrane separation processes have a complex, multifaceted nature. For this reason it has been necessary to examine specific aspects of the system separately, before it can be understood as a whole. In each previous chapter, individual aspects of the separation process have been examined, to develop an understanding of the complete membrane process:

- Chapter 2 reviewed common flowsheet designs and methods of improving separation performance
- Chapter 3 presented methods of developing a dynamic process model
- Chapters 4 & 5 investigated the inherent characteristics of multistage membrane separations
- Chapter 6 examined closed-loop process behaviour and strategies for SISO controller implementations

It is now possible to revisit each aspect of the process, and consider options to remove, avoid or minimise limitations on closed-loop performance.

A variety of separation flowsheets were presented in Chapter 2, a subset of which are capable of fulfilling the operating requirements of the two case studies (Section 2.5). In both cases it was necessary that the plant operate with constant processing capacity for a (relatively) long period of time. This implies that the process must be (batchwise) continuous, and thus all batch flowsheets are removed from the set of viable alternatives.

High capital costs for membrane area strongly favour designs that maximise separation efficiency, and minimise membrane fouling. Analysis in Chapter 2 showed that sequentially staged flowsheets offer the highest separation efficiencies possible with a continuous flowsheet. Efficiency increased with number of stages, suggesting that it is desirable for a plant design to have a large number of separation stages. Consequent analysis in Chapters 4 & 5 showed that processes with more stages exhibited greater levels of interaction and were more likely to have oscillatory characteristics. This behaviour is highly undesirable and such flowsheets should be avoided, or modified to mitigate such characteristics. With design optimisation strongly favouring flowsheets with many stages, the only economically feasible alternatives are small modifications to the process flowsheet, or the development of superior control strategies. The level of interaction within the process may be reduced by inserting well-mixed 'buffer' tanks between each stage, but for a plant with many stages, this represents a large capital cost and excessive residence times that would not satisfy the food safety requirements stipulated in Section 2.5. A trade-off therefore exists between process design and controllability which is difficult to avoid.

Closed-loop analysis in Chapter 6 identified the disturbances associated with membrane area addition as having a significant effect on controller performance. Unfortunately, variable area operation is necessary if a constant feed flow rate is to be maintained. Large variations in feed flow rate have an associated economic cost, since they create the need for a larger buffer tank between upstream operations and the membrane plant. More significantly, larger intermediate storage corresponds to greater residence times within the process and increased (food) safety risks. Whilst it is desirable, from the process control perspective, to avoid variable area operation, the costs and risks associated with such a decision outweigh potential controller performance improvements.

The high product purity and permeate yield requirements of the case studies mean that diafiltration injection is necessary to achieve sufficient fractionation of the feed stream. Dynamic analysis in Chapters 4 & 5 showed that the application of diafiltration injection generally caused undesirable process behaviour. However, since diafiltration is a necessity, the only opportunity for improvement lies in developing and implementing better strategies for composition control. It was found in Chapter 6 that implementing a plantwide diafiltration strategy using SISO control loops was quite restricting:

- Feedback composition control (assuming the availability of predicted or measured retentate composition data) could not easily be implemented, due to poor closed-loop plant dynamics. For a variable area plant, selection of the manipulated variable(s) was difficult.
- Specifying the diafiltration flow rate as a ratio of permeate flow rate achieved good servo control but created a disturbance feedback loop within the stage.

Having reviewed the feasible options for modifying the process flowsheet design (none) and operating strategy (few), it can be concluded that the only possibilities for improvement lie with the implementation of alternative process control strategies and technologies. Surveying the control literature, it quickly becomes apparent that a wide range of advanced control theory exists. Interaction was previously identified as being one of the most significant control difficulties for this process. Mitigation or management of this issue would provide significant opportunities for improvement in controller performance. Options to achieve this can be divided into two broad categories; addition of decouplers to existing control loops, and full multivariable controller design. Adding a decoupler to each PID controller may well reduce the level of interaction between each loop, but it will not address the limitations of the SISO controller structure. It is therefore likely that pursuing this approach will not yield significant performance improvements.

Multivariable controllers offer good capabilities for managing process interaction by simultaneously manipulating several inputs to track the desired setpoints or reject disturbances. However, significantly more effort is required to implement a controller with this level of sophistication. A number of different technologies have been developed in the field of multivariable control, some of the more common ones being; model predictive control (Seborg *et al.*, 1989; Ogunnaike & Ray, 1994; Meadows & Rawl-

ings, 1997), internal model control (Garcia & Morari, 1985; Morari & Zafiriou, 1989; Shinskey, 1994), multivariable adaptive control (Krstiz *et al.*, 1995; Landau & Lozano, 1998), robust control (Green & Limebeer, 1995; Skogestad & Postlethwaite, 1996) and linear quadratic control (Mosca, 1995). Each strategy offers different advantages, but all require a process model either directly for controller synthesis or as a predictive tool. Multivariable controller performance is therefore highly dependent on the quality and accuracy of the process model (Morari & Zafiriou, 1989). For this reason it is worthwhile revisiting the dynamic process model developed in Chapter 3, and considering its suitability as a basis for a multivariable control strategy.

7.2 Development of an accurate model for advanced process control

The development of a simple, representative membrane process model was discussed in detail in Chapter 3. A set of non-linear ordinary differential equations was developed to describe the dynamic behaviour of a separation stage. This was a lumped-parameter model, based on the assumption of perfect mixing within the recirculation loop. These equation sets were then combined to produce an overall dynamic process model representing the structure of the process flowsheet. Modelling a specific situation required additional information about the actual separation. This information was supplied by a supplementary set of models describing the fractionation and permeate flux occurring across the membrane (Figure 7-1). The development of an accurate process representation is highly dependent on the accuracy of this second equation set. In Chapter 3 an algebraic equation was used to predict a component concentration in the

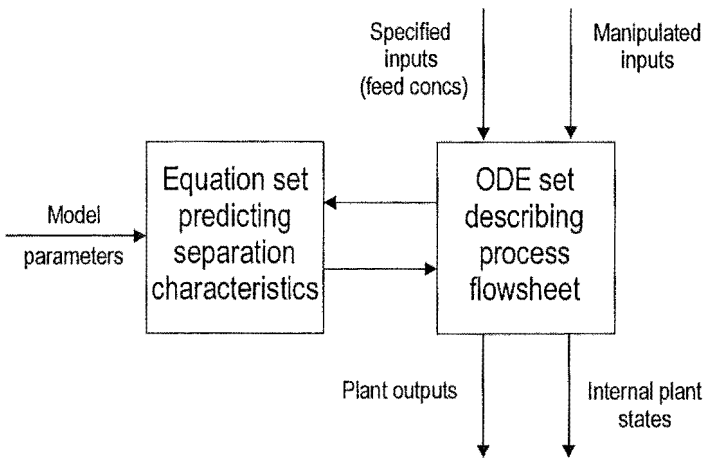

Figure 7-1 Dynamic process simulation using predicted permeate flow rates

permeate stream, based on the retentate-side concentration. This relationship was based on the observed retention coefficient of each component (Equation 3-4), an approach commonly described in literature, and widely employed in process design and industrial contexts (de Rham & Chanton, 1986; Pradanos *et al.*, 1994). Coefficient values are either constant or a simple function of concentration (Equation 3-6), and are usually well known for any industrial installation, since they play an important role during plant design calculations. The coefficients for an existing plant can easily be checked by performing laboratory analysis on samples simultaneously collected from the retentate and permeate sides of a membrane.

It was explained in Section 3.3.2 that the accurate prediction of permeate flux is extremely difficult, since this entity is a complex function of time, concentration, trans-membrane pressure and temperature. Process design data is of limited use, since equipment sizing uses approximate 'steady state' fluxes (Figure 2-4), whereas a dynamic model requires an accurate estimate of permeate flow rates at all times. The issues of permeate flux prediction were examined in Chapter 3, and it was concluded that empirical models were too simplistic whilst mechanistic models were generally very complex, requiring many coefficients and parameters. A significant amount of effort could easily be expended gathering data and calculating these parameters, with no guarantee of model accuracy. Even the pure water permeate fluxes of an industrial WPC process can show poor repeatability on consecutive production runs (She, 1998).

The development of a process model is generally a compromise between accuracy and complexity. When emphasis is placed on accuracy a greater level of rigor is accepted as being necessary to achieve the desired precision. However, for a membrane process, complex phenomenological models still may not achieve the desired level of accuracy. From a process control perspective this poses significant difficulties, for which two alternatives exist; accept limited model accuracy and implement a robust control technology, or consider alternative model structures and implement a control technology that does not require a fully predictive model. Robust controller designs are able to accommodate structural and parametric uncertainty, but achievable controller performance is limited by the accuracy of the process model (Morari & Zafiriou, 1989). For a complex process such as this, it is conceivable that the estimated model uncertainties will result in a complex multivariable controller that provides no better performance

than the current SISO implementation. It is instead preferable to explore the possibilities for developing alternative process modelling methods.

In the absence of a full predictive model, the best alternative is a process simulation based on sampled process data. This approach is particularly attractive for a membrane plant, since the most difficult parameters to predict (flow rate) are the easiest to measure. Indeed, in a modern membrane plant all permeate flow rates are usually measured and passed to the SCADA (supervisory control) system. Plant feed, retentate and diafiltration flow rates are usually measured online, along with the number of stages in operation. It is feasible to obtain this information from the SCADA system and use the data in place of predicted values, as shown in Figure 7-2. Given the unavailability of online composition measurement, an estimated feed stream composition must be supplied to the model, possibly based on daily laboratory analysis. A process model which uses sampled plant data has superior accuracy, but its use as a predictive tool is now restricted; no longer is it possible to predict long-term plant responses to controller inputs. Although this tool is now only a real-time process model the additional information it provides still offers opportunities for improving controller performance.

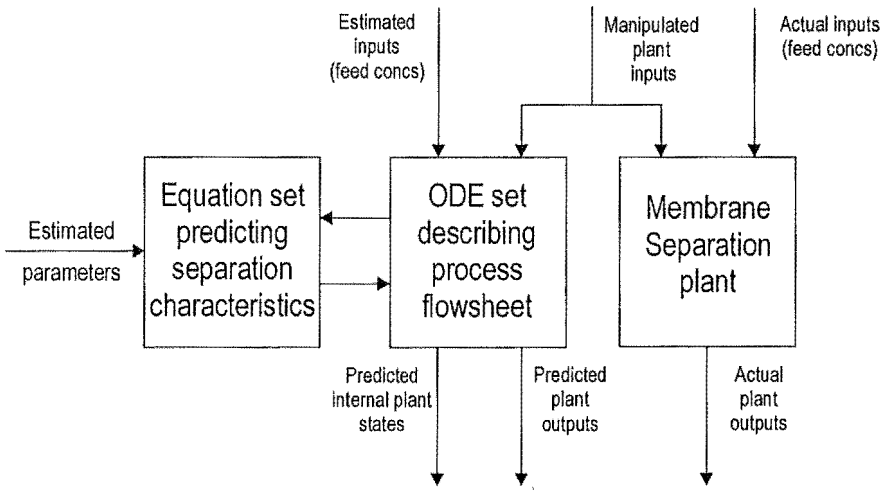

Figure 7-2 Real-time dynamic process simulation using measured process flow rates

7.3 Sensitivity of prediction model to modelling errors

The availability of a real-time process model enables multivariable controller strategies to be developed and trialled for membrane multistage plants. However, conclusions drawn from such analysis will only be useful if the limitations of this work are well understood. It is impossible to model the behaviour of an actual process with perfect

accuracy since any model will contain both structural and parametric uncertainties. Structural uncertainty usually corresponds to unmodelled high-order process dynamics whilst parametric uncertainty is often caused by the inability to measure or estimate certain variables. The true accuracy of the real-time model developed here can only be determined by analysis using actual process data. This validation can be performed using data collected from the SCADA system of an industrial multistage plant, but is outside the scope of this theoretical analysis.

The Simulink simulation environment, which operates with the Matlab software package (MathWorks, 1999) was used for the numerical modelling and analysis work performed in this chapter. In the Simulink implementation shown in Figure 7-3, membrane plant behaviour is simulated using the dynamic process model developed in Chapter 3. Each permeate flow rate is sampled using a zero-order hold, and considered to represent plant data collected from the SCADA system. In this approach both the plant and real-time model in the simulation have been constructed from the same ODE set, and so will be structurally identical, meaning that there is no structural uncertainty present in the real-time model. For this reason it is likely that the real-time model predictions shown in this chapter will have greater accuracy than could be expected when implemented on an actual plant. However, it is possible to introduce parametric uncertainty by ensuring mismatch between the retention coefficients and feed concentrations of the plant and the real-time model. Model accuracy is also affected by the rate at which plant data is sampled and passed to the real-time model. It is preferable to sample as fast as possible, although in an industrial setting the available sampling rate

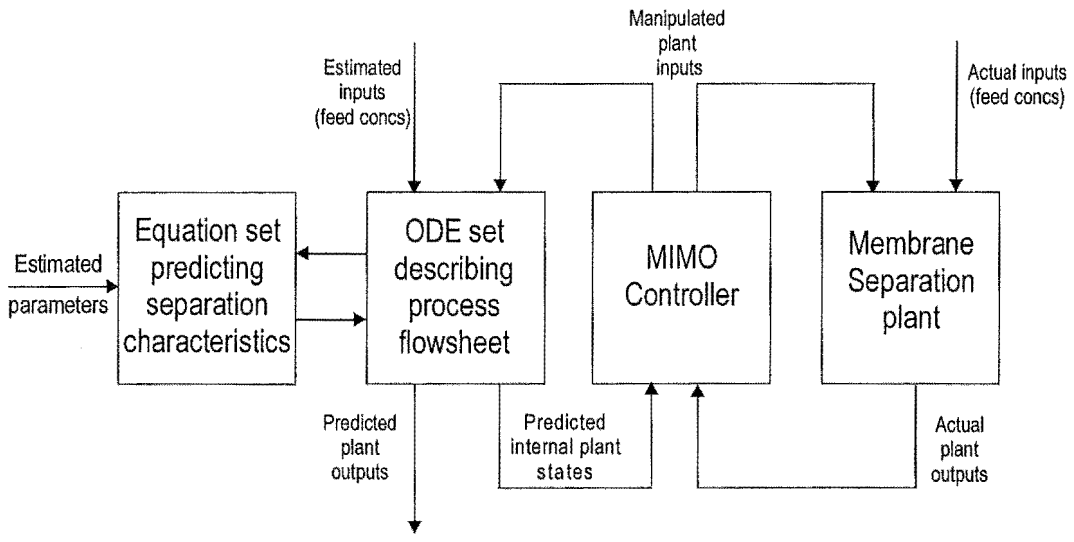

Figure 7-3 Simulink implementation of actual plant and real-time model

will be limited by the abilities of the SCADA system, and available computational power.

The non-linear time-variant nature of a membrane process makes rigorous investigation of model sensitivity an enormous task. For the purposes of brevity the effect of parameter uncertainty was only examined under a single set of operating conditions. For each case study, process behaviour was simulated for 60 minutes, covering plant startup, the addition of a new stage and return to setpoint. For sampling frequency analysis, the normalised IAE was calculated over the duration of the simulation. Relative system sensitivity was calculated by comparing the plant and model outputs at $t = 60$ minutes for a specified parameter uncertainty.

7.3.1 Case study 1: Whey protein concentrate production

The effect of sampling rate on model accuracy was examined by repeating the same closed-loop SISO plant simulation with different sample times set in the zero-order hold blocks of the real-time model. Closed-loop plant operation was simulated using the SISO control strategy discussed in Section 6.4. Retentate total solids setpoint was specified as 27 wt %. Plant startup strategy was identical to that shown in Figure 6-10. Not surprisingly, normalised IAE values for these trials (Table 7-1) increased with sample time. As a general trend the quality of prediction was poorest during initial plant startup, when changes in permeate flow rates were most significant. Once the plant reached setpoint all predicted total solids concentrations and purities quickly converged to the actual plant values. Overall it was concluded that a 10 second sampling time provided a suitable compromise between prediction accuracy and computational effort, so will be used during further analysis in this chapter.

Table 7-1 Effect of sampling time on real-time model accuracy - case study 1

	Normalised IAE	
Sampling period [seconds]	Retentate Total Solids Concentration $C_{R\,TS,16}$	Retentate Protein purity $P_{R\,Protein,16}$
1	0.023	0.007
5	0.165	0.022
10	0.334	0.062
20	0.670	0.151
30	0.996	0.248
60	1.796	0.491
120	2.920	0.827

Model sensitivity to parametric error was examined for the feed concentration and retention coefficients of protein and lactose components. Analysis was performed for a 20 % discrepancy between the predicted and actual component feed concentration, with the 'plant' operating at the usual feed conditions. A 10 % discrepancy was used for the retention coefficient mismatch, with the component j retention coefficient for any given stage calculated by:

$$R_j' = 0.9a_j + b_j\left(C_{R,foul}\right) \quad \textbf{(7-1)}$$

This is based on the algebraic retention coefficient model presented in Equation 3-6, with the prime denoting variables in the real-time model. Normalised sensitivities for the real-time model are shown in Table 7-2 for parametric uncertainties in feed concentration and retention coefficients. A relative sensitivity of 1.0 meant that a 10 % parameter mismatch caused a 10 % error in the model output when operating at setpoint. The results show that the real-time model was extremely sensitive to mismatch in the protein parameters, due to the high protein purity of the retentate product, and the effect of protein concentration on other retention coefficients. Because the retention coefficient of protein is very close to 1.0 for WPC plants using ultrafiltration membranes (Section 3.5.1):

$$0.98 \leq R_{Protein} \leq 1.0$$

a variation of $R_p \pm 0.02$ represents only a small percentage uncertainty. Therefore a 10 % disparity between the plant and the model coefficients is unlikely. However significant feed concentration disturbances in this component are highly possible and should be considered as being the most likely source of modelling error in an industrial situation. The predicted retentate total solids concentration was most sensitive to such uncertainty, hence it is strongly desirable to use the online total solids data to correct the real-time model. A method of achieving this is presented in Section 7.7.

Table 7-2 Effect of uncertainty on real-time model accuracy - case study 1

Parameter	Relative sensitivity at setpoint	
	Retentate Total Solids Concentration	Retentate Protein purity
$R_{Protein}$	4.761	1.305
$R_{Lactose}$	0.027	-0.027
$C_{F,Protein}$	0.901	0.141
$C_{F,Lactose}$	0.058	-0.059

7.3.2 Case study 2: Permeate product separation

Sensitivity analysis was carried out for this permeate product case study using the SISO control strategy presented in Section 6.5.1. The Simulink simulation was run for $t = 60$ minutes using the startup strategy shown in Figure 6-12, with retentate setpoint of 17 wt % total solids concentration. Accuracy of the prediction model was examined for a range of sampling times, with the normalised IAE values presented in Table 7-3. Comparing these values with the results of case study 1, it can be seen that the modelling errors at small sampling periods were generally smaller for this system. Again, all predictive models rapidly converged to the plant values once setpoint was reached. A sampling time of 10 seconds was also chosen for this case study.

Table 7-3 Effect of sampling time on real-time model accuracy - case study 2

	Normalised IAE	
Sampling period [seconds]	Retentate Total Solids Concentration	Retentate protein purity
1	0.038	0.004
5	0.143	0.010
10	0.316	0.020
20	0.635	0.043
30	0.887	0.055
60	1.895	0.139
120	4.261	0.218

Sensitivity of the real-time model to errors in the estimated model parameters (retention coefficient and feed concentration) was analysed using the same approach as for case study 1. The relative sensitivities for mismatch in Component A and B parameters are given in Table 7-4. Just like the first case study, this model was found to be highly sensitive to errors in the parameters of the dominant retentate stream component (Component A). However it is again unlikely that the retention coefficient of this component ($R_A = 1.0$) will vary significantly. The results also showed the retentate total solids concentration to be more sensitive to parameter uncertainty than purity, but the availability of measured retentate total solids concentration data allows the real-time model to be corrected and this sensitivity reduced. In a physical plant, the most likely uncertainty would be associated with the component feed concentrations. In both cases the real-time model for this separation was less sensitive to errors in these parameters than the WPC case study.

Table 7-4 Effect of uncertainty on real-time model accuracy - case study 2

Parameter	Relative sensitivity at setpoint	
	Retentate Total Solids Concentration	Retentate Component A purity
R_A	3.088	0.797
R_B	0.501	0.199
$C_{F,A}$	1.124	0.239
$C_{F,B}$	-0.532	-0.210

7.4 Selection of a new strategy for MIMO control of multistage membrane plants

The development of a multivariable controller is a three step process:

1) *Specifying the control strategy* - selection of process inputs, controlled variables and reference values for the process
2) *Defining an objective function* - numerical definition of the controller error between the desired and recorded or predicted process condition.
3) *Selecting an appropriate multivariable technology to implement the control strategy* - finding a control theory which matches both the characteristics of the process and the specified control strategy.

Using an advanced controller technology to implement a poorly conceived strategy is unlikely to achieve the desired performance improvements. Likewise, the selection of an inappropriate technology can lead to implementation difficulties.

Analysis in previous chapters showed retentate composition control to be a challenging task, particularly for variable area plants. For many membrane separation plants, including those studied here, the most important objective is to achieve and maintain the desired retentate stream purity. For a retentate product this is crucial since it is unlikely that any further purification will occur downstream of this process. For a permeate product, maintaining the desired retentate purity ensures that the desired recovery rate or yield is achieved (assuming constant feed composition). Maintaining a constant total solids concentration in the retentate stream is less important, since permeate product yield has a low sensitivity to this parameter. For a retentate product separation small concentration fluctuations in the total solids concentration can be mitigated by downstream operations. It is also desirable to maintain a constant plant feed flow rate, to aid process integration. Short-term deviations from the feed setpoint are tolerable, provided

they are not too extreme, since this controlled variable has no direct effect on product quality.

Typically, a process is controlled by maintaining a set of specified variables at desired values by manipulating selected plant inputs. The choice of inputs and output variables, and relationships between the two, constitutes the process control strategy. Preferred pairings of input and output variables for a SISO control strategy were considered in Chapter 5 using the relative gain array (RGA). Closed-loop performance of the preferred pairings was examined in Chapter 6. Analysis concluded that achievable closed-loop performance was affected by interaction between the individual control loops.

It was suggested, following analysis in Chapter 6, that a MIMO control strategy may offer improved levels of closed-loop performance. It is likely that using a MIMO controller to implement a SISO-style control strategy will encounter the same composition control difficulties (see Section 6.3.3). The availability of a real-time model presents the opportunity to develop new control strategies able to utilise this additional information. Given the widespread disturbance propagation characteristics of multi-stage membrane plants, it is preferable for a controller to act as promptly as possible to reject a disturbance. Controlling some or all internal process states may make it possible to achieve superior disturbance rejection, and improved retentate setpoint tracking.

The MIMO control strategy proposed and developed in the remainder of this thesis is best explained using the separation trajectory shown in Figure 7-4. In this strategy, the plant is considered to consist of two individual separations connected in series; the primary objective of the first is to concentrate the feed stream, while the second must achieve sufficient fractionation (via diafiltration injection) to satisfy the purity specifications for the retentate stream. The concentration (non-diafiltration) section has a known feed concentration (Figure 7-4, Point 1) which, except for small disturbances, can be assumed to be fixed. The separation trajectory from this point is also fixed, since it is determined by the characteristics of components in the feed stream. Therefore, it is not possible to independently control both concentration and purity in this section. At some chosen point along this trajectory, diafiltration will commence (Figure 7-4, Point

2). In this work, Point 2 is called the midpoint of the process, since it occurs between the concentration and fractionation sections. Because the separation trajectory is fixed, the total solids concentration and protein purity of the retentate stream from the concentration section can be uniquely defined solely by the midpoint concentration. Thus, *it is desired to maintain the total solids concentration of the last non-diafiltration stage as near as possible to the desired midpoint concentration.*

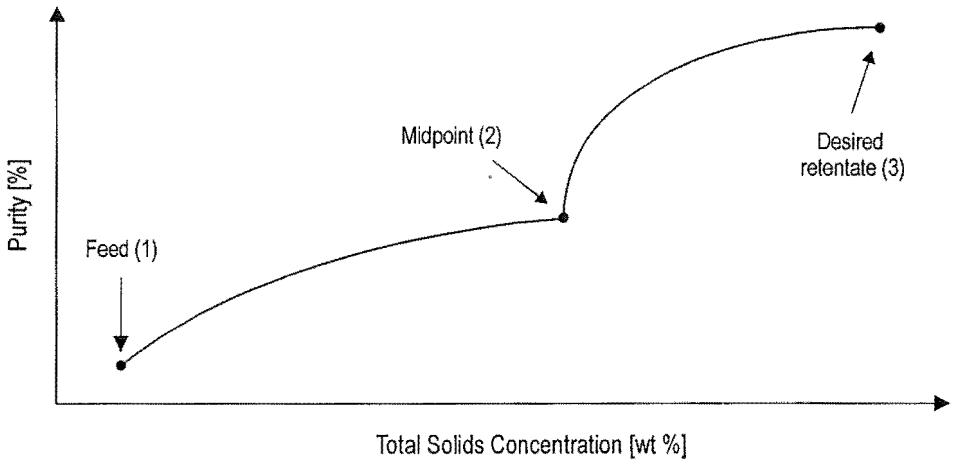

Figure 7-4 Generic separation trajectory

In the absence of online concentration measurement at the midpoint of the plant, two options are available; controlling the predicted midpoint concentration supplied by the real-time model, or inferring the plant concentration from the midpoint flow rate. The latter option was pursued here, since this approach could also be applied to a SISO controlled plant where no real-time model was available. In this strategy, it is desirable to maintain the midpoint flow rate as close to the setpoint as possible. The desired midpoint flow rate is most easily calculated from the current retentate flow of the plant:

$$F_{mid,sp} = F_R VCF_f \quad \textbf{(7-2)}$$

where

$F_{mid,sp}$ = midpoint flow rate setpoint [L s^{-1}]

F_R = plant retentate flow rate [L s^{-1}]

VCF_f = volume concentration factor corresponding to the fractionation section of the plant

Equation 7-2 allows the setpoint to track changes in the plant flow rates during startup. In practice some filtering would be required to ensure that fluctuations in the retentate flow rate did not cause difficulties. An appropriate value of VCF_f corresponding to the

desired midpoint concentration can be determined either from the plant design calculations or operating data.

Although the desired midpoint is easily defined, there is no obvious corresponding input available to maintain this value, since the flow rate at the midpoint cannot be manipulated independently of the plant retentate flow rate. The strategy proposed here is to add new membrane area in a manner which maintains a consistent midpoint flow rate. Previously identified as a significant disturbance, membrane area addition now offers the means to simultaneously achieve two objectives; maintain the required plant feed flow rate, and stabilise the midpoint flow rate. An increasing midpoint flow rate corresponds to a declining midpoint total solids concentration. Thus, when the flow rate exceeds the setpoint, new membrane area (when next required) should be added to the concentration section of the plant. When the midpoint flow rate declines below the setpoint, the next area should be added to the diafiltration section. This approach will not achieve tight control, but it will stop the midpoint concentration from drifting during production.

With limited ability to manipulate the concentration section, a MIMO control strategy must focus on the fractionation section of the plant. Achieving good controller performance is extremely important since the product stream is drawn from here. A fixed trajectory can be specified from the desired midpoint (Figure 7-4, Point 2) to the desired retentate condition (Point 3), and used as a reference for the controller. Stated simply, *it is desired that the co-ordinate of each operating diafiltration stage lie somewhere on the reference trajectory, with the retentate stream from the plant achieving the desired concentration and purity specifications.* The fractionation section has neither the midpoint nor the separation trajectory fixed, hence both of these can, and will, vary during the course of operation. Manipulated variables available to maintain the desired trajectory are the flow rate of diafiltration water added to each fractionation stage, as well as the retentate flow rate of the plant. A key point of this strategy is that the actual diafiltration flow rate to each stage is directly manipulated by the controller. This approach replaces the ratio-controlled diafiltration strategy previously discussed and criticised at length.

Distillation is an obvious situation where it is desirable to maintain a fixed composition profile within the process. Han & Park (1993) successfully controlled the composition profile of a high purity distillation column using a generic model controller (GMC), combined with a non-linear observer which predicted the composition profile within the process. However a continuous distillation column significantly differs from a multi-stage membrane plant, since the number of separation stages (trays) remains constant, and the operating efficiency of each remains fixed. Some parallels exist between continuous membrane separation and batch distillation, but in this situation the separation trajectory within a column will change over time as the separation progresses. In general, parallels between distillation and membrane separation are poor, since it is possible to independently manipulate the amount of diafiltration applied to each stage in a membrane plant, but the reflux ratio of each tray in a column cannot be independently manipulated.

Profile control is also important within paper-making machines and sheeting or rolling mills, where it is important to produce a specified thickness profile through the press or mill (Liang *et al.*, 1998). However in both cases, the situation more closely represents that of distillation than variable area membrane separation, since the number of rollers or stands is fixed, and conditions within the process are relatively constant. Overall it can be concluded that the characteristics of single phase, variable area multistage membrane plants are essentially unique. The profile control strategy is not new, but the challenges faced in implementing this approach on a multistage membrane plant are.

7.5 Selection of a reference trajectory for a MIMO controller

Under the SISO controller regime of Chapter 6, a diafiltration strategy was defined in terms of an overall diafiltration ratio ϕ_o and maximum stage ratio ϕ_{max}. However in a variable area plant, maintaining the desired ϕ_o does not necessarily produce a constant retentate purity, since the diafiltration efficiency is generally dependent on the number of stages in operation. The MIMO control strategy presented in the previous section offers the opportunity to maintain a fixed separation trajectory, and hence retentate purity, for the duration of production. The desired or reference trajectory for such a controller should be selected with care since it is likely that the characteristics of this path will affect closed-loop process behaviour. A multistage membrane process can be considered as a 2-point boundary value problem, with the co-ordinates of the boundary

conditions set by the expected feed concentration and purity, and desired retentate specifications. Any reference trajectory must traverse both points, and is usually specified in terms of a desired midpoint concentration (representing the point at which diafiltration injection commences) and a chosen path from the corresponding co-ordinate to the retentate stream boundary condition.

It is possible to construct a reference trajectory for any single phase membrane plant without the need for a permeate flux model. This makes it possible to implement the reference trajectory concept during preliminary design stages. If it is assumed that all streams have equal density then the concentration of component j within a theoretical stage i can be calculated using the steady state component balance originally presented in Equation 3-1:

$$C_{Ri,j} = \frac{F_{R,j}C_{Fi,j}}{F_{P,j}(1-R_{i,j})+F_{R,j}} \tag{7-3}$$

Provided a plant is divided into a sufficient number of theoretical stages (say $n > 30$), then this reference trajectory is stable, and independent of the exact number of stages in operation. For each theoretical stage operating in the fractionation section of the reference trajectory, diafiltration is added as a given proportion $\phi_{ref,i}$ of the permeate stream flow rate. For this analysis, it is assumed that stage i has a permeate flow rate which is proportional to the feed flow rate, i.e. each stage has a constant VCF:

$$F_{P,i} = \delta F_{F,i} \tag{7-4}$$

where δ is a proportionality constant. For a theoretical fixed volume stage receiving diafiltration, the retentate flow rate can be expressed as a function of the feed flow:

$$\begin{aligned} F_{R,i} &= F_{F,i} + F_{DF,i} - F_{P,i} \\ &= F_{F,i} + \left(\phi_{ref,i} - 1\right) F_{P,i} \\ &= F_{F,i}\left(1 + \delta\left(\phi_{ref,i} - 1\right)\right) \end{aligned} \tag{7-5}$$

Substituting the algebraic retention coefficient model of Equation 3-6, the retentate concentration of component j in the i^{th} reference stage can be expressed using the simple relation:

$$C_{Ri,j} = \frac{C_{Ri-1,j}}{1+\delta\left(\phi_{ref,i} - R_{i,j}\right)} \tag{7-6}$$

In the concentration section, no diafiltration injection is applied, hence $\phi_{ref,i}$ is set to zero. The concentration profile of each component can be calculated through the plant

using Equation 7-6, with the total solids concentration and purity of each theoretical stage calculated in the usual way and plotted to produce a reference trajectory. A 'continuous' reference trajectory can be constructed if $\delta << 1$, representing an ideal plant with a large number of very small stages (based on the approach of Morison, 1997).

It is known (Section 2.3.2) that separation efficiency is dependent on the number of stages in operation. Diafiltration efficiency is particularly sensitive to staging effects. As $\delta \rightarrow 1$ the number of stages in the theoretical plant decreases, and greater levels of diafiltration are required to maintain a desired fractionation trajectory. For this reason the SISO diafiltration strategy was unable to maintain a constant retentate purity because ϕ_o was fixed, but the number of stages in operation changed over time. The MIMO strategy is based on the concept of manipulating the diafiltration flow rates to each stage as necessary to maintain the desired concentration and purity within each fractionation stage. Thus, this controller type has the potential to maintain a specified reference trajectory (and hence the desired retentate purity) throughout production, independent of the number of stages in operation.

Using Equation 7-6 it is possible to construct a range of different reference trajectories for a process, and analyse the characteristics of each. Two possible reference trajectories for case study 1 (whey protein retentate product) are presented in Figure 7-5, constructed using midpoint concentrations of 15 and 23.5 wt %. These trajectories corresponded to a plant operating with 16 stages, using the SISO diafiltration strategy with ϕ_{max} = 0.7 and 0.85 respectively. The shaded grey areas indicate regions of *decreasing* total solids concentration, i.e. the occurrence of backup within the plant.

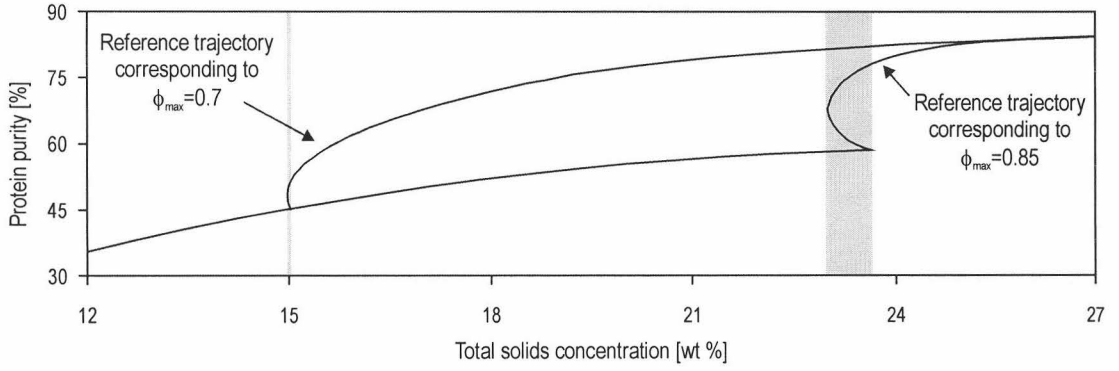

Figure 7-5 Effect of midpoint concentration on separation trajectory

The MIMO control strategy provides the opportunity to select a reference trajectory from a large set of feasible alternatives. To uniquely define a reference trajectory it is necessary to specify both a midpoint concentration at which diafiltration injection should commence, and a desired path from this point to the specified retentate concentration and purity. The midpoint concentration determines the relative size of the concentration and fractionation sections of a membrane plant. For an existing plant design, a high midpoint concentration places the majority of the stages in the concentration section, with increased flow rates of diafiltration applied to fewer stages in the fractionation section. Thus, operating at higher midpoint concentrations requires a more aggressive diafiltration strategy, but can achieve superior separation efficiencies and reduced diafiltration water requirements (depending on the permeate flux characteristics of the separation). For the SISO strategy examined in Chapter 6, a high midpoint concentration corresponds to operating at high ϕ_{max}. Analysis in Chapter 5 showed that such conditions generally made the process more difficult to control. Selection of a midpoint concentration is therefore a trade-off between improved operating efficiencies and possible degradation in controller performance.

The conditions causing backup within the plant become evident if Equation 7-6 is modified to express the total solids concentration of a theoretical stage as a function of diafiltration ratio ϕ_{ref}:

$$C_{R\,i,j} = \frac{C_{R\,i-1,j}}{1+\delta\left(\phi_{ref\,j} - R_i^{'}\right)} \tag{7-7}$$

with the overall retention coefficient $R_i^{'}$ for stage i with k components calculated by:

$$R_i^{'} = \frac{\sum_{j=1}^{k} C_{R,j}\, R_j}{\sum_{j=1}^{k} C_{R,j}} \tag{7-8}$$

From Equation 7-7 it is clear that backup occurs when the diafiltration ratio of a stage equals or exceeds the corresponding retention coefficient. Such behaviour can be avoided if the diafiltration strategy satisfies Equation 7-9 for all n theoretical stages comprising the reference trajectory:

$$\phi_i < R_i^{'} \qquad for \quad 1 \le i \le n \tag{7-9}$$

The same requirement applies for an actual process with n diafiltration stages, and non-ideal behaviour. It is possible that severe backup in the plant may cause numerical

difficulties for a MIMO controller, particularly for diafiltration stages near the midpoint. Backup does not occur in case study 2 due to the characteristics of the separation, however the same cannot be said for case study 1. In situations where backup is likely to be significant, the diafiltration ratio ϕ_{max} can be constrained if it is specified as a fixed proportion α of the corresponding retention coefficient:

$$\phi_{\max,j} = \alpha R' \quad for \quad \alpha < 1 \tag{7-10}$$

For a chosen midpoint concentration there will exist no more than one value of α which achieves the desired retentate specification. If the specified midpoint concentration is too high, then no value of α will exist which satisfies both Equation 7-10 and achieves the desired retentate specification.

For case study 1, reference trajectories can be defined on this basis using $\alpha = 0.753$ and 0.864 for midpoint concentrations of 15 and 23.5 wt % respectively (Figure 7-6A). The effective diafiltration ratio rises with total solids concentration, until it exceeds ϕ_{max} in the second half of the fractionation section. The constrained diafiltration strategy may offer superior separation efficiency and reduced diafiltration water use, since diafiltration injection is being applied more aggressively to fewer stages at the retentate end of the plant. Figure 7-6B & C show that at higher midpoint concentrations a controller

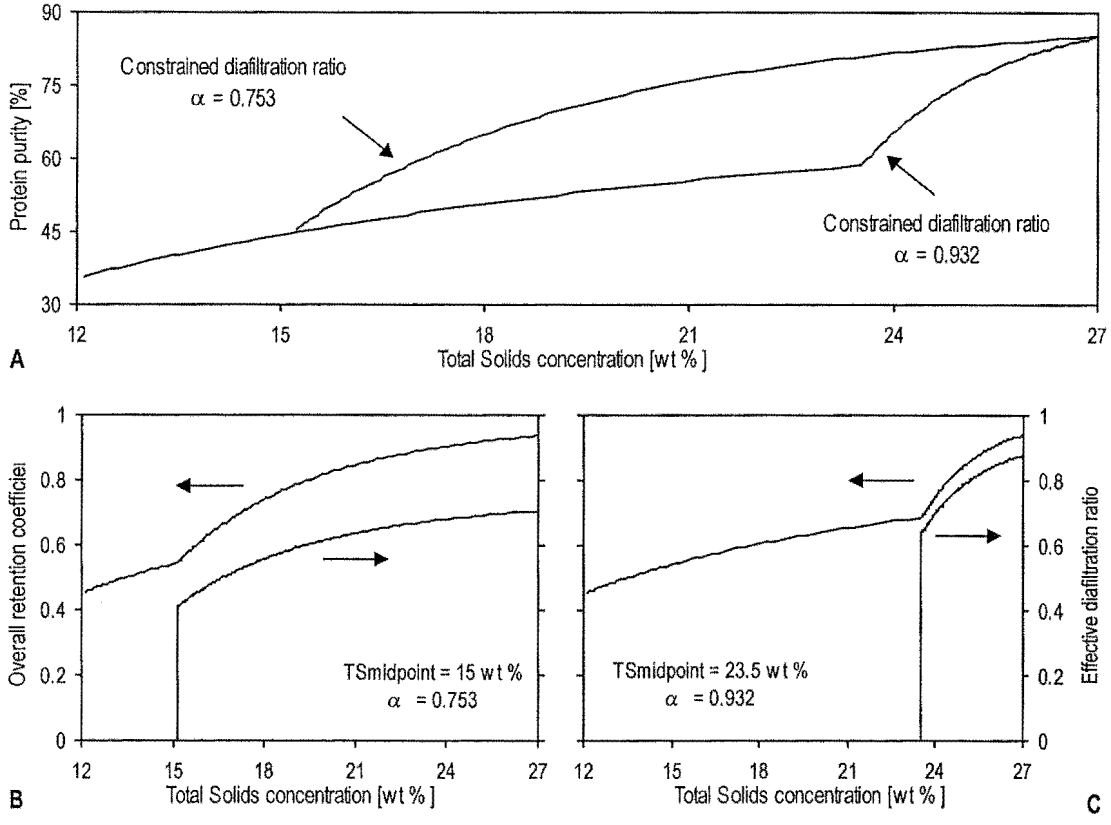

Figure 7-6 Comparison of fixed equivalent diafiltration ratios and overall retention coefficients

must operate closer to the constraint posed by Equation 7-9.

A number of other trajectories also satisfy Equation 7-9 and achieve the desired retentate specifications. One interesting candidate is a linear trajectory traversing the boundary conditions of the fractionation section. However previous analysis has shown that linear trajectories are not a natural characteristic of multistage membrane separations, suggesting that a controller may struggle to maintain such a profile. A second alternative is to divide the plant into more than two sections. For example, it may be desired that the process operate with concentration sections at both feed and retentate ends on the plant, and a fractionation section between these two. Such a strategy is feasible, and represents a common industrial operating practice in New Zealand, where diafiltration may not be applied to the final stage(s) of the plant (Morison, 1998). In certain situations, aggressive diafiltration injection into the final stages of a plant can reduce the diafiltration water requirements, but may also reduce the operating capacity of the plant Morison (1998). For such separations, moving the fraction section upstream offers a compromise between diafiltration water usage and processing capacity.

These two alternatives represent a small fraction of a large set of feasible reference trajectories that are possible for a multistage membrane plant. Some of these will offer better closed-loop process behaviour, whilst others will provide superior separation efficiency. The purpose of this chapter is to demonstrate the implementation of MIMO control on membrane plants for a chosen reference trajectory. Further discussion on the choice of the reference trajectory is outside the scope of this work.

7.6 Defining an objective function for MIMO control of multistage membrane plants

In order to implement a multivariable process controller, it is necessary to mathematically define the control objective. Such a definition is used to calculate input (error) signals for the controller, and provides a framework for a feedback control structure. The control strategy presented in Section 7.4 formally partitioned the plant into concentration (non-diafiltration) and fractionation (diafiltration) sections, with most control objectives defined in the context of a desired fractionation separation trajectory. However this framework does not easily accommodate plant feed flow rate control or membrane area addition, since the reference trajectory is independent of flow rate. Feed

flow rate control was previously implemented separately, with associated supervisory logic for membrane area addition. Given its success, this strategy will be retained, with the supervisory logic modified to also include the midpoint flow rate control objectives discussed in Section 7.4.

Formally defining a MIMO controller objective is not as simple as it may appear. In fact, the situation is complicated by three factors;

- The desired concentration and purity for each diafiltration stage (except the last) are not explicitly defined, and will actually change over time as fouling occurs and new area is added. Calculating the error between the current and desired condition of each stage is not easy, since the 'setpoint' is actually a continuous reference trajectory. For a plant with n diafiltration stages in operation, there are $2n$ controlled variables.
- It is possible to control both the concentration and purity of a single diafiltration stage by manipulating the retentate and diafiltration flow rates, but it is not possible to independently manipulate the retentate flow rate of several stages connected in series. In addition, analysis has shown high levels of interaction to be present in the system; manipulating the diafiltration flow rate of one stage will disturb the retentate flow rates of all upstream stages, due to the constant volume plant design. For a fractionation section with n stages in operation, there are $n+1$ available manipulated variables.
- Periodic addition of new diafiltration stages means that the number of controlled and manipulated variables changes over time.

The development of a multivariable objective function is best achieved by considering the situation in two dimensions, as illustrated in Figure 7-7. The i^{th} operating diafiltration stage will have the co-ordinate ($TS_{predicted,i}$, $P_{predicted,i}$) predicted by the real-time plant model. On this basis it is possible to calculate a single scalar error d_i which represents the distance between the predicted stage co-ordinate and a chosen point ($TS_{reference,i}$, $P_{reference,i}$) on the reference trajectory.

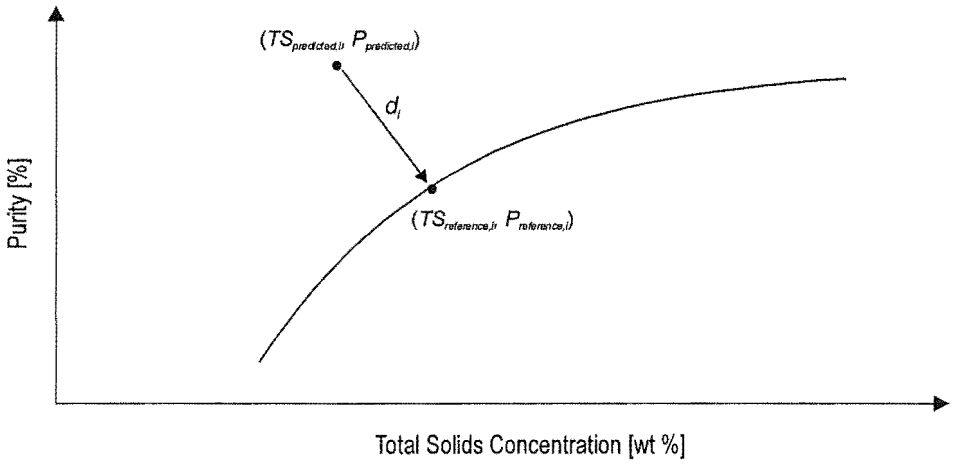

Figure 7-7 Two-dimensional representation of controller objective

This distance is best expressed on a normalised basis:

$$d_i = \sqrt{\left(\frac{TS_{reference,i} - TS_{predicted,i}}{TS_{reference,i}}\right)^2 + \left(\frac{P_{reference,i} - P_{predicted,i}}{P_{reference,i}}\right)^2} \quad \textbf{(7-11)}$$

where:

$TS_{reference,i}$ = selected reference total solids concentration [wt %]

$TS_{predicted,i}$ = total solids concentration predicted by real-time process model [wt %]

$P_{reference,i}$ = selected reference purity [%]

$P_{predicted,i}$ = purity predicted by real-time process model [%]

The difficulty lies in selecting an appropriate reference co-ordinate for each stage. The approach proposed here is to select the reference co-ordinate $(TS_{reference,i}, P_{reference,i})$ which minimises the error term d_i for the stage. This means that the controller will try to simultaneously move each stage toward the nearest point on the reference trajectory.

It is necessary to add one further term to the objective function, expressing the distance between the predicted and desired retentate stream total solids and purity. If this is not done, the controller is not forced to the achieve the specified product specifications. For a process with n diafiltration stages in operation

$$d_{n+1} = \sqrt{\left(\frac{TS_{SP} - TS_{predicted,n}}{TS_{SP}}\right)^2 + \left(\frac{P_{SP} - P_{predicted,n}}{P_{SP}}\right)^2} \quad \textbf{(7-12)}$$

where:

TS_{SP} = specified retentate total solids concentration setpoint [wt %]

P_{SP} = specified retentate purity setpoint [%]

The individual error terms can be combined into a single vector e which is supplied to the controller:

$$e = \left[d_1 \quad \cdots \quad d_n , d_{n+1} \right] \tag{7-13}$$

For a plant with n diafiltration stages in operation, the control strategy now has $n+1$ controlled variables, and $n+1$ manipulated inputs. This is a feasible input-output structure, with sufficient degrees of freedom. As the number of operating diafiltration stages increases, so too will the number of manipulated and controlled variables.

7.7 Selecting and implementing a controller technology for MIMO control of a multistage membrane plant

With the control strategy and objective function now defined, the implementation of a MIMO controller becomes possible. A number of different controller technologies were mentioned in Section 7.1, from which a suitable candidate must be selected. After careful consideration, the model predictive control (MPC) methodology was selected due to its ability to cope with 'difficult' processes. Ogunnaike & Ray (1994) state that MPC is typically best suited to processes with any combination of the following characteristics:

- Multiple input and output variables with significant interaction between SISO loops
- Either equal or unequal number of inputs and outputs
- Complex and unusually problematic dynamics (such as long time delays, inverse response, or even unusually large time constants)
- Constraints on inputs and/or output variables

Within this field there exist a number of different implementations of this methodology, including dynamic matrix control, quadratic dynamic matrix control, model algorithmic control, generic model control and forward modelling control (Ogunnaike & Ray, 1994). Given the unusual real-time model implementation and controller objective, it is not immediately clear which implementation is most suitable for a variable area membrane process. For this reason, a custom implementation was developed for multistage membrane plants. More elegant and complex strategies may be developed at a future date, should the need arise.

A general overview of MPC theory is presented here, however a thorough review of the field is outside the scope of this work. A more rigorous examination of MPC theory is presented by Ogunnaike & Ray (1994). The MPC strategy generally consists of four elements:

1. Specification of a desired time-domain reference trajectory
2. Prediction of the process output at future times
3. Computation of optimal controller action
4. Prediction of model errors and identification of unmeasured disturbances

These elements are examined in detail in the following sections, and a custom MPC implementation developed for the specific requirements of a multistage membrane process.

7.7.1 Specification of a desired time-domain reference trajectory

Model-predictive theory is based, like many control strategies, around achieving good setpoint step change response. For this reason, the controller objective focuses on moving the plant from the current to a desired condition. It is intended that each controlled variable reach a desired value within a specified time or event horizon. This desired time domain trajectory (not to be confused with the separation trajectory discussed earlier) serves as a sequence of 'setpoints' specified over successive time steps, which guide the plant towards the desired condition in a controlled manner. A long event horizon ensures that the control action is not overly-aggressive, but may produce a sluggish controller with poor performance.

Unfortunately, such a framework is not particularly compatible with the controller objective function defined in Equation 7-13. Defining a desired path for each stage from the current co-ordinate to a desired point on the reference trajectory is unwieldy, particularly since there is no clear target co-ordinate for each stage to attain. For this reason, the MPC implementation developed here discards the concept of a desired time domain trajectory, and instead retains the error definition of Equation 7-11.

7.7.2 Prediction of process output at future times

To predict the process output an accurate process model **M** is required. Discrete or sampled data MPC implementations often use a moving average ARMAX method (Box

et al., 1994) to predict future process outputs y from the plant response to past inputs u. Such a model is generally represented in the form:

$$y = \mathbf{M}u \tag{7-14}$$

However, the non-linear time invariant behaviour of a membrane process means that the relationship between inputs and outputs continuously changes, and cannot easily be represented by such a model. The addition of new stages also makes forward prediction a difficult task since the size of **M**, y and u periodically change. A common MPC implementation strategy uses the inverted process model $\mathbf{M}^*$ to determine an input sequence which will guide the process along the specified reference trajectory, from the current to the desired condition.

$$u = \mathbf{M}^* y \tag{7-15}$$

The real-time process model developed in Section 7.2 provides accurate prediction of the concentration and purity of each separation stage, but cannot be inverted unless it is linearised, and the current permeate flow rates are assumed to remain constant over the specified event horizon. The accuracy of this assumption will become increasingly inaccurate over longer event horizons.

7.7.3 Computation of optimal controller action

In a standard MPC implementation, good control is achieved by minimising deviation between the predicted plant outputs y and the specified time domain reference trajectory y^*. In this situation, an optimal controller sequence is chosen which minimises the error integral over the complete event horizon. Such an approach is not feasible for the membrane implementation, since it has already been decided to discard the time domain reference trajectory. Instead, it is assumed that all system flow rates (both input variables u and sampled permeate flow rate values) remain constant until the end of the specified event horizon. For a selected input set u the real-time plant model predicts the states at time $t + t_f$, at which point the error vector e (Equation 7-13) is evaluated. The optimal controller input set u is selected to satisfy the linear quadratic optimisation:

$$\min_u J(u) = e_{t_f} \mathbf{Q}\, e_{t_f}^T + x\mathbf{R}x^T \tag{7-16}$$

where:

e_{t_f} = vector of controller errors calculated at the event horizon t_f.

x = vector of controller action terms $\left[x_1 \ \cdots \ x_{n+1}\right]$, representing deviation from a specified 'base' value

Q = matrix of controller error cost weightings

R = matrix of controller action cost weightings

The matrices **Q** and **R** can be considered to contain tuning parameters, since these terms affect controller behaviour. Although the process behaviour is evaluated at the end of the event horizon, the optimal input set u is actually only applied for the current sampling period, after which time the permeate flow rates are resampled, the real-time model is updated, and a new optimal controller input set u is calculated and applied to the plant.

Controller action cost is based on the deviation of the controller inputs from specified 'base' values, calculated on a normalised basis. For the i^{th} operating fractionation stage the normalised deviation is given by:

$$x_i = \frac{F_{DF,i} - F_{DF\,base,i}}{F_{DF\,base,i}} \tag{7-17}$$

where $F_{DF\,base,i}$ is the 'base' value diafiltration flow rate to the i^{th} fractionation stage [L s^{-1}], specified using:

$$F_{DF\,base,i} = \phi_{base} F_{P,i} \tag{7-18}$$

For a fixed ratio trajectory $\phi_{base} = \phi_{max}$, however the situation is not as straightforward for the constrained diafiltration ratio strategy, since ϕ_{base} is not constant. In such circumstances it is preferable to remove the base terms for diafiltration flow rates, and only associate a control action cost with manipulation of the retentate flow rate.

The final controller cost term is associated with manipulation of the plant retentate flow rate. This is calculated using:

$$x_{n+1} = \frac{F_R - F_{R\,base}}{F_{R\,base}} \tag{7-19}$$

with the base value for the retentate flow rate $F_{R,base}$ [L s^{-1}] is related to the plant feed flow rate setpoint $F_{F,SP}$:

$$F_{R,base} = \frac{F_{F,SP}}{VCF} \tag{7-20}$$

The optimal controller action u, i.e. the solution of Equation 7-16 can be determined reasonably easily, although the method is rather more numerically intense than the general MPC strategy due, to the time-variant nature of the process. If Equation 7-14 is

used to predict process behaviour, it becomes necessary to invert the plant model **M** at each time step, since the permeate flow rates (and occasionally the number of stages) change. Solution of Equation 7-16 is subject to a set of constraints on the diafiltration flow rate to each stage $F_{DF,i}$, since it is generally desirable that the diafiltration flow rate not exceed the permeate flow rate from that stage:

$$0 \leq F_{DF,i} \leq F_{P,i} \tag{7-21}$$

A stricter constraint is posed by Equation 7-9, which requires:

$$0 \leq F_{DF,i} \leq R_o F_{P,i} \tag{7-22}$$

It is important that the diafiltration limits (either Equation 7-21 or 7-22) are updated at each time step to track changes in the permeate flow rates. The retentate flow rate is also constrained by physical factors such as valve size and rangeability:

$$F_{R,min} \leq F_R \leq F_{R,max} \tag{7-23}$$

The field of linear quadratic control theory is well developed, with a number of techniques available for the solution of the constrained optimisation (e.g. Ricker, 1985). However, for case study 1, this strategy requires the inversion of a process model **M** which may have up to 96 states. Although only the diafiltration stages are of interest, the response of the non-diafiltration stages will affect the feed concentration of the fractionation section, so must be included in the process model.

Although it is feasible to invert the process model **M** at each time step, an alternative approach is pursued in this thesis. Instead of linearising and inverting the real-time process model, the existing non-linear differential (real-time) equation set is directly used to predict future process behaviour via numerical integration. Thus, the numerical optimisation method will select a trial input set u, with the plant response simulated to the event horizon t_f, and the cost function J calculated at this point. A numerical optimisation method can be used to find an optimal u which satisfies Equation 7-16, subject to the specified constraints. Using this method allows additional rate-of-change constraints to be applied to the controller action. The numerical optimisation approach allows the same dynamic process model to be used for both real-time simulation and MIMO control. Greater flexibility is also possible in the choice of process model, with the use of a distributed parameter model now feasible if necessary, to represent dynamic process behaviour. This approach has similarities to the non-linear MPC strategy

outlined by Biegler & Rawlings (1991), which uses non-linear programming methods to solve the objective function.

7.7.4 Error correction in process model

The final part of a MPC strategy is the identification of errors or inaccuracy in the process model. Such errors can result from data sampling (see Section 7.3), modelling error or unmeasured disturbances entering the process. Identification of these inaccuracies is usually achieved by calculating the differences between the predicted process outputs, and those measured from the plant. It is generally assumed that any offset will remain constant, so is applied as a correction to the next model output (Luyben & Luyben, 1997). Utilising the measured retentate total solids concentration to correct plant-model mismatch is not easy, since discrepancies identified in the retentate stream are difficult to relate to other stages within the plant. With a number of stages connected in series, it is unlikely that any discrepancy between the predicted and measured retentate concentration will be simultaneously occurring in all other stages of the plant. The simplest approach is to assume that, in the absence of online data, the predicted midpoint concentration is correct, and the discrepancy occurs linearly between this point and the retentate stream. This is a gross assumption, but it serves to provide a basis for implementing some form of error correction using the available online data. Should the midpoint concentration be measured online, then this strategy could easily be modified to utilise this additional information. For a fractionation section with n stages in operation, a correction term can be calculated by:

$$\varepsilon = \frac{1}{n}\left(\frac{\textit{Measured total solids concentration}}{\textit{Predicted total solids concentration}} - 1\right) \qquad \textbf{(7-24)}$$

The term ε could then be used to correct the total solids concentration predicted by a fractionation stage i:

$$TS'_{predicted,i} = TS_{predicted,i} \times \left(1 + i\varepsilon\right) \qquad \textbf{(7-25)}$$

The correction term ε is assumed to remain constant for the duration of the current event horizon t_f. Given the short event horizon used for this MPC implementation, this is a fair assumption. Shinskey (1994) states that PID controllers often have superior disturbance rejection performance to MPC systems. In many cases this may be true, however for a multistage membrane plant this is unlikely, since the MPC strategy provides a framework where predicted internal states can be used to identify, and ultimately reject disturbances before they enter the retentate stream.

7.7.5 Implementation of the MIMO controller strategy in Matlab

The modified MPC strategy was written as a function constructed and implemented within a 'user-defined function' block in Simulink, using the data from the real-time model discussed in Section 7.3. For ease of implementation the multivariable optimisation used a separate (but identical) non-linear ODE set to the real-time model. In an industrial implementation, it is likely that the controller could be implemented in a compiled language, allowing sufficient flexibility to use the same equation set for both the real-time model and controller simulation. The constrained multivariable optimisation function '*fmincon*' (Coleman *et al.*, 1999) was used to find the optimal manipulated variable set u, subject to the constraints specified in Equations 7-21 or 7-22, and 7-23. For each case study, the retentate flow rate was initially fixed at $F_{R,min}$ the minimum allowable retentate flow rate, with automatic control only commencing once the retentate total solids concentration exceeded the desired midpoint concentration.

In this strategy the controller could apply diafiltration to any stage operating in the fractionation section once the controller switched to automatic. This occurred when the predicted total solids concentration of any stage in the plant exceeded the desired midpoint concentration. As new diafiltration stages are added to the plant, the controller has an increasing number of measured and manipulated variables to manage. The weighting matrix **Q** must therefore vary in size to match the number of stages in operation.

7.8 Model-predictive control of variable area multistage membrane plants

The control strategy discussed in Section 7.6 was trialled for each case study, using the MPC implementation developed in the Section 7.7. Trials were performed in Simulink to assess the feasibility and performance of this MIMO strategy, and provide comparative data for the SISO trials performed in Chapter 6. The operating conditions and online data available to the controller were identical to the closed-loop SISO trials performed in Sections 6.4 and 6.5.

Shinskey (1994) states that model-predictive controllers have poor rejection of unmeasured disturbances. Given such an allegation, it is important to examine MIMO controller performance under such conditions when subjected to unmeasured disturbances in

the feed stream. For this reason two further sets of closed-loop trials were performed, where the plant was subject to one of the following disturbance regimes:

1. Unmeasured sinusoidal variation in feed stream total solids concentration: amplitude 2 %, period 40 minutes.
2. Unmeasured sinusoidal variation in feed stream protein concentration: amplitude 2 %, period 40 minutes.

The period of these disturbances was consistent with the characteristics of a casein plant producing the feed stream for case study 1. In the absence of more specific data, the same disturbance characteristics were also used for case study 2. Sensor noise was not included in these simulations, since it is assumed that the continuously measured values were filtered or averaged prior to sampling.

Plant feed flow rate was maintained by a PID controller, with additional area added as complete stages. These were added to either the concentration or fractionation section as appropriate to minimise variation in the midpoint flow rate, in the manner discussed in Section 7.4. A 10 second sampling time was used for both real-time models, combined with a 20 second controller event horizon. Discrete outputs from the controller were passed through a continuous first order filter before entering the plant.

7.8.1 Case study 1: Whey protein concentrate production

Model-predictive control of the whey protein concentrate plant was trialled for the same retentate specifications as examined in Sections 5.2.1, 5.4.3, 5.5.1, 5.7.1 and 6.4; namely 85 % protein purity, and 27 wt % total solids concentration. The midpoint concentration of the reference trajectory was specified as 15 wt %, corresponding to the SISO simulations for this case study presented in Section 6.4. Analysis in Section 7.5 showed the fixed diafiltration ratio strategy to cause backup within the plant, so a constrained diafiltration ratio strategy was used to generate the reference trajectory ($\alpha = 0.753$).

The model-predictive controller was tuned by manipulating values in the weighting matrix **Q**, where terms in the matrix correspond to 'costs' of controller error in each objective term. For this case study, terms in the matrix were dynamically scaled, depending on the number of diafiltration stages in operation. For the i^{th} diafiltration stage in the fractionation section (with n stages in operation):

$$q_i = \left(q_{\min} + i \frac{q_{range}}{n} \right) \quad \textbf{(7-26)}$$

where

q_{min} = minimum weighting value, set as 0.15 for this case study

q_{range} = range between minimum and maximum weighting values, set as 1.85 for this case study

The overall weighting matrix **Q**, with n stages operating in the fractionation section, was therefore:

$$\mathbf{Q} = diag\left[q_1 \cdots q_n \;\; 40 \right]$$

where the final term represented the cost weighting on the error (distance) between the predicted and desired retentate stream total solids and purity. No costs were associated with manipulation of the control variables, i.e. $R = 0$. Error correction was implemented using the measured retentate total solids concentration, as defined by Equation 7-24 and 7-25.

During startup, it is desirable to draw as little off-specification retentate from the plant as possible. For this reason, the retentate flow rate was fixed at the $F_{R,min}$ until the controller switched to automatic, when the controller optimisation was constrained within the range:

$$5\times10^{-5} \leq F_R \leq 2.5\times10^{-3} \qquad [m^3\ s^{-1}]$$

For these trials, a feed flow rate setpoint of 2.17×10^{-3} m^3 s^{-1} was used, the same as specified for the Chapter 6 closed-loop trials. A VCF_f of 2.8 was used to calculate the desired midpoint flow rate.

The closed-loop behaviour of the MIMO controller is presented in Figure 7-8, operating under equivalent conditions as the SISO controller design presented in Table 6-2. The action of the MIMO controller differed significantly during startup, with diafiltration injection applied aggressively as the retentate total solids concentration approached setpoint, ensuring that overshoot did not occur. Retentate flow rate was only increased as the predicated protein purity approached setpoint. Under the SISO strategy, the retentate flow rate was paired with total solids concentration, whilst diafiltration injection was applied according to a predetermined schedule. Selection of the SISO variable pairings was based on RGA analysis, performed for a plant operating at setpoint. The behaviour of the MIMO controller suggests that dynamic characteristics at

startup may be different to when the process is operating at setpoint. It is possible that the preferred pairings for servo (startup) and regulatory (disturbance rejection) requirements are different. Most importantly, these trials show that the MIMO controller structure has sufficient flexibility to accommodate changes which occur in dynamic plant behaviour.

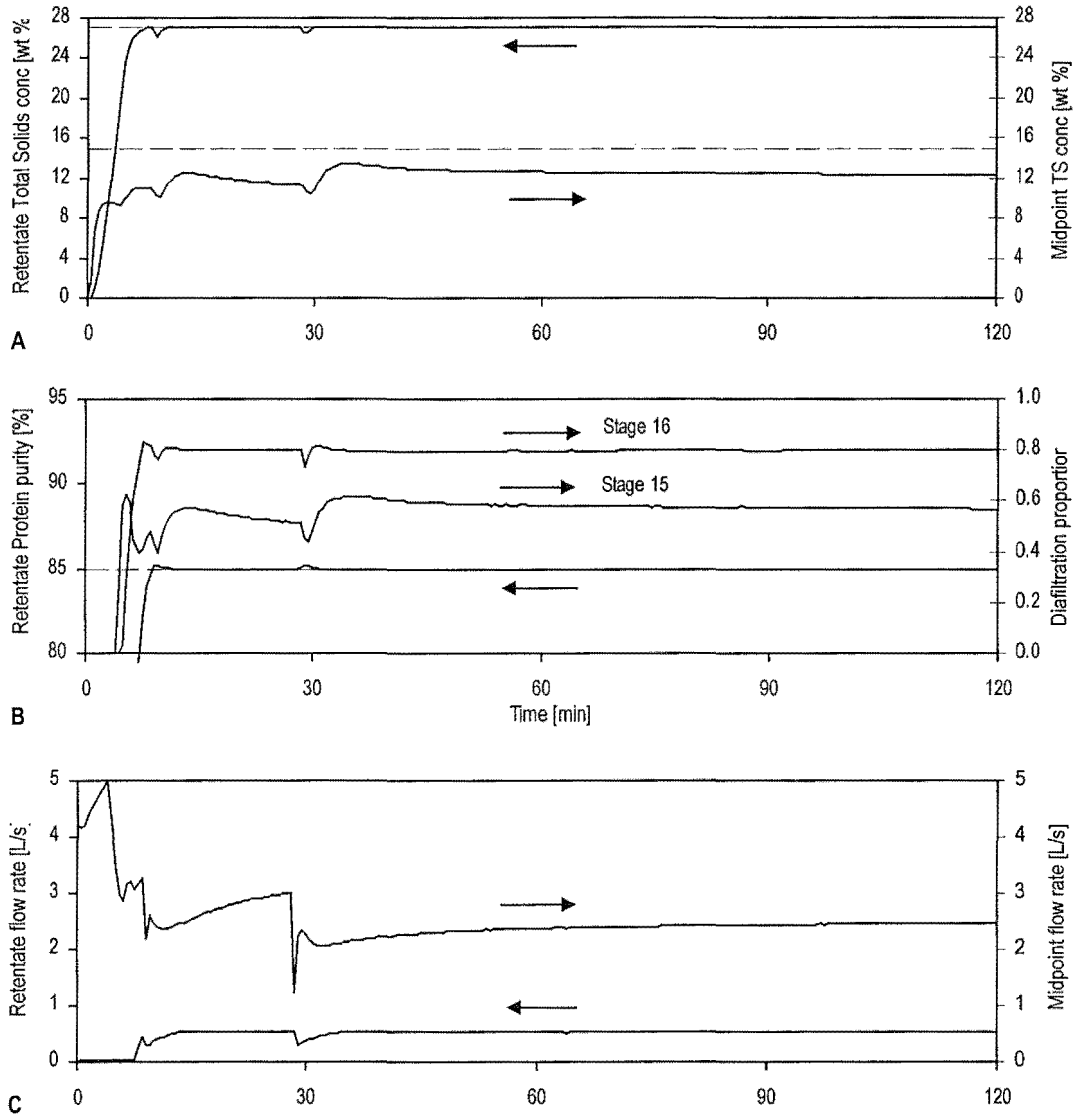

Figure 7-8 Closed-loop MIMO operation - case study 1 with variable membrane area

New stages were added by MIMO controller after 9 and 28 minutes of operation. Simulation conditions and controller parameters are presented in Appendix B.

The diafiltration flow rates applied to each stage in the fractionation section were expressed as a proportion of the permeate flow (Figure 7-8B), calculated in the same manner as the stage diafiltration ratios used in Chapter 6. The high levels of diafiltration injection applied to the final stages of the plant reflected the characteristics of the constrained reference trajectory used for this separation. This compared with the SISO strategy which applied diafiltration at lower rates to four stages. Interestingly, the

MIMO controller still preferentially manipulated the diafiltration flow rate to the first diafiltration stage in order to reject disturbances, exhibiting behaviour which mirrored the overall diafiltration ratio strategy employed by the SISO controller.

An advanced controller strategy is only worthwhile if the additional effort required to implement such a strategy is rewarded with tangible improvements in performance. The quality of control achieved by the two strategies is compared in Figure 7-9, focusing specifically on the consistency of the retentate properties. SISO performance was simulated using the 'optimal' startup strategy presented in Figure 6-10. The MIMO controller clearly achieves faster startup with less overshoot (superior servo characteristics). In contrast, the SISO controller strategy achieved superior disturbance rejection (regulatory characteristics) for the retentate total solids concentration. However, the SISO strategy also displayed significantly poorer protein purity control, exhibiting noticeable drift in the protein purity as the plant fouled and new stages were added. At the end of the 9 hour production run, the protein purity had risen significantly. Careful selection of the overall diafiltration ratio $\phi_\%$ may reduce the initial offset in protein purity, but little can be done to improve the poor setpoint tracking. This difficulty will

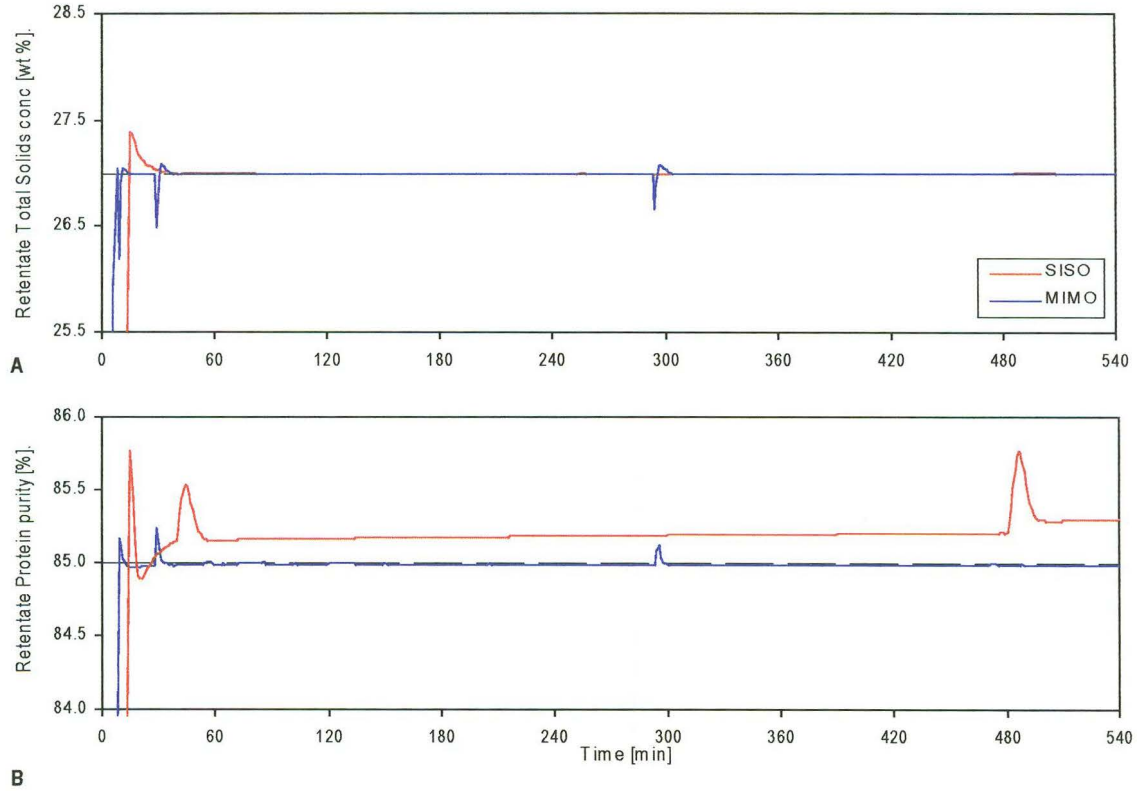

Figure 7-9 Comparison of SISO and MIMO controller performance - case study 1

New stages were added by MIMO controller after 9, 28 and 293 minutes of operation. New stages were added by SISO controller after 4, 9, 38 and 478 minutes of operation. Simulation conditions and controller parameters are presented in Appendix B.

be even more significant in a low temperature WPC plant, which may operate continuously for up to 20 hours. The controller objectives outlined in Section 7.4 placed greatest emphasis on consistency of product purity, since variations in retentate concentration could be mitigated by downstream processing. The performance of the MIMO control strategy most closely matches these objectives.

Shinskey (1994) states that model-predictive controllers usually have poorer ability to reject unmeasured disturbances than single-loop PID controllers. This generalisation was tested by comparing the closed-loop performance of the SISO and MIMO controllers when subjected to unmeasured sinusoidal variations in total solids feed concentration (Figure 7-10) and protein feed concentration (Figure 7-11).

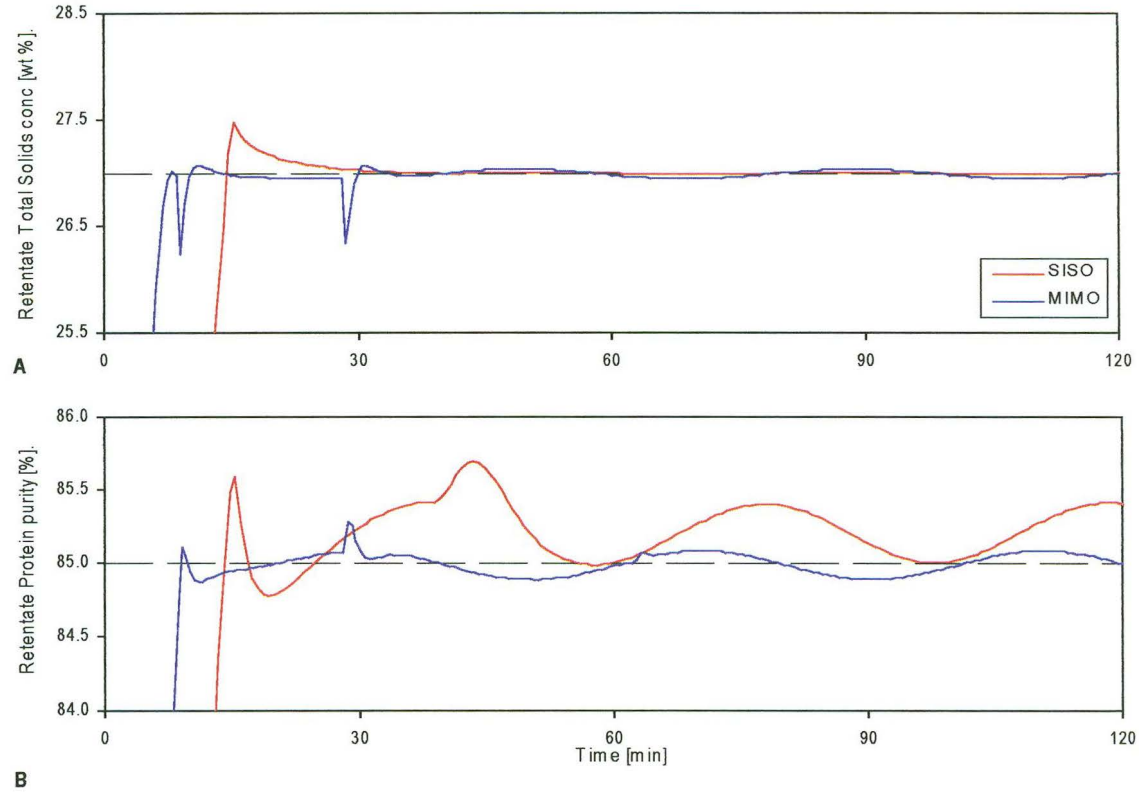

Figure 7-10 Comparison of SISO and MIMO controller performance for total solids feed concentration disturbance - case study 1

New stages were added by MIMO controller after 9 and 28 minutes of operation. New stages were added by SISO controller after 4, 9 and 38 minutes of operation. Simulation conditions and controller parameters are presented in Appendix B.

The SISO control strategy showed no degradation in performance for the retentate total solids concentration (Figure 7-10A), completely rejecting the total solids feed concentration disturbance. Whilst the same cannot be said for the MIMO controller, variation in the retentate concentration was not excessive (27 ± 0.05 wt %), and the superior startup performance was maintained. Retentate protein purity (Figure 7-10B) was a

rather different situation, with the MIMO controller displaying superior performance (85 ± 0.09 %) over the SISO strategy (85.2 ± 0.2 %).

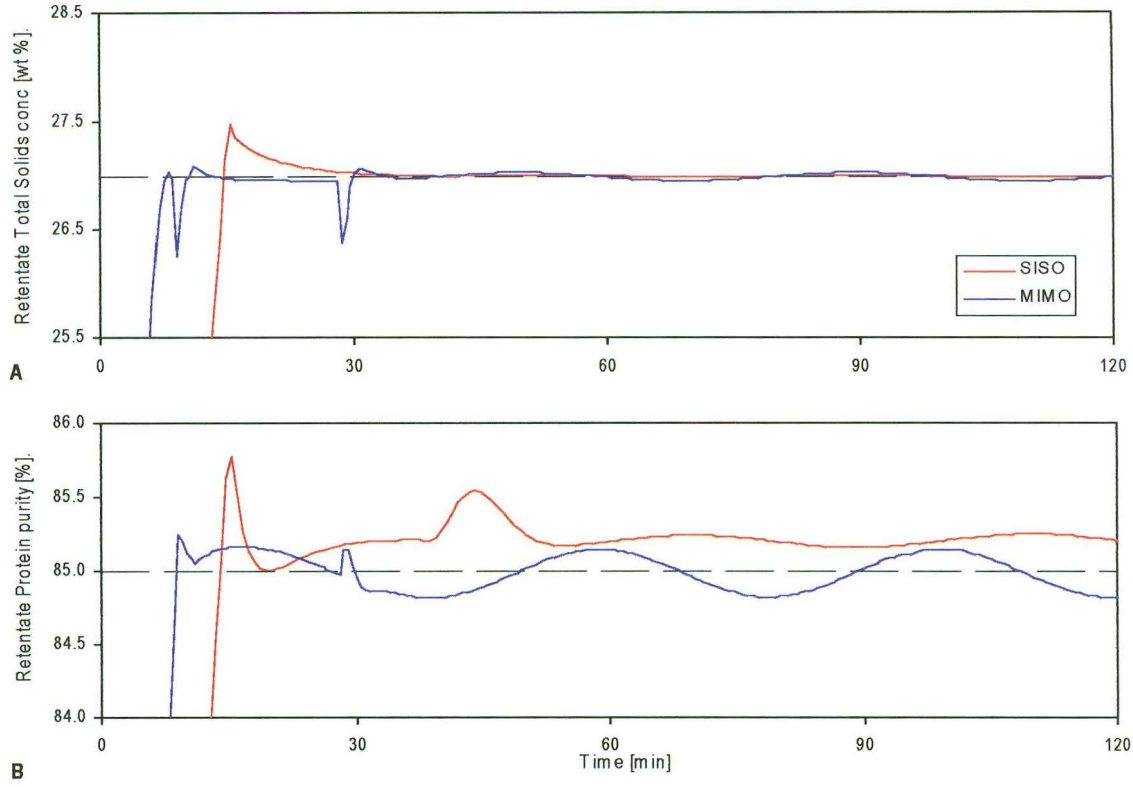

Figure 7-11 Comparison of SISO and MIMO controller performance for protein feed concentration disturbance - case study 1

New stages were added by MIMO controller after 9 and 28 minutes of operation. New stages were added by SISO controller after 4, 9 and 38 minutes of operation. Simulation conditions and controller parameters are presented in Appendix B.

Sinusoidal variation in protein concentration represents both a concentration and composition disturbance in the feed stream. Closed-loop performance for the retentate total solids concentration (Figure 7-11A) was almost identical, with the PID controller completely rejecting the disturbance but still displaying slower startup and greater overshoot. However controller performance was quite different for the retentate protein purity (Figure 7-11B), with the model predictive controller (85 ± 0.15 %) displaying poorer performance than the SISO strategy (85.2 ± 0.05 %) for this disturbance. In both situations, the MIMO controller successfully maintained the predicted protein purity at the setpoint, but the sensitivity of the real-time model to unmeasured feed concentration disturbances caused difficulties. Little can be done to solve this problem. Overall, the model predictive strategy offered faster startup, and more importantly, the protein purity did not drift from the setpoint over the course of production.

7.8.2 Case study 2: Permeate product separation

This case study has also been examined extensively in previous sections. The desired retentate purity was specified as that necessary to achieve the required permeate yield of 75 %. This recovery was achieved at a retentate concentration of 17 wt % and Component A purity of 79.9 %. A midpoint concentration of 9.25 wt % was specified for the reference trajectory, corresponding to the SISO simulations presented in Section 6.5.1. A fixed diafiltration ratio strategy was used to generate the reference trajectory for the controller. Backup did not occur within the plant due to the high retention coefficients of the components in the feed stream ($R_A = 1.0$, $R_B = 0.7$).

A dynamically scaled error weighting matrix **Q** was also used for this case study (Equation 7-27) with $q_{min} = 1.5$, $q_{range} = 1.5$, and a retentate stream error weighting $q_{n+1} = 50$. By choosing a fixed diafiltration ratio strategy when defining the reference trajectory, it was possible to associate a control action cost with deviation of the diafiltration flow rates from specified base values. The base value $F_{DF\,base,i}$ for each stage operating in the fractionation section was calculated using Equations 7-17 and 7-18, with $\phi_{base} = \phi_{max} = 0.7$. The cost weighting matrix **R** was specified as:

$$\mathbf{R} = diag\left[\, 0.02, \cdots 0.02, 0.05 \,\right]$$

where the final term corresponded to the deviation of the retentate flow rate from the base value $F_{R\,base}$. During startup the base value $F_{R,base}$ was set equal to $F_{R,min}$ until the controller switched to automatic, when $F_{R\,base}$ was calculated using Equation 7-20, for a *VCF* of 11.25. Upper and lower constraints on the diafiltration flow rates were specified as:

$$0 \leq F_{DF,i} \leq F_{P,i}$$

Limits were also specified on the plant retentate flow rate:

$$1\times10^{-4} \leq F_R \leq 2.5\times10^{-3} \qquad [m^3\ s^{-1}]$$

For these trials, a feed flow rate setpoint of 1.5×10^{-2} m^3 s^{-1} was used, the same as used previously for this case study. Membrane area addition was used to maintain a stable midpoint flow rate corresponding to the desired midpoint concentration. The desired midpoint flow rate was calculated using Equation 7-2, with $VCF_f = 2$. Real-time model correction using the measured retentate total solids concentration was applied using Equations 7-24 and 7-25.

The closed-loop performance of the MIMO controller is shown in Figure 7-12 for the permeate product case study. The high permeate yield requirement for this separation mean that large amounts of diafiltration must be injected into this plant, making it slow

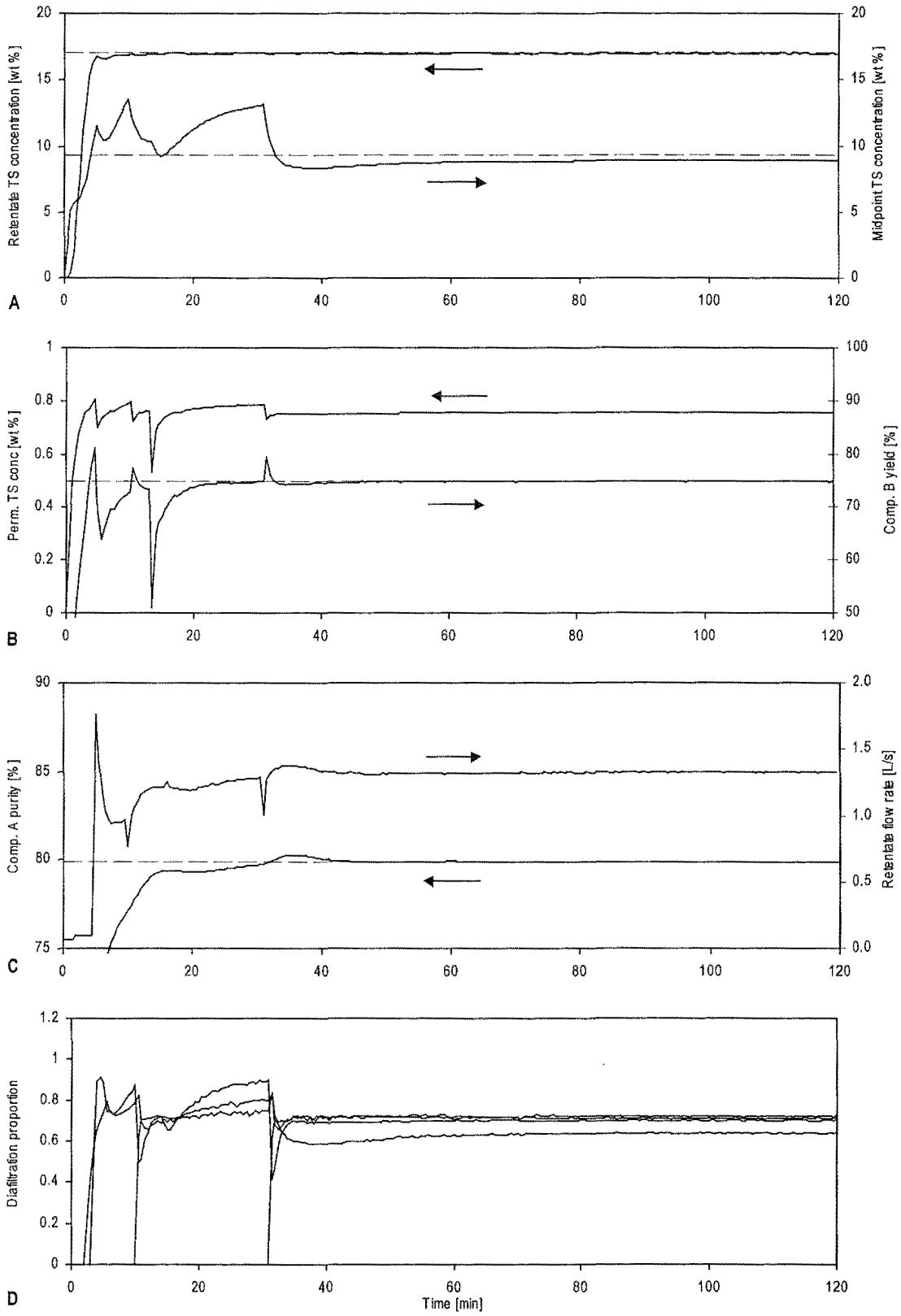

Figure 7-12 Closed-loop MIMO operation - case study 2 with variable membrane area

New stages were added by MIMO controller after 4, 13 and 31 minutes of operation. Simulation conditions and controller parameters are presented in Appendix B.

to reach the desired retentate purity (Figure 7-12C). At startup the model-predictive controller applied diafiltration injection quite differently to the SISO strategy (Figure 6-16). Diafiltration water was applied at high rates initially by the MIMO controller to hasten the rise of the retentate purity, with these flow rates reducing as the purity approached setpoint (Figure 7-12D). The use of cost penalties encouraged the controller to operate with diafiltration proportions close to 70 %. This helped to stabilise the system, but 'noise' was still evident in the diafiltration flow rates employed by the MIMO controller. The desired midpoint concentration was successfully attained through careful management of membrane area addition by the feed flow rate controller. After approximately 40 minutes of operation, sufficient stages had been added to the plant to allow the separation trajectory to become fully established.

Direct comparison of the SISO and MIMO controller simulations (Figure 7-13) shows the model-predictive controller to achieve superior performance at startup for the retentate total solids concentration although a small offset was evident. Overshoot for this case study was very undesirable since the plant operated relatively close to the gel concentration (C_{gel} = 20 wt %). The model-predictive controller achieved better setpoint tracking for the retentate purity (Figure 7-13B), and also exhibited superior rejection of disturbances associated with the addition of new membrane area. Both controllers were able to maintain the desired permeate yield (Figure 7-13C), however the MIMO strategy was better able to accommodate disturbances associated with the addition of a new stage. There may seem to be little significant difference between the characteristics of the two controllers, but this is not surprising since the reference trajectory for the MIMO strategy was identical to the SISO diafiltration strategy. However it is believed that the MIMO controller showed superior performance and stability overall, as well as offering the potential to operate with alternative reference trajectories which may provide significant performance or efficiency gains.

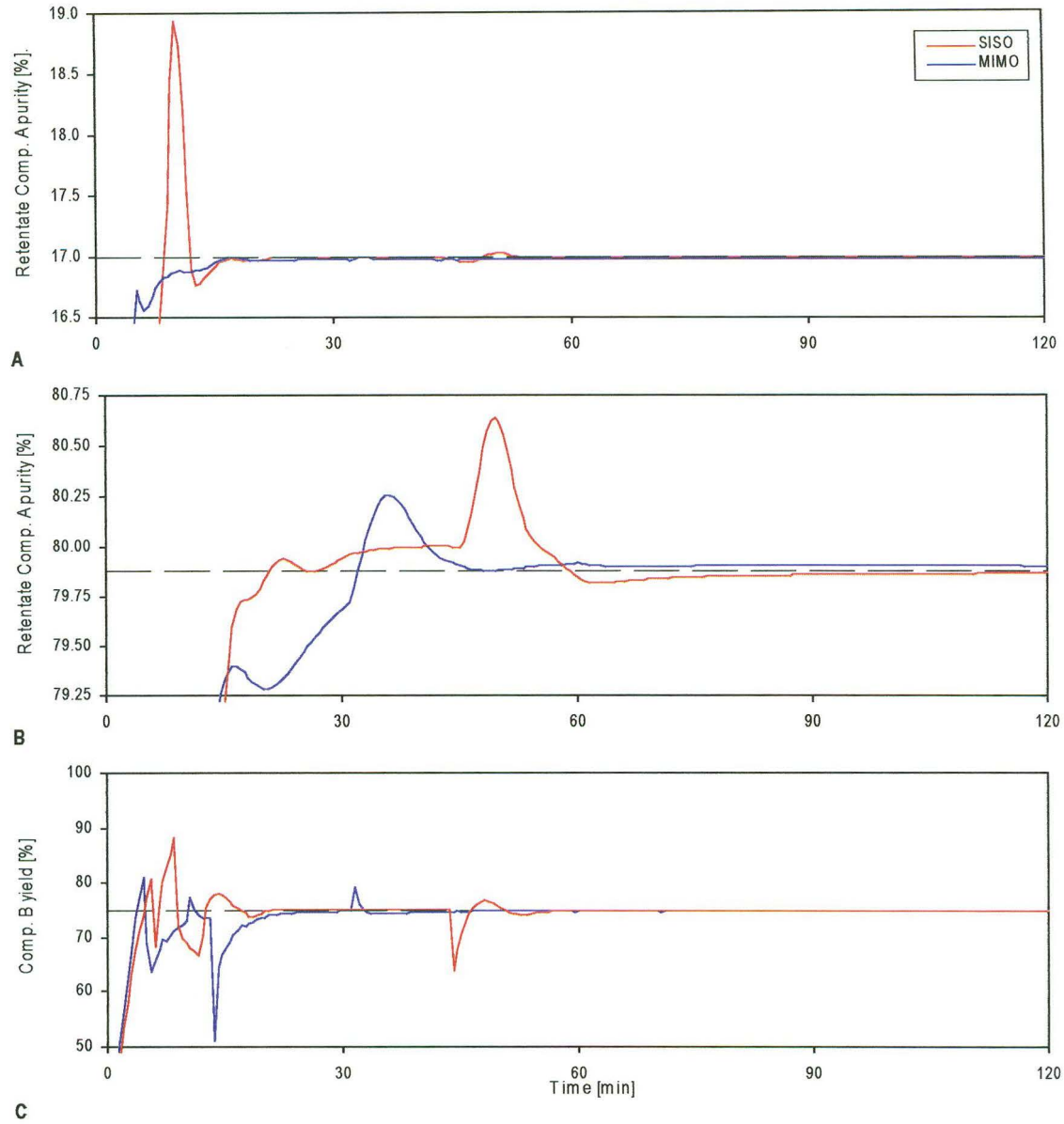

Figure 7-13 Comparison of SISO and MIMO controller performance- case study 2

New stages were added by MIMO controller after 4, 13 and 31minutes of operation. New stages were added by SISO controller after 5, 9 and 44 minutes of operation. Simulation conditions and controller parameters are presented in Appendix B.

It is also useful to examine the closed-loop performance of the model-predictive controller when subjected to unmeasured disturbances. Figure 7-14 and Figure 7-15 present comparisons between SISO and MIMO controller performance in the presence of sinusoidal disturbances in total solids and Component A feed stream concentrations respectively. Overall, both controller types exhibited similar behaviour, achieving almost identical permeate yield performance. Most importantly, the model-predictive controller did not exhibit excessive signs of sensitivity to unmeasured system disturbances compared to the PID-based approach.

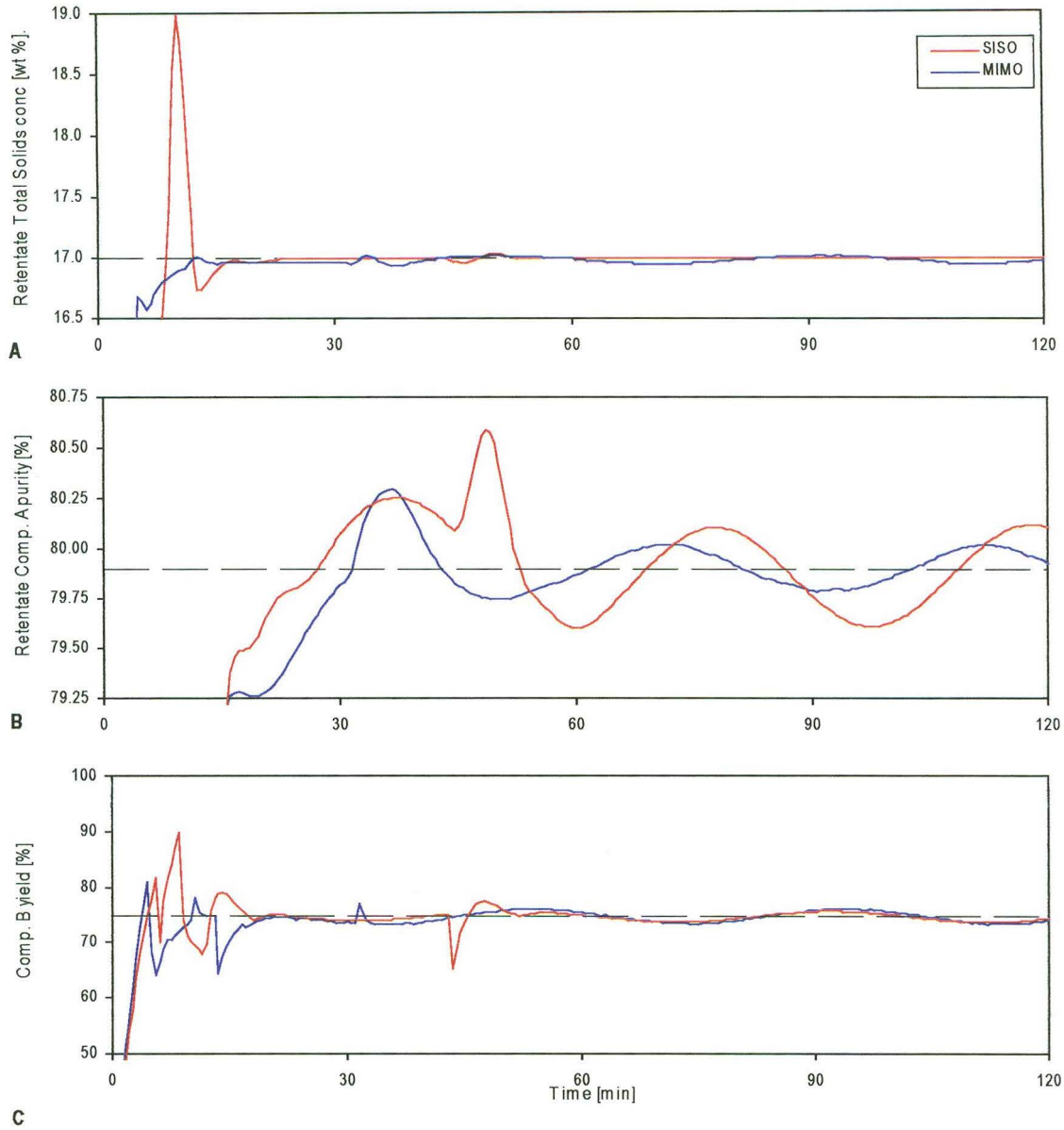

Figure 7-14 Comparison of SISO and MIMO controller performance for total solids feed concentration disturbance - case study 2

New stages were added by MIMO controller after 4, 13 and 31 minutes of operation. New stages were added by SISO controller after 5, 9 and 43 minutes of operation. Simulation conditions and controller parameters are presented in Appendix B.

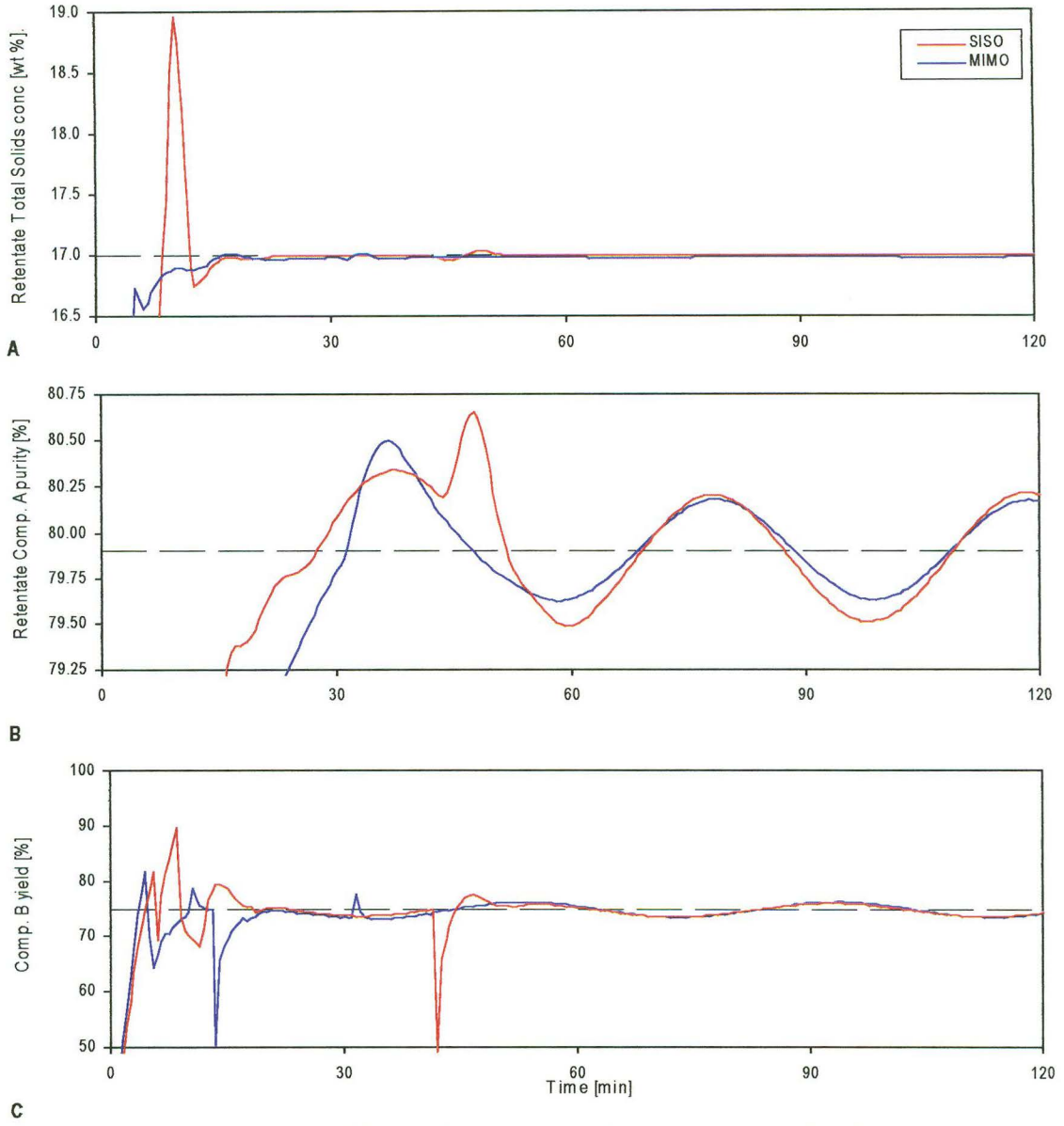

Figure 7-15 Comparison of SISO and MIMO controller performance for Component A feed concentration disturbance - case study 2

New stages were added by MIMO controller after 4, 13 and 31 minutes of operation. New stages were added by SISO controller after 5, 9 and 43 minutes of operation. Simulation conditions and controller parameters are presented in Appendix B.

7.9 MIMO controller performance under aggressive diafiltration regimes

The greatest achievement that a new control strategy can offer, is the ability to operate a process under previously unattainable conditions. For a multistage membrane plant this corresponds to operating under more aggressive diafiltration regimes than previously possible. The model-predictive controller directly manipulates diafiltration flow rates to the plant, avoiding the need to specify diafiltration as ratios of permeate flow rates. This removes the disturbance feedback loop present under the SISO diafiltration control strategy. It is therefore useful to compare the closed-loop performance of the SISO and MIMO controllers under more aggressive diafiltration strategies.

7.9.1 Case study 1: Whey protein concentrate production

The weighting matrices and controller structure used for these trials were identical to that outlined in Section 7.8.1. Only the reference trajectory for the controller differed from the previous implementation, with midpoint concentration of 23.5 wt %, and α = 0.932. This midpoint concentration corresponded to an SISO strategy operating with ϕ_0 = 0.092 and ϕ_{max} = 0.85. The closed-loop performance of the two controller types is shown in Figure 7-16 for an unmeasured sinusoidal disturbance in the total solids concentration of the feed stream. The MIMO controller performance was almost identical to that achieved under the less aggressive diafiltration regime (Figure 7-13), with equivalent variation in the retentate total solids concentration (27 ± 0.05 wt %) and protein purity (85 ± 0.1 %). However the SISO controller performance was noticeably poorer for this operating condition, exhibiting slower startup and significantly greater overshoot. A constant total solids concentration was maintained, but variation in the protein purity was greater (85 ± 0.25 %).

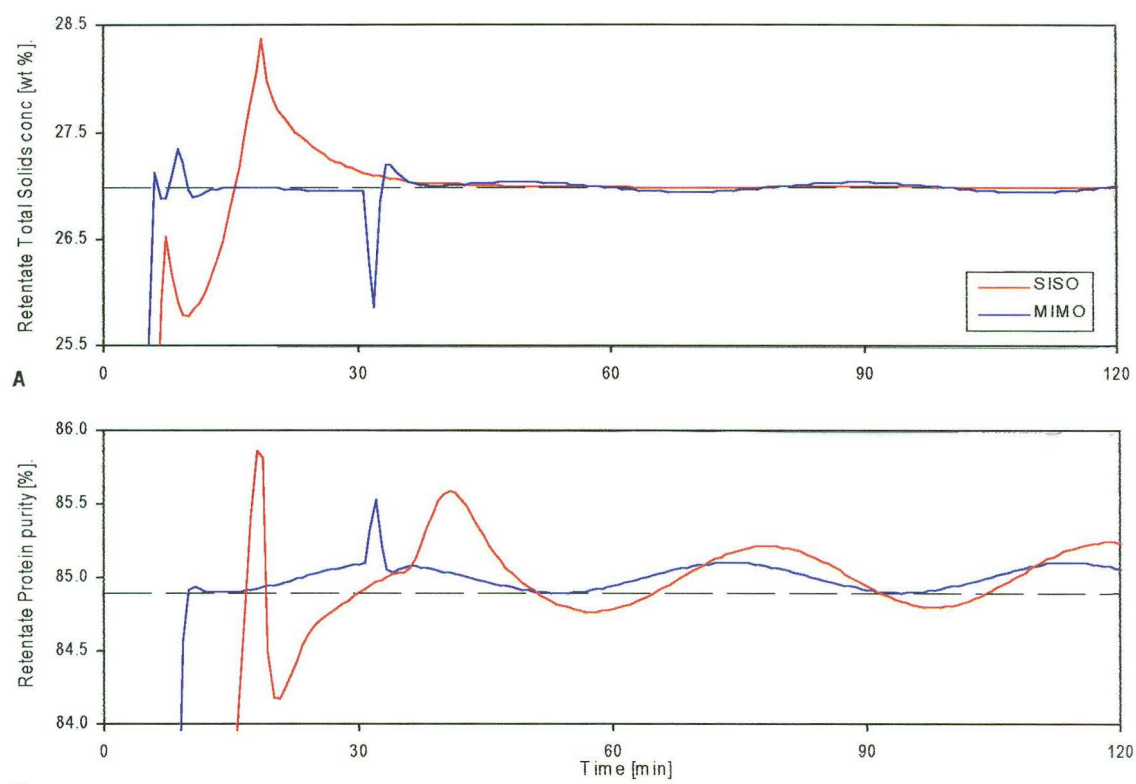

Figure 7-16 Comparison of SISO and MIMO controller performance at high diafiltration for total solids feed concentration disturbance - case study 1

New stages were added by MIMO controller after 31 minutes of operation. New stages were added by SISO controller after 11, 18 and 35 minutes of operation. Simulation conditions and controller parameters are presented in Appendix B.

Closed-loop controller performance for an unmeasured sinusoidal disturbance in the feed stream protein concentration is presented in Figure 7-17. The same trends were present in this data, with consistent closed-loop performance achieved by the MIMO controller and poorer plant startup evident under the SISO strategy. Overall, it can be concluded that the model-predictive controller was able to successfully accommodate unmeasured disturbances or model uncertainty under different operating conditions, and maintain consistent closed-loop performance. Degradation of the SISO controller performance, particularly at startup, was evident under the more aggressive diafiltration regime, which was consistent with industrial experiences with WPC production in New Zealand.

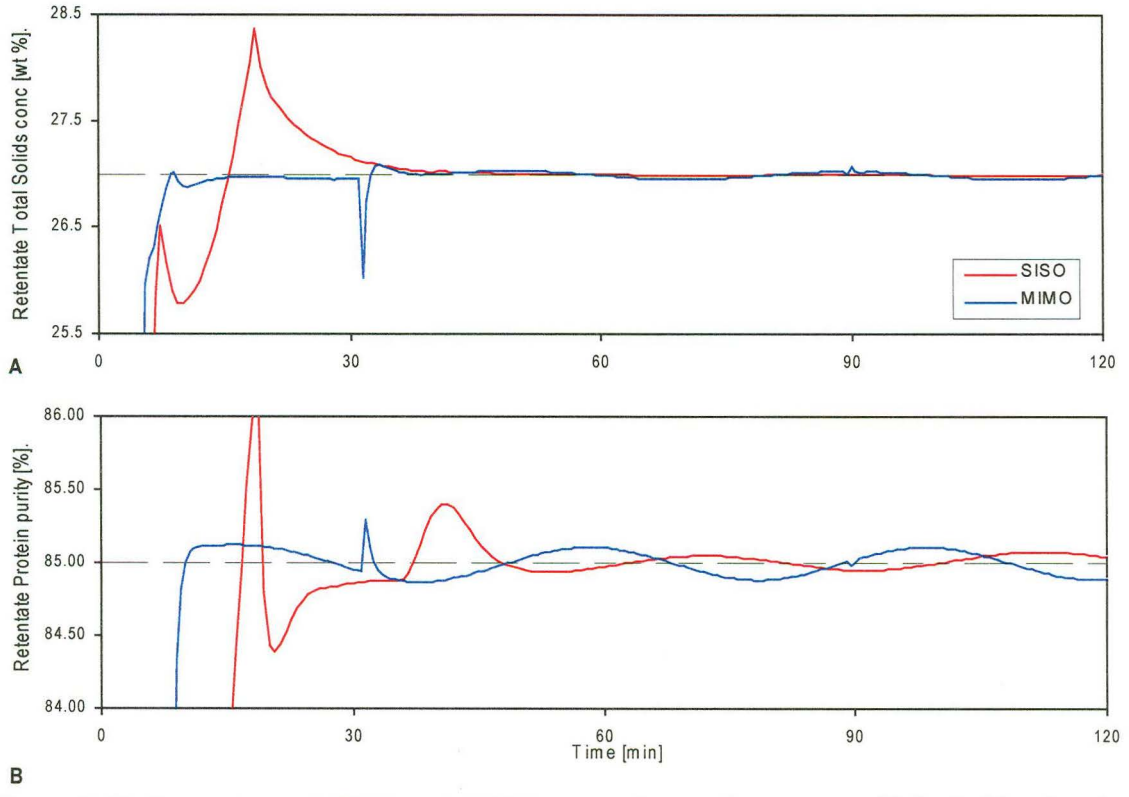

Figure 7-17 Comparison of SISO and MIMO controller performance at high diafiltration for protein feed concentration disturbance - case study 1

New stages were added by MIMO controller after 31 minutes of operation. New stages were added by SISO controller after 11, 18 and 35 minutes of operation. Simulation conditions and controller parameters are presented in Appendix B.

7.9.2 Case study 2: Permeate product separation

The same controller structure and weighting matrices were used for these trials as was used previously for the permeate product case study. The reference trajectory was defined for a midpoint concentration of 14 wt %, corresponding to a SISO strategy operating with $\phi_o = 0.23$ and $\phi_{max} = 0.85$. Simulated closed-loop performance for the SISO and MIMO controller is shown in Figure 7-18 with *no* unmeasured disturbances

entering the system. The model-predictive controller displayed almost identical behaviour as the first trials presented in Section 7.8.2, although plant startup was slower. However SISO controller performance was markedly poorer under the more aggressive diafiltration regime. It was only possible to achieve stable (though underdamped) controller behaviour by significantly detuning the retentate total solids and feed flow rate PID controllers. Figure 7-18 shows the best achievable controller performance.

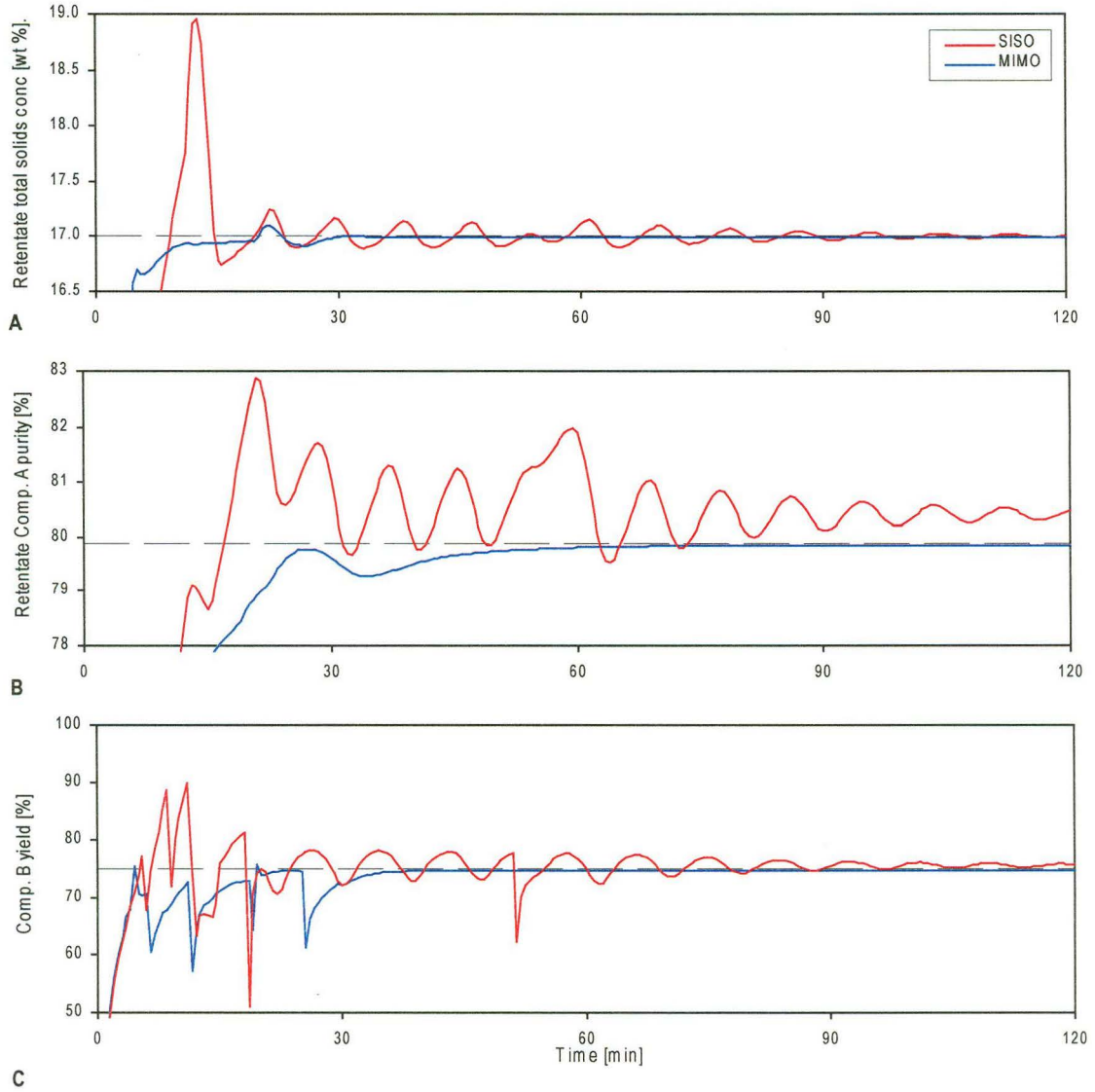

Figure 7-18 Comparison of SISO and MIMO controller performance at high diafiltration - case study 2

New stages were added by MIMO controller after 6, 11, 18, and 25 minutes of operation. New stages were added by SISO controller after 5, 8, 11, 18 and 51 minutes of operation. Simulation conditions and controller parameters are presented in Appendix B.

The low plant VCF contributed to the high levels of interaction between the feed and retentate flow rates. Increased levels of disturbance feedback, caused by operating at higher diafiltration ratios, also contributed to oscillatory plant behaviour. Because the MIMO strategy does not specify diafiltration flow rates as a ratio of permeate flows, the

disturbance feedback difficulties were not encountered and controller performance did not decline under a more aggressive diafiltration regime.

7.10 Conclusion

An innovative controller strategy was developed in this chapter and trialled for the two case studies. This strategy was based on the concept of manipulating process inputs to maintain a desired separation trajectory through the plant. The strategy was implemented using model-predictive controller technology, with the behaviour of internal system states predicted by a real-time process model. Diafiltration flow rates were directly manipulated rather than maintained as specified proportions of the permeate flows. This removed the undesirable disturbance feedback characteristics that were present under the SISO strategy. Simulations performed for the two case studies suggested that this control strategy was able to achieve superior process startup and good control of retentate purity, even when subject to unmeasured feed disturbances. Most importantly, closed-loop simulations showed that, unlike the SISO strategy of Chapter 6, the model-predictive controller was able to maintain a consistent level of performance over a range of operating conditions.

The reference trajectory strategy offered great flexibility, since any specified set of operating requirements (e.g, retentate purity, midpoint concentration) there will exist a number of feasible operating strategies (i.e. reference trajectories). Thus it becomes possible to develop and implement improved operating strategies for existing membrane separations. Although controller trials were performed exclusively in Matlab, it is believed that this MIMO strategy can achieve equivalent performance improvements over traditional SISO strategies on an industrial plant.

7.11 References

Biegler L T & Rawlings J B (1991), Optimization approaches to Nonlinear Model Predictive Control. *Proceedings of Chemical Process Control - CPC IV,* pp. 543-571, New York.

Box G E P, Jenkins G N & Reinsel G C (1994), *Time Series Analysis: Forecasting and Control,* Prentice-Hall Inc., New Jersey.

Coleman T, Branch M A & Grace A (1999), *Optimisation Toolbox User's Guide,* 2nd Ed., The MathWorks Inc., MA.

de Rham O & Chanton S (1986), An empirical mathematical model of retentate composition in ultrafiltration of dairy products, *Journal of Dairy Research,* **53**, 271-283.

Garcia C E & Morari M (1985), Internal Model Control 2. Design procedure for multivariable systems, *Ind. Eng. Chem. Process Des. Dev.,* **24**, 472-484.

Green M & Limebeer D J N (1995), *Linear Robust Control,* Prentice-Hall Inc., New Jersey.

Han M & Park S (1993), Control of high-purity distillation column using a non-linear wave theory, *AIChE Journal,* **39**, May 787-796.

Krstiz M, Kanellakopoulos I & Kokotovic P (1995), *Nonlinear and Adaptive Control Design,* John Wiley and Sons Inc., Canada.

Landau I D & Lozano R (1998), *Adaptive Control,* Springer-Verlag, Great Britain.

Liang Y, Kurihara K & Siato K (1998), Profile control of plastic sheet in an industrial polymer processing process, *Polymer Engineering and Science,* **38**, (10), 1740-1750.

Luyben M L & Luyben W L (1997), *Essentials of Process Control,* McGraw-Hill International, USA.

MathWorks (1999), *Matlab User's Guide v 5.3,* The MathWorks Inc., USA.

Meadows E S & Rawlings J B (1997), Model Predictive Control. In *Nonlinear Process Control* (Ed. Henson M A & Seborg D E), pp. 233-310, Prentice-Hall Inc., New Jersey.

Morari M & Zafiriou E (1989), *Robust Process Control,* Prentice-Hall International, New Jersey.

Morison K R (1997), Developing a design methodology for ultrafiltration plants. *CHEMECA 97,* pp. PD4e:1-PD4e:11, Rotorua, New Zealand.

Morison K R (1998), Department of Chemical and Process Engineering, University of Canterbury, Personal communication

Mosca E (1995), *Optimal, Predictive and Adaptive Control,* Prentice-Hall Inc., New Jersey.

Ogunnaike B A & Ray W H (1994), *Process Dynamics, Modeling, and Control,* Oxford University Press, New York.

Pradanos P, Arribas J I & Hernandez A (1994), Retention of proteins in cross-flow UF through asymmetric inorganic membranes, *AIChE Journal,* **40**, (11), 1901-1910.

Ricker N L (1985), The use of Quadratic Programming for Constrained Intenal Model Control, *Ind. Eng. Chem. Process Des. Dev.,* **24**, 925-936.

Seborg D E, Edgar T F & Millichamp D A (1989), *Process Dynamics and Control,* Wiley, New York.

She X (1998), New Zealand Dairy Group, Personal communication

Shinskey F G (1994), *Feedback Controllers for the Process Industries,* McGraw-Hill Inc., USA.

Skogestad S & Postlethwaite I (1996), *Robust Multivariable Feedback Control: Analysis and Design,* John Wiley and Sons, England.

8 Conclusions And Recommendations

The aim of this thesis was to examine the dynamic characteristics of multistage membrane separation plants, with the aim of identifying methods to improve the closed-loop performance of such processes.

A general review of membrane separation process was presented in Chapter 2, where the importance of staging membrane separations was illustrated. In Chapter 3 a dynamic model was developed for a generic multistage separation process using differential component balances. Dynamic models were developed for two case study systems, one producing a retentate and the other a permeate product, by substituting permeate flux and membrane fractionation relations into the general dynamic model. Membrane separation processes have non-linear, time variant behaviour, making formal controllability assessment a difficult task. For this reason it was necessary to explore the characteristic behaviour of membrane processes using a number of tools and assessment methods. The dynamic characteristics of the two case studies were analysed extensively in Chapters 4 and 5. Chapter 6 examined the closed-loop performance of each case study using multi-loop PID strategies. An innovative multivariable control strategy was developed in Chapter 7, and trialled using the case studies.

Overall, this thesis developed an understanding of dynamic membrane process behaviour, which was then used to identify constraints on closed-loop process behaviour and to develop methods to avoid or overcome these limitations. In this chapter, the findings of this thesis are reviewed, and recommendations for further work made.

8.1 Dynamic characteristics of multistage membrane processes

Structural analysis performed in Chapter 4 identified the presence of widespread disturbance propagation paths, and possible oscillatory characteristics within the plant. Possible inverse response behaviour was also identified. The inherent characteristics of the permeate and retentate product case studies were shown to be very similar, although the permeate stream response had lower order dynamics for feed concentration and diafiltration inputs.

In Chapter 5 pole-zero maps of the simplified steady state case study models confirmed the presence of inverse response and oscillatory behaviour within both processes. It was found that flowsheet designs with more stages have higher order dynamics, greater levels of interaction and increased likelihood of having oscillatory characteristics. A compromise was identified between process design, where optimisation may favour a greater number of separation stages, and process controllability, which improved with fewer stages in the plant. It was concluded that constant volume plant designs and concentration dependent permeate fluxes cause the high levels of interaction and widespread disturbance propagation present within each case study. This behaviour will be present in any multistage retentate or permeate product membrane separation.

Interaction between different control variable pairings was quantified using the relative gain array. This analysis indicated that high levels of interaction were present between certain input-output variable combinations in both case studies. Overall it can be concluded that such behaviour will be present, to some degree, in all liquid phase multistage membrane separations regardless of feed stream, product type or membrane specification.

It was also found that diafiltration injection has a significant effect on dynamic process behaviour. Analysis shows that when the diafiltration rates are maintained as a fixed proportion of the permeate flow, disturbance feedback loops are created within each stage. Such behaviour hastens the onset of oscillatory behaviour in plants with few stages. Aggressive diafiltration injection strategies increase the disturbance feedback gain within a stage, contributing to poor process behaviour for both retentate and permeate product separations.

8.2 Closed-loop control of multistage membrane processes

Closed-loop controller performance was examined for each case study through simulation, using a multi-loop PID strategy representative of that used industrially for a retentate product plant. In both case studies, the retentate stream maintained a retentate composition corresponding to the desired retentate purity or permeate yield, using the preferred input-output variable pairings identified by the relative gain analysis. Moderate controller performance was achieved, but overall both case studies had poor ability to reject retentate purity disturbances. Measurement difficulties have traditionally

precluded the industrial implementation of closed-loop composition control using diafiltration injection. Analysis in this thesis identified the presence of complex process dynamics and inverse response behaviour for this control variable pairing. It can therefore be concluded that, regardless of measurement difficulties, closed-loop composition control has limited feasibility within the multi-loop PID framework.

With a sound understanding of dynamic membrane system behaviour, general process flowsheet design was reviewed, along with the industrial control strategies commonly employed in the New Zealand dairy industry. Limitations on closed-loop performance were identified, but few feasible solutions were evident. A trade-off exists for multistage membrane processes, between optimal design and process controllability. It seems very unlikely that a simple control system will be found that gives a high level of performance for current, and sensible, designs of multistage membrane processes with diafiltration.

Separation trajectories, originally presented by She (1998) were explored as a tool for closed-loop process control, and a control strategy based on this approach was developed. An accurate real-time process model was implemented for each case study, allowing model-predictive control strategies to be developed. This approach represents a departure from standard control methodologies for membrane separations, since a desired concentration and purity is identified for each diafiltration stage within the process, rather than just the retentate stream.

The framework of a multivariable control strategy was then developed and implemented using general model-predictive methods, where the process inputs were manipulated to ensure the desired separation trajectory was maintained. This is a significant shift in strategy, since the diafiltration flow rates are directly manipulated, rather than maintained as proportions of the permeate flow rates. Such a strategy removes the disturbance feedback loop associated with each diafiltration stage, which was identified in Chapters 5 and 6 as placing significant constraint on closed-loop performance. Closed-loop simulation for each case study showed that the multivariable controller is affected by unmeasured feed concentration disturbances, but still provides superior disturbance rejection, particularly when new separation stages are added to the plant. Most importantly, the MIMO controller is able to maintain the desired retentate purity or permeate

yield for the duration of production despite changes in process behaviour during this time. Under more aggressive diafiltration regimes the MIMO controller is able to achieve superior performance to equivalent SISO controller strategies. For the permeate case study, the MIMO controller is able to operate at conditions where the multi-loop PID strategy is barely stable. The controller strategy developed in this chapter could easily be applied to any other multistage membrane plant using diafiltration injection to achieve enhanced separation and controller performance.

8.3 Recommendations

From the investigation presented in this thesis, it is believed that multivariable control strategies offer significant opportunities for improving controller performance. Such strategies rely on an accurate process model to predict internal process states. The commercial feasibility of a model-predictive strategy is therefore dependent on the successful development of a process model for an industrial membrane plant. Tangible improvements in controller performance will be dependent on the accuracy of this model. For this reason it is recommended that further work be focused in this area.

A trade-off exists for multistage membrane processes, between optimal design (which favours a large number of separation stages) and process controllability (which improves with fewer stages). It is likely that an equivalent trade-off also exists in the selection of a reference trajectory for a process. Aggressive diafiltration strategies can reduce the diafiltration water requirement of a process, but may also reduce the processing capacity of the plant. The shape of the trajectory from the midpoint to the retentate co-ordinate also affects closed-loop controller performance. It is recommended that the steady state and dynamic characteristics of different reference trajectories be investigated, to ensure the significant factors determining the optimal path selection are understood.

8.4 References

She X (1998), *Design and Optimisation of Multistage Ultrafiltration Plants.* M.E. Thesis, Department of Chemical and Process Engineering, University of Canterbury, New Zealand.

Symbols

A	membrane area [m^2]
B_v	viscosity coefficient
C	concentration [wt %]
F	flow rate [m^3 s^{-1}]
J	permeate flux [m s^{-1}]
K_m	mass transfer coefficient [m s^{-1}]
L	membrane permeability [m]
P	purity [%]
R	retention coefficient
R_m	membrane resistance [m^{-1}]
R_p	polarisation resistance [m^{-1}]
R_{sf}	short-term fouling resistance [m^{-1}]
R_{lf}	long-term fouling resistance [m^{-1}]
t	time [sec]
u	system input
V	stage volume [m^3]
x	system state
Y	yield

Subscripts

DF	diafiltration
F	feed
foul	fouling component(s)
i	stage property
j	component property
max	maximum
mid	midpoint
o	overall
P	permeate
R	retentate
SP	setpoint
TMP	trans-membrane pressure

TS total solids

W wall

Greek letters

$\Delta\pi$ osmotic pressure differential [Pa]

ΔP mechanical pressure differential [Pa]

ϕ diafiltration ratio

λ relative gain

μ dynamic viscosity [Pa.s]

ρ density [kg m^{-3}]

τ time constant [sec]

Appendix A - Multistage Membrane Model Equation Set

The dynamic multistage model developed in Chapter 3 is summarised in this Appendix.

A.1 Case study 1: Whey protein concentrate production

A.1.1 Assumptions

The following assumptions were made when developing the final equation set

1. Each separation stage had sufficiently high recirculation rate that it was well mixed, and could be represented by a lumped parameter model.
2. Osmotic pressure effects were negligible.
3. Membrane resistance R_m was equal for all stages, and constant throughout production.
4. Mass transfer coefficient K_m was assumed equal for all stages, and constant throughout production.
5. Trans-membrane pressure ΔP_{TMP} within each stage was equal.
6. All stream densities within the process were constant and equal to that of water at 50 °C.
7. The dynamic viscosity of all permeate streams was constant and equal to that of water at 50 °C.

A.1.2 Equation set

The set of equations presented in this section is used in Chapters 3 to 7, to model the dynamic behaviour of case study 1. Equation numbers quoted in this section correspond to the equation numbering used in each chapter.

The differential balance for component j in the i^{th} stage in a flowsheet with manipulated retentate flow rate is given by:

$$\frac{d\left(\rho_i V_i C_{Rj,i}\right)}{dt} = \left(\rho_{R,i}F_{R,i} - \rho_{DF,i}F_{DF,i} + \rho_{P,i}F_{P,i}\right)C_{Fj,i} + \rho_{DF,i}F_{DF,i}C_{DFj,i} - \rho_{P,i}F_{P,i}\left(1 - R_{j,i}\right)C_{Rj,i} - \rho_{R,i}F_{R,i}C_{Rj,i} \quad \textbf{(3-25)}$$

The observed retention coefficient $R_{j,i}$:

$$R_{j,i} = a_j + b_j C_{Rfoul,i} \quad \textbf{(3-6)}$$

Total concentration of fouling components:

$$C_{R\,foul,i} = C_{R\,Protein,i} + C_{R\,Fat,i} \quad \textbf{(3-28)}$$

Permeate flow rate F_{pi}:

$$F_{P,i} = A_i J_i \quad \textbf{(3-7)}$$

Permeate flux resistance model for stage i:

$$J_i = \frac{\Delta P_{TMP}}{\mu_{P,i}\left(R_m + R_{p,i} + R_{f,i}\right)} \quad \textbf{(3-16)}$$

Concentration polarisation resistance for stage i:

$$R_{p,i} = \max\left\{\begin{array}{c} \dfrac{\Delta P_{TMP} - \Delta\pi_i}{\mu_{P,i} K_{m,i} \ln\left(\dfrac{C_{gel,i}}{C_{R\,foul,i}}\right)} - R_m \\ 0 \end{array}\right\} \quad \textbf{(3-18)}$$

Fouling resistance for stage i:

$$R_{f,i} = R_{sf,i} + R_{lf,i} \quad \textbf{(3-20)}$$

Differential short-term fouling resistance model for stage i:

$$\frac{dR_{sf,i}}{dt} = \frac{k_1 J_i C_{R\,foul,i} \mu_{R,i}}{\rho_{R,i}} - k_2 R_{sf,i} \quad \textbf{(3-21)}$$

Differential long-term fouling resistance model for stage i:

$$\frac{dR_{lf,i}}{dt} = k_3 R_{sf,i} \quad \textbf{(3-22)}$$

Dynamic viscosity of the retentate stream from the i^{th} stage:

$$\mu_{R,i} = \mu_w e^{\sum_{j=1}^{k} B_{v,j} C_{Rj,i}} \quad \textbf{(3-23)}$$

A.1.3 Model parameters

Parameters used in Chapters 3 to 7 for case study 1 are summarised in Table A-1 to Table A-3.

Table A-1 Stage-specific model parameters – case study 1

Stage Number	Membrane Area A_i [m²]	Volume V_i [m³]	Fouling coefficient K_l [m s^{-4}]
1	285	0.18	3.0×10^{23}
2	285	0.18	3.0×10^{23}
3	285	0.17	2.4×10^{23}
4	285	0.17	2.4×10^{23}
5	285	0.18	2.4×10^{23}
6	285	0.18	2.4×10^{23}
7	285	0.17	2.4×10^{23}
8	285	0.17	1.2×10^{23}
9	230	0.16	8.2×10^{22}
10	215	0.16	3.0×10^{22}
11	215	0.16	1.0×10^{22}
12	168	0.16	1.0×10^{22}
13	178	0.16	1.8×10^{22}
14	178	0.15	5.0×10^{21}
15	134	0.14	1.0×10^{22}
16	59	0.12	1.3×10^{22}

Table A-2 Component-specific model parameters – case study 1

Component	Feed concentration $C_{Fl,j}$ [wt %]	Retention coefficient parameter a_j	Retention coefficient parameter b_j	Retentate viscosity parameter $B_{v,j}$
Protein	0.56	0.993	0.0004	17
NPN	0.19	0.080	0.0390	5
Lactose	4.89	0.120	0	5
Lactic acid	0.05	0.120	0	5
Minerals	0.78	0.034	0.0130	5
Fat	0.04	1.000	0	20

Table A-3 General model parameters – case study 1

Parameter	Value
Maximum continuous operating time	9 hours
Plant cleaning (CIP) time	3 hourts
Maximum trans-membrane pressure	$\Delta P_{TMP,max} = 3.0 \times 10^5$ Pa
Minimum trans-membrane pressure	$\Delta P_{TMP,min} = 1.75 \times 10^5$ Pa
Crossflow pressure drop	$\Delta P_{crossflow} = 2.0 \times 10^5$ Pa
Stream density	$\rho = 998.14$ kg/m^3
Diafiltration and permeate dynamic viscosity	$\mu = 5.44 \times 10^{-4}$ Pa.s
Gel concentration	$C_{gel} = 40$ wt %
Mass transfer coefficient	$K_m = 1.39 \times 10^{-5}$ m s^{-1}
Membrane resistance	$R_m = 1.2 \times 10^{12}$ s^{-1}
Fouling constants	$k_2 = 8.33 \times 10^{-4}$ s^{-1}
	$k_3 = 1.67 \times 10^{-5}$ s^{-1}

A.2 Case study 2: Permeate product separation

A.2.1 Assumptions

The following assumptions were made when developing the final equation set

1. Each separation stage has sufficiently high recirculation rate that it was well mixed, and could be represented by a lumped parameter model.
2. Osmotic pressure effects were negligible.
3. Membrane resistance R_m was equal for all stages, and constant throughout production.
4. Mass transfer coefficient K_m was assumed equal for all stages, and constant throughout production.
5. Trans-membrane pressure ΔP_{TMP} within each stage was equal.
6. All stream densities within the process were constant and equal to that of water at 50 °C
7. The dynamic viscosity of all permeate streams was constant and equal to that of water at 50 °C

A.2.2 Equation set

The set of equations presented in this section is used in Chapters 3 to 7, to model the dynamic behaviour of case study 1. Equation numbers quoted in this section correspond to the equation numbering used in each chapter.

The differential balance for component j in the i^{th} stage in a flowsheet with manipulated retentate flow rate is given by:

$$\frac{d\left(\rho_i V_i C_{Rj,i}\right)}{dt} = \left(\rho_{R,i}F_{R,i} - \rho_{DF,i}F_{DF,i} + \rho_{P,i}F_{P,i}\right)C_{Fj,i} + \rho_{DF,i}F_{DF,i}C_{DFj,i} - \rho_{P,i}F_{P,i}\left(1 - R_{j,i}\right)C_{Rj,i} - \rho_{R,i}F_{R,i}C_{Rj,i} \quad \textbf{(3-25)}$$

The observed retention coefficient $R_{j,i}$:

$$R_{j,i} = a_j + b_j C_{R\,foul,i} \quad \textbf{(3-6)}$$

Total concentration of fouling components:

$$C_{R\,foul,i} = C_{RA,i} \quad \textbf{(3-28)}$$

Permeate flow rate F_{pi}:

$$F_{P,i} = A_i J_i \quad \textbf{(3-7)}$$

Permeate flux resistance model for stage i:

$$J_i = \frac{\Delta P_{TMP}}{\mu_{P,i}\left(R_m + R_{p,i} + R_{f,i}\right)} \quad \textbf{(3-16)}$$

Concentration polarisation resistance for stage i:

$$R_{p,i} = \max\left\{\begin{matrix} \dfrac{\Delta P_{TMP} - \Delta\pi_i}{\mu_{P,i}K_{m,i}\ln\left(\dfrac{C_{gel,i}}{C_{R\,foul,i}}\right)} - R_m \\ 0 \end{matrix}\right\} \quad \textbf{(3-18)}$$

Fouling resistance for stage i:

$$R_{f,i} = R_{sf,i} + R_{lf,i} \quad \textbf{(3-20)}$$

Differential short-term fouling resistance model for stage i:

$$\frac{dR_{sf,i}}{dt} = \frac{k_1 J_i C_{R\,foul,i} \mu_{R,i}}{\rho_{R,i}} - k_2 R_{sf,i} \quad \textbf{(3-21)}$$

Differential long-term fouling resistance model for stage i:

$$\frac{dR_{lf,i}}{dt} = k_3 R_{sf,i} \quad \textbf{(3-22)}$$

Dynamic viscosity of the retentate stream from the i^{th} stage:

$$\mu_{R,i} = \mu_w e^{\sum_{j=1}^{k} B_{v,j} C_{Rj,i}} \quad \textbf{(3-23)}$$

A.2.3 Model parameters

Parameters used in Chapters 3 to 7 for case study 1 are summarised in Table A-4 to Table A-6.

Table A-4 Stage-specific model parameters – case study 2

Stage Number	Membrane Area A_i [m²]	Volume V_i [m³]	Fouling coefficient K_1 [m s^{-4}]
1	285	0.18	4.0×10^{23}
2	285	0.18	4.0×10^{23}
3	285	0.17	2.8×10^{23}
4	285	0.17	2.8×10^{23}
5	285	0.18	2.8×10^{23}
6	285	0.18	2.6×10^{23}
7	285	0.17	2.6×10^{23}
8	285	0.17	2.0×10^{23}
9	230	0.16	2.0×10^{23}
10	215	0.16	1.75×10^{22}
11	215	0.16	1.75×10^{22}
12	168	0.16	1.5×10^{22}
13	178	0.16	1.5×10^{22}
14	178	0.15	1.0×10^{23}
15	134	0.14	1.0×10^{22}
16	59	0.12	1.0×10^{22}

Table A-5 Component-specific model parameters – case study 2

Component	Feed concentration $C_{F1,j}$ [wt %]	Retention coefficient parameter a_j	Retention coefficient parameter b_j	Retentate viscosity parameter $B_{v,j}$
A	1.20	1.0	0	10
B	1.20	0.7	0	4

Table A-6 General model parameters – case study 2

Parameter	Value
Maximum continuous operating time	9 hours
Plant cleaning (CIP) time	3 hours
Maximum trans-membrane pressure	$\Delta P_{TMP,max} = 3.0 \times 10^5$ Pa
Minimum trans-membrane pressure	$\Delta P_{TMP,min} = 1.75 \times 10^5$ Pa
Crossflow pressure drop	$\Delta P_{crossflow} = 2.0 \times 10^5$ Pa
Stream density	$\rho = 998.14$ kg/m³
Diafiltration and permeate dynamic viscosity	$\mu = 5.44 \times 10^{-4}$ Pa.s
Gel concentration	$C_{gel} = 20$ wt %
Mass transfer coefficient	$K_m = 1.60 \times 10^{-5}$ m s^{-1}
Membrane resistance	$R_m = 1.2 \times 10^{12}$ s^{-1}
Fouling constants	$k_2 = 6.67 \times 10^{-4}$ s^{-1}
	$k_3 = 1.33 \times 10^{-5}$ s^{-1}

Appendix B - Simulation And Controller Parameters

This Appendix presents a summary of the conditions, and PID controller tuning parameters used in the simulations presented in Chapters 5 to 8.

B.1 Chapter 5: Numerical Analysis of Multistage Membrane Plants

B.1.1 Case study 1: Whey protein concentrate production

Desired retentate protein purity = 85 wt %

Table B-1 Simulation conditions – case study 1

Controlled variable	Feed flow rate	Overall diafiltration ratio	Retentate total solids concentration
Setpoint / desired value	*	Various	27 wt %
Manipulated variable(s)	Baseline pressure	Stage diafiltration ratios	Retentate flow rate

*A fixed baseline pressure was used for all steady state simulations: P_{Base}= 1.75 × 10^5 Pa

B.1.2 Case study 2: Permeate product separation

Desired Component B yield in permeate = 75 %

Component A purity in retentate, corresponding to desired Component B yield in permeate: 79.9 wt %

Table B-2 Simulation conditions – case study 2

Controlled variable	Feed flow rate	Overall diafiltration ratio	Retentate total solids concentration
Setpoint / desired value	*	Various	17 wt %
Manipulated variable(s)	Baseline pressure	Stage diafiltration ratios	Retentate flow rate

*A fixed baseline pressure was used for all steady state simulations: P_{Base}= 1.75 × 10^5 Pa

B.2 Chapter 6: Closed-loop Behaviour of Multistage Membrane Plants

Tuning parameters for process controllers are presented for each case study. The PID controller algorithm used in Simulink is of the form:

$$u = K_c e + T_i \int e\,dt + T_d \frac{de}{dt}$$

B.2.1 Case study 1: Whey protein concentrate production

Desired retentate protein purity = 85 wt %

Minimum time delay between the introduction of new stages = 180 sec

Table B-3 SISO PID controller settings – case study 1

Controlled variable	Feed flow rate	Overall diafiltration ratio	Retentate total solids concentration
Setpoint / desired value	2.17×10^{-2} m^3 s^{-1}	0.118	27 wt %
Manipulated variable(s)	Baseline pressure	Stage diafiltration ratios	Retentate flow rate
Controller limits	$P_{base,min} = 0.75 \times 10^5$ Pa	$\phi_{min} = 0.00$	$Fr_{min} = 0.05 \times 10^{-3}$ m^3 s^{-1}
	$P_{base,max} = 2.00 \times 10^5$ Pa	$\phi_{max} = 0.70$	$Fr_{max} = 2.50 \times 10^{-3}$ m^3 s^{-1}
Gain	$K_c = 10000$	$K_c = 0.5$	$K_c = 5.5$
Integral time	$T_i = 3000$	$T_i = 0.1$	$T_i = 0.015$
Derivative time	$T_d = 0$	$T_d = 0$	$T_d = 0$

B.2.2 Case study 2: Permeate product separation

Desired Component B yield in permeate = 75 %

Desired Component A purity in retentate, corresponding to desired Component B yield in permeate = 79.9 wt %

Minimum time delay between the introduction of new stages = 180 sec

Table B-4 SISO PID controller settings – case study 2

Controlled variable	Feed flow rate	Overall diafiltration ratio	Retentate total solids concentration
Setpoint / desired value	1.50×10^{-2} m^3 s^{-1}	0.260	17 wt %
Manipulated variable(s)	Baseline pressure	Stage diafiltration ratios	Retentate flow rate
Controller limits	$P_{base,min} = 0.75 \times 10^5$ Pa	$\phi_{min} = 0.00$	$Fr_{min} = 0.05 \times 10^{-3}$ m^3 s^{-1}
	$P_{base,max} = 2.00 \times 10^5$ Pa	$\phi_{max} = 0.70$	$Fr_{max} = 2.5 \times 10^{-3}$ m^3 s^{-1}
Gain	$K_c = 2500$	$K_c = 0.1$	$K_c = 4.0$
Integral time	$T_i = 1000$	$T_i = 0.005$	$T_i = 0.015$
Derivative time	$T_d = 0$	$T_d = 0$	$T_d = 0$

B.3 Chapter 7: Novel Strategies for Improving Membrane Plant Behaviour

B.3.1 Case study 1: Whey protein concentrate production

Desired retentate protein purity = 85 wt %

Minimum time delay between the introduction of new stages = 180 sec

Table B-5 SISO PID controller settings – case study 1

Controlled variable	Feed flow rate	Overall diafiltration ratio	Retentate total solids concentration
Setpoint / desired value	2.17×10^{-2} m^3 s^{-1}	0.118	27 wt %
Manipulated variable(s)	Baseline pressure	Stage diafiltration ratios	Retentate flow rate
Controller limits	$P_{base,min} = 0.75 \times 10^5$ Pa	$\phi_{min} = 0.00$	$Fr_{min} = 0.05 \times 10^{-3}$ m^3 s^{-1}
	$P_{base,max} = 2.00 \times 10^5$ Pa	$\phi_{max} = 0.70$	$Fr_{max} = 2.5 \times 10^{-3}$ m^3 s^{-1}
Gain	$K_c = 10000$	$K_c = 0.5$	$K_c = 5.5$
Integral time	$T_i = 3000$	$T_i = 0.1$	$T_i = 0.015$
Derivative time	$T_d = 0$	$T_d = 0$	$T_d = 0$

Full details of the MIMO controller tuning parameters are presented in Section 7.8.1. Tuning parameters for the PID loop controlling feed flow rate are presented in Table B-6

Table B-6 PID controller settings – MIMO case study 1

Controlled variable	Feed flow rate
Setpoint / desired value	2.17×10^{-2} m^3 s^{-1}
Manipulated variable(s)	Baseline pressure
Controller limits	$P_{base,min} = 0.75 \times 10^5$ Pa
	$P_{base,max} = 2.00 \times 10^5$ Pa
Gain	$K_c = 7500$
Integral time	$T_i = 2500$
Derivative time	$T_d = 0$

B.3.2 Case study 2: Permeate product separation

Desired Component B yield in permeate = 75 %

Desired Component A purity in retentate, corresponding to desired Component B yield in permeate = 79.9 wt %

Minimum time delay between the introduction of new stages = 180 sec

Table B-7 SISO PID controller settings – case study 2

Controlled variable	Feed flow rate	Overall diafiltration ratio	Retentate total solids concentration
Setpoint / desired value	1.50×10^{-2} m^3 s^{-1}	0.260	17 wt %
Manipulated variable(s)	Baseline pressure	Stage diafiltration ratios	Retentate flow rate
Controller limits	$P_{base,min} = 0.75 \times 10^5$ Pa	$\phi_{min} = 0.00$	$Fr_{min} = 0.05 \times 10^{-3}$ m^3 s^{-1}
	$P_{base,max} = 2.00 \times 10^5$ Pa	$\phi_{max} = 0.70$	$Fr_{max} = 2.5 \times 10^{-3}$ m^3 s^{-1}
Gain	$K_c = 2500$	$K_c = 0.1$	$K_c = 4.0$
Integral time	$T_i = 1000$	$T_i = 0.005$	$T_i = 0.015$
Derivative time	$T_d = 0$	$T_d = 0$	$T_d = 0$

Full details of the MIMO controller tuning parameters are presented in Section 7.8.2. Tuning parameters for the PID loop controlling feed flow rate are presented in Table B-8.

Table B-8 PID controller settings – MIMO case study 2

Controlled variable	Feed flow rate
Setpoint / desired value	1.50×10^{-2} m^3 s^{-1}
Manipulated variable(s)	Baseline pressure
Controller limits	$P_{base,min} = 0.75 \times 10^5$ Pa
	$P_{base,max} = 2.00 \times 10^5$ Pa
Gain	$K_c = 4700$
Integral time	$T_i = 800$
Derivative time	$T_d = 0$